Defining the inner membrane proteome of *Pseudomonas aeruginosa* with particular focus on small proteins

Von der Fakultät für Lebenswissenschaften
der Technischen Universität Carolo-Wilhelmina zu Braunschweig
zur Erlangung des Grades
eines Doktors der Naturwissenschaften
(Dr. rer. nat.)
genehmigte
Dissertation

von Erik Lehmann
aus Frankfurt/Oder

1. Referentin: Professorin Dr. Susanne Engelmann
2. Referent: Professor Dr. Dieter Jahn

eingereicht am: 27.05.2020
mündliche Prüfung (Disputation) am: 08.02.2021

Druckjahr 2021

Vorveröffentlichungen der Dissertation

Teilergebnisse aus dieser Arbeit wurden mit Genehmigung der Fakultät für Lebenswissenschaften, vertreten durch die Mentorin der Arbeit, in folgenden Beiträgen vorab veröffentlicht:

Tagungsbeiträge

Lehmann E., Kucklick M., Fuchs S., Wissing J., Jänsch L., Jahn D. & Engelmann S.: Identifying small proteins of the inner membrane proteome of *Pseudomonas aeruginosa*. (Poster). PROCOMPAS PhD Symposium, Braunschweig (2018)

Lehmann E., Kucklick M., Wissing J., Jänsch L., Fuchs S. & Engelmann S.: Identification of small proteins in the membrane-associated proteome of *Pseudomonas aeruginosa* strain PA01. (Poster). 11th International PhD Symposium (HZI), Braunschweig (2018)

Lehmann E., Kucklick M., Wissing J., Jänsch L., Fuchs S. & Engelmann S.: Identification of small proteins in the membrane-associated Proteome of *Pseudomonas aeruginosa* strain PA01. (Talk). Jahrestagung der Vereinigung für Allgemeine und Angewandte Mikrobiologie (VAAM), Mainz (2019).

"The mind will not be cultivated at the expense of the heart."

Basil Moreau

Table of Contents

I. List of tables

II. List of figures

III. List of equations

IV. Abbreviations

Table 1 List of abbreviations used and introduced during this work.

%	percent, percentage
°C	Celsius degree
µ	micro
µg	microgram
µl	microliter
µm	micrometer
∞	infinite
Å	angstrom; unit of length equal to 10^{-10} m
ACN	acetonitrile
Anr	anaerobic regulation of arginine deiminase and nitrate reduction
bp	base pair(s)
CF	cystic fibrosis
ddH_2O	double-distilled water
DMSO	dimethyl sulfoxide
DNA	deoxyribonucleic acid
Dnr	dissimilatory nitrate respiration regulator
e.g.	*exempli gratia*; for example
EDTA	ethylene diamine tetra acetic acid
et al.	*et alteri*; and others
FA	formic acid
FAD	flavine adenine dinucleotide
FAD^+/ H	flavine adenine dinucleotide (oxidized/ reduced)
FDR	false discovery rate; rate of type I errors (false-positive)
fs	femtosecond; 1 fs = 10^{-15} s
Fw	forward
FWER	family-wise error rate; probability for type I error (false-positive)
g	gram
GAPDH	glyceraldehyde 3-phosphate dehydrogenase

h	hour(s)
HQNO	2-n-heptyl-4-hydroxyquinoline N oxide
kb	kilobase(s)
kDa	kilo Dalton(s)
kg	kilogram
kV	kilovolt
l	liter(s)
LB	lysogeny broth
LC-MS/MS	liquid chromatography coupled with tandem mass spectrometry
M	molar
mg	milligram
min	minute(s)
µl	microliter
ml	milliliter
mM	mmol/l; millimoles per liter
MS	mass spectrometry
N_2	dinitrogen
N_2O	nitrous oxide
NAD	nicotinamide adenine dinucleotide
NAD^+/H	nicotinamide adenine dinucleotide (oxidized/ reduced)
$NADP^+/H$	nicotinamide adenine dinucleotide phosphate (oxidized/ reduced)
ncRNA	non-coding ribonucleic acid
nm	nanometer(s)
NO	nitric oxide
NO_2	nitrite
NO_3	nitrate
nts	nucleotides
OD	optical density
ORF	open reading frame
PBS	phosphate-buffered saline
PCR	polymerase chain reaction

p-value	probability value
PVDF	polyvinylidene difluoride
RBS	ribosomal binding site
Rev	reverse
RNA	ribonucleic acid
rpm	revolutions per minute
rRNA	ribosomal ribonucleic acid
S	Svedberg unit; non-metric unit for sedimentation coefficient (1 S = 10^{-13} s = 100 fs)
SDS-PAGE	sodium dodecyl sulfate polyacrylamide gel electrophoresis
sec	second(s)
SSC	saline-sodium citrate
SSPE	saline-sodium phosphate-EDTA
TBE	tris-borate-EDTA
TBS	tris-buffered saline
TCA cycle	tricarbolic acid cycle; citric acid cycle, Krebs cycle
tRNA	transfer ribonucleic acid
UV	ultraviolet light
v/v	volume/ volume
w/v	weight/ volume
WT	wild type
x *g*	gravitational force
Ω	ohm; unit of electrical resistance

1 Introduction

1.1 *Pseudomonas aeruginosa*

Pseudomonas aeruginosa belongs to the Gram-negative Gammaproteobacteria. Normally, its cells are rod shaped and highly motile. Here, a polar flagellum promotes swimming motility in aqueous environments whereas type IV pili are used for twitching motility (Dasgupta, *et al.*, 2003) (Matticks, 2002). Members of the family of the *Pseudomonadaceae* are ubiquitous distributed and resident in aquatic to terrestrial environments (Silby, *et al.*, 2011). *P. aeruginosa* is a facultative anaerobic microorganism, using aerobic respiration with oxygen as a terminal electron acceptor. However, in anoxic environments it is also able to respire anaerobically using nitrate as the primary alternative electron acceptor. Otherwise, even without alternative electron acceptor *P. aeruginosa* can also survive using arginine or pyruvate for fermentation (Schobert, *et al.*, 2010). Despite its ubiquitous habitats, *P. aeruginosa* is an opportunistic pathogen infecting immunocompromised patients. In 2017, the World Health Organization (WHO) published a list of priority pathogens highlighting *P. aeruginosa* as one of the critical pathogens, substantiating its leading role among all Gram-negative bacteria in nosocomial infections with 40 – 60% mortality (Botzenhart, *et al.*, 1993) (Matos, *et al.*, 2018). Additionally, *P. aeruginosa* complicates about 90% of cystic fibrosis infections by exploiting the oxygen-depleted environment in the patients' lung. There, *Pseudomonas* forms biofilms and thus, causes chronic infections (Fick, 1993).

Over the time, various *P. aeruginosa* strains were characterized and among these is strain PAO1. This strain is a chloramphenicol-resistant mutant of the original PAO strain, which was isolated in 1954 in Australia and nowadays is widely used as a reference strain (Holloway, 1955). The genome of this reference strain was first sequenced in 2000 reporting 6.3 million base pairs with 5570 predicted open reading frames (Stover, *et al.*, 2000). Following, an analysis of 389 genomes of different *P. aeruginosa* strains showed that 17.5% are shared between all genomes, representing the core genome of *P. aeruginosa*. Further preliminary analyses showed that these 389 strains clustered into three major groups around the strains PAO1, PA7 and PA14 (Freschi, *et al.*, 2015).

1.1.1 *Pseudomonas aeruginosa* and cystic fibrosis

P. aeruginosa causes a variety of infections ranging from urinary to wound infections and infections of the respiratory tract. The later are even more severe for patients already suffering from cystic fibrosis (CF), which is an autosomal disease caused by a genetic defect in the gene coding for the cystic fibrosis transmembrane conductance regulator (CFTR) (Riordan, *et al.*, 1989). CFTR has regulatory function and is also responsible for the secretion of chloride ions. Furthermore, CFTR shows inhibitory function towards the epithelial sodium channel ENaC, which transports sodium ions into the cell. During CF, a defective CFTR results in the deregulation of the chloride and sodium ions. Subsequently, this leads to an increased water absorption by the cell and eventually to an increase of viscosity of the mucus layer (O'Sullivan, *et al.*, 2009). Moreover, the resulting thicker mucus layer cannot be removed by the cilia and favors bacterial and fungal infections in the mucus causing strong immune reactions and irreversible tissue damage (Knowles, *et al.*, 2002) (Worlitzsch, *et al.*, 2002). Differences in physiology of a healthy compared to a CF lung are depicted in Figure 1, showing that the defect in the CFTR not only results in a thicker mucus layer, but also in a decrease of the oxygen concentration generating a micro-anaerobic to anaerobic environment (Williams, *et al.*, 2007).

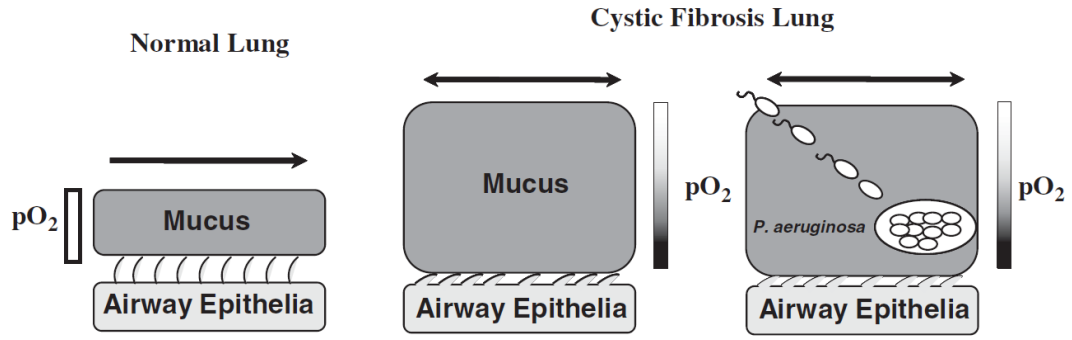

Figure 1 Physiologic comparison of a healthy and a CF lung (adapted from Williams, *et al.* 2007).
The genetic defect in the CFTR results in a thicker and more viscous mucus layer compared to the layer in healthy lungs, where the mucus is aerated and constantly cleared by the cilia. Due to continuous mucus secretion, the layer gets thicker and eventually generates a hypoxic gradient in the mucus. Subsequently, obligate anaerobic bacteria like *P. aeruginosa* colonize the mucus layer where they are protected from the immune system.

In addition to its ability to survive in harsh oxygen-limited environments, *P. aeruginosa* also harbors a multitude of virulence factors. Currently, studies display a variety of antibiotic resistant strains, e.g. strains showing resistance against fluoroquinolones (Rizvi, *et al.*, 2011). This inherent resistance against antibiotics and antimicrobial agents is mainly achieved by the possibility to form biofilms (Lambert, 2002). Furthermore, antibiotic resistance is mediated by a number of antibiotic efflux systems such as MexAB-OprM and MexCD-OprJ (Poole, 2001). In addition to its resistance against antibiotics, *P. aeruginosa* possesses a variety of secretion systems to directly inject or secrete proteases and toxins into the host cells or environment, respectively (Figure 2).

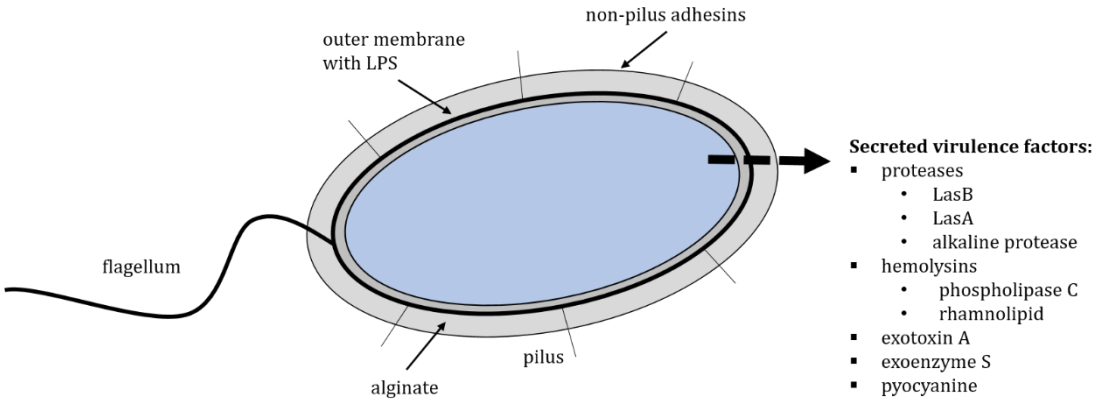

Figure 2 Schematic view of the virulence factors of *P. aeruginosa* (adapted from Van Delden, *et al.*, 1998).
Cell-associated virulence factors like the flagellum, pili or the alginate capsule contribute to motility and resistance, respectively. Extracellular virulence factors, like proteases, exotoxins and pyocyanin are actively secreted by the cell via type II or type III secretion systems.

In *P. aeruginosa*, the type II secretion system is used to secrete virulence factors like exotoxin A, metalloproteases like LasB and phospholipases (Filloux, *et al.*, 1998). Moreover, toxins like the exoenzyme (Exo) S, ExoT, ExoU and ExoY are secreted by the type III secretion system (Hueck, 1998). Other important virulence factors are the siderophores pyoverdine and pyocyanin, both fluorescent compounds and important for iron-uptake. Pyoverdine is the primary iron-uptake system in *P. aeruginosa,* whereas pyocyanin shows less affinity for iron in comparison to pyoverdine. Especially in iron-limited environments, like the mucus layer of CF patients, siderophores are necessary for the survival of *P. aeruginosa* and are thus essential for its virulence.

1.1.2 Membrane structure of *P. aeruginosa*

The cell envelope of Gram-negative bacteria, like *P. aeruginosa* and *Escherichia coli*, consists of three distinct layers as depicted in Figure 3: the outer membrane (OM), the cell wall consisting of peptidoglycan (PG) and the inner membrane (IM). Both, the OM and the IM are lipid bilayers, composed of phospholipids, separating the aqueous periplasm from the cytoplasm and the environment (Silhavy, *et al.*, 2010). These phospholipids are arranged in a way that the polar head-groups form the surface of the membrane while the hydrophilic fatty acid tails form the center. Here, the OM is rich in lipopolysaccharides (LPS) consisting of poly- or oligosaccharides with exposed phosphoryl and carboxyl groups resulting in a high negative charge of the OM (Beveridge, 1999). Furthermore, to resist the strong turgor pressure from the cytoplasm, interconnected peptidoglycan is linked to the OM via lipoproteins.

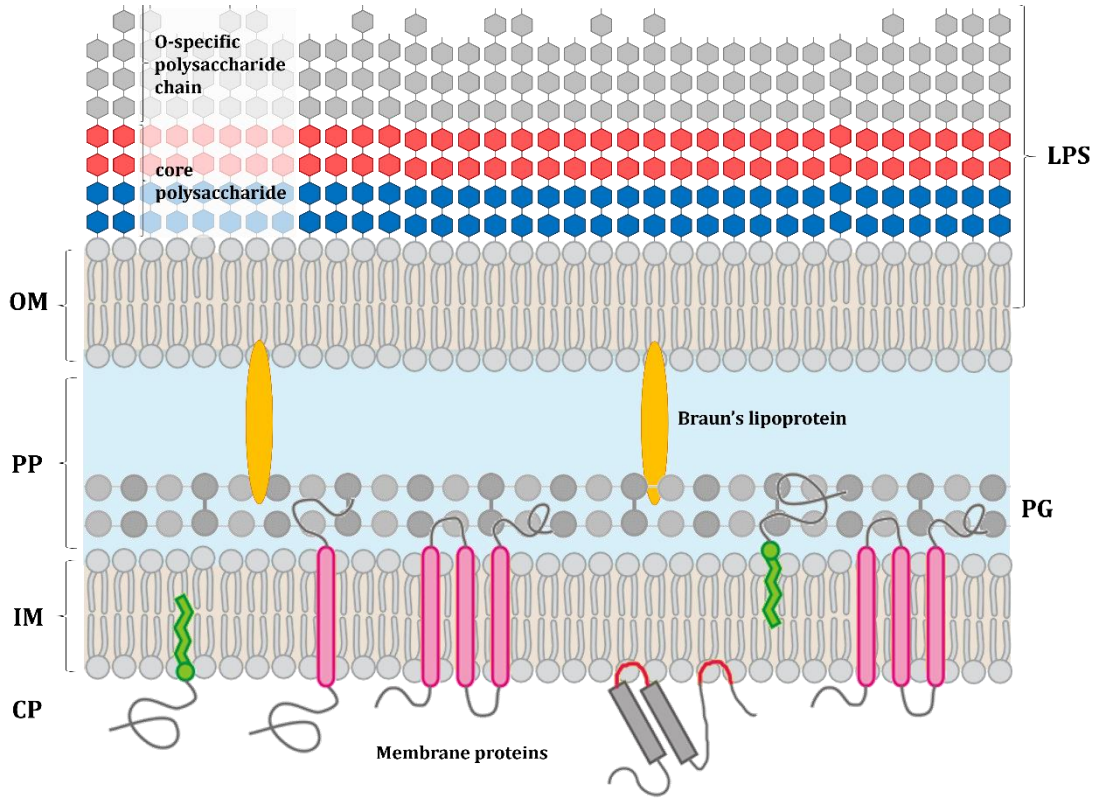

Figure 3 Schematic view of the membrane structure of Gram-negative bacteria.
The cell envelope of Gram-negative bacteria consists of three layers where the outer and the inner membrane delimit the aqueous periplasm. LPS = Lipopolysaccharides; OM = Outer membrane; PG = Peptidoglycan; PP = Periplasm; IM = Inner membrane; CP = Cytoplasm

1.1.2.1 Outer Membrane

The outer membrane is the first contact point of the bacterium with the environment. As described previously, the OM is a lipid bilayer with an asymmetric distribution of lipids over its inner and outer leaflet. The inner leaflet consists of phospholipids whereas the outer leaflet is composed of LPS (Silhavy, *et al.*, 2010). LPS contribute to the structural integrity of the bacteria and also stabilize the membrane structure. They are also referred to as endotoxins, as LPS are responsible for the endotoxic shock that is associated with sepsis caused by Gram-negative bacteria (Raetz, *et al.*, 2002). Structurally, LPS are built by three domains: the lipid A, a core polysaccharide, and the O-antigen. Lipid A consists of two phosphorylated glucosamine molecules with multiple fatty acid chains that anchor the LPS into the OM (Raetz, *et al.*, 2009). Connected to the lipid A domain is the core polysaccharide, which is a short chain of sugar residues. The core polysaccharide can be further divided into the inner and the outer core. Here, the inner core is directly attached to lipid A and consists of one to three keto-deoxyoctulosonate (KDO) residues of which the last KDO is often modified with a phosphate or ethanolamine group. On the contrary, the outer core is built of hexose residues. Subsequently, comparative studies showed that the overall core polysaccharide domain is highly diverse among bacteria species and strains (Heinrichs, *et al.*, 1998). Additionally, repetitive carbohydrate polymers, the O-antigens, are attached to the outer core. In *P. aeruginosa*, two distinct forms of O-antigens are produced by each strain: the common polysaccharide chain (CPA) and the O-specific antigen (OSA). The CPA is produced in the majority of *P. aeruginosa* strains and is a neutral polysaccharide composed of D-rhamnose that causes a weak antibody response (Yokota, *et al.*, 1987). Contrary to this, the OSA is a heteropolymer of three to five sugars that built repetitive O units and elicit a strong antibody response. Until now, various compositions of O units have been found, leading to the classification of *P. aeruginosa* strains into 20 major serotypes (O1 - O20) (Knirel, *et al.*, 2006)

1.1.2.2 Peptidoglycan cell wall

In Gram-negative bacteria, the peptidoglycan layer is about seven to eight nanometers thick and contributes up to 10% to the dry weight (Esko, *et al.*, 2017). It is formed by two alternating amino sugars, *N*-acetylmuramic acid (MurNAc) and

N-acetylglucosamine (GlcNAc5) that are connected via β-(1,4)-glycosidic bonds. Additionally, a short amino acid chain is attached to each MurNAc and the specific amino acid sequences vary among bacteria. Here, Gram-negative bacteria show more uniformity in their peptidoglycan structure, while this sequences are more diverse among Gram-positive bacteria (Schleifer, *et al.*, 1972). For *P. aeruginosa* it was shown that glutamate, alanine and 2, 5-diaminopimelate are commonly joined to MurNAc (Heilmann, 1972). In *E. coli*, the peptidoglycan layers are connected to the outer membrane by the lipoprotein Lpp, also called Braun's lipoprotein (Braun, 1975).

1.1.2.3 Periplasm

The periplasm is a gel-like concentrated matrix and is confined by the OM and the IM. It can contribute up to 40% to the total cell volume of Gram-negative bacteria (Holst, *et al.*, 1982). This cellular compartmentalization enables Gram-negative bacteria to separate degrading enzymes like the alkaline phosphatase, whose activity may be harmful in the cytoplasm (Beveridge, 1995). Moreover, the periplasm also harbors assembly platforms for the secretion of lipoproteins like the β-barrel assembly machinery (BAM) complex (Typas, *et al.*, 2011) (Noinaj, *et al.*, 2017). Furthermore, in *P. aeruginosa* it was shown that virulence factors, that are prominent during CF, first need to be activated in the periplasm before they are released (Passador, *et al.*, 1993).

1.1.2.4 Inner Membrane

The inner membrane (IM) or cytoplasmic membrane is a lipid bilayer consisting of 40% phospholipids and 60% proteins. Phospholipids show amphiphilic characteristics due to the hydrophilic 'head' and the hydrophobic fatty acid 'tail' that naturally form a bilayer in aqueous environments. In comparison to eukaryotic cells, bacteria lack organelles and thus, membrane-linked reactions like aerobic respiration and denitrification are located and performed in the IM (Silhavy, *et al.*, 2010). It was also observed that membrane junctions, so-called Bayer's junctions, are formed between the IM and the OM which offer another way of secretion of e.g. exotoxins in *P. aeruginosa* (Bayer, 1991) (Kadurugamuwa, *et al.*, 1995).

1.1.3 Membrane proteins in bacteria

Membrane proteins are either directly incorporated into the cell membrane of the organism or are associated with the membrane via various interactions. It is presumed that 20 - 30% of the genome code for membrane proteins (Krogh, *et al.*, 2001) (Andreeva, *et al.*, 2014). Membrane proteins offer a variety of vital functions including receptor, transporter, and enzyme functions. Additionally, they are also important for cell adhesion such as integrins and cadherins (Brackenbury, *et al.*, 1981) (Almén, *et al.*, 2009). Based on their topology in the membrane, membrane proteins are subdivided into peripheral and integral membrane proteins as depicted in Figure 4 (Johnson, *et al.*, 1999). Peripheral membrane proteins are associated with the membrane via an amphipathic α-helix or a hydrophilic loop, or directly bound to a membrane lipid. Also, electrostatic interactions occur between positively charged proteins and the negatively charged membrane. Thus, these proteins can dissociate from the membrane very easily by changing the pH or due to high salt concentrations. Contrary to this, integral membrane proteins (IMPs) are permanently integrated into the membrane and can only be isolated by solubilizing the membrane with detergents or denaturing agents. Furthermore, integral membrane proteins are incorporated either by one or more transmembrane α-helices and described as bitopic or polytopic membrane proteins (Ott, *et al.*, 2002). Integral membrane proteins in the OM consist of a large β-sheet formation, called β-barrel (Selkrig, *et al.*, 2014).

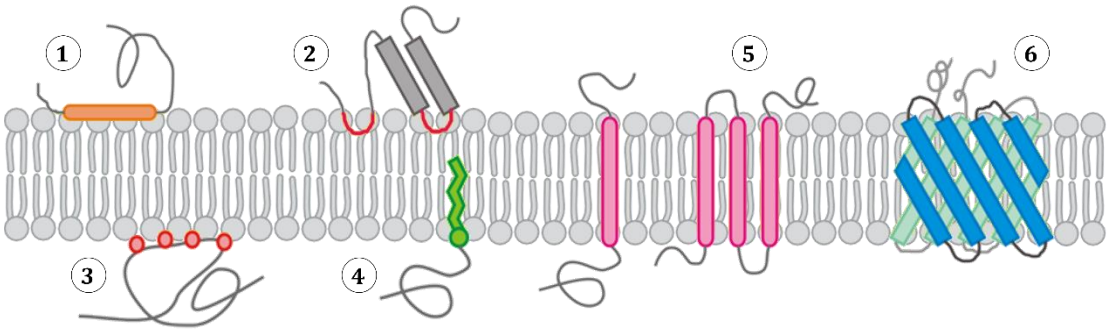

Figure 4 Schematic representation of peripheral and integral membrane proteins.
Peripheral membrane proteins are simply associated to the membrane by 1) an amphipathic α-helix, 2) hydrophilic loops, 3) electrostatic interactions, or 4) directly bound to membrane lipids. In contrast, integral membrane proteins are directly incorporated into the membrane by 5) one or more transmembrane α-helices or by 6) large β-sheets forming a so-called β-barrel.

In the past, proteomic studies of *P. aeruginosa* analyzed the whole proteome by using two-dimensional gel electrophoresis (2D PAGE) in combination with MALDI-MS peptide fingerprint identification (Nouwens, *et al.*, 2000) (Sriramulu, *et al.*, 2005). Additional studies applied both, a theoretical and an experimental approach, albeit only few took a further look at the inner membrane proteome of *P. aeruginosa* (Nouwens, *et al.*, 2002) (Lecoutere, *et al.*, 2012) (Magnowska, *et al.*, 2014). In 2000 Nouwens, *et al.* were able to identify 80 of 1500 known membrane proteins by enrichment of the membrane fraction, representing about 5% of the assumed membrane proteins in *P. aeruginosa*. Nevertheless, in all previous studies, the weakness lies in the utilization of 2D PAGE for protein separation. Here, the first dimension of separation is based on isoelectric focusing, thus the proteins were separated on an immobilized pH gradient within an electric field according to their respective isoelectric point. Thereby, most of the hydrophobic proteins will usually precipitate and then are excluded from the second dimension separation (Bunai, *et al.*, 2005). Using ultracentrifugation prior to digestion and LC-MS/MS analyses, resulted in the identification of over 60% of predicted membrane proteins in *P. aeruginosa.* This emphasizes the importance of proper sample preparation (Kamath, *et al.*, 2016). Furthermore, the enrichment of membrane proteins can also be achieved by various other methods. One possibility is the selective biotinylation of whole bacterial cells using different biotinylation agents followed by affinity chromatography and mass spectrometric analysis of the labeled proteins (Sabarth, *et al.*, 2002). In addition, applying a density-based isopycnic gradient centrifugation allows the separation and enrichment of the outer and inner membrane fractions (Stasyk, *et al.*, 2004).

In addition to membrane preparation, protein preparation and digestion for LC-MS/MS analyses are also crucial points for the analysis of membrane proteins (Speers, *et al.*, 2007). Contrary to soluble proteins, membrane proteins are rather low abundant and display a hydrophobic character, which is characterized by the specific amino acid composition of the integral membrane protein domains. Here, arginine and lysine rarely occur, and thus trypsin activity, which is commonly used for protein digestion, is limited, exacerbating the identification of these proteins. Alternatively, chymotrypsin, which preferably cleaves hydrophobic residues, can be applied. Here, several studies displayed almost the same peptide coverage on

both qualitative and quantitative levels for chymotrypsin as found for trypsin (Peng, *et al.*, 2012) (Low, *et al.*, 2013). Regarding the preparation of membrane proteins, selection of methods strongly depends on the type of membrane proteins that want to be analyzed. Peripheral or associated membrane proteins are usually easier to receive due to their loose interactions with the membrane. Moreover, the majority of peripheral membrane proteins can be prepared by washing membranes with high-pH or high-ionic-strength buffers. A combination of both buffer systems enables a higher yield of peripheral membrane proteins. However, it was shown that the efficiency of this method is strongly membrane-dependent (Fischer, *et al.*, 2006). In addition, the preparation of integral membrane proteins is usually achieved by first solubilizing the membrane, followed by protein solubilization and denaturation. Here, a broad range of solubilization agents is available ranging from harsh to mild detergents and varying in their MS compatibility. Application of chaotropic agents like urea and thiourea facilitates strong protein denaturation with a mild potential for membrane disruption and are often combined with other detergents. However, prior MS/MS analyses urea-treated samples require an additional desalting step (Makhatadze, *et al.*, 1992) (Möglich, *et al.*, 2005). Additionally, classical ionic and anionic detergents like SDS or Triton X-100 are amphipathic molecules mimicking membrane lipids. SDS has a strong potential to disrupt membranes, but must be removed completely from the sample as it severely suppresses ionization during MS/MS analyses (Reynolds, *et al.*, 1970) (Loo, *et al.*, 1994). In comparison to this, Triton X-100 is much less efficient in denaturation and membrane solubilization but it has also less effects on ionization (le Maire, *et al.*, 2000). Another possibility to circumvent the loss of signals during MS/MS analyses is the utilization of MS-compatible detergents. For example RapiGest, an ionic detergent, showed moderate denaturation and membrane disruption potential. Furthermore, RapiGest can be easily removed from the samples by acidification. Upon acidification, the labile ketal functional group between the hydrophilic head group and the hydrophobic tail is hydrolyzed resulting in two products. The insoluble product can be removed via centrifugation, while the second soluble product does not influence LC-MS/MS analyses (Yu, *et al.*, 2004).

1.1.4 Aerobic respiration in *P. aeruginosa*

Respiration under aerobic conditions is a processes that occurs at the inner membrane of Gram-negative bacteria since the majority of the involved proteins and protein complexes are membrane-resident (Matsushita, *et al.*, 1980). In general, this process can be described as a series connection of various electron-transfer components that contribute to the proton motive force to generate ATP. The respiratory chain consists of the five complexes: the NADH dehydrogenase (complex I), the succinate dehydrogenase (complex II), the bc_1 complex (complex III), the terminal oxidase (complex IV) and the ATP synthase (complex V) as depicted in Figure 5.

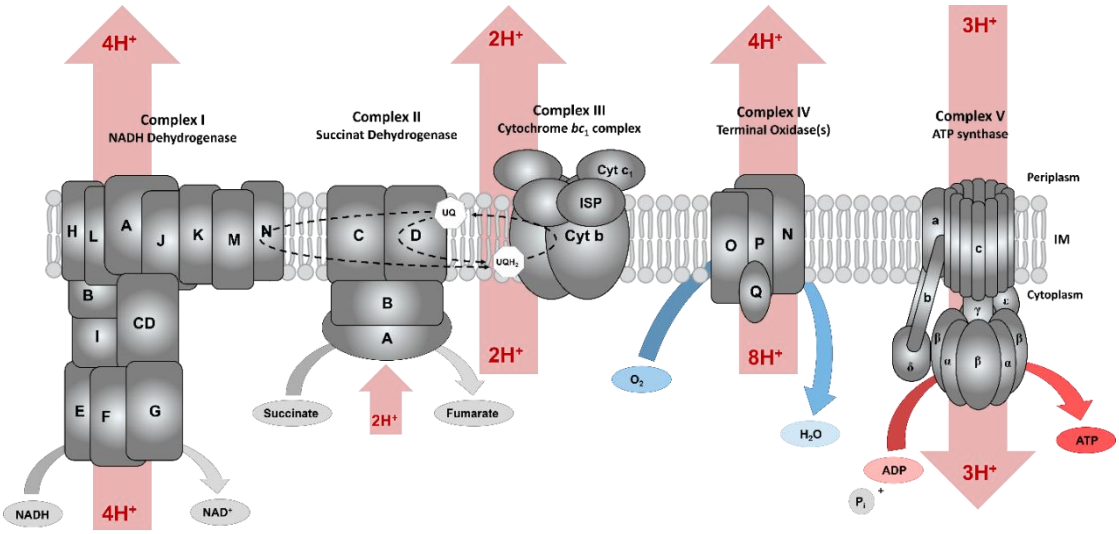

Figure 5 Schematic depiction of the respiratory chain of aerobic respiration.
The NADH dehydrogenase contributes to the generation of the proton motive force by transferring electrons from NADH to the ubiquinone (UQ) pool. Complex II oxidizes succinate to fumarate thus delivering additional electrons to the ubiquinone pool that are used by complex III resulting in the translocation of four additional protons into the periplasm. The terminal oxidase/s take the electrons from cytochrome *c* and transfer them to oxygen. Simultaneously four protons are translocated from the cytoplasm to the periplasm contributing to the proton gradient. The proton gradient is used by the F_0F_1 ATP synthase (complex V) to generate ATP.

Complex I - NADH dehydrogenase

In bacteria, three types of NADH dehydrogenases are currently known and *P. aeruginosa* possesses all of them. The most studied one is the proton translocating NADH dehydrogenase NDH-1. The NDH-1 of *P. aeruginosa* consists of 13 subunits encoded by the *nuoABDEFGHIJKLMN* operon (PA2637 – PA2649) and contains two [2Fe-2S] and six [4Fe-4S] clusters. This enzyme complex transduces electrons from NADH to the quinone pool while a conformational change leads to the translocation of four protons over the IM into the periplasm. Simultaneously, two protons are removed from the cytoplasm by the reduction of

the quinols (Brandt, 2006) (Hunte, *et al.*, 2010). In addition to NDH-1, a non-proton-translocating type II NADH dehydrogenase (NDH-2) is encoded by the *ndh* gene (PA4538) (Yagi, *et al.*, 2001). NDH-2 is composed of a single FAD-containing subunit and a deletion of both NDH-1 and NDH-2 leads to a loss of NADH enzymatic activity (Torres, *et al.*, 2019). Furthermore, the third NADH dehydrogenase is a Na^+-translocating NADH dehydrogenase (NQR) encoded by the *nqrABCDEF* operon (PA2999 - PA2994). While the physiologic role of NQR in *P. aeruginosa* is unclear, it was shown that the expression of the *nqr* genes were increased in cystic fibrosis patients (Kamath, *et al.*, 2016). Furthermore, NQR seems to be resistant to the quinolone 2-heptyl-4-hydroxyquinoline N-oxide secreted by *P. aeruginosa* during infection. This quinoline acts as a quorum sensing molecule and has bactericidal properties against other bacteria suggesting that NQR plays a role in the adaption against autotoxicity (Hazan, *et al.*, 2016) (Raba, *et al.*, 2018).

Complex II - Succinate dehydrogenase

The succinate dehydrogenase (SDH) is part of the TCA cycle and catalyzes the oxidation of succinate to fumarate. In parallel, electrons are transferred to complex I. In *P. aeruginosa*, the *sdhCDAB* (PA1581 - PA1584) operon encodes the respective subunits of the succinate dehydrogenase. Both, SdhC and SdhD are the membrane-anchored subunits of the complex containing a single heme B. Furthermore, the SdhA subunit is a flavoprotein containing FAD and SdhB is an iron-sulfur protein containing a [2Fe-2S], a [4Fe-4S] and a [3Fe-4S] cluster, respectively. FAD is used as a cofactor and is subsequently reduced to $FADH_2$ while the two released electrons are transferred to ubiquinol (Cecchini, *et al.*, 2002) (Hederstedt, 2002) (Oyedotun, *et al.*, 2004).

Complex III - Cytochrome bc_1 complex

The cytochrome bc_1 complex or ubiquinol: ferricytochrome-*c* oxidoreductase functions as an enzymatic relay between the quinone pool and cytochrome *c*. Thus, it contributes to the formation of the electrochemical gradient (Berry, *et al.*, 2000). Here, four protons are translocated across the IM for every two electrons that pass through complex III. It was reported that prokaryotic bc_1 complexes vary in their composition but generally consist of three subunits: two or more cytochrome *b*

subunits with two B-type hemes, a cytochrome c_1 subunit with a C-type heme and a Rieske Iron-Sulfur protein (ISP) (Berry, *et al.*, 2009). The last one is required in the periplasm and is therefore translocated in its folded state via the twin-arginine translocation (TAT) system (Sargent, 2007). In addition, the corresponding genes of complex III, PA4429 - PA4431, are organized in an operon together with the genes *sspBA* (PA4427, PA4428) encoding the stringent-starvation protein A and B respectively that are produced in response to amino acid starvation (Williams, *et al.*, 1994).

Complex IV - Terminal cytochrome oxidases

Five terminal oxidases are currently annotated in *P. aeruginosa,* each with a different affinity for oxygen as shown in Figure 6. Three of them, the cbb_3-1 oxidase (Cco1), the cbb_3-2 oxidase (Cco2) and the aa_3 oxidase (Cox) are cytochrome *c* oxidases and thus, receive electrons via the cytochrome bc_1 complex and *c*-type cytochromes. Contrary, the bo_3 oxidase (Cyo) and the cyanide-insensitive oxidase (Cio) are quinol oxidases and receive the electrons directly from ubiquinol (Arai, 2011). The two oxidases Cco1 and Cco2 are encoded by the tetracistronic operons *ccoN1O1Q1P1* (PA1554 - PA1552) and *ccoN2O2Q2P2* (PA1557 - PA1555) respectively. Both operons are consecutively clustered in *P. aeruginosa* and positively regulated by the RoxSR two-component system (Fernández-Piñar, *et al.*, 2008). Furthermore, the expression of Cco2 is also induced by Anr (anaerobic regulator of arginine deiminase and nitrate reductase) thus emphasizing the role of Cco2 in low-oxygen environments whereas Cco1 was shown to be constitutively expressed under aerobic conditions (Kawakami, *et al.*, 2010). Both Cco oxidases display a high affinity towards oxygen and their subunits share functionality. Moreover, CcoN is the catalytic subunit containing a high spin heme b_3 and Cu_B. CcoO and CcoP are transmembrane monoheme and di-heme cytochrome *c* subunits, respectively. While CcoQ is assumed to stabilize the core complex of the cbb_3-type oxidases (Zufferey, *et al.*, 1996) (Peters, *et al.*, 2008).

Terminal oxidase	Affinity for O_2	Inducing conditions
Cco1	High	Constitutive
Cco2	High	Low O_2, Stationary phase
Cox	Low	Nutrient starvation
Cyo	Low	Iron starvation
Cio	Low	Cyanide, Copper starvation, Inhibition of other oxidases

Figure 6 Overview of terminal oxidases in *P. aeruginosa* (modified from: Arai, 2011).
In *P. aeruginosa,* five terminal oxidases are currently annotated. Both Cco1 and Cco2 have a high affinity towards oxygen whereas Cox, Cyo and Cio display a low oxygen affinity. Conditions under which the corresponding terminal oxidases are upregulated are displayed in the right column.

Contrary to this, the three terminal oxidases Cox, Cyo and Cio have low oxygen affinities and their expression is upregulated under various nutrient limiting conditions (Kawakami, *et al.*, 2010) (Ochsner, *et al.*, 2002). In *P. aeruginosa*, the Cox oxidase is encoded by the *coxBA-PA0107-coIII* gene cluster (PA0105 - PA0108). There, the *coxA*, *coxB* and *coIII* genes encode the subunits I, II and III of the Cox oxidase, respectively. Subunit I contains a heme a_3-Cu_B binuclear catalytic center and subunit II a Cu_A binding site corresponding to the electron transfer site. PA0107 encodes a putative cytochrome *c* assembly protein presumably involved in the insertion of copper into subunit I. Furthermore, the expression of the *cox* genes is negatively regulated by RoxSR, while the stationary phase sigma factor RpoS (PA3622) has a positive effect (Schuster, *et al.*, 2004). In contrast, Cyo and Cio are positively regulated by the RoxSR system. Cio is additionally activated by RpoS (Kawakami, *et al.*, 2010). Moreover, the transcriptional regulator Fur (ferric uptake regulator) and Anr have negative effects on the expression of the Cyo oxidase and Cio (Vasil, *et al.*, 1999) (Cooper, *et al.*, 2003). In *P. aeruginosa,* Cyo is encoded by the *cyoABCDE* genes (PA1317 - PA1321) and the genes *cyoA*, *cyoB* and *cyoC* code for subunits II, I and III of the bo_3 oxidase. *CyoD* encodes the subunit IV that is assumed to assist in Cu_B-binding to subunit I and *cyoE* encodes a heme *o* synthetase, which is required for production of heme *o* using heme *B* (Saiki, *et al.*, 1992) (Saiki, *et al.*, 1996). Interestingly, Cio is the only copper-free terminal oxidase of *P. aeruginosa* and is encoded by the *cioAB* genes (PA3930 - PA3929) (Matsushita, *et al.*, 1983). Analyses showed that respiratory chain inhibitors and cyanide induce the expression of the *cioAB* genes. Interestingly, *P. aeruginosa*

produces hydrogen cyanide during stationary growth phase or at low oxygen concentrations and with up to 300 µM, the concentration of cyanide is high enough to inhibit the activity of the heme-copper oxidases (Cunningham, *et al.*, 1997). Furthermore, the expression of the *cioAB* genes is upregulated at stationary phase or at low oxygen concentrations. Notably, Cio has a higher resistance to cyanide than Cyo, leading to the assumption that Cio is required under cyanogenic conditions (Cooper, *et al.*, 2003) (Mogi, *et al.*, 2009).

Complex V - F_0F_1 ATP synthase

The ATP synthase consists of two subunits, the F_1 and the F_0 subunit. The F_1 subunit is the more hydrophilic part of the ATP synthase and consists of the five subunits α, β, γ, δ and ε. It is responsible for the hydrolyzation of ATP. In contrast, the F_0 region is more hydrophobic and is localized in the inner membrane (Kagawa, *et al.*, 1966). In *P. aeruginosa,* the nine subunits of the ATP synthase are encoded by the *atpCDGAHFEBI* operon (PA5553 – PA5561), in which the F_1 part is encoded by *atpCDGAH* and the F_0 region by *atpFEB*. In addition, the ATP synthase protein I, encoded by the *atpI* gene, is predicted to be important for the assembly and stability of ATP synthase complex (Liu, *et al.*, 2012).

1.1.5 Anaerobic lifestyle and denitrification of *P. aeruginosa*

P. aeruginosa is a denitrifying bacterium and is able to utilize various N-oxides as terminal electron acceptors in the absence of oxygen. Here, the reduction of nitrate to N_2 is catalyzed by four enzymes: nitrate reductase (Nar), nitrite reductase (Nir), nitric oxide reductase (cNor) and nitrous oxide reductase (Nos) (Zumft, 1997). Furthermore, electrons are used from quinones or the cytochrome bc_1 complex which are key components of the respiratory chain. At the same time, protons are transferred into the periplasm, as shown in Figure 7 (Chen, *et al.*, 2013).

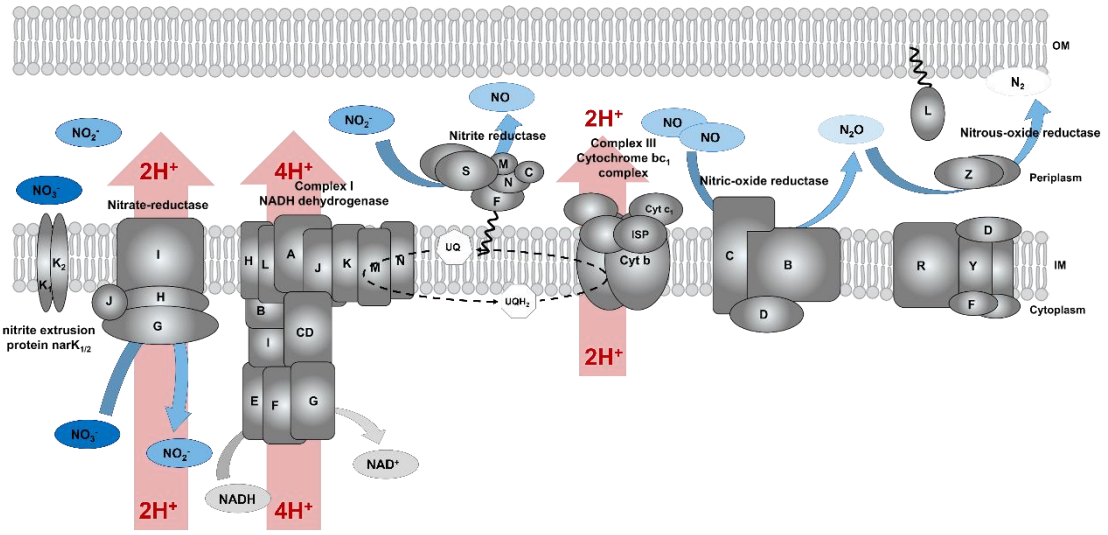

Figure 7 Arrangement of the respiratory chain of denitrification (altered and adapted from Chen, *et al.*, 2013). The NADH dehydrogenase transfers electrons from the NADH to the ubiquinone (UQ) pool. Nitrate is transported from the environment through the periplasm into the cytoplasm by the nitrite extrusion protein $NarK_{1,2}$, which also transports the nascent nitrite back into the periplasm. Following, nitrite is reduced by the cd_1 nitrite reductase by oxidization of the cytochrome c_{551} (NirM) and simultaneously, electrons are transferred via c-type cytochromes from the quinone pool to the nitrite reductase, which is mediated by the cytochrome bc_1 complex. The nitrogen of two molecules of nitric-oxide are reduced resulting in one molecule nitrous-oxide which, in the last step of the denitrification, is reduced to nitrogen. Again, the cytochrome bc_1 complex mediates the transfer of electrons via cytochrome *c* to both the nitric-oxide and the nitrous oxide reductase.

Nitrate reductases

Nitrate reductases catalyze the reduction of nitrate to nitrite and are part of the molybdopterin oxidoreductase-family. Two dissimilatory nitrate reductases are currently known in *P. aeruginosa* PAO1. The first one, the nitrate reductase NAP is localized in the periplasm and is encoded by the *napEFDABC* (PA1177 - PA1172) operon. Nap is essential for aerobic denitrification and thus being important for survival in g oxygen-depleting environments. Interestingly, nitrate reduction via Nap does not lead to ATP production, while nitrate reduction via the membrane bound dissimilatory nitrate reductase Nar does (Van Alst, *et al.*, 2010). The membrane localized nitrate reductase Nar is essential for denitrification under anaerobic conditions and is encoded by the genes *narGHIJ* (PA3877 - PA3872). Here, the cytochrome *b* subunit (NarI) oxidizes ubiquinol resulting in the translocation of two protons to the periplasm. Simultaneously, electron flow across the membrane via the hemB group of NarI to the Fe-S centers of NarH on to the active site of the molybdenum cofactor-containing protein NarG (Carlson, *et al.*, 1982). NarG is required for the reduction of nitrate to nitrite by consuming two protons from the cytoplasm. Furthermore, the *narJ* gene encodes a protein involved in the assembly of the nitrate reductase complex (Blasco, *et al.*, 1992).

The expression of the *narGHIJ* genes are dependent on the oxygen-sensing regulator Anr, the nitric oxide sensing regulator Dnr and the nitrate responsive two-component regulatory system NarXL (Schreiber, *et al.*, 2007).

Nitrite reductase

The reduction of nitrite to nitric oxide is catalyzed by the periplasmic nitrite reductase. In *P. aeruginosa* this enzyme is a cytochrome cd_1, carrying two monoheme *c* and one heme d_1 and is encoded by the *nirSMCFDLGHJEN* operon. The first gene, *nirS* encodes the structural gene for the nitrite reductase which is translocated into the periplasm via the Sec pathway. In the periplasm, the protein forms a complex with NirN and NirF (Thöny-Meyer, *et al.*, 1997) (Nicke, *et al.*, 2013). Additionally, the two monoheme c-type cytochromes are encoded by *nirM* and *nirC,* where NirM is the physiological electron donor for the nitrite reduction (Kawasaki, *et al.*, 1997). Furthermore, *in vitro* experiments showed that cytochrome c_{551} and azurin, a blue copper protein, can compensate each other, but cytochrome c_{551} is the more efficient electron donor (Silvestrini, *et al.*, 1981) (Silvestrini, *et al.*, 1982). Azurin forms a complex with the cytochrome c_{551} NirM and mediates the electron transfer from the cytochrome bc_1 complex to various terminal reductases (Santini, *et al.*, 2014). Additionally, NirF is important for insertion of the heme d_1 into the nitrite reductase and the synthesis of heme d_1 is catalyzed by the proteins encoded by *nirDLGHJEN*. Here, the uroporphyrin-III *c*-methyltransferase NirE, the siroheme decarboxylase NirDL/NirGH, the presumed S-adenosylmethionine enzyme NirJ and the electron-bifurcating dehydrogenase NirN are involved in the heme d_1 biosynthesis (Kawasaki, *et al.*, 1997)(Bali, *et al.*, 2011) (Adamczack, *et al.*, 2014). Furthermore, the substrate for the nitrite reductase is facilitated via the nitrate/nitrite antiporter $NarK_1K_2$. Moreover, due to the periplasmic localization of the nitrite reductase, the reduction of nitrite does not contribute to the generation of the proton gradient.

Nitric oxide reductase

The membrane-bound nitric oxide reductase in *P. aeruginosa* PAO1 is a heterodimeric enzyme containing heme *c* and heme *b*. The two subunits, the membrane-anchored NorC and the transmembrane protein NorB are encoded by the *norCBD* operon. The third protein of the nitric oxide reductase NorD is important for the maturation of the NorCB protein complex (Bartnikas, *et al.*, 1997). There, the NorC subunit contains a low-spin heme *c* that is responsible for the electron transport from a cytochrome *c* to the catalytic subunit NorB. Here, the binuclear active site is composed of a high-spin heme b_3 and non-heme Fe_B. Both coordinate the two NO molecules which are subsequently reduced to N_2O (Hino, *et al.*, 2010). Like the reduction of nitrite, the reduction of nitric oxide to nitrous oxide via cNor does not contribute to the generation of the proton motive force, rather utilize protons from the periplasmic side of the inner membrane (Reimann, *et al.*, 2007). Interestingly, the *norCBD* operon is downstream located to the *nirQOP* operon. There, the ATP-binding protein NirQ encoded by the corresponding gene also appears to be important for the cNor maturation while the role of the NirO and NirP proteins is still unclear (Hayashi, *et al.*, 1998).

Nitrous oxide reductase

Lastly, the reduction of nitrous oxide to nitrogen is catalyzed by the periplasmic and homodimeric nitrous oxide reductase encoded by *nosZ*. The enzyme contains two copper centers: a binuclear electron transfer side Cu_A and a tetranuclear catalytic site Cu_Z (Charnock, *et al.*, 2000) (Brown, *et al.*, 2000). Here, electrons, originating from cytochrome *c*, are relayed from Cu_A to Cu_Z, where nitrous oxide binds and is reduced to nitrogen. The NosZ encoding gene is localized in the *nosRZDFYL* operon of which *nosDFY* encode proteins important for processing and insertion of copper into NosZ (Zumft, *et al.*, 1990). Furthermore, *NosL* encodes the periplasmic lipoprotein NosL that is bound to the outer membrane and involved in the NosZ maturation (McGuirl, *et al.*, 2001). In addition, the transmembrane iron-sulfur flavoprotein NosR is proposed to be an N_2O-sensing regulator of the *nosZDFYL* genes and is essential for the functionality of NosZ (Vollack, *et al.*, 2001) (Wunsch, *et al.*, 2005). Interestingly, *P. aeruginosa* is not able to grow on exogenous nitrous oxide as an alternative electron acceptor, though it can use

endogenous nitrous oxide for growth via denitrification and energy generation (Carlson, *et al.*, 1983).

1.1.6 Regulation of the oxygen-dependent energy metabolism

In *P. aeruginosa* the main regulator of denitrification is the anaerobic regulator of arginine deiminase and nitrate reduction (Anr), analogous to the regulator of fumarate and nitrite reduction (Fnr) in *Escherichia coli*. Fnr directly senses oxygen via a $[4Fe\text{-}4S]^{2+}$ cluster that is coordinated by four cysteine residues. These are also conserved in Anr (Sawers, 1991). Thus in the presence of oxygen, the $[4Fe\text{-}4S]^{2+}$ cluster is partly oxidized or even destroyed. Subsequently, under anaerobic conditions, activated Anr leads to the activation of the expression of *dnr* and the nitrate reduction genes (Trunk, *et al.*, 2010). Dnr is the dissimilatory nitrate respiration regulator that is also related to Fnr but lacks the cysteine residues and is assumed to sense N-oxides via a heme cofactor (Arai, *et al.*, 1995) (Giardina, *et al.*, 2008). Extracellular nitrate is sensed by the two-component transcriptional regulator NarXL, consisting of the nitrate or nitrite sensor kinase NarX and the response regulator NarL (Krieger, *et al.*, 2002). In the presence of nitrate, the two-component system NarXL induces the expression of $narK_1$, *nirQ*, *dnr* and *hemA* while simultaneously repressing the genes necessary for arginine fermentation. Altogether, Dnr and NarXL form a complex regulatory network to facilitate the expression of proteins for anaerobic denitrification. Both, Anr and NarXL are important for the expression of the nitrate reductase and Dnr regulates the expression of *nir*, *cNor* and *nos* , as depicted in Figure 8 (Arai, *et al.*, 2003) (Schreiber, *et al.*, 2007)(Trunk, *et al.*, 2010).

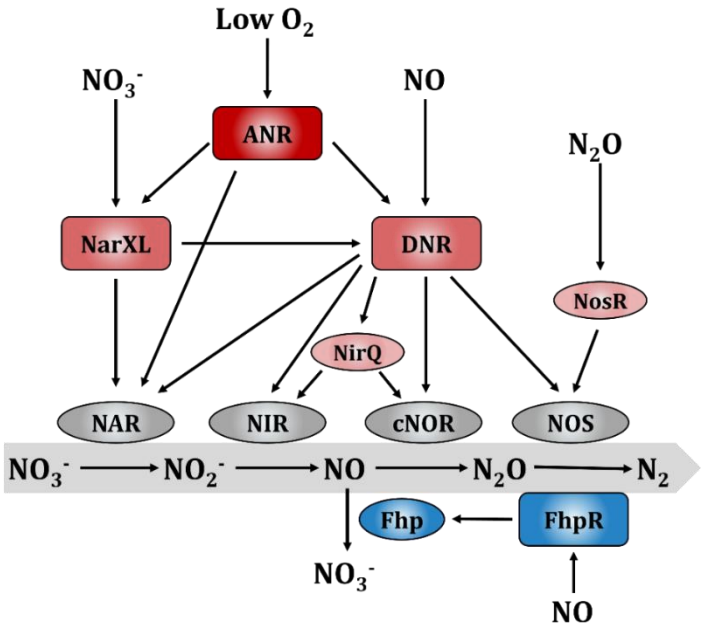

Figure 8 Regulatory network of denitrification in *P. aeruginosa*.
The subsequent reduction of nitrate to nitrogen is displayed in the grey arrow with the corresponding catalyzing enzymes above each arrow. The transcriptional regulators are presented in blunt boxes with Anr on top as the oxygen-sensing anaerobic regulator controlling the expression of the regulators NarXL and Dnr as well as the expression of the nitrate reductase (Nar). Upon activation, Dnr induces the expression of Nir, cNor and Nos while Dnr expression itself is also regulated by NarXL. While the regulatory function of NirQ and NosR remains still unclear, both are part of the regulatory network due to their importance during protein complex maturation of the corresponding enzymes. The flavohemoglobin regulator FhpR also senses nitric oxide and regulates the expression of Fhp that is required for the detoxification of NO under aerobic conditions.

1.1.7 Arginine and pyruvate fermentation

P. aeruginosa prefers denitrification for energy generation under anaerobic conditions; however, if no terminal electron acceptors are present *P. aeruginosa* is able to survive by arginine and pyruvate fermentation (Gamper, *et al.*, 1991) (Eschbach, *et al.*, 2004).

Arginine fermentation

Arginine fermentation is performed by the arginine deiminase (ADI) pathway. Here, L-arginine is first hydrolyzed into citrulline which is phosphorylated, resulting in L-ornithine and carbamoyl phosphate. Subsequently, the later one is used to generate ATP from ADP, as shown in Figure 9. The three enzymes involved in the ADI pathway, the arginine deiminase, the catabolic ornithine carbamoyltransferase (cOTC) and the carbamate kinase (CK), are encoded by *arcABC.* Localized in the same operon, the *arcD* gene encodes an arginine/ornithine antiporter (Mercenier, *et al.*, 1980) (Lüthi, *et al.*, 1990). The

expression of this operon is induced under anaerobic conditions and further enhanced by arginine (Mercenier, *et al.*, 1980). Similar to the denitrification, Anr is the major regulator for arginine fermentation by inducing the expression of the *arcDABC* operon under anaerobic conditions. Furthermore, the regulatory protein ArgR further enhances the expression of the operon dependent on the arginine level by binding to a conserved motif in the *arcD* promotor (Williams, *et al.*, 2007). Furthermore, the two component system NarXL is also involved. NarL binds upstream of the *arcD* promotor resulting in repression of the *arcDABC* operon in the presence of nitrate (Benkert, *et al.*, 2008).

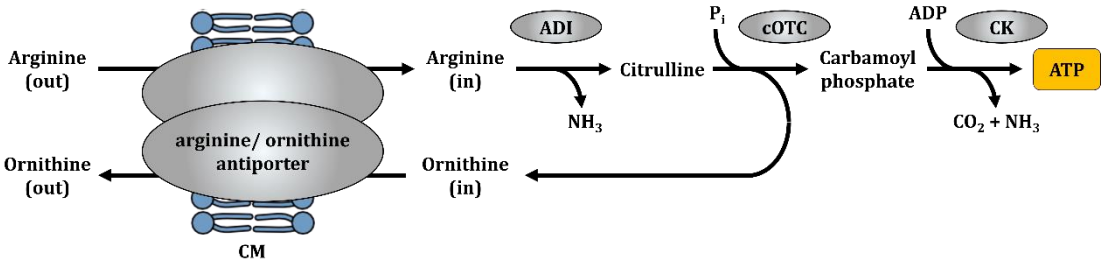

Figure 9 The arginine deiminase pathway of *P. aeruginosa* (altered from: Gamper, *et al.*, 1991).
Catalyzing enzymes are depicted as grey ovals. CM = cytoplasmic membrane; ADI = arginine deiminase; cOTC = catabolic ornithine carbamoyltransferase; CK = carbamate kinase

Pyruvate fermentation

Similar to arginine, *P. aeruginosa* can also utilize pyruvate to establish a long-term anaerobic survival (Petrova, *et al.*, 2012). Altogether, several genes are important for the fermentation of pyruvate such as *ldhA*, *adhA*, *Pta* and *AckA*. Again, the anaerobic regulator Anr is involved in the expression of *Pta* and *AckA* as it was shown that these genes are induced under anaerobic conditions in an Anr-dependent manner. Furthermore, a still unknown universal stress protein (Usp)-type protein seems to be involved in the pyruvate fermentation (Eschbach, *et al.*, 2004) (Schreiber, *et al.*, 2006). Moreover, the classical fermentation products such as lactate, acetate and succinate that occur during pyruvate fermentation lead to a proposed model for pyruvate fermentation as depicted in Figure 10. Under fermentative conditions pyruvate is converted into acetyl-CoA followed by the conversion of acetyl-CoA to CoA and acetyl-phosphate, where the later one is used

for the generation of ATP via an acetate kinase (Eschbach, *et al.*, 2004) (Yasid, *et al.*, 2016).

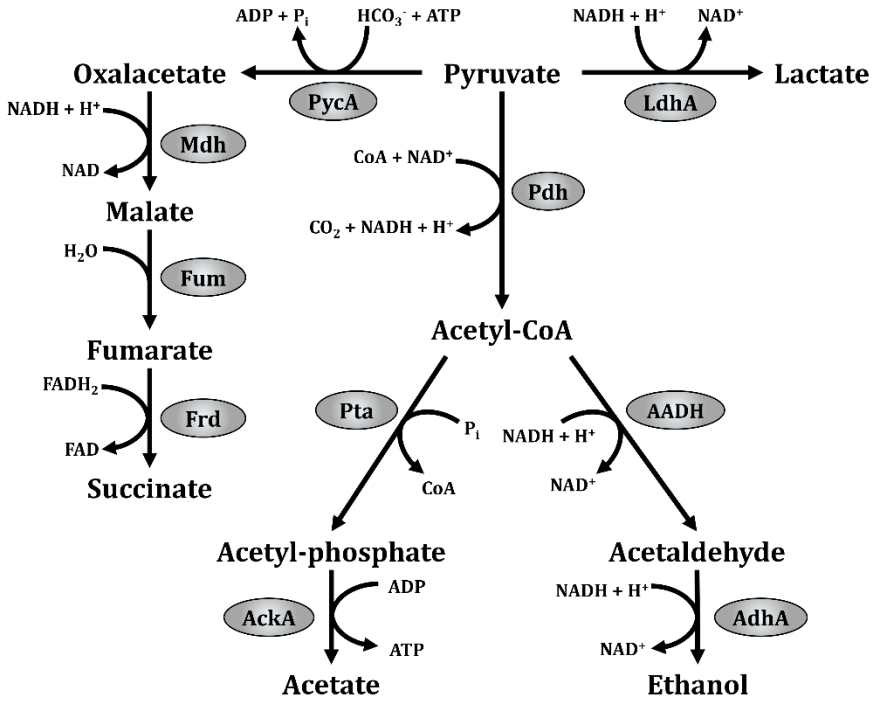

Figure 10 Scheme of the pyruvate fermentation in *P. aeruginosa* (Adapted from: Eschbach, *et al.*, 2004).
Catalyzing enzymes are depicted as grey ovals. PycA = pyruvate carboxylase; LdhA = fermentative lactate dehydrogenase; Pdh = pyruvate dehydrogenase; Pta = phosphotransacetylase; AckA = acetate kinase; AADH = acetaldehyde dehydrogenase; AdhA = alcohol dehydrogenase. Enzymes involved of the reductive citric acid cycle: Mdh = malate dehydrogenase; Fum = fumarase; Frd = fumarate reductase

1.2 Protein degradation in bacteria

Proteolysis describes the degradation of proteins into polypeptides or amino acids. In bacteria, targeted protein degradation plays an important role in the processing, quality control and turnover of proteins. Thus, offering a fast and efficient mechanism to adapt the proteome to environmental changes. Here, the enzymes catalyzing proteolysis are classified into seven groups based on the catalytic residue (Oda, 2012). In bacteria, AAA$^+$ proteases (**A**TPases **a**ssociated with various cellular **a**ctivities) are responsible for quality control and processing of proteins (Sauer, *et al.*, 2011). In addition, well researched members of AAA$^+$ proteases are the ClpXP, ClpAP, HslUV and Lon proteases that are important for intracellular proteolysis in the cytoplasm (Gur, *et al.*, 2011). Overall, ATP-dependent proteases consist of a compartmentalized proteolytic chamber and a substrate-binding domain that possesses ATP-binding and hydrolysis properties. Both compartments of AAA$^+$ proteases display an oligomeric structure;

however, each ATP-dependent protease has its own specific substrate. The substrates are determined by a short sequence described as degradation tag or degron (Baker, *et al.*, 2006). Degrons are present at the N- or C-terminus of the corresponding substrate. For example in *E. coli*, a short amino acid sequence (AANDENYALAA), described as SsrA-tag, is appended to the C-terminus of proteins. In case of a shortage of charged tRNAs or a lack of a STOP codon, the A-site of the ribosome becomes unoccupied whereupon a tmRNA enters the empty A-site. This tmRNA carries the corresponding SsrA-tag coding sequence resulting in a polypeptide carrying the SsrA degron (Gottesmann, *et al.*, 1998) (Moore, *et al.*, 2005). Furthermore, the mechanism of proteolytic degradation of ATP-dependent proteases follows a three-step mechanism as displayed in Figure 11. First, the substrate binds at the corresponding binding domain of the protease. Following, repetitive cycles of ATP hydrolysis lead to unfolding and translocation of the substrate. After unfolding the protein, the peptide bonds are cleaved inside the proteolytic chamber in an ATP-independent manner and the peptides or single amino acids are released.

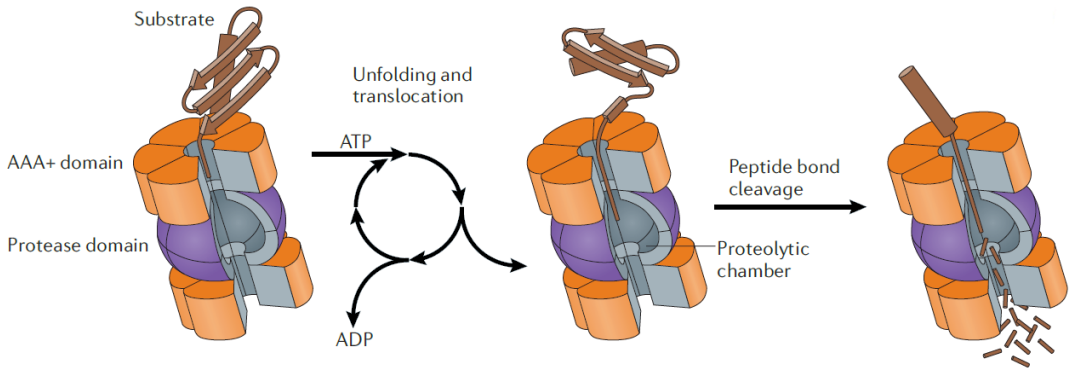

Figure 11 Mechanism of ATP-dependent proteases (adapted and altered from Gur, *et al.*, 2011).
ATP-dependent proteases catalyze a three-step proteolysis. After substrate binding, cycling ATP-hydrolysis drives repeatedly unfolding and translocation of the substrate. Inside the proteolytic chamber, the peptide bonds are cleaved ATP-independently and the peptides or single amino acids are releases from the ATP-dependent protease.

Among all AAA+ proteases, FtsH (also known as HflB) is the only membrane-bound protease and degrades both membrane-embedded and soluble substrates (Akiyama, *et al.*, 1996). This zinc-containing metalloprotease consists of two N-terminal transmembrane helices followed by an AAA+ ATPase domain and the zinc-containing active site (Tomoyasu, *et al.*, 1993). As observed previously in *E. coli*, known membrane-integrated substrates of the FtsH protease are the SecY

subunit of the bacterial Sec-pathway, also known as the SecYEG translocon (Kihara, *et al.*, 1995), and the subunit *a* of the F_0 component of the ATP synthase (Akiyama, *et al.*, 1996). However, the complete mechanism of the proteolysis via the FtsH protease remains unclear, but it is assumed that the enzyme dislocates the membrane-embedded regions of a substrate to the cytoplasm where the active site of the enzyme resides (Kihara, *et al.*, 1999). Furthermore, there seems to be no common degron for FtsH substrates, in fact, the recognition by FtsH depends on exposed N or C termini of about 20 residues (Chiba, *et al.*, 2002). Besides its function as a protease, FtsH, in combination with HflC, HflK and YidC, may act as a chaperone to sustain the quality of inner membrane proteins (van Bloois, *et al.*, 2008). Both HflC and HflK are single-pass inner membrane proteins that form a complex with FtsH and thus regulate the FtsH activity for degrading inner membrane substrates like SecY (Kihara, *et al.*, 1996) (Kihara, *et al.*, 1998).

Like FtsH, HtpX is also a membrane-integrated metalloprotease containing four transmembrane helices. Again, the zinc-containing protease domain is localized in the cytoplasm but unlike FtsH, HtpX lacks the AAA^+ ATPase domain. This heat shock-inducible protease is also involved in the quality control of folding and assembly of membrane proteins and knock out experiments suggest that HtpX and FtsH share one or more functions (Ogura, *et al.*, 1999) (Shimohata, *et al.*, 2002) (Sakoh, *et al.*, 2005).

1.3 Small proteins

Proteins with a length up to 100 amino acids without post-translational processing are called small proteins (SP100) and they are encoded by small open reading frames (sORF). Due to their size of less or equal than 303 nucleotides, sORFs were not assigned any coding potential and thus were overlooked in previous genome annotations (Frith, *et al.*, 2006). In addition to the bioinformatic challenge of the identification of sORFs, another problem lies in the detection of the encoded proteins. Due to their small molecular weight, small proteins tend to be washed out during the running or staining process if analyzed via conventional gel systems. However, in recent years the progress in bioinformatics and the development of analytical methods lead to the identification of a large number of small proteins displaying a wide range of different functions (Storz, *et al.*, 2014). Hundreds of small proteins have been identified in various organisms, including

Escherichia coli, *Arabidopsis thaliana* and *Saccharomyces cerevisiae* (Kastenmayer, *et al.*, 2006) (Yang, *et al.*, 2011). This led to the assumption that sORFs comprise around 5 - 10% of the genome of any organism (Saghatelian, *et al.*, 2015).
An example of an SP100 present in various bacteria is the transmembrane protein KdpF that is associated with virulence. KdpF was first discovered in *E. coli* and is involved in the stabilization of an ATPase transporter. However, in *S. aureus* it regulates the transcription of a number of virulence factors depending on the external K^+ ion concentration (Gassel, *et al.*, 1999) (Xue, *et al.*, 2011). Another known small protein is SpoVM, which is also membrane-associated and involved in spore formation in *Bacillus subtilis* (Sandman, *et al.*, 1987). Here, at least four functions were allocated to SpoVM; among them are the marking the membrane of the pre-pore for further assembly and recruiting the protein SpoIVA to the forespore for further spore formation (Roels, *et al.*, 1992) (Ramamurthi, *et al.*, 2009). Currently, the smallest protein described so far is the TAL protein in *Drosophila melanogaster* with a length of 11 amino acids that controls gene expression, tissue formation and necessary for embryonic development (Galindo, *et al.*, 2007).

Despite the large number of newly discovered SP100, in many cases they were discovered and characterized by chance. Due to their diverse functions, the investigation of small proteins offers new opportunities for the better understanding of complex mechanisms and processes within an organism, which of course is and will be of enormous importance for the development of new treatment methods for bacterial infections.

1.3.1 Small proteins in *P. aeruginosa*

The genome of *P. aeruginosa* PAO1 contains 5697 genes of which 5572 encode for proteins. 344 of these genes encode proteins smaller than 101 amino acids. Interestingly, over 70% are still uncharacterized and are annotated as hypothetical proteins with little to no knowledge about their functionality. Twenty of the annotated SP100 are ribosomal proteins and either part of the small (30 S) or the large (50 S) subunit of the 70 S ribosome (Garret, *et al.*, 2010). Among the annotated SP100, the TatA protein encoded by the gene PA5068 is one of the best characterized. TatA together with the proteins TatB and TatC forms the twin

arginine translocation (Tat) export system. While TatA and TatB contain one transmembrane helix, TatC contains six transmembrane helices and is involved in the twin-arginine signal peptide recognition and protein translocation. Upon recognition and binding of the signal peptide, the polymerization of TatA is initiated resulting in the formation of the protein-conducting channel. This formation is driven by the proton motive force and subsequently the substrate is transported via the TatA pore (Gohlke, *et al.*, 2005). Contrary to the Sec pathway, the Tat pathway transports proteins that require proper folding in the cytoplasm prior to transport across the IM (Palmer, *et al.*, 2012). Prominent Tat-dependent proteins in *Pseudomonas* are NapA and NapF, two proteins of the periplasmic nitrate reductase as well as the nitrous oxide reductase NosZ, which catalyzes the last reduction step from nitrous oxide to nitrogen (Berks, *et al.*, 2000) (Heikkilä, *et al.*, 2001). Additionally, the Tat pathway is important for the transport of several virulence factors and disruption of this pathway results in a reduced virulence (Ochsner, *et al.*, 2002).

Another annotated SP100 is the lipoprotein OprI that is localized in the OM of *P. aeruginosa*. OprI is one of the major OM lipoproteins and exists in two forms: a peptidoglycan-linked form and a free form carrying a C-terminal lysine residue (Inouye, 1974) (Mizuno, *et al.*, 1979). OprI forms a ternary complex with OprF and OprL that contributes to the shape of the cell and outer membrane stability (Navare, *et al.*, 2015). A similarity was observed in *E. coli* where sequence homologues of OprI, OprF and OprL, namely LPP, OmpA and Pal form a multi-protein complex and as such playing a role in cell membrane integrity (Cascales, *et al.*, 2002). Furthermore, LPP-lacking mutants of *E. coli* leak enzymes from the periplasm into the media, form large blebs on their surface and also show difficulties in septum formation during cell division emphasizing the importance of the small lipoprotein OprI (Fung, *et al.*, 1978).

1.4 Aim of this work

The first part of this thesis aims at the investigation of the inner membrane proteome of *Pseudomonas aeruginosa* under aerobic and anaerobic conditions. As described previously, NDH-1, cytochrome bc_1 and the ATP synthase are necessary for respiration under both, aerobic and anaerobic conditions and thus might build

the respiratory core complex. Analyses of the changes among protein composition in response to oxygen availability contribute to the better understanding of important processes like aerobic respiration and denitrification. Furthermore, proteases are known to be involved in a variety of processes and their role in aerobic and anaerobic respiration will be assessed.

In the second part, new *in-silico* approaches were combined to predict sORFs and subsequently identify non-annotated and annotated small proteins that are associated to the inner membrane of *P. aeruginosa.* Here, non-annotated small ORFs of identified non-annotated proteins will be further analyzed by transcriptional analyses with the aim to characterize the corresponding small proteins. Additionally, already annotated small proteins will be analyzed using cluster analyses to investigate a possible involvement in respiration under aerobic and anaerobic conditions.

2 Materials and Methods

2.1 Software

Table 2 List of software used in this work.

description	manufacturer
Software and Databases	
Pseudomonas Genome DB	(Winsor, *et al.*, 2016)
Python	Version 2.7.; Python software foundation
sORF finder	(Hanada, *et al.*, 2010)
AIDA Image Analyzer v. 4.15	Elysia-raytest GmbH, Straubenhardt, Germany
MultAlin	(Corpet, 1988)
ESPrint 3.0	(Robert, *et al.*, 2014)
Quantity One® software (GS-800 Calibrated Imaging Densitometer)	Bio-Rad, Düsseldorf, Germany
BioCapt 1 (Gel documentation software)	Herolab GmbH, Wiesloch, Germany
MaxQuant 1.5.2.8	(Cox, *et al.*, 2008)
Perseus 1.5.2.8	(Tyanova, *et al.*, 2016)
GraphPad Prism	GraphPad Software, San Diego, California
Geneious	Biomatters Ltd., Auckland, New Zealand
Pepper	Dr. Stephan Fuchs, Wernigerode, Germany

2.2 Chemicals and Enzymes

Table 3 List of used chemicals and reagents

description	manufacturer
3-[(3-cholamidopropyl) dimethylammonio]-1-propanesulfonate (CHAPS)	Merck KGaA
acetic acid	Carl Roth
acetonitrile (ACN)	Rotisolv
acrylamide/bisacrylamide 30% (37.5 : 1)	Applichem
Agar-Agar bacterial	Carl Roth
Agar-Agar KOBE I	Serva
Agarose Broad Range (DNase- und RNase-free)	Carl Roth
ammonium bicarbonate	Sigma Aldrich

ammonium persulfate (APS)	GE Healthcare
calcium chloride x 6 H_2O	Carl Roth
chymotrypsin	Sigma Aldrich
Coomassie Brilliant Blue G-250	Serva
ethylenediaminetetraacetic acid (EDTA)	Carl Roth
formic acid 50% in water (FA)	Fluka
glycerol	Carl Roth
iodoacetamide (IAA)	GE Healthcare
lithium chloride	Carl Roth
magnesium chloride x 6 H_2O	Merck KGaA
maleic acid	Carl Roth
methanol	Carl Roth
potassium chloride	Carl Roth
proteinase K	Sigma Aldrich
sodium carbonate	Carl Roth
sodium chloride	Carl Roth
sodium dodecyl sulfate	Carl Roth
tris(2-carboxyethyl)phosphine (TCEP)	Carl Roth
tetramethyl ethylenediamine (TEMED)	GE Healthcare
triethylammonium bicarbonate (TEAB)	Fluka
tris(hydroxymethyl)aminomethane (TRIS)	Carl Roth
trypsin	Promega
urea	Merck KGaA
β-mercaptoethanol	GE Healthcare

2.3 Media

LB medium (Lennox; Carl Roth, Karlsruhe, Germany) was prepared according to the manufacturer's guidance. 20 g were solved in 1 L ddH_2O followed by heat sterilization. Prepared LB medium was stored at RT until usage.

2.4 Bacteria strain and primers

Table 4 Table of bacteria strains and primer used in this work.

The T7 RNA polymerase recognition side is displayed in red.

	description and characteristics	source/ reference
P. aeruginosa		
PAO1 wt	parental strain	DSMZ, Braunschweig, Germany
primer (5' – 3')		
PAO1_RNA_14524_F	ATGCTTTGGGTCAAGCGTACGTTAATGGCGGT	Life Technologies, Darmstadt, Germany
PAO1_RNA_14524_R	CTAATACGACTCACTATAGGGAGATCACCGCAGGGCGGTAGACT	Life Technologies, Darmstadt, Germany

PAO1_RNA_PA3160_F	ATGACTGACGAAATACAAAAGCACGGCGGT	Life Technologies, Darmstadt, Germany
PAO1_RNA_PA3160_R	CTAATACGACTCACTATAGGGAGACTAACGAGCATACTTCTTCA	Life Technologies, Darmstadt, Germany
PAO1_RNA_PA3161_F	ATGACCAAGTCGGAGTTGATCGAACGGATCGTT	Life Technologies, Darmstadt, Germany
PAO1_RNA_PA3161_R	CTAATACGACTCACTATAGGGAGATCACTCCGGCTCGTTGACCC	Life Technologies, Darmstadt, Germany
PAO1_RNA_26594_F	TTGGCTAAACTGCAGCTTTCTCC	Life Technologies, Darmstadt, Germany
PAO1_RNA_26594_R	CTAATACGACTCACTATAGGGAGATCAGCGCGCACGGTC	Life Technologies, Darmstadt, Germany
PAO1_RNA_igr2243_F	ATGTCCAGCAGCACCCTGGC	Life Technologies, Darmstadt, Germany
PAO1_RNA_igr2243_R	CTAATACGACTCACTATAGGGAGATCAGTGGCAGGGGAAGCCGG	Life Technologies, Darmstadt, Germany

2.5 Database development for prediction of small proteins in *P. aeruginosa*

For the identification of yet unknown small proteins in *P. aeruginosa* strain PAO1, two different approaches were used to determine the amino acid sequence of these SP100. Both approaches used the genome of *P. aeruginosa* NC_002516 (downloaded from: https://www.ncbi.nlm.nih.gov/, 06.02.2018, 9.30 am). The six frame translation covered the whole genome and made use of all six possible reading frames (Rainey, *et al.*, 2006). In comparison, the second approach focused on the prediction of small open reading frames in intergenic regions. Both databases were designed in cooperation with Dr. Stephan Fuchs (Robert-Koch Institute, Wernigerode, Germany).

2.5.1 Six frame translation

For the six frame translation approach, the genome was first translated in all six possible reading frames. This *in-silico* translation was done using a pipeline in the Linux shell. First, each sequence was wrapped after every three nucleotides resulting in a list of base triplets. Each triplet was translated according to the translational table 11. Stop codons were marked as an asterisk. Following, line breaks were removed to restore the sequence character and all translated six reading frames were stored in a .fasta-file. Each amino acid sequence was 'cut' at every asterisk generating a list of predicted proteins. The six-frame translation database (TRDB) contained a total of 155,396 entries.

2.5.2 Prediction of small open reading frames using the sORF finder

The second approach for the prediction of small open reading frames has been performed using the online algorithm sORF finder. This algorithm predicts the coding potential nucleotide sequences based on the nucleotide composition (Hanada, *et al.*, 2010). The frequency of the nucleotides is determined by the ratio of the nucleotides of the coding and non-coding sequences (Hanada, *et al.*, 2007). Here, all known coding nucleotide sequences present in the genome of *P. aeruginosa* PAO1 were used as a positive training set (5572 entries). The negative training set contained all known noncoding nucleotide sequences (tRNA, rRNA and ncRNA; 106 entries). Training, modelling, and the final prediction of coding nucleotide sequences were carried out using a p value of 0.3. Following, the sequences of the predicted sORFs were translated into their respective amino acid sequence. The resulting sequences were combined with the *P. aeruginosa* PAO1 annotation resulting in the prediction database (PRDB) containing 6,213 entries.

2.6 Microbiological methods

2.6.1 Growth conditions and cultivation of *P. aeruginosa* PAO1

For aerobic growth, *P. aeruginosa* strains were grown in liquid LB medium Lennox (Carl Roth, Karlsruhe, Germany) at 37 °C and 140 rpm in an incubator shaker (Multitron, Infors, Switzerland). Therefore, 100 ml LB medium was either inoculated with 200 µl glycerol stock of the respective strain or with an inoculation loop with bacterial material grown on a LB agar plate and cultivated over night at 37 °C and 140 rpm in an incubation shaker. Following, 1.3 L LB medium were inoculated with *P. aeruginosa* overnight culture to an OD_{540} of 0.07 and the main culture was grown until an OD_{540} of 0.5. To investigate the growth behavior under denitrifying conditions, 1 L schott flasks were supplemented with 50 mM potassium nitrate and upon reaching an OD_{540} of 0.5, main cultures were filled to the brim into the prepared schott flasks, tightly screwed and cultivated at 37 °C and 180 rpm in the incubator.

2.6.2 Determination of cell growth

The cell density of liquid cultures was determined via optical density measurements at a wavelength of 540 nm. An OD_{540} of 1.0 corresponded to approximately 1×10^9 cells per ml culture. Four biological replicates were cultivated to an OD_{540} of 0.5 followed by shifting cells to anaerobic conditions in the presence of 50 mM KNO_3. Cell densities were determined every two hours up to 16 hours under anaerobic conditions. Subsequently, cells were shifted back to aerobic conditions and cell densities were further measured every hour for 16 hours.

Relative growth rates μ and the doubling time t_D were determined according to the following equations:

$$\mu = \left(\frac{ln(OD_1) - ln(OD_0)}{t_1 - t_0}\right) \quad (1)$$

$$t_D = \frac{ln\,(2)}{\mu} \quad (2)$$

During cultivation both under anaerobic and aerobic conditions, samples for nitrate concentration analyses were taken every two hours and stored at -20 °C until analysis.

2.6.3 Determination of nitrate concentration

The nitrate concentration was determined using the Nitrate Spectroquant® Analytical Test Kit (Merck KgaA). The kit is based on the reaction of 2,6-dimethylphenol to 4-nitro-2,6-dimethylphenol which determines the amount of nitrate-nitrogen (NO_3-N) photometrically at a wavelength of 375 nm. Based on the amount of NO_3-N, the NO_3 concentration is determined as $NO_3 = NO_3\text{-N} \times 4.43$. Subsequently, a calibration line was determined using ddH_2O as a blank and defined concentrations of nitrate following the scheme as described in Table 5. Upon next, each sample was diluted 1 : 100 with autoclaved ddH_2O and the measurements were carried out as described by the manufacturer. Nitrate concentrations of the samples were determined be rearranging the linear equation of the determined calibration line. Next, nitrate consumption rates μ_{NO_3} were determined according to the following equation:

$$\mu_{NO_3} = \left(\frac{[NO_3]_1 - [NO_3]_0}{t_1 - t_0}\right) \quad (3)$$

Table 5 Pipette scheme for calibration line for nitrate concentration determination.
NO_3-1 and NO_3-2 were referring to solutions from the Nitrate Spectroquant® Analytical Test Kit. This kit determined the level of nitrate-nitrogen (NO_3-N) correlating with the amount of nitrate as follows: $NO_3 = NO_3$-N x 4.43. For example, 2 ml of NO_3-1 solution were mixed with 250 µl KNO_3 and 250 µl NO_3-2, vigorously mixed and incubated for ten minutes at RT. Next, the absorbance was measured at a wavelength of 357 nm.

NO_3-N [mg/l]	NO_3^- [mg/l]	NO_3-1 [µl]	KNO_3 solution [µl]	NO_3-2 [µl]	357 nm
0.00	0.00	2000	250	250	0.024
1.00	4.43	2000	250	250	0.047
3.00	13.28	2000	250	250	0.083
5.00	22.14	2000	250	250	0.148
10.00	44.28	2000	250	250	0.246
15.00	66.42	2000	250	250	0.357
20.00	88.56	2000	250	250	0.462
25.00	110.70	2000	250	250	0.527

2.6.4 Genomic DNA isolation

Genomic DNA of *P. aeruginosa* PAO1 wt was used for the construction of DNA templates for RNA probes against small ORFs. The isolation of the genomic DNA was performed using the Bacterial Genomic DNA Isolation kit (Norgen Biotek Corp., #17900) according to the manufacturer protocol for Gram-negative bacteria with slight variation at the elution step. For elution, 100 µl pre-warmed ddH_2O were added to the column and were centrifuged for one minute at 6'000 x g. The flow through was added a second time onto the column and centrifuged again for two minutes at 14'000 x g. The DNA concentration was determined using a nanophotometer (IMPLEN Nanophotometer P330; Implen, Munich, Germany) and the DNA was stored at -20 °C until further use.

2.6.5 Template generation via PCR

DNA templates of the corresponding genes were amplified using the polymerase chain reaction (PCR) technique. DMSO was added to the whole PCR reaction mix to lower the annealing temperature and for easier denaturation of the GC-rich genomic DNA of *P. aeruginosa* (Hardjasa, *et al.*, 2010). DMSO binds to the minor and major cleft of the DNA double helix allowing an easier denaturation of the DNA double strand (Simon, *et al.*, 2009). A PCR master mix was prepared in 1.5 ml reaction tubes whereas one 20 µl PCR reaction was composed of 150 to 200 ng genomic DNA, 1x Phusion HF buffer (Thermo Scientific, Waltham, USA), 500 nm of each primer, 3% DMSO (Thermo Scientific), 500 µM dNTPs, 0.4 U Phusion polymerase (Thermo Scientific) and ddH_2O, as described in Table 6.

Table 6 Composition of one PCR reaction for the amplification of specific DNA fragments for template generation for RNA probes.

Component	Volume [µl]	Final concentration
Genomic DNA [150 - 200 ng]	X	
5x Phusion HF buffer	4	1x
Forward Primer (10 µM)	1	500 nM
Reverse Primer (10 µM)	1	500 nM
DMSO	0.6	3%
dNTPs (10 mM)	0.4	500 µM
Phusion Polymerase (2 U/µl)	0.2	
ddH_2O	Y	
Total volume	20	

Following, the PCR reactions were centrifuged down shortly and placed into the thermocycler (peqSTAR 96X Universal or peqSTAR 2X Universal; Peqlab). For the PCR reaction itself, annealing temperature and elongation time were selected based on the primer melting temperature and the expected product length as shown in Table 7.

Table 7 Conditions for amplification of selected genes and small open reading frames.

Gene	PCR product length	primer	Annealing Tm	Elongation time
PA3160	1071 nts	PAO1_RNA_PA3160_F PAO1_RNA_PA3160_R	57 °C	40 s
PA3161	309 nts	PAO1_RNA_PA3161_F PAO1_RNA_PA3161_R	59 °C	30 s
6frt_14524	321 nts	PAO1_RNA_14524_F PAO1_RNA_14524_R	59 °C	30 s
igr2243	207 nts	PAO1_RNA_igr2243_F PAO1_RNA_igr2243_R	65 °C	20 s
6frt_26594	309 nts	PAO1_RNA_26594_F PAO1_RNA_26594_R	59 °C	30 s

The following settings were used for the amplification of the DNA fragments:

	temperature	time
	98 °C	30 s
37x	98 °C	20 s
	annealing Tm	30 s
	72 °C	elongation time
	72 °C	10 min
	8 °C	∞

Afterwards, the PCR reactions were loaded onto a 1.5% agarose gel in 1x TBE buffer (10 x TBE: 900 mM Tris, 900 mM boric acid, 10 mM EDTA) containing 0.005% (v/v) Roti®-GelStain (Carl Roth, Karlsruhe, Germany). Additionally, 6 µl of GeneRuler™ 1 kb DNA ladder or GeneRuler™ 100 bp DNA ladder (Thermo Fisher Scientific) was loaded onto the gel to determine the fragment sizes. Samples and marker were separated for about one hour at 120 V and 350 mA. DNA fragments were visualized using a gel documentation system (E.A.S.Y. Doc plus; Herolab, Wiesloch, Germany) and band sizes were estimated using the visualized marker bands (App. 8.8). In case the fragment sizes matched the expected sizes, fragments were purified from the agarose gel using the NucleoSpin® Gel and PCR Clean-up kit (Macherey-Nagel, Düren, Germany) according to the manufacturer's instructions with a modified elution step. For the elution, 30 µl of pre-warmed ddH_2O was used. Finally, the concentration of the DNA fragments was determined using a nanophotometer and the DNA fragments were stored at -20 °C.

2.7 Preparation and analysis of inner membrane proteins

Proteins of the inner membrane of *P. aeruginosa* were prepared by performing two complementary approaches as described by Sievers and colleagues (Sievers, 2018). The first approach aims at the preparation of peripheral membrane proteins, in the following referred to as the solubilization approach. In the second approach, soluble parts of the membrane proteins are removed by membrane shaving and, finally, the remaining hydrophobic domains of the proteins were prepared from the membranes, in the following referred to as the shaving approach. All ultracentrifugation steps were performed at 4 °C and 100'000 x *g* for one hour unless otherwise specified. Furthermore, all working steps were carried out on ice to avoid possible protein degradation.

2.7.1 Cell harvest

P. aeruginosa cultures were cultivated as described previously (ch. 2.6.1) and cells were harvested at an OD_{540} of 0.5 and 2 h, 4 h, 8 h and 16 h after shift to anaerobic

growth conditions. Additionally, an aerobic shift assay was done after 16 h cultivation at anaerobic conditions. For this purpose, cultures were shifted back from anaerobic to aerobic growth (5 L Erlenmeyer flasks at 37 °C and 140 rpm in an incubation shaker). Cells were again harvested 2 h, 4 h, 8 h and 16 h after the aerobic shift. Each culture was split up into four 500 ml centrifuge tubes and centrifuged for ten minutes at 4 °C and 8'000 x *g*. The supernatant was discarded, and the pellets were washed in 20 ml ice-cold TBS buffer (50 mM Tris, 150 mM NaCl, pH 8.0). Subsequently, the cell pellets were resuspended in 15 ml lysis buffer (20 mM Tris, 10 mM $MgCl_2$, 1 mM $CaCl_2$, pH 7.5) and transferred into 50 ml reaction tubes containing 5 g glass beads (Ø 0,1 µm). Cell disruption was performed using the Fast-Prep®-24 (MP Biomedicals) in two cycles, each at 6 m/s for 40 seconds, with samples cooled on ice for five minutes between each cycle. The cell suspension was then centrifuged for ten minutes at 4 °C and 10'000 x *g* and the supernatant containing the crude protein extract was stored at -20 °C.

2.7.2 Preparation of the inner membrane fraction

For the separation of the inner and outer membrane, the crude cell lysate was treated with an isopycnic sucrose gradient. Therefore, 2 M, 1.5 M and 0.5 M sucrose solutions were prepared and filled into 14 x 89 mm ultracentrifugation tubes (Beckmann Coulter, Indianapolis, Indiana) in the following order: 3 ml 2 M, 3 ml 1.5 M and 3 ml 0.5 M. Subsequently, 7 ml of each protein extract was carefully transferred on top of the sucrose gradient and centrifuged in a SW41 swinging-bucket rotor (Beckman Coulter) at 100'000 x *g* and 4 °C for an hour. This resulted in one low-density and one high-density band, of which the first corresponded to the inner membrane and the second to the outer membrane (Morein, *et al.*, 1994). The bands were carefully removed using a Pasteur pipette and transferred into a new ultracentrifugation tube. Each membrane fraction was washed with ice-cold ddH_2O by centrifugation. The supernatant was removed, and tubes containing the pellets were dried upside down at RT for about five minutes. Following, the pellets were completely dried overnight at 4 °C and stored at -80 °C until further use.

2.7.3 Solubilization approach

2.7.3.1 Protein extraction

The inner membrane pellets were resuspended in 2 ml of ice-cold high-salt buffer (20 mM Tris, 1 M NaCl, pH 7.5), transferred into a 15 ml reaction tube and filled with high-salt buffer to 6 ml. The samples were incubated for one hour at 4 °C in an overhead shaker to break ionic bonds between integral and peripheral membrane proteins. Following, samples were ultracentrifuged, the supernatant was discarded and the pellets were resuspended in 6 ml of ice-cold carbonate buffer (100 mM Na_2CO_3, 100 mM NaCl, pH 11). Subsequently, the extracts were incubated for one hour at 4 ° C in an overhead shaker and homogenized every

15 minutes by pipetting up and down with a syringe. Due to the very alkaline pH of the buffer, the membranes were solubilized and the containing proteins released (Fujiki, *et al.*, 1982). After solubilization, the samples were again ultracentrifuged, the supernatant discarded and the purified membrane pellets resuspended in 500 µl solubilization buffer (50 mM Tris, 8 M urea, 1% CHAPS, pH 7.5). This step served to dissolve the hydrophobic components of the proteins. Consequently, TCEP was added in a final concentration of 5 mM to reduce the disulfide bridges in cysteine-containing proteins and the samples were incubated for one hour at 30 °C. The protein samples were then supplemented with IAA to a final concentration of 10 mM and incubated for 30 minutes at RT in the dark to alkylate thiol groups. Subsequently, the protein concentration was determined using Roti®-Nanoquant (Roth, Germany).

2.7.3.2 Determination of protein concentration according to Bradford

For the determination of the protein concentration, Roti®-Nanoquant (Carl Roth) was used. This assay is based on a modified Bradford assay utilizing the chemical properties of the dye Coomassie Brilliant Blue. In its unbound, red form it has an absorption maximum at 470 nm. Upon addition of proteins, complex formation between the dye and the proteins occurred and the dye was stabilized in its blue, bound form. This then led to a shift of the absorption maximum to 590 nm (Compton, *et al.*, 1985). The quotient of the measured absorbance of the bound and unbound dye corresponded to the amount of protein in the samples. First of all, a calibration line was prepared with a standard protein solution, as displayed in Table 8 and solubilization buffer according to the manufacturer's instructions. The protein concentrations were plotted against the determined quotients and a regression line was drawn through the points as shown in Figure 12. For determination of the protein concentration in the membrane protein samples, the photometer was first blanked with ddH_2O. Subsequently, 180 µl of ddH_20 were mixed with 20 µl buffer and 800 µl of Roti-Nanoquant in a cuvette to determine the value for a protein concentration of 0 µg/µl. For each protein sample, 10 µl of the respective protein extract were mixed with 180 µl ddH_2O and 10 µl buffer in a cuvette and measured after addition of 800 µl Roti-Nanoquant. The OD_{590}/OD_{450} ratios had to be above the value determined for a protein concentration of 0 µg/µl. Following, the amount of used protein sample was adjusted so that the measured OD_{590}/OD_{450} ratios were nearly the same and thus comparable.

Table 8 Composition of the protein standard solution used for the calibration curve.

protein	MW [kDa]	origin	manufacturer
aprotinin	6.5	bovine	Sigma Aldrich
bradykinin	1.0	synthetic	Sigma Aldrich
cytochrome C	12.0	bovine	Sigma Aldrich
GAPDH	36.0	chicken, muscle	Sigma Aldrich
insulin	5.8	bovine, pancreas	Sigma Aldrich
ribonuclease A	13.7	unknown	Pharmacia Biotech
A - carbonic anhydrase	30.0	bovine, erythrocytes	Sigma Aldrich

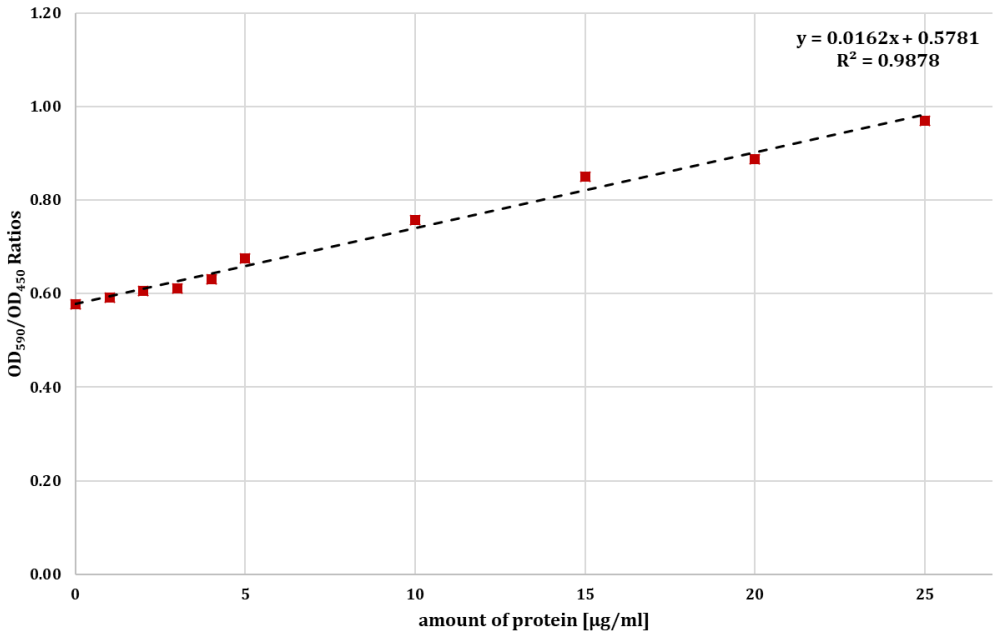

Figure 12 Calibration curve for the protein concentration determination of samples of the solubilization approach using solubilization buffer.
The protein concentrations on the x-axis were plotted against the determined ratios of OD590/OD450 on the y-axis. The regression line was represented by the formula y = 0.0162 x + 0.5781. With a coefficient of determination R^2 of 0.9878, the formula represented the course of the regression line well.

2.7.3.3 One-dimensional sodium dodecyl sulfate polyacrylamide gel electrophoresis

For One-dimensional sodium dodecyl sulfate polyacrylamide gel electrophoresis (1D SDS-PAGE), a 1 mm thick, 12% separating gel (3.35 ml ddH_2O, 4.0 ml 30% acrylamide/bisacrylamide (37.5 : 1), 2.6 ml Tris pH 8.8, 106 µl 10% SDS, 100 µl 10% APS, 10 µl TEMED) was prepared. The separating gel was covered with 100% ethanol and polymerized for one hour. The ethanol was then removed, the stacking gel (3.05 ml ddH_2O, 0.65 ml 30% acrylamide/bisacrylamide (37.5 : 1), 1.3 ml 0.4% SDS in 0.5 M Tris pH 6.8, 50 µl of APS, 10 µl of TEMED) was pipetted between the glass plates and a 1 mm comb was inserted. After polymerization, the gels were

placed into the gel holder, the minitank was filled with 1x electrophoresis buffer (10x buffer: 250 mM Tris, 1.92 M glycine, 1% SDS) and the comb was removed. Protein solutions containing 20 µg protein were mixed with the same volume of loading buffer (125 mM Tris pH 6.8, 20% glycerol v/v, 20% SDS w/v, 10 mg BPB) and loaded onto the gel. 10 µl of LMW-protein-SDS marker (GE Healthcare) served as a protein standard for size determination. Per gel, 15 mA were applied and the SDS gels ran at 150 V for approximately two hours.

Subsequently, gels were washed with water and fixed in 40% ethanol/ 10% acetic acid solution for one hour, followed by two washing steps using water for 30 minutes. The washed gels were stained for one hour in 100 ml Coomassie staining solution on a shaker (Candiano, *et al.*, 2004). For the Coomassie dye stock solution, 50 g of ammonium sulfate were dissolved in 400 ml ddH_2O and then mixed with 6 ml of 85% ortho-phosphoric acid. The final volume was adjusted to 490 ml by adding ddH_2O. Finally, 10 ml of 5% (w/v) Coomassie Brilliant Blue G-250 in ddH_2O stock solution was added and mixed well. The stock solution was stored in the dark at RT. The Coomassie staining solution contained 80% Coomassie dye stock solution and 20% methanol. After staining, gels were washed several times with ddH_2O until the background was sufficiently destained (App. 8.3).

2.7.3.4 Tryptical in-gel digestion

SDS gels were scanned and evaluated using the Aida Image Analyzer software v.4.15. The amount of protein in each lane was determined by comparing the intensity of the BSA marker band with the intensity of the protein sample. First, the integral of the intensity of the BSA band of the LMW Marker was formed, subtracting the background staining, which corresponded to 0.5 µg of protein. The protein concentration in each lane was densitometrically determined by the known amount of protein in the BSA band and the values of the integral (4). Based on this, each lane was divided into eight fractions and the amount of trypsin for the in-gel digestion of each fraction was calculated (App. 8.4).

$$\frac{Integral\ (sample) - Background}{(Integral\ (BSA) - Background)\ \times 2} \qquad (4)$$

Afterwards, each lane of the SDS gel was cut into eight pieces according to the previous evaluation. Each of the eight gel pieces was further cut into 1 x 1 mm pieces and transferred to a new 1.5 ml reaction tube. The gel pieces were then destained repeatedly in 50% acetonitrile (ACN) and 50 mM ammonium bicarbonate until the pieces were colorless. Subsequently, gel pieces of each sample were dehydrated in 100% ACN. Each sample was supplemented with 20 µl trypsin solution (0.1 µg/ ml, ratio trypsin : protein 1:20 (w/ w)). After absorption of the solution through the gel pieces, 50 mM ammonium bicarbonate was added

in small increments until all gel pieces were completely rehydrated and slightly covered. The tryptic in-gel digestion was carried out at 37 °C overnight.

2.7.3.5 Peptide extraction

Peptides were extracted from the gel pieces using the protocol described by Lassek and colleagues (Lassek, *et al.*, 2015). 200 µl of each solution were used and in between, the supernatants of each sample were collected. Gel pieces of each sample were first dehydrated two times with acetonitrile and then rehydrated with 1% acetic acid. Following, gel pieces of each sample were again dehydrated two times with acetonitrile, then treated with 5% acetic acid and incubated for ten minutes in an ultrasonic bath. Finally, 100% acetonitrile was added to the gel pieces of each sample and again incubated in the ultrasonic bath. The collected supernatants were dried in a vacuum concentrator (Concentrator plus, Eppendorf, Germany) and stored at -20 °C.

2.7.3.6 Desalting of peptide samples using ZipTips

To remove interfering salts, samples were desalted using ZipTip tips (Bagshaw, *et al.*, 2000). These tips contain a matrix of C18 covered silicon dioxide to which the peptides bind. Desalting and cleaning were based on the different polarities of the used solutions. The samples were resuspended in 20 µl wash solution II (5% ACN with 0.1% FA in UPLC water) and incubated for one hour at RT in the dark. Afterwards, it was cautiously snipped against the reaction tube and briefly centrifuged. The following steps were performed with a pipette of 10 µl and it was pipetted up and down very slowly to increase binding to the matrix and to minimize peptide loss. First, the ZipTip tips were moistened three times with wetting solution (50% ACN in UPLC water), which was then discarded. This was followed by two washing steps with wash solution I (5% ACN with 0.1% FA in UPLC water), which was also discarded. Peptides of the sample were bound to the matrix by pipetting the peptide solution up and down ten times. This was followed by three times washing with wash solution II, which was also discarded. The elution of the bound peptides was performed by aspiring the elution solution (60% ACN with 0.1% FA in UPLC water) five times at the edge of a new reaction tube. This process was repeated twice. The desalted samples were dried in a vacuum concentrator and stored at -20 °C.

2.7.3.7 Sample preparation for LC-MS/MS analyses

For LC-MS/MS analyses, the peptide samples were dissolved in 16 µl of buffer A (0.1% formic acid/ 3% ACN) and incubated for one hour at RT in the dark. Subsequently, samples were incubated for ten minutes in an ultrasonic bath at 37 kHZ. The samples were centrifuged at 4 °C and 109'000 x *g* for 20 minutes and transferred to an UPLC glass vial.

2.7.4 Membrane Shaving approach

2.7.4.1 Preparation of integral membrane proteins

The membrane pellet (ch. 2.7.2) was homogenized in 500 µl of carbonate buffer. Protein concentrations were determined as described previously (ch. 2.7.3.2). The calibration line was determined using the standard protein solution and carbonate buffer according to the manufacturer's instructions. The protein concentrations were plotted against the determined quotients and a linear regression was performed through the points as shown in Figure 13. Subsequently, the protein concentration of the samples was adjusted with carbonate buffer to 1 mg/ml and samples were incubated for one hour at 4 °C in an overhead shaker and further homogenized every 15 minutes with a syringe. Afterwards, the sample temperatures were adjusted to RT and solid urea was added to a final concentration of 8 M. The high urea concentration enhances the cleaning effect and breaks hydrophobic bonds between proteins and the membrane (Okamoto, *et al.*, 2001). Additionally, peripheral membrane proteins are removed from the membrane fraction and integral proteins are denatured, leaving their cysteine residues accessible for subsequent reduction and alkylation. Subsequently, TCEP was added at a final concentration of 5 mM and the sample was incubated for one hour at 30 °C. For alkylation and reduction of the proteins, IAA was added to a final concentration of 10 mM and incubated for 30 minutes at RT in the dark.

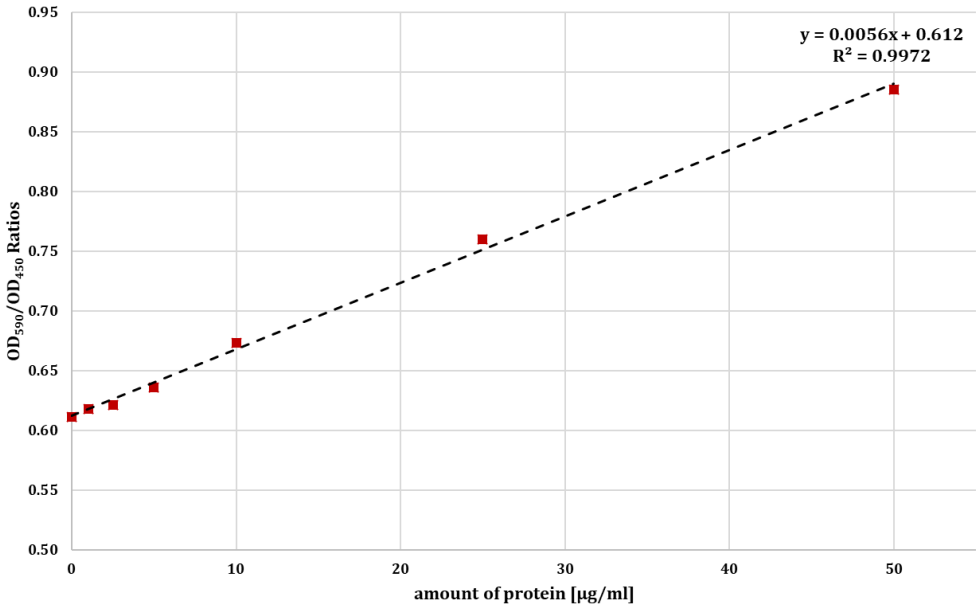

Figure 13 Calibration curve for the protein concentration determination of samples of the shaving approach using carbonate buffer.
The protein concentrations on the x-axis were plotted against the determined ratios of OD_{590}/OD_{450} on the y-axis. Here, the regression line was represented by the formula $y = 0.0056 x + 0.612$ and the coefficient of determination R^2 of 0.9972 represented the course of the regression line well.

2.7.4.2 Proteinase K digestion

Proteins were digested using proteinase K, which cuts protruding transmembrane proteins unspecific (Morihara, *et al.*, 1975). Therefore, proteinase K was added in an enzyme-protein ratio of 1 : 50 (w/w) and incubated for 15 hours in a thermomixer at 900 rpm and 37 °C. This resulted in the removal of all peripheral membrane protein parts ('Shaving'), leaving membrane-bound proteins and protease-accessible peptides in the membrane extract (Blackler, *et al.*, 2008). Subsequently, one volume of 10% acetonitrile was added to the membrane extract, the samples were cooled on ice and ultracentrifuged. The supernatant was discarded and the pellets were washed with 50 mM TEAB, pH 7.8. The samples were ultracentrifuged again and the supernatant was discarded.

2.7.4.3 Chymotrypsin digestion

After the proteinase K digestion, samples were digested using chymotrypsin which, in contrast to trypsin, cleaves peptides at aromatic amino acids such as tryptophan, tyrosine and phenylalanine as well as leucine and methionine at the C-terminus (Burrel, 1993). Furthermore, RapiGest™ was used in the digestion buffer, which is an acid-labile surfactant that improves the speed and efficiency of digestion (Yu, *et al.*, 2003). The proteins are unfolded and thus more accessible for subsequent digestion. Due to its acid lability, RapiGest™ can be degraded in solutions with a pH lower than two. This results in a water-insoluble product, which pelletizes during centrifugation, and a water-soluble product, which does not affect later LC-MS analyses.

The protein pellet was first resuspended in 100 µl chymotrypsin buffer (50 mM TEAB, 10 mM $CaCl_2$, pH 7.8). Subsequently, the protein concentration was again determined using a modified Bradford assay (2.7.3.2) with the calibration line depicted in Figure 14. The samples were mixed with 100 µl chymotrypsin buffer containing 0.5% RapiGest™. Chymotrypsin was added in an enzyme-protein ratio of 1 : 100 (w/w) and incubated for six hours at 900 rpm and 30 °C (App. 8.5). Subsequently, 10% formic acid was added to adjust the pH below two and the samples were incubated for 45 minutes at 37 °C. The samples were cooled on ice and centrifuged for 15 minutes at 4 °C and 20'000 x *g*. Finally, the supernatant was transferred into a new reaction tube, centrifugation was repeated two more times and the purified supernatant was stored at -20 °C.

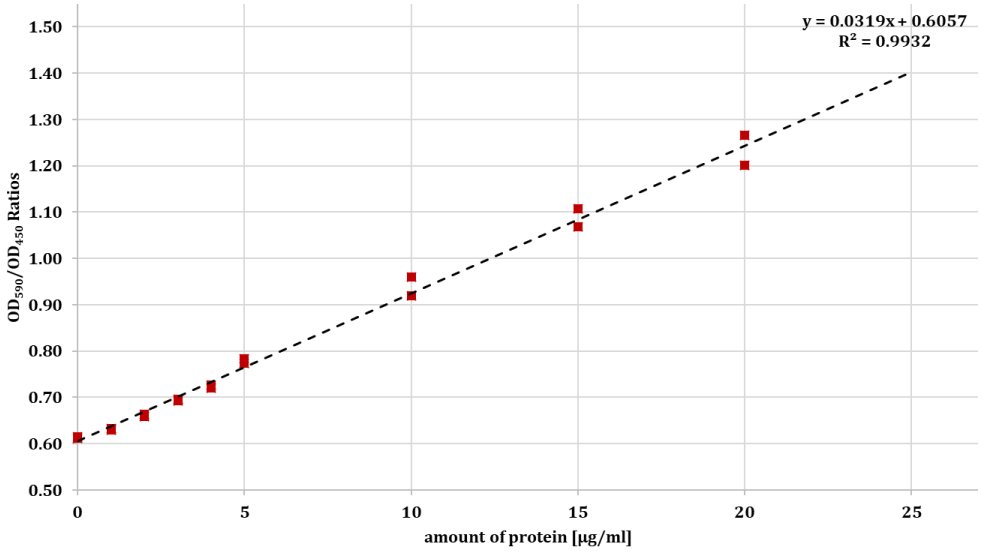

Figure 14 Calibration curve for the protein concentration determination of samples of the shaving approach using chymotrypsin buffer.
Values of OD_{450} and OD_{590} were determined in duplicates. The protein concentrations on the x-axis were plotted against the determined ratios of OD_{590}/OD_{450} on the y-axis. The regression line, represented by the formula y = 0.0319 x + 0.6057, showed a coefficient of determination R^2 of 0.9932 that represented the course of the regression line well.

2.7.4.4 Sample preparation for LC-MS/MS analyses

For LC-MS/MS analyses, samples of the membrane shaving approach were thawed on ice, 4 µg per sample were transferred into ultracentrifugation vials and buffer A was added to a total volume of 16 µl. In case the protein concentration was lower than 0.25 µg/µl, 16 µl of the corresponding sample were directly transferred into ultracentrifugation vials. The samples were centrifuged at 4 °C and 109'000 x *g* for 20 minutes and transferred into UPLC glass vials.

2.7.5 LC-MS/MS analyses

Samples of the solubilization approach were analyzed with an UPLC-coupled to an Orbitrap Velos Pro mass spectrometer. The samples were prepared as described previously (2.7.3.7). The samples were separated by liquid chromatography on a BEH C18 column (130 Å, 1.7 µm, 75 µm X 250 mm) at 35 °C using a nanoAcquity UPLC with a flow rate of 0.35 µl/ min. Solvent A consisted of 0.1% (w/v) FA in UPLC water, solvent B of 80% ACN with 0.1% FA. 5 µL were injected on column and the following gradient was used: 0-30 min 3.7% B, 30-65 min 3.7-22.1% B, 65-88 min 22.1-29.3% B, 88-148 min 29.3-48.3% B, 148-175 min 48.3-62.5% B, 175-192 min 62.5-99% B, 192- 195 min 99% B, 195-200 min 99-3.7% B.

The column was connected to the mass spectrometer by a nanospray emitter. For primary MS-scans the orbitrap (FTMS) was used scanning a range from 350 – 1900 m/z with a resolution of 60,000 (Marshall, *et al.*, 1998). An internal mass calibration was performed with the universal polysiloxane contaminant of mass 445.12030. For MS/MS scans in an ITMS, the 20 most abundant mass signals of the

MS were ionized by CID (normalized collision energy: 35, Activation Q: 0.25, activation time 10 ms, isolation width: 2 m/z, charge state: 4, scan rate: rapid). The signal threshold has been set to 2,000. A dynamic exclusion list was introduced (repeat count: 1, repeat duration: 12 s, size of the exclusion list: 500, exclusion duration: 12 s). The allowed charge states were: +2 or more.

For samples of the membrane shaving approach a Dionex Ultimate 3000 nHPLC (Thermo Scientific) was used for separation. The column was pre-heated to 60 °C. Upon next, 7 µl per sample were first injected onto the pre-column (Acclaim PepMap 100, 75 µm x 20 mm, nanoViper, C18, 3 µm, 100 Å; Thermo Scientific) followed by the pre-heated analytical column (Acclaim PepMap RSLC, 75 µm x 500 mm, vanoViper, C18, 2 µm, 100 Å; Thermo Scientific). The samples were eluted from the precolumn with the following gradient starting with 3.7% buffer B (80% acetonitrile and 0.1% formic acid, 5% DMSO) and 96.3% buffer A (0.1% formic acid, 5% DMSO): 3-35 min 3.7% B, 35-125 min 3.7-31.3% B, 125-145 min 31.3-62.5% B, 145-152 min 62.5-90% B, 152-157 min 90% B, 157-162 min 90-3.7% B, 162-180 min 3.7% B.

The column was connected to an Orbitrap Fusion mass spectrometer where MS scans were conducted in the FT-MS mode using a scan range from 350 to 1750 m/z with a resolution of 120,000 and a lock mass of 445.12030. The Top Speed Method in a data dependent mode was used to select the most abundant ions with charges from +2 to +5 for fragmentation. A dynamic exclusion list was applied (repeat number: 1, exclusion time 13 s). Ions for fragmentation were selected by a quadrupole and analyzed by an ion trap (normalized collision energy: 35, activation Q: 0.25, , isolation width: 1.6 m/z, scan rate: rapid).

The raw data files obtained from both the solubilization and shaving samples were analyzed separately with the MaxQuant software using the *P. aeruginosa* databases developed in this work.

2.7.6 Protein identification using MaxQuant and *Pepper*

For the identification of proteins and possible small proteins, .raw-files containing the data from the mass spectrometric analyses were analyzed using the quantitative proteomic software MaxQuant (www.maxquant.org, version 1.5.2.8). The software first aligns the retention times between different runs and corrects the peptide masses followed by the detection and quantification of the peptides. In the next step, the MS/MS ions are identified. A theoretical digestion based on the chosen enzyme was done by the software based on the introduced database to generate a list of all possible peptides. For these peptides, a theoretical MS/MS spectrum was generated, which was then compared to the determined MS/MS spectra of the sample peptides. Subsequently, the final protein identification is done by assigning matches between theoretical and sample peptide spectra to the corresponding, originating protein sequence of the database (Cox, *et al.*, 2008).

First, the files were loaded into the program and were assigned to their corresponding sample. All samples were searched with a false discovery rate (FDR) of 0.0001 on peptide and 0.01 on protein level. At least one unique peptide with a minimal length of seven amino acids was necessary for the identification of a protein. Additionally, the internally calculated peptide scores for both modified and unmodified peptides were set to 40. The delta scores, describing the difference in scores of the best and the second-best identified peptide, were set to 6 and 17 for unmodified and modified peptides, respectively.

As most protein samples exhibit some degree of modification either due to post translational modifications or accidental modifications which are artefacts of sample handling, such as oxidation these modifications also have to be considered during database searches. Peptides above 5400 Da were discarded for the identification and a maximum of four different modifications per peptide was permitted. During the sample preparation, peptides could be oxidized at their methionyl group resulting in $[M+H+16]^+$-ions. Therefore, the detected peptide mass increases by 16 Da (Morand, *et al.*, 1993). Additionally, proteins could be acetylated at the N-terminus, which is proposed to be a signal for degradation of the respective protein resulting in an increase of the peptide mass by 42 Da (Hwang, *et al.*, 2010). During preparation, the protein samples were alkylated with iodoacetamide to prevent the formation of disulfide-bridges resulting in carbamidomethyl-modified cysteine residues (Waterman, 1976). This carbamidomethylation resulted in an increase of the mass of the resulting peptide for each cysteine residues by 57 Da and was also considered as a fixed modification. To increase the number of identifications, match between runs was enabled (Matching time window: 0.7 min, Alignment time window: 20 min). This FDR-controlled algorithm enables the MS/MS-free identification of peptides if retention time and mass are reasonably similar to their MS/MS-identified counterpart (Cox, *et al.*, 2008). The enzyme for the theoretical digestion of samples of the solubilization approach was trypsin, which cleaves at the C-terminal side of lysine and arginine residues (Olsen, *et al.*, 2004). Two missed cleavages were allowed and a maximal charge of 5+ for the identified peptides. For samples of the solubilization approach, iBAQ values were determined, meaning the protein intensity is divided by the number of theoretical tryptic peptides (Schwanhäusser, *et al.*, 2011).

For database searches of samples of the shaving approach, three different digestions were chosen to cover all possible resulting peptides. This was accomplished by triplicating the set of .raw-files and assigning each set to one of the three different parameter groups. The first parameter group was defined as chymotrypsin cutting completely enzymatically at WYMFL (four missed cleavages) and the second one was defined as chymotrypsin cutting partially enzymatically (four missed cleavages) to identify peptides that were cut by both proteinase K and by chymotrypsin. For the third parameter group, no defined

enzyme specificity was chosen due to the unspecific cleavage properties of proteinase K (no missed cleavages). All samples were searched against both the PRDB and the TRDB generated in this work (ch. 2.5).

The resulting evidence-files containing all identified peptides were further validated by applying additional criteria to the identified peptide sequences and additionally back matching the peptide sequences onto their position within the genome of *P. aeruginosa* PAO1. This was accomplished by using the *Pepper* (https://gitlab.com/s.fuchs/pepper) algorithm that translates the peptide sequences back into the corresponding nucleotide sequences followed by mapping to the genome sequence. This algorithm was developed by Dr. Stephan Fuchs (RKI, Wernigerode, Germany). The algorithm also predicts open reading frames (ORF) for each DNA match in case they do not match to an annotated ORF. For this purpose, the next stop codon downstream within the same frame of the respective DNA match is considered as the end of the ORF. In case the match is not a result of digestion by the used protease (n-terminal peptide match), the sequence between match start and the closest downstream in-frame stop codon is considered as the only possible ORF. In case a methionine is encoded immediately upstream of an n-terminal peptide match, this methionine is considered as the start of the ORF. In case of non-terminal DNA matches, the sequence between the closest stop codon upstream and downstream of the respective DNA match is considered as the longest possible ORF. Alternative potential ORFs are considered by screening for potential in-frame start codons which are located upstream of the respective DNA match. Additionally, for predicted open reading frames, the encoded start codon, the Shine-Dalgarno sequence and the length of the ribosomal binding site (RBS) spacer are also determined. Open reading frames were then classified based on this information to give insight about their coding potential, as described in Table 9. The final ORF classification can be found in App. 8.6. For these analyses, peptides corresponding to reverse identified proteins and contaminants as well as peptides displaying no intensity were removed from the evidence files. The pepper algorithm only considered peptides which were only identified in at least two different samples with a minimum of two MS/MS scans.

Table 9 Pepper classification and scoring of start codons, RBS as well as RBS spacer length.
Start codons were classified based on the common start codons ATG, GTG and TTG encoding for methionine. Considered alternative start codons were CTC encoding for leucine and the triplets ATA, ATT and ATC encoding for isoleucine. All other codons were ranked in class 3. For the ribosomal binding sites (RBS), GGAGG as the most common motif was ranked in class 1. Class 2 considered nucleotide changes at position 1, 3 or 5 respectively and class 3 considered two nucleotide changes at the corresponding positions. The length of the RBS spacer was ranked in class 1 or class 2 based on the distance between the RBS and the start codon.

Start codons		**RBS**		**RBS spacer**	
class 1:	ATG, GTG, TTG	class 1:	GGAGG	class 1:	> 2 nts
class 2:	CTG, ATA, ATT, ATC	class 2:	T, C or A at position 1	class 2:	< 3 nts
class 3:	all other codons		T or G at position 3		
			T, C or A at position 5		
		class 3:	two variations of class 2		

2.7.7 Quantification of identified proteins

After the verification of identified proteins based on their identified peptides, further criteria were applied using the proteinsgroups.txt file created by the MaxQuant software. Contaminants, reverse identified proteins, and proteins with no intensity were discarded and only proteins that were previously identified via the *Pepper* algorithm were further analyzed. Following, only proteins with at least two unique peptides (for SP100 at least one unique peptide) detected somewhere in all samples were considered and proteins that did not met this criterion were removed. The sum of the protein intensities of all three replicates of a time point divided by the number of identified, unique peptides had to be larger than 100.000 in samples of the solubilization approach or ≥ 200.000 for proteins prepared via shaving approach. Eventually, only proteins that were identified in at least two replicates or samples by a MS/MS scan qualified for quantification. The software Perseus (Version 1.5.2.6) was used for statistical testing. This software covers normalization, pattern recognition, time-series analysis, cross-omics comparisons, and multiple hypothesis testing (Tyanova, *et al.*, 2016).

For proteins of the solubilization approach, the relative iBAQ (riBAQ) values were determined, a normalized measure of molar abundance (Shin, *et al.*, 2013). These were determined by dividing each proteins' iBAQ value by the sum of all non-contaminant and non-reverse iBAQ values of the sample (Krey, *et al.*, 2014). Following, the riBAQ values were Log2 transformed and grouped for each time point. A one-way analysis of variance (ANOVA) was performed with an FDR of 0.05 to test for statistical significance among all sample groups (Diez, *et al.*, 2019). For all proteins that were ranked as significant by the ANOVA, a t-test (FDR = 0.05)

comparing anaerobic and aerobic time points directly with the aerobic control was performed (Gosset 'Student', 1908).

For quantification of proteins identified via the membrane shaving approach, the intensities of the corresponding proteins were determined based on the intensities of their corresponding peptides. Due to the possibility of identifying a peptide more than once using three different parameter groups for the database search with MaxQuant resulting in a multiplication of identified peptides per sample and thus artificially altering the protein intensities, all identified peptides were introduced to the EvProc.py algorithm developed by M.Sc. Alexander Beckmann (TU Braunschweig, Braunschweig, Germany). This algorithm determined the protein intensities based on the corresponding peptide intensities in each sample followed by computation of the normalization and statistical quantification. Therefore, peptides that were identified in a sample by two or all three digestion modes were selected based on the number and appearance of modifications as well as the charge state of the peptide and the identification type (via MS/MS, via second peptide search and match-between runs respectively). Peptide intensities were than normalized via total normalization, meaning the peptide intensity was divided by the sum of all peptide intensities of the corresponding sample (5).

$$x_{norm} = \frac{x_i}{\sum_{i=1}^{n} x} \tag{5}$$

After normalization, normalized intensities were also Log2-transformed followed by Z-score standardization. Due to the fact that the intensities of the identified proteins were not nearly normally distributed as was the case with the solubilization samples, a non-parametric Kruskal-Wallis test (KW test) was performed to determine changes in protein level (Kruskal, *et al.*, 1952). For the direct comparison of samples to the aerobic control as well as to the 16 h anaerobic sample, post hoc analyses for large data sets based on the Dunn's test were performed (Dunn, 1961). Additionally, Family-wise error rate (FWER) corrections were performed due to the reason that both the KW test and Dunn's test calculate statistical significance based on the p-value. The p-value represents the probability that, assuming the null hypothesis is true, the statistical observation is greater or equal to the actual observed results and thus giving no clue about the statistical significance of the gene expression (Wasserstein, *et al.*, 2016). FWERs were controlled by applying the Bonferroni-Holm method, which is uniformly more powerful than the Bonferroni method and less prone to positive and negative dependence (Holm, 1979). Proteins, whose values were both lower than 0.05 were described as significantly changed in their abundance distribution between the samples.

Following, based on the averaged riBAQ values or the normalized intensities for the solubilization approach or membrane shaving approach respectively, the ratios between the normalized (riBAQ) intensity of all time points and the aerobic control were calculated for each protein to determine the biological changes in the expression of the respective gene over the period of time under anaerobic and aerobic conditions. Ratios ≥ 1.5 (Log2-transformed: 0.58) indicated that the gene was significantly more expressed in the sample in comparison to the aerobic control. In case the ratios ≤ 0.669 (Log2-transformed: -0.58) the gene was significantly lower expressed in the sample compared to the aerobic control. Ratios were also determined for the aerobic shift samples compared to the 16h anaerobic sample to investigate changes in gene expression occurring after shifting the bacteria back to aerobic conditions. Expression rates were analyzed for differences in the expression of genes encoding for proteins important for aerobic and anaerobic respiration.

2.7.8 Cluster analyses

For the identification of proteins with similar time-dependent distribution and kinetic, hierarchical clustering was performed using the software Perseus (Version 1.5.2.6). For the comparison of the normalized protein intensities of the identified proteins of both the solubilization and the shaving approach, these normalized intensities had first to be standardized. A commonly used method for standardization is the Z-Score (6) which uses both the mean μ and the standard deviation σ of a given data set (Dubes, *et al.*, 1980). Here it was important to consider that the number of total samples changed in case proteins were not identified at every time point.

$$z = \frac{(x - \mu)}{\sigma} \qquad (6)$$

To detect similarities in protein kinetics, the datasets containing the Z scores of the identified proteins for each time point were analyzed using the Perseus software. Following, *k*-means clustering of the 20 most similar protein kinetics using Spearman's correlation coefficient ρ and the corresponding Spearman correlation distance were performed for proteins of interest. *K*-means clustering is a method that partitions a number of observations into a pre-defined number of clusters, here grouping proteins with a similar mean into one group until all proteins are divided onto *k* groups (Lloyd, 1982). Furthermore, Spearman's correlation coefficient is, in comparison to the more popular Euclidean or Pearson correlation coefficient, more robust to outliers by determining the statistical dependence between the rankings of two variables (Spearman, 1904) (Daniel, 1990). The correlation coefficient ρ is calculated using the difference between ranks d and the number of observations n (7).

$$\rho_{x,y} = 1 - \frac{6 \sum d_i^2}{n(n^2 - 1)} \quad (7)$$

Following, ρ is transformed into a distance (8) and resulting clusters were investigated for proteins and SP100 that displayed similar kinetic profiles like proteins involved in respiration and denitrification.

$$d(x,y) = 1/2(1 - \rho_{x,y}) \quad (8)$$

2.8 Transcriptional analyses of newly identified sORFs

2.8.1 Digoxigenin-labeling of RNA probes

For later detection of transcriptional activity, RNA probes were synthesized by *in-vitro* transcription using the T7 polymerase and DIG-11-UTP (Fuchs, *et al.*, 2007). Specific genes were amplified using genomic DNA of *P. aeruginosa* PAO1 and the corresponding primer pairs as described previously (ch. 2.6.5). For *in vitro* transcription, 500 ng PCR template were used and the reaction mixture contained 1x DIG RNA Labeling Mix (Roche), 1x transcription buffer (Thermo Scientific, Waltham, USA), 40 U T7 RNA polymerase (Thermo Scientific, Waltham, USA) and 40 U rRNasin® (Promega, Mannheim, Germany). The final volume was adjusted with DEPC-water to 20 µl per reaction and the mixture was incubated for two hours at 37 °C. Afterwards, 2 µl of DNase (1 U/µl; Thermo Scientific, Waltham, USA) were added and incubated for additional 15 minutes at 37 °C. The reaction was stopped by adding EDTA pH 8.0 to a final concentration of 20 mM. Subsequently, 2.5 µl 4 M lithium chloride and 75 µl 96% ethanol were added and the RNA probes were precipitated for 30 minutes at -80 °C. After centrifugation for ten minutes at 12'000 x g at 4 °C, the supernatant was removed and the pellet was washed with 50 µl ice-cold 70% ethanol. The RNA pellet was dried at RT under the hood and solved in 100 µl DEPC-water for 30 minutes at 37 °C. Afterwards, the RNA probes were stored until further use at -80 °C.

2.8.2 Efficiency test of RNA probes

The labeling efficiency of the RNA probes was tested by probing various dilutions of the probes. Dilutions were prepared using DEPC-water, the RNA probes were mixed and 1 µl of each diluted RNA probe was spotted onto a positively-charged nylon membrane. Following, the RNA probes were covalently bound to the nylon membrane via UV cross-linking (120 J/ cm^2) and the membrane was equilibrated for 30 minutes in buffer II (1% (v/v) blocking reagent in buffer I [100 mM maleic acid, 150 mM NaCl]) at RT. Subsequently, the membrane was incubated with anti-Digoxigenin-AP (Sigma Aldrich, St. Louis, USA) 1 : 10,000 in buffer II for 30 minutes at RT. Afterwards, the membrane was washed two times for

15 minutes with buffer I followed by equilibration for one minute in buffer III (100 mM Tris, 100 mM NaCl, pH 9.5). After incubating the membrane for five minutes in CDP-Star (Sigma Aldrich) 1 : 200 in buffer III at RT in the dark, chemiluminescence signals were detected using the Luminescent Image Analyzer LAS-3000 (Fujifilm, Minato, Japan) (App. 8.9).

2.8.3 Cultivation and cell harvest

For transcriptional analyses, *P. aeruginosa* PAO1 cells were cultivated under aerobic and anaerobic conditions as described previously (ch. 2.6.1). Pre-cultures of 120 ml LB-medium were cultivated overnight. Main cultures were cultivated in triplicates. Anaerobic cultures were cultivated in 15 ml reaction tubes supplemented with 50 mM KNO_3, filled to the brim, and screwed tightly. Cells were harvested after reaching an OD_{540} of 0.5 and after 30 minutes, 1 h, 2 h, 3 h and 6 h of cultivation under anaerobic conditions. The cultures were mixed with ice-cold killing buffer (20 mM Tris pH 7.5, 20 mM sodium azide, 5 mM magnesium chloride) in a ratio of 2 to 1 and centrifuged for five minutes at 18'514 x *g* at 4 °C. The supernatant was removed and the pellet was resuspended in 1 ml ice-cold killing buffer. After a second centrifuging step at 20'879 x *g*, the supernatant was discarded and the cell pellet was stored at -80 °C.

2.8.4 Phenol-based RNA extraction

Samples were stored on ice during cell disruption and the RNA preparation was performed using acidic-phenol-chloroform extraction (Majumdar, *et al.*, 1991). Frozen cell pellets were resuspended in 500 µl suspension buffer (200 mM NaCl, 3 mM EDTA, pH 8.0) and transferred into 1.5 ml cell disruption tubes containing 500 µl glass beads (Ø 0,1 µm) and 500 µl phenol-chloroform-iso-amyl alcohol (PCI; acidic phenol : chloroform : iso-amyl alcohol, 25:24:1). Cell disruption was done for one minute at 6.5 m/s using the Fast-Prep® 24. Following, the cell lysate was centrifuged for five minutes at 12'000 x *g* at RT and the upper, aqueous phase was transferred carefully into a new 1.5 ml reaction tube. 500 µl PCI were added, incubated for five minutes at RT in a shaker at 9.5 m/s (1,000 m^{-1}) and centrifuged for five minutes at 15'000 x *g* and RT. The upper phase was again removed, transferred into a new reaction tube, supplemented with 500 µl chloroform-iso-amyl alcohol (CI; chloroform : iso-amyl alcohol, 24:1) and incubated for five minutes at RT in a shaker at 9.5 m/s (1,000 m^{-1}). Again, the samples were centrifuged at 15'000 x *g* and RT for five minutes. Afterwards, the upper phase was removed and treated with CI one more time. After centrifugation, the supernatant was transferred into a new reaction tube and supplemented with two volumes of ice-cold 98% ethanol and 0.1 volume of ice-cold 3 M sodium acetate pH 5.2. The RNA was precipitated overnight at -20 °C.
Precipitated RNA was centrifuged for 30 minutes at 15'000 x *g* and 4 °C. After removing the supernatant, the RNA pellet was washed with 500 µl ice-cold 70%

ethanol and centrifuged for ten minutes at 15'000 x *g* and 4 °C. The supernatant was discarded and the pellet was dried under the hood until a translucent pellet was visible. 50 µl DEPC-water were added and the RNA was solved overnight on ice at 4 °C. Following, the RNA concentration was photometrical determined (IMPLEN Nanophotometer P 330; Implen GmbH, Munich, Germany) and the RNA was stored at -80 °C.

2.8.5 Denaturing RNA gel

For the separation of the RNA samples, a denaturing formaldehyde-agarose gel was used. Formaldehyde denatures RNA by forming Schiffs-bases with guanine and prevents the formation of hydrogen bonds between cytosine and guanine. Furthermore, formaldehyde is easier to remove from the RNA compared to glyoxal/ DMSO. Additionally to this, the sample buffer contains formamide, which suppressed RNase-activity and also stabilizes the RNA. A 1.5% (w/v) agarose gel was prepared by solving 3 g agarose in 20 ml 10x MOPS (200 mM MOPS, 50 mM sodium acetate, 10 mM EDTA, pH 7.0) and 146 ml ddH_2O. The solution was cooled down to 65 °C and 34 ml pre-warmed 35% formaldehyde were added. The agarose gel was cast and solidified for one hour at RT. Of each RNA sample, 10 µg were used and filled with DEPC-water to the same volume. 4 µl of DIG labeled RNA molecular weight marker I (Roche, Rotkreuz, Swiss) were adjusted with DEPC-water to the volume of the samples and both samples and marker, were supplemented with one volume of RNA sample buffer (64% (v/v) formamide, 12% (v/v) 35% formaldehyde, 20% (v/v) 10x MOPS, 4% (v/v) 50% sucrose, 0.2% (w/v) BPB, 0.2% (w/v) xylene cyanole). Both samples and marker were heated for ten minutes at 65 °C and immediately cooled down on ice afterwards. The samples and the marker were carefully loaded onto the gel and were subsequently separated at 120 V for two to three hours (Sub-Cell® GT Cell, Bio-Rad, California, USA).

2.8.6 Northern Blot analyses

RNA separated on the denaturing agarose gel was transferred onto a positively-charged nylon membrane (Ziebandt, *et al.*, 2001). Following separation using a 1.5% denaturing agarose gel, a vacuum blot was used to transfer the RNA onto the membrane (Zeta-Probe® Blotting Membranes; Bio-Rad, California, USA) at 55 mbar using a vacuum blotting device (VacuGene™ XL Vacuum Blotting System; Fisher Scientific, New Hampshire, USA) (Wetzstein, *et al.*, 1992). The agarose gel was placed onto the nylon membrane and RNA was denatured for five minutes adding denaturing solution (50 mM NaOH, 10 mM NaCl). Following, the denaturing solution was removed and neutralizing solution (100 mM Tris, pH 7.4) was added and incubated for additional five minutes. The neutralizing solution was removed and subsequently, the RNA was blotted onto the nylon membrane for four hours with 20 x SSPE (3 M NaCl, 200 mM sodium dihydrogen phosphate.

20 mM EDTA, pH 7.4). After the transfer, the RNA was covalently bound to the nylon membrane via UV cross-linking (120 J/ cm^2). To control of the transfer efficiency, the nylon membrane was incubated for five minutes in methylene blue solution (0.1% (w/v) methylene blue, 400 mM sodium acetate, 2% (v/v) acetic acid) followed by destaining three times with ddH_2O (App. 8.10). After controlling the transfer efficiency, the nylon membrane was incubated at least one hour in hybridization buffer (5 x SSPE, 0.1% (w/v) N-lauroyl sarcosine, 7% (w/v) SDS, 1% blocking reagent (Sigma Aldrich), 50% (v/v) formamide) at 68 °C. Meanwhile, the RNA probe was diluted in hybridization buffer as displayed in Table 10, and was denatured for five minutes at 95 °C followed by storing on ice for additional five minutes. After addition of the RNA probe, the membrane was hybridized over night at 68 °C.

Table 10 Used RNA probes and corresponding dilutions.

RNA probe	dilution
PA3160	1 : 1000
PA3161	1 : 5000
6frt_14524	1 : 1000
igr2243	1 : 2000
6frt_26594	1 : 2000

The next day, the RNA probe was removed and stored for further use at -20 °C. The membrane was washed two times for five minutes each in wash buffer I (2 x SSC [20x SSC: 3 M NaCl, 300 mM trisodium citrate], 0.1% (w/v) SDS) followed by washing two times for 15 minutes each with pre-warmed wash buffer II (0.2 x SSC, 0.1% (w/v) SDS) at 68 °C. After one minute incubation in buffer I (100 mM maleic acid, 150 mM NaCl), the membrane was equilibrated for 30 minutes in buffer II (1% (v/v) blocking reagent in buffer I) at RT. Subsequently, the membrane was incubated with anti-Digoxigenin-AP (Sigma Aldrich, St. Louis, USA) 1 : 10,000 in buffer II for 30 minutes at RT. After the antibody incubation, the membrane was washed two times for 15 minutes each with buffer I followed by equilibration for one minutes in buffer III (100 mM Tris, 100 mM NaCl, pH 9.5). CDP-Star (Sigma Aldrich) in a ratio of 1 : 200 in buffer III was added and incubated for five minutes at RT in the dark and the chemiluminescence signals were detected using the Luminescent Image Analyzer LAS-3000 (Fujifilm, Minato, Japan).

3 Results and Discussion

3.1 Growth behavior and nitrate consumption

To determine time points for the cell harvest for the proteogenomics approach, the growth behavior of *P. aeruginosa* under aerobic and anaerobic conditions was observed. The *P. aeruginosa* strain PA01 was cultivated in complex medium to determine its growth behavior before and after shifting the cells from aerobic to anaerobic conditions and vice versa. Therefore, four biological replicates were used and the bacterial culture density started at an OD_{540} around 0.06 (App. 8.1). Regression curves were determined for each observed phase (App. 8.2). Here, the determined slop corresponded to the growth rate during this phase. First, the cells grew roughly two hours until they reached an optical density of 0.5 (Figure 15). Thereby, the growth rate under aerobic conditions lay around 0.432 with a doubling time of roughly 22 min (C). The determined growth rate remained constant over the selected period of time, indicating that the cells were in the exponential growth phase (Table 11). Afterwards, the cultures were shifted to anaerobic conditions. During growth under anaerobic conditions, two different growth phases A1 and A2 were observed. The first phase A1, lasted until ten hours after shifting to anaerobic conditions. In this phase the cells were in a lag-like phase showing a growth rate of 0.016. Then, the second phase A2 followed, whereby the growth rates increased resulting in a growth rate of 0.091, which was reduced by a factor of 4.7 compared to aerobic conditions. Moreover, during anaerobic cultivation, cells reached a maximum OD_{540} of 1.8. Furthermore, nitrate consumption rates of all four replicates showed a mean nitrate consumption of around 22% under anaerobic conditions (Table 12). During cultivation under anaerobic conditions the nitrate concentration in the medium decreased significantly from 7.2 g/l to 4.2 g/l indicating that nitrate was used by the cells for dissimilatory nitrate reduction. After 16 h of anaerobic cultivation, the bacteria were shifted back to aerobic conditions. Here, the cells reached a maximum OD_{540} of 2.9 after a total of 34 hours of cultivation and again two growth phases A3 and A4 were observed. During 10 h after shift (A3), the growth rate was 0.039. Afterwards the cells reached the stationary phase (A4). At the same time, the determined nitrate consumption rates decreased by factor 10 compared to

anaerobic conditions (from -0.218 to -0.024.) The nitrate concentration in the medium remained unchanged during this time.

Table 11 Determined growth rates of *P. aeruginosa* wt under aerobic and anaerobic conditions.
μ R1, μ R2, μ R3 and μ R4 = growth rates of replicate 1, 2, 3 and 4, respectively; t_D = doubling time of cells in the corresponding phase; slope = slope of determined regression curve; STDV = standard deviation of determined slope

time [h]	condition	phase	μ R1	μ R2	μ R3	μ R4	t_D [h]	slope	STDV
0									
2	aerobic	C	0.907	1.013	0.978	0.916	0.36	0.432	0.012
2.08			4.622	1.965	1.652	3.399			
4.08			-0.100	0.027	0.032	-0.066			
6.08			0.109	-0.127	0.059	-0.058			
8.08		A1	0.178	0.109	0.008	0.215	29.03	0.016	0.005
10.08	anaerobic		-0.136	0.009	-0.058	-0.033			
12.08			0.069	0.042	0.157	0.041			
14.08			0.067	0.115	-0.020	0.045			
16.08		A2	0.107	0.000	0.063	0.109	4.41	0.091	0.013
18.08			0.307	0.356	0.420	0.317			
19.08			-0.389	-0.333	-0.471	-0.505			
20.08			0.591	0.473	0.705	0.625			
21.08			-0.149	0.084	-0.151	0.011			
22.08			0.080	0.187	0.187	0.121			
23.08		A3	0.142	-0.143	-0.102	0.060	12.81	0.039	0.006
24.08			-0.004	0.164	0.050	0.118			
25.08			-0.013	-0.037	0.048	0.008			
26.08			0.138	0.146	0.034	0.061			
27.08	aerobic		-0.057	-0.080	0.030	-0.007			
28.08			0.082	0.151	0.146	0.165			
29.08			-0.130	-0.216	-0.282	-0.230			
30.08			0.020	0.037	0.103	0.077			
31.08		A4	0.043	0.071	0.066	0.043	-151.86	0.005	0.003
32.08			-0.031	0.026	0.035	0.024			
33.08			0.105	0.011	0.050	0.017			
34.08			-0.025	0.050	-0.003	0.030			

Table 12 Determined nitrate consumption rates of *P. aeruginosa* wt during anaerobic and aerobic cultivation.
R1, R2, R3 and R4 = replicate 1, 2, 3 and 4, respectively; STDV = standard deviation; ΔOD_{540} = difference in OD between last and first time point; mean $\mu/\Delta OD_{540}$ = nitrate consumption per OD unit

	time	R1	R2	R3	R4	mean	STDV	ΔOD_{540}	mean/ ΔOD_{540}
anaerobic	4.08 - 18.08 h	-0.327	-0.199	-0.217	-0.129	-0.218	0.071	1.220	-0.179
aerobic	18.08 - 34.08 h	-0.004	-0.003	0.009	-0.098	-0.024	0.043	1.173	-0.020

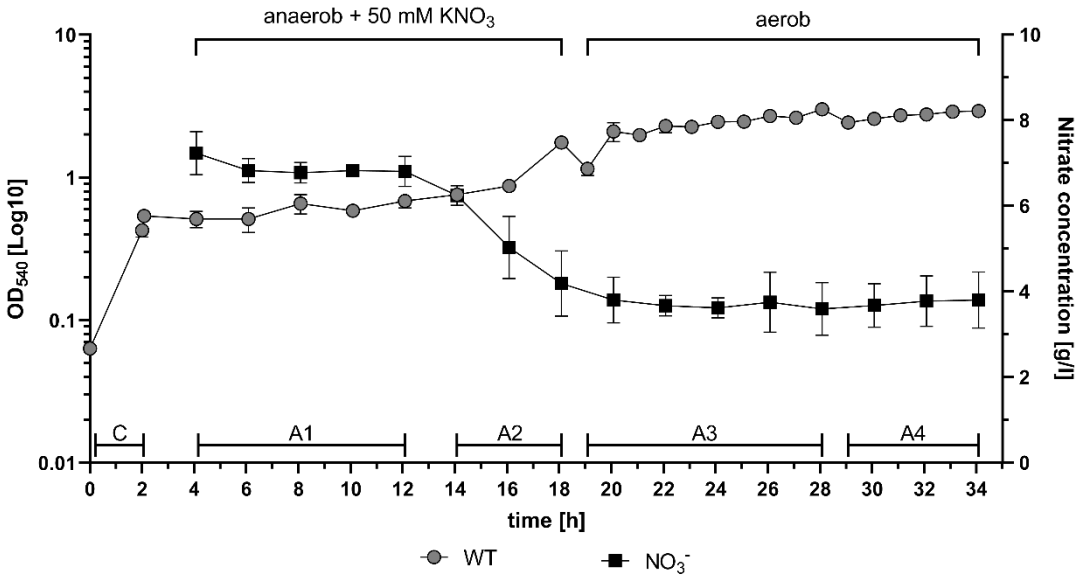

Figure 15 Growth curve of *P. aeruginosa* wt under anaerobic and aerobic conditions.
Grey circles = OD_{540} of *P. aeruginosa* WT, black squares = nitrate concentration in g/l. Four biological replicates were cultivated in LB medium to an OD_{540} of 0.5 followed by shifting cells to anaerobic conditions in the presence of 50 mM KNO_3. Cell densities were determined every two hours up to 16 hours under anaerobic conditions and after that, cells were shifted back to aerobic conditions and cell densities were further measured every hour for 16 hours. During cultivation, samples for nitrate concentration analyses were taken every two hours and nitrate concentration was determined using the Nitrate Spectroquant® Analytical Test Kit. Before shifting to anaerobic conditions, the OD increased significantly indicating exponential growth. During anaerobic cultivation cell growth was significantly reduced and after 12 hours, an increase of the cell density was observed. These observations correlated with the nitrate concentration present in the medium, which decreased significantly from 6.5 g/l to 4.2 g/l nitrate during the time from 12 to 16 hours. Cells reached a maximal density of 1.8 under anaerobic conditions and showed a significant onset after shifting to aerobic conditions. Following, measured cell densities leveled out around 2.5 indicating that cells were now in the stationary phase. Similarly, the concentration of nitrate in the medium remained stagnant around 3.5 g/l implying that nitrate was not further used for respiration.

Altogether, *P. aeruginosa* wt displayed a slow growth during cultivation under anaerobic conditions as growth rates decreased from 0.432 to 0.091. In parallel, the nitrate concentration in the medium decreased and the determined nitrate consumption rate of about 22% under anaerobic conditions. Furthermore, the nitrate consumption rate per OD unit was higher under anaerobic conditions than under aerobic conditions further substantiating the utilization of nitrate for denitrification. Interestingly after shifting back to aerobic conditions, growth rates

decreased further from 0.091 to 0.039 and subsequently to 0.005. Moreover, eleven hours after the shift to aerobic conditions, the growth rates indicated that cells were in the stationary phase.

Based on these results, the time points for cell harvest for proteome analyses of the inner membrane fractions were selected. Samples with an OD_{540} of 0.5 cultivated under aerobic conditions were used as control samples. Two, four, eight and sixteen hours under anaerobic conditions were chosen to cover the lag-like anaerobic phase and the later anaerobic phase, respectively. After shifting back to aerobic conditions, again two, four and eight hours of cultivation under aerobic conditions were selected to collect samples of early shifting conditions. Furthermore, sixteen hours after cultivation under aerobic conditions were selected for harvest, as cells were in the stationary phase at this point.

3.2 Identified proteins using complementary approaches

In this work, two complementary approaches have been used to prepare peripheral as well as integral membrane proteins of the inner membrane of *P aeruginosa.* Using both approaches followed by LC-MS/MS analyses, a total of 2461 proteins was identified representing 44% of the proteome encoded in the genome of *P. aeruginosa* PAO1 (App. 8.12). Of these proteins, 978 proteins (40%) were solely identified in the solubilization approach and 428 (17%) proteins were exclusively identified via the membrane shaving approach (Figure 16). Both approaches shared 1055 (43%) identified proteins.

The software LocateP v.2 was used to predict the localizations of the proteins identified by the different approaches, (Zhou, *et al.*, 2008). Accordingly, 67.4% of the proteins detected by the solubilization approach (n = 1370) were cytoplasmic proteins and only 319 (15.7%) proteins were predicted to be integrated in or associated with the inner membrane. However using the shaving approach, 46.2% of the identified proteins were predicted to localized in the cytoplasm and 36.9% to be integral and inner membrane-associated proteins.

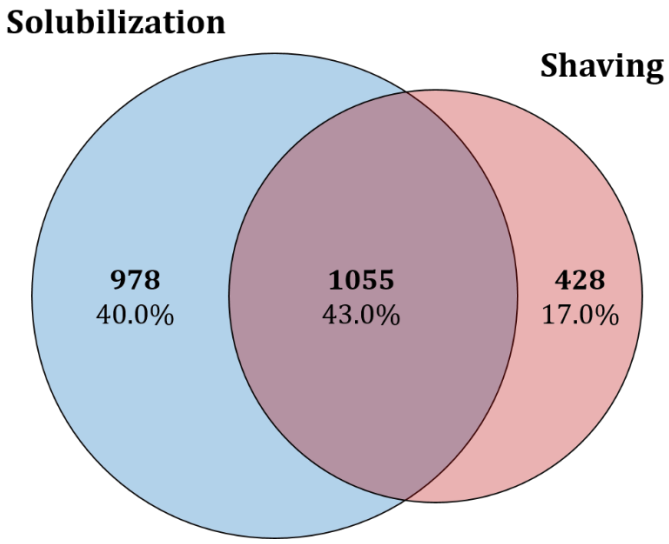

Figure 16 Number of identified proteins using the solubilization and membrane shaving approach.
Altogether, 2461 proteins were identified of which 978 (40%) proteins were solely identified using the solubilization approach. Contrary, 428 (17%) proteins were only identified via the membrane shaving approach and both approaches shared 1055 (43%) identified proteins.

Interestingly, the percentages of periplasmic, extracellular as well as OM proteins and IM associated proteins were quite similar between both approaches, while the number of integral inner membrane proteins was 1.5 times higher using the shaving approach (Figure 17).

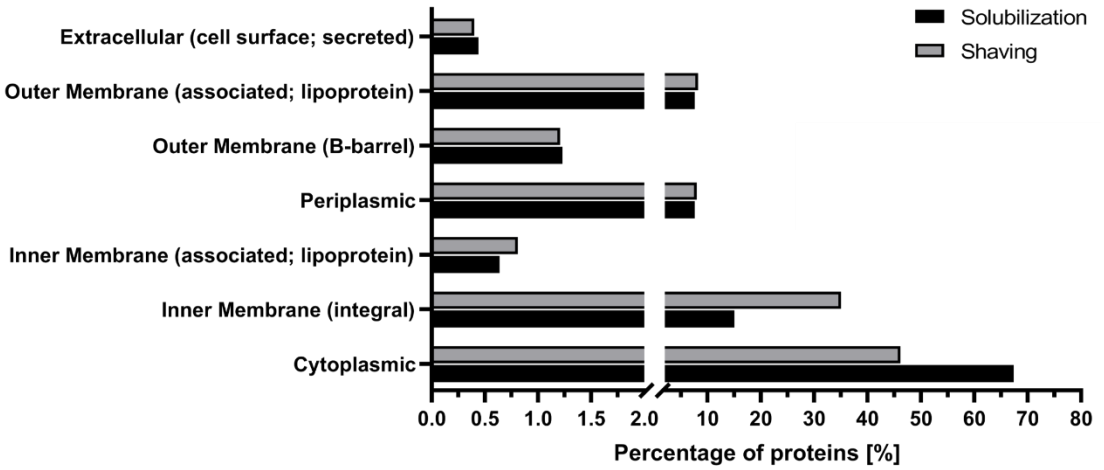

Figure 17 Predicted localizations of the identified proteins.
Predicted localizations of the identified proteins according to LocateP v.2. Using the solubilization approach (black), 1370 (67.4%) cytoplasmic proteins were identified whereas 306 (15.1%) proteins where predicted as integral inner membrane proteins. Contrary to this, 685 (46.2%) cytoplasmic proteins were identified using the shaving approach (grey) while 520 (35.1%) proteins were predicted as integral inner membrane proteins. The percentage of IM-associated, periplasmic as well as OM and extracellular proteins was similar between the solubilization and shaving approach.

Next, total protein intensities for the different predicted localizations were determined. Accordingly, the percentage of total intensities for integral IM proteins was about 60% using the shaving approach (Figure 18). In contrast, using the solubilization approach, these proteins constitute about 13% of the total protein intensity. According to the higher number of cytoplasmic proteins identified by the solubilization approach, these proteins made up almost 60% of the total protein intensity. However, using the shaving approach cytoplasmic proteins constitute only 11% of the total intensity. Furthermore, using the solubilization approach, β-barrel OM proteins and extracellular proteins contributed to the intensity of all identified proteins with a higher percentage in comparison to the shaving approach. Overall, these results clearly show, that the shaving approach supported the preparation of integral membrane proteins while the solubilization approach was more specific for soluble membrane associated proteins.

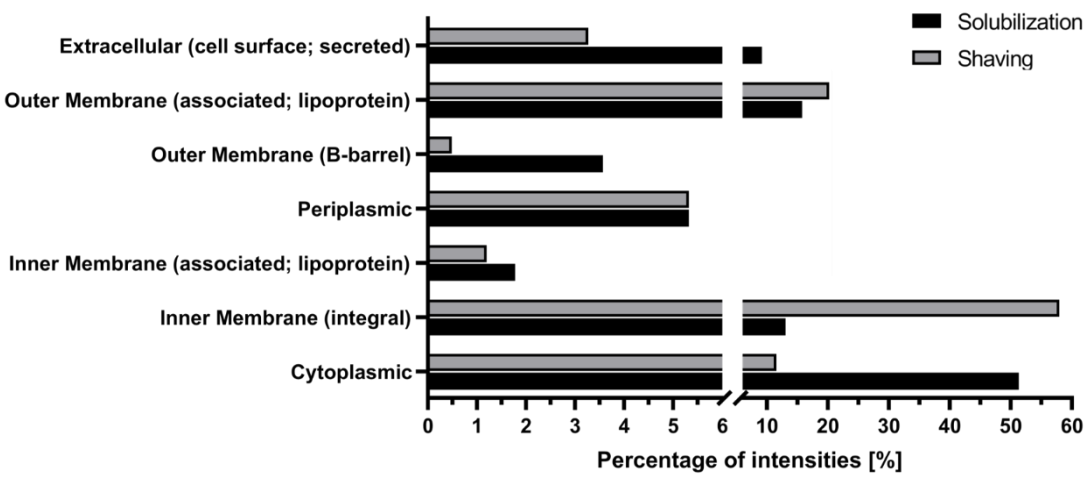

Figure 18 Intensity distribution of identified proteins with respect to their localization.
Cytoplasmic proteins represent more than 50% to the total protein intensity of the solubilization approach while the percentage of the intensity of integral IM proteins was only about 10%. Furthermore, percentage of extracellular proteins and OM beta-barrel proteins was higher in the solubilization approach compared to the shaving approach. Contrary, with 60 % of the total protein intensity integral IM proteins were significantly more abundant in in the shaving approach while here cytoplasmic proteins were significantly were significantly less abundant (11% of the total intensity). In both approaches, the intensity percentage of proteins associated with the IM and OM as well as periplasmic proteins are similar distributed.

It was expected that the shaving approach supports the identification of proteins with more than one transmembrane helices (TMHs). To confirm this hypothesis, the number of TMHs of identified inner membrane proteins was predicted using the software TMHMM Server v. 2.0 (Moller, *et al.*, 2001). Using the solubilization and shaving approach, 472 (64.0%) and 676 (91.7%) proteins were predicted to contain at least one TMH (Figure 19). Among them, 57 are proteins with more than 10 TMH identified with the solubilization approach and 115 proteins identified with the shaving approach. Overall, more proteins, predicted to contain two or more TMHs, were identified using the shaving approach. While proteins with a higher number of TMHs were also identified via the solubilization approach, the number of these proteins was at least two times higher using the shaving approach, providing again evidence for the efficiency of the shaving approach for the preparation of integral membrane proteins.

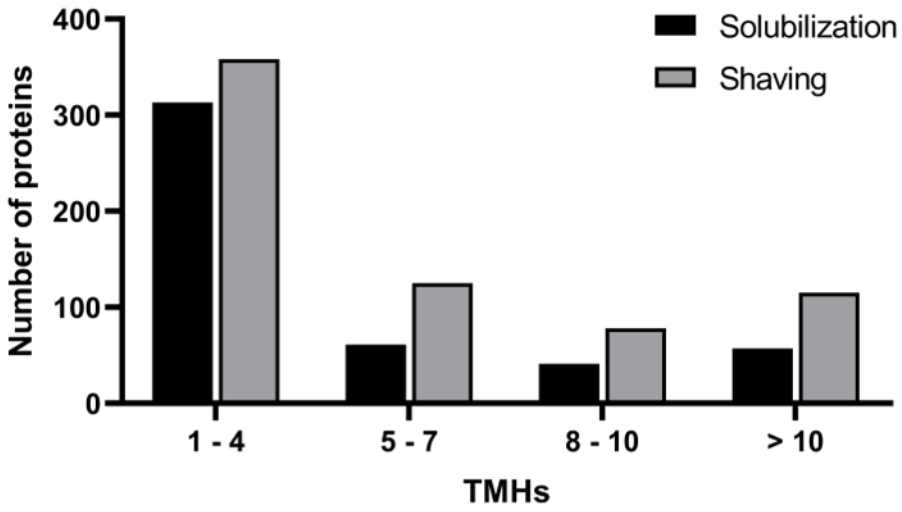

Figure 19 Distribution of proteins identified with at least one TMH.
Using the solubilization (black) and shaving (grey) approach lead to the identification of 737 proteins containing at least one TMH. Of these 472 were identified using the solubilization approach representing 64.0% to the total number of identified proteins carrying TMH. In contrast, 676 proteins (91.7%) of identified proteins carrying TMH were identified using the shaving approach. With increasing number of TMHs, the shaving approach was more efficient in identifying these proteins than the solubilization approach.

As membrane proteins are known to be more hydrophobic than cytoplasmic proteins, GRAVY scores (grand average of hydropathy) of all identified proteins were determined, with positive GRAVY values representing higher hydrophobicity (Kyte, *et al.*, 1982). Most proteins identified using the solubilization and shaving approach displayed GRAVY scores around -0.2 (Figure 20). Using the solubilization approach, 1417 proteins (69.7%) had a negative GRAVY value and are thus more hydrophilic. In contrast, using the shaving approach, 849 proteins (57.2%) also displayed negative GRAVY values. 616 (30.3%) and 634 (42.8%) hydrophobic proteins were identified using the solubilization and shaving approach, respectively, which was represented by positive GRAVY values. Overall, the percentage of hydrophobic proteins was higher in the shaving approach than in the solubilization approach. The obtained results support to the expectations, that the shaving approach supports the identification of integral membrane proteins.

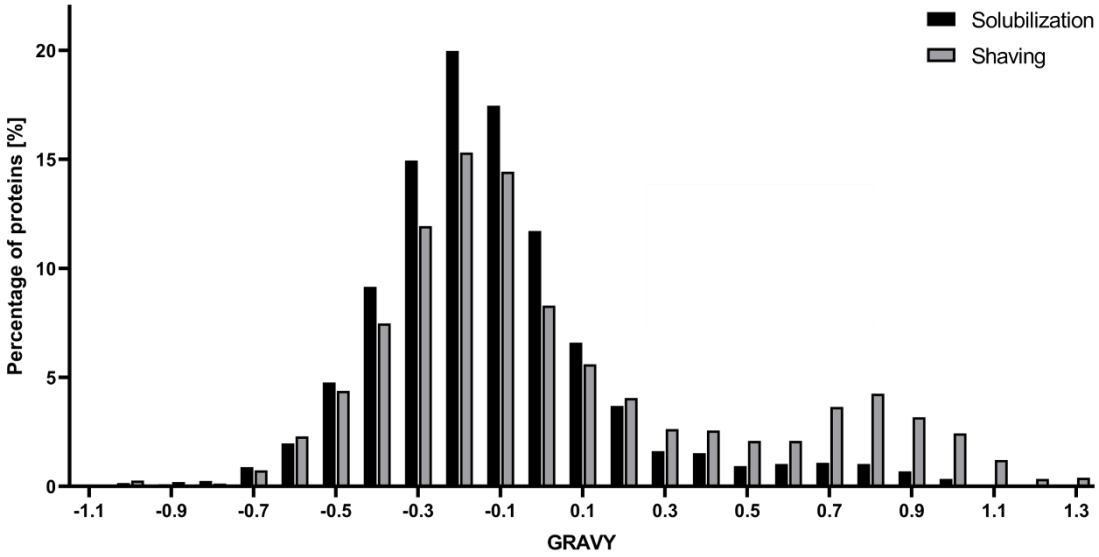

Figure 20 GRAVY distribution of all identified proteins.
GRAVY values of all identified proteins using the solubilization (black) and shaving (grey) approach. In both approaches, most proteins are characterized by a GRAVY value of -0.2. Using the solubilization approach, 1417 proteins (69.7%) displayed negative GRAVY scores and were thus hydrophilic. Using the shaving approach, only 57.2% of the identified proteins (n= 849) were hydrophilic. Of both the solubilization and the shaving approach, 616 (30.3%) and 634 (42.8%) hydrophobic proteins were identified indicated by positive GRAVY values, respectively. Altogether, a higher percentage of hydrophobic proteins was identified using the shaving approach in comparison to the solubilization approach.

Altogether, 737 integral inner membrane proteins were identified making up 48% of all known membrane proteins of *P. aeruginosa*. By combining two complementary preparation methods after the separation of the membrane fractions, almost half of the proteins currently predicted to be either associated with or integrated into the membrane in *P. aeruginosa* have been identified. The results corroborate the suitability of the membrane shaving approach for the preparation of both membrane associated and integrated proteins. Interestingly, a high number of cytoplasmic proteins were also identified with the shaving approach and the question still remains whether they are simply 'contaminants' that were not fully removed during sample preparation. Another explanation might be, that these cytoplasmic proteins are tightly interacting with integral membrane proteins and thus were prepared and identified. Furthermore, deficiencies in the prediction of the localization cannot be fully excluded; for instance 76 of the identified proteins were assigned to cytoplasmic proteins using the LocateP algorithm while TMH analyses predicted one or more TMHs (Table 13). A detailed list of predicted cytoplasmic proteins containing at least one TMH is displayed in App. 8.7.

Table 13 Number of identified TMHs in proteins predicted to be localized in the cytoplasm .
Localizations were predicted using LocateP v.2; TMHs were predicted using TMHMM Server v. 2.0. Overall, 1509 identified proteins were predicted as cytoplasmic proteins using LocateP. For the 76 at least one TMH was identified by TMHMM algorithm.

pred. localization (LocateP v.2)	pred. TMHs (TMHMM v.2.0)	proteins
Cytoplasmic	0	1433
	1	73
	4	1
	5	1
	6	1

Furthermore, both approaches led to the identification of a high number of OM associated proteins, even though inner and outer membrane fractions were separated beforehand. Here, it is possible that proteins, which are associated to the OM facing the periplasm, are also part of a larger protein complex not fully disintegrated during sample preparation. Such interactions were observed in previous studies between the FliC protein and NirS indicating that this complex is necessary for flagellum formation (Borrero-de Acuña, *et al.*, 2017).

3.3 Analyses of proteins of the respiratory complex

Under aerobic conditions, *P. aeruginosa* utilizes oxygen as the primary electron acceptor for the generation of ATP via the respiratory complex. At least five protein complexes are working interconnected to ensure a stable electron transfer. In this work, 44 of 49 proteins were identified that are known to be involved in aerobic respiration. Of these, 26 proteins were predicted to contain one or more TMHs and most proteins of the respiratory complex were identified using both approaches. In many cases, the shaving approach was slightly more efficient regarding the identification of proteins that carried one or more transmembrane helices.

Altogether, complex I, complex III and complex V play a significant role during aerobic and anaerobic respiration. Thus it was expected that proteins of these complexes were minor or unchanged in their amounts under aerobic and anaerobic cultivation. Complex II, the succinate dehydrogenase was expected to decrease in its amount under anaerobic conditions due to the reduced activity of the TCA cycle. Regarding the terminal oxidases that comprise the complex IV of the respiratory complex it was expected to primarily observe the oxidases Cco1 and Cco2 under aerobic and anaerobic conditions, respectively. The oxidases Cox and Cyo were expected to be present in higher amounts after shifting back to aerobic conditions as these oxidases are primarily present under nutrient starvation conditions.

3.3.1 Complexes I, III and V provide the core complex for respiration

As described previously, the NADH dehydrogenase, the cytochrome bc_1 complex and the ATP synthase are involved in respiration under both aerobic and anaerobic conditions. Thus, it was expected to observe only few changes in the expression of the proteins of the corresponding complexes. Most subunits of the complexes I, III and V were identified with both the solubilization and the shaving approach (Figure 21). Of complex I, the membrane resident subunits NuoA, NuoH, and NuoJKLMN were present in higher amounts under aerobic control conditions compared to the cytoplasmic subunits NuoBCDEFGI. After shifting back to aerobic conditions, proteins of complex I decreased in their amount also indicating a decrease of the amount of total NDH-1 protein complexes in the membrane.

A similar behavior was observed for the complexes III and V, the cytochrome bc_1 complex and the ATP synthase, respectively (Figure 21). Here, results from the shaving approach displayed high abundances for all three proteins of the cytochrome bc_1 complex after two hours of cultivation under anaerobic conditions, which than decreased during the remaining time and remained consistently low after shifting to aerobic conditions. It was shown that the cytochrome bc_1 complex is also involved in denitrification by mediating electrons to the cytochromes of the nitrite reductase NirM and NirC. Thus the observed kinetic profiles support an involvement of the cytochrome bc_1 complex during aerobic and anaerobic respiration (Hasegawa, *et al.*, 2003).

Regarding the proteins of the ATP synthase, the AtpI protein, which is predicted to be important for the assembly and stability of ATP synthase complex was not identified. However, this protein possesses four TMHs and it should have been possible to prepare it during the membrane shaving approach. Altogether, the subunits AtpFEB, comprising the hydrophobic part of the ATP synthase, displayed different protein kinetics than the proteins AtpCDGAH, which build the hydrophilic part. Here, results of the shaving approach showed proteins of the hydrophilic part in high abundance after two hours of cultivation under anaerobic conditions, followed by a decrease in their amount afterwards. Contrary, the three subunits that build the hydrophobic part displayed low amounts during cultivation under denitrifying conditions which than increased in their amount after shifting back to aerobic conditions.

Altogether, the obtained results showed that the proteins of the three complexes NDH-1, the cytochrome bc_1 complex and the ATP synthase were unchanged in their amount under aerobic and anaerobic conditions as expected. These findings indicate that these three complexes build the core complex of respiration independently of oxygen availability and growth phase. Furthermore, the succinate dehydrogenase remained low abundant even after shifting back to aerobic conditions indicating that cells were indeed already in the stationary phase indicating a depletion of nutrients.

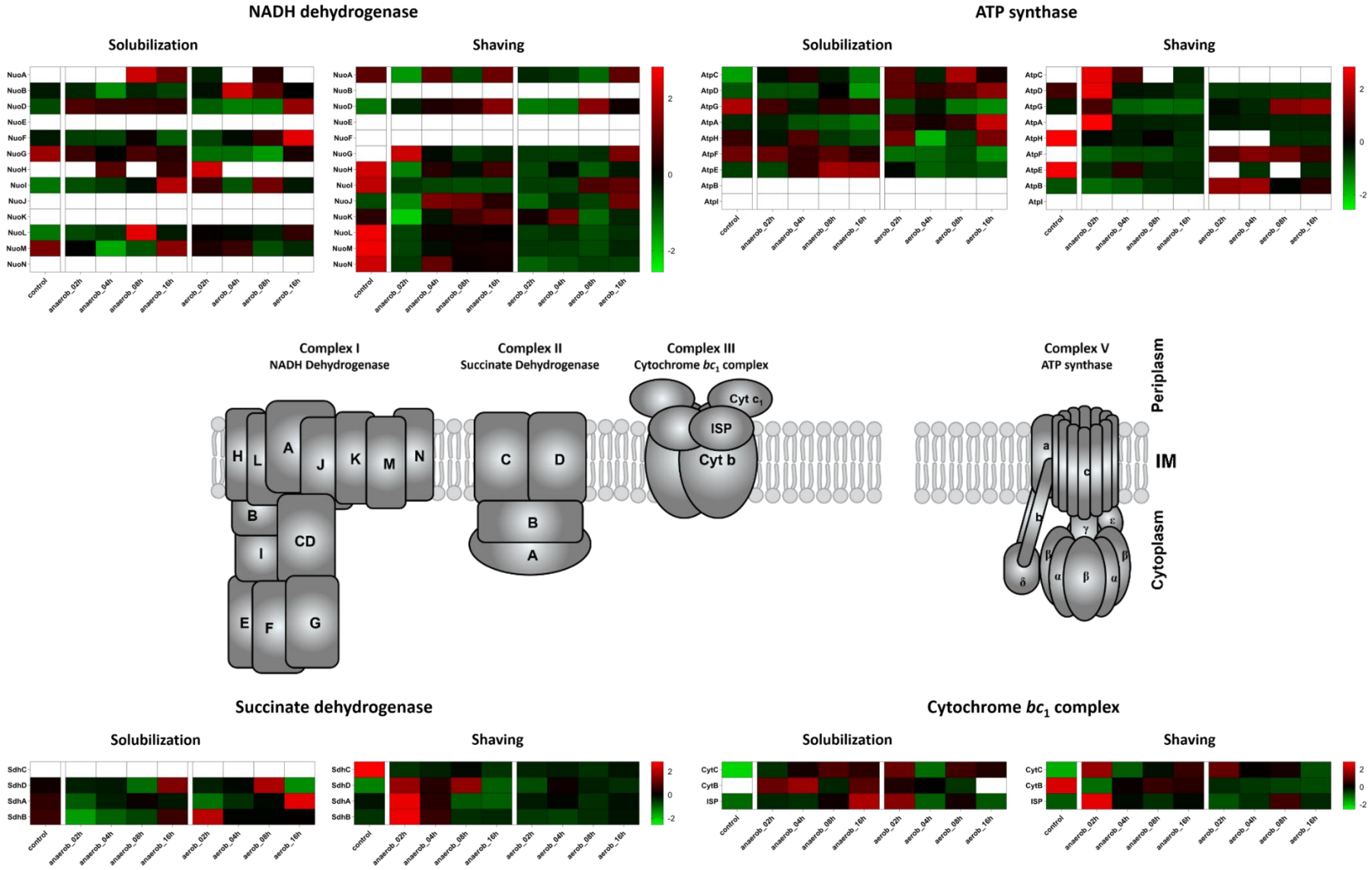

Figure 21 Kinetic profiles of complexes I, II, III and V of the respiratory chain of *P. aeruginosa* under aerobic and anaerobic conditions.
Z scores of normalized protein intensities ranging from 2.826 (red) to -2.563 (green), the baseline was set to 0 (black) and proteins that were not identified were displayed as an empty cell (white).

3.3.2 Succinate dehydrogenase during anaerobic conditions

For proteins of complex II, the succinate dehydrogenase, different kinetic profiles were observed. Three of the four subunits of the succinate dehydrogenase were identified with both approaches, while the C subunit, one of the two transmembrane subunits, was solely identified using the shaving approach (Figure 21). Interestingly, only the C subunit was highly abundant in the control samples, whereas the remaining Sdh proteins were identified in higher amounts after two hours of cultivation under anaerobic condition. Subsequently, the amount of all Sdh subunits decreased over the remaining time under anaerobic conditions and remained at a constant low level after shifting back to aerobic conditions. However, it was unexpected to observe higher amounts of subunits of complex II under anaerobic conditions.

The succinate dehydrogenase connects the TCA cycle with the aerobic respiration. In *E. coli*, the expression of the *sdhCDAB* genes is higher under aerobic conditions while under anaerobic conditions, expression of the *sdh* genes is about 10-fold lower also implying a reduced activity of the TCA cycle under anaerobic conditions (Park, *et al.*, 1995). In addition to the SDH, *E. coli* possesses a quinole:fumarate dehydrogenase (QFR) that catalyzes the reverse reaction under anaerobic conditions using fumarate as an alternative electron acceptor (Lancaster, 2002). Contrary to *E. coli, P. aeruginosa* does not possess a QFR. Here, the roles of SDH and QFR seem to be performed by a single succinate dehydrogenase as also observed in *Campylobacter jejunii* as no QFR homologue has been identified so far (Weingarten, *et al.*, 2009). In addition, it was also proposed that fumarate promotes TCA cycle activity resulting also in an increase of reduced electron carriers that drive the electron transport chain (Meylan, *et al.*, 2017). Based on this, the observed protein kinetics under anaerobic conditions of the SDH might be the result of the aftermath of the higher TCA activity under aerobic conditions. Intracellular fumarate levels might have been high enough to induce SDH activity resulting in the observed protein 'peak' after two hours of cultivation under denitrifying conditions.

3.3.3 Complex IV composition is influenced by oxygen availability

Complex IV implies one or more terminal oxidases of these *P. aeruginosa* contains five different enzymes in total. Both, the cbb_3-type oxidases Cco1 and Cco2 are known to be important for aerobic respiration and Cco1 is constitutively expressed under these conditions. Interestingly as displayed in Figure 22, not all subunits of Cco1 and Cco2 were identified during aerobic control conditions and again, the results from the solubilization and shaving approach differ from each other. The Results from the solubilization approach showed that most subunits of Cco1 and Cco2 were present in low amounts in control samples while their amount increased during cultivation under anaerobic conditions. Contrary to this, the results of the shaving approach displayed most subunits abundant during control conditions while decreased during cultivation under denitrifying conditions. Altogether, the observed kinetic profiles of both approaches might indicate that both Cco1 and Cco2 were fully assembled and integrated in the membrane after shifting to anaerobic conditions. However, results of both approaches showed an increase of the subunits P1, Q1, O1 as well as P2, Q2 and O2 after shifting to aerobic conditions.

The third terminal oxidase, the bo_3 oxidase was almost exclusively identified via the shaving approach. Furthermore, the CyoE protein that is required for the production of heme *o* was not identified with neither approach. While the bo_3 oxidase has a lower oxygen affinity than Cco1 and Cco2, it was also present in high amounts during aerobic control conditions. Interestingly, all subunits of the bo_3 oxidase Cyo remained abundant during the first two time points of anaerobic cultivation while their amount decreased after eight hours of cultivation under denitrifying conditions. After shifting to aerobic conditions, the amount of Cyo subunits further decreased and remained low over all time points.

Similarly to the bo_3 oxidase Cyo, the aa_3 oxidase Cox also has a lower oxygen affinity than Cco1 and Cco2. Of the terminal oxidase Cox, only CoxB and CoxA were identified solely with the shaving approach. Interestingly, the Cox11 and CoIII subunits were not identified, even though both were predicted with one and eight TMHs, respectively and thus should have been identified with the shaving approach. Analyses revealed that both Cox11 and CoIII were identified by only one

unique peptide (length of larger than 100 aa) and did not met the criteria to be reliably identified. Contrary to the kinetic profile of Cyo, CoxB and CoxA of the aa_3 oxidase displayed low abundancies during control conditions as well as after two and four hours of cultivation under denitrifying conditions. However, after eight hours of growth under denitrifying conditions the amount of both CoxB and CoxA increased and remained high until shifting to aerobic conditions. After that shift, the amount of both subunits decreased and remained constantly low during this period of aerobic cultivation.

Surprisingly, both subunits of the cyanide-insensitive cytochrome *bd* oxidase Cio were high abundant during control conditions and rapidly decreasing in their amount after shifting to denitrifying conditions. After shifting back to aerobic conditions, both subunits did not increase in their amounts.

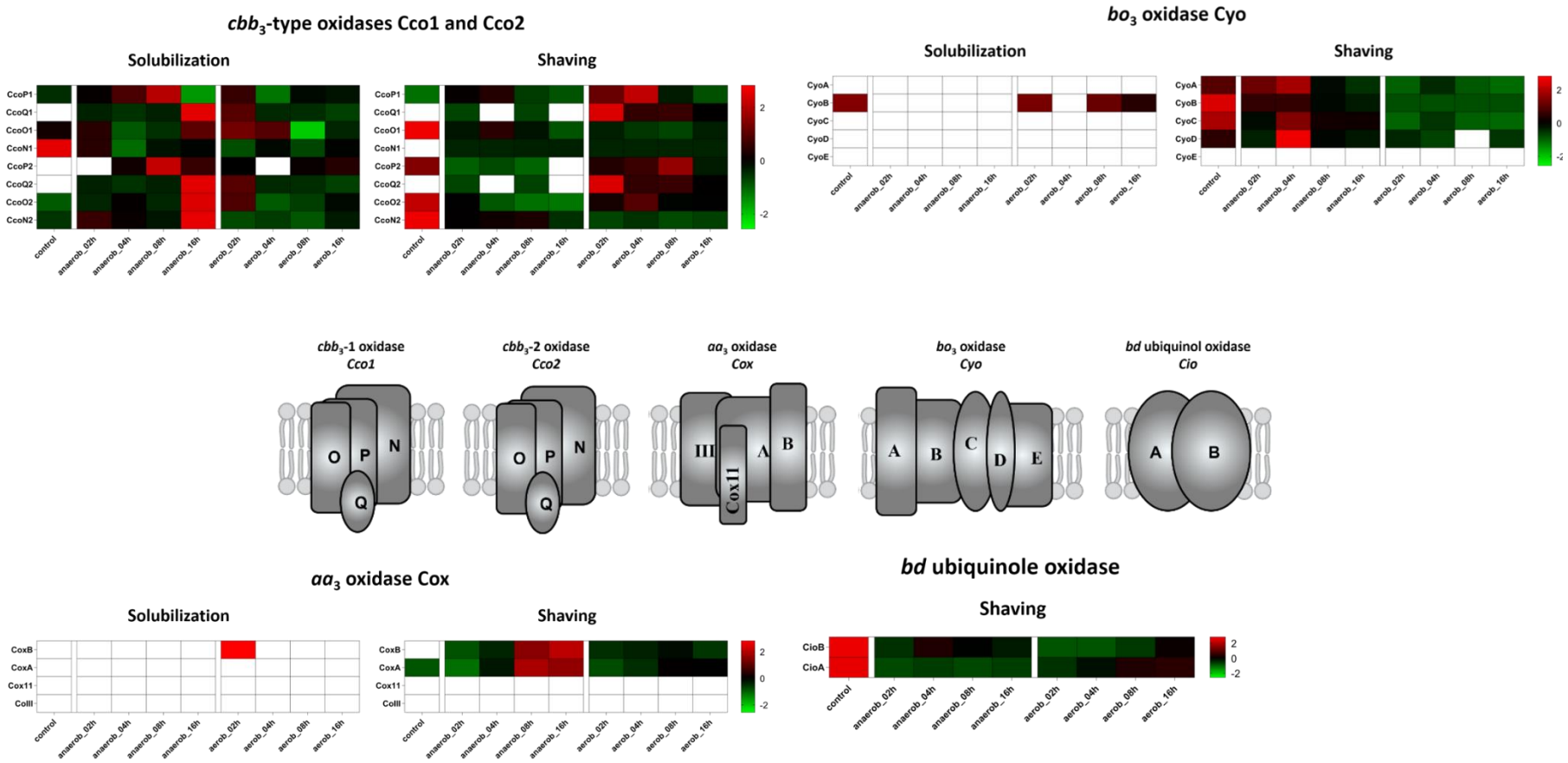

Figure 22 Kinetic profiles of currently known terminal oxidases of *P. aeruginosa* under aerobic and anaerobic conditions.
Z scores of normalized protein intensities ranging from 2.826 (red) to -2.563 (green), the baseline was set to 0 (black) and proteins that were not identified were displayed as an empty cell (white). Both subunits of the cyanide-insensitive oxidase Cio were exclusively identified using the shaving approach.

Altogether, the obtained results indicated that the composition of complex IV of the respiratory chain changes depending on the oxygen availability and the growth phase. Arai *et al.,* (2011) suggested the following model for the regulation of terminal oxidases of *P.* aeruginosa (Figure 23).

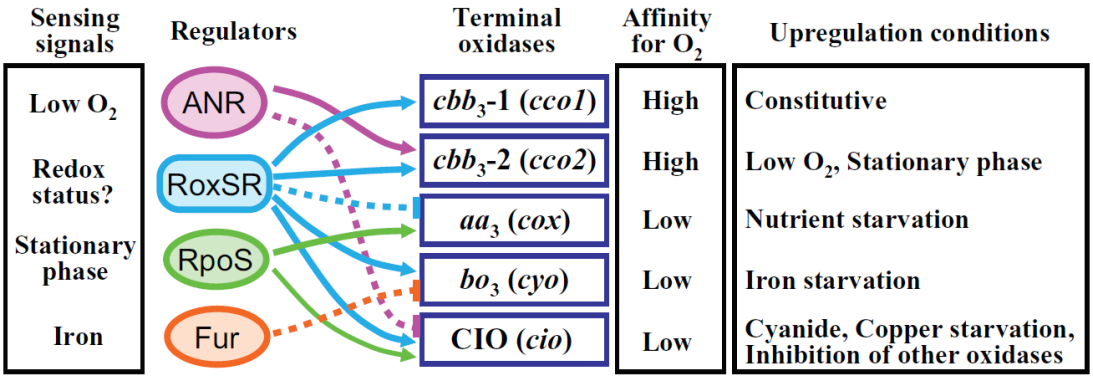

Figure 23 Suggested model of the regulatory network of the terminal oxidases in *P. aeruginosa* (adapted from Arai *et al.,* 2011).
Signals for the regulators are shown in the left column. Activation is indicated by arrows and bars with dotted lines indicate inhibition. Subsequently, oxygen affinity and upregulation conditions of the terminal oxidases are shown in the right columns.

Anr as the primary regulator for anaerobiosis was found to activate the expression of *cco2* genes and also inhibit the expression of *cio* (Comolli, *et al.*, 2004). Based on this, it was expected that Cco2 was also present in higher amounts under anaerobic conditions however a different kinetic profile was observed.

Furthermore, the stationary phase sigma factor RpoS and the RoxRS system were both found to be involved in the expression of the terminal oxidases (Kawakami, *et al.*, 2010). RpoS was observed to activate the expression of both *cox* and *cio* genes. The RoxRS system positively regulates the expression of the *cco1*, *cco2*, *cyo* and *cio* genes while the expression of *cox* is negatively regulated (Comolli, *et al.*, 2002) (Cooper, *et al.*, 2003). While RpoS was not identified, RoxR and RoxS were identified with both approaches. The RoxRS two-component system of *P. aeruginosa* is related to the PrrAB system of *Rhodobacter spaeroides* that regulates photosynthesis, CO_2 fixation and elements of the electron transport chain in response to the redox status (Dubbs, *et al.*, 2006). In *P. aeruginosa,* RoxR is the response regulator encoded by PA4493 and is co-transcribed with PA4494, which encodes the cognate sensor histidine kinase RoxS (Comolli, *et al.*, 2002). The response regulator RoxR was present in higher amounts during cultivation under anaerobic conditions and its amount decreased after shifting back to aerobic

conditions (Figure 24). The histidine kinase RoxS however remained low during denitrifying conditions and was later abundant after shifting to aerobic conditions.

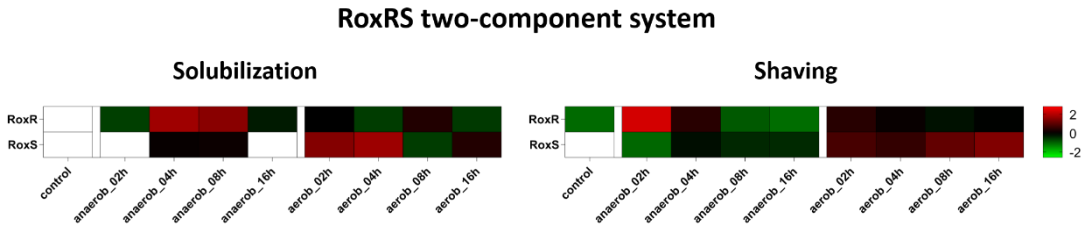

Figure 24 Kinetic profiles of the response regulator RoxR and the cognate histidine kinase RoxS.
Z scores of normalized protein intensities ranging from 2.826 (red) to -2.563 (green), the baseline was set to 0 (black) and proteins that were not identified were displayed as an empty cell (white). While the response regulator RoxR was present in higher amounts during cultivation under denitrifying conditions, the amount of the cognate histidine kinase RoxS remained low. After shifting to aerobic conditions, RoxR decreased in its amount while RoxS was high abundant.

As previously reported, expression of the *cox* genes is repressed by RoxR as observed in this work. Furthermore, expression of the genes of the remaining terminal oxidases was reported to be induced by RoxR, this also confirms the observed kinetic profiles of the terminal oxidases Cco1, Cco2 and Cyo (Kawakami, *et al.*, 2010).

Interestingly, the results obtained in this work displayed not the proposed correlation between RoxRS and Cio. Furthermore, Cio was expected to be present in higher amounts in the stationary phase though the amount of both CioA and CioB remained low after the aerobic shift, where results of the growth experiment clearly showed stationary behavior. Here, the cbb_3-type oxidase Cco1 might influence the expression of the *cioAB* genes as their expression was observed to be inhibited by Cco1 (Comolli, *et al.*, 2004). Cco1 was found in relative low amounts during control conditions and thus expression of *cio* genes was unhindered. After shifting back to aerobic conditions, Cco1 was present in higher amounts and thus might have inhibited the expression of c*ioAB*.

Even though the mechanism of how Cco1 might inhibit *cio* gene expression is not known yet, this work shows a correlation between the activity of both terminal oxidases. It is assumed that Cyo and Cox are partly involved in denitrification and might take over the role of Cco1 and Cco2 during anaerobic conditions, further studies need to be performed to clarify the regulatory interactions of the terminal oxidases under aerobic and anaerobic conditions.

3.3.4 Orphan cytochrome *c* oxidases

Besides the two isoforms of the *cbb*$_3$-type cytochrome *c* oxidase Cco1 and Cco2 *P. aeruginosa* possesses two additional orphan *ccoNQ* genes clustered in the operons PA1856 - PA1855 and PA4133 - PA4134, respectively. CcoN3 and CcoN4 are each 78 aa and 75 aa long and sequence analyses showed high sequence similarities to their well characterized isoforms CcoN1 and CcoN2, as displayed in Figure 25 A. In contrast, CcoQ3 and CcoQ4 are longer than CcoQ1 and CcoQ2 and displayed only few sequence similarities, as shown in Figure 25 B. Additionally, CcoQ1 and CcoQ2 both possess one transmembrane helix and are localized at the inner membrane while ccoQ3 and ccoQ4 are predicted to be localized in the periplasm.

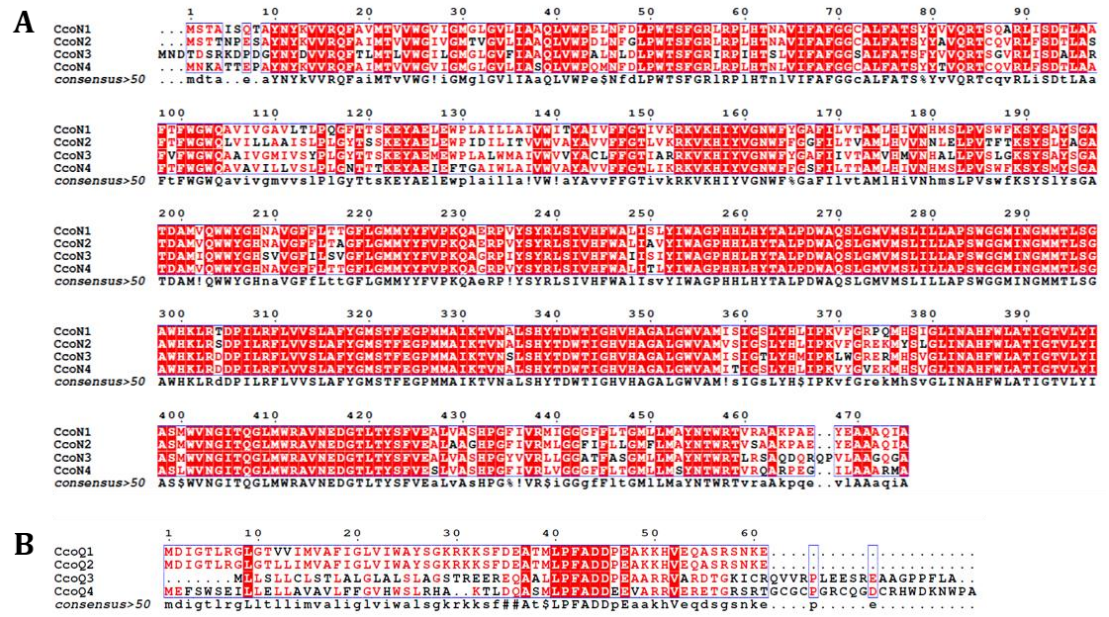

Figure 25 Sequence alignment of the orphan CcoNQ proteins in *P. aeruginosa* with annotated CcoNQ.
Sequences were analyzed using the MultAlin website followed by alignment visualization vie ESPrint 3.0. **A**) Sequence alignment of CcoN1 and CcoN2 of the annotated cbb3-type oxidases and the CcoN3 and CcoN4 subunits of the orphan *ccoNQ* genes. **B**) Sequence alignment of CcoQ1 and CcoQ2 of the annotated *cbb*$_3$-type oxidases and the CcoQ3 and CcoQ4 subunits of the orphan *ccoNQ* genes.

Recently it was observed that the gene products of *ccoNQ3* and *ccoNQ4* could produce active isoforms of *cbb*$_3$ oxidases in combination with CcoO1 or CcoO2 and CcoP1 or CcoP2 respectively (Hirai, *et al.*, 2016). While *ccoN3* was found to be expressed under aerobic conditions in the presence of nitrite, *ccoN4* expression was described higher during exponential growth under aerobic conditions in the presence of cyanide or in the stationary phase. In this work, both CcoN3 and CcoN4 subunits were identified, but not the corresponding CcQ3 and CcoQ4 subunits,

respectively. CcoN3 was present in low amounts during cultivation under denitrifying conditions while the amount increased after shifting back to aerobic conditions (Figure 26).

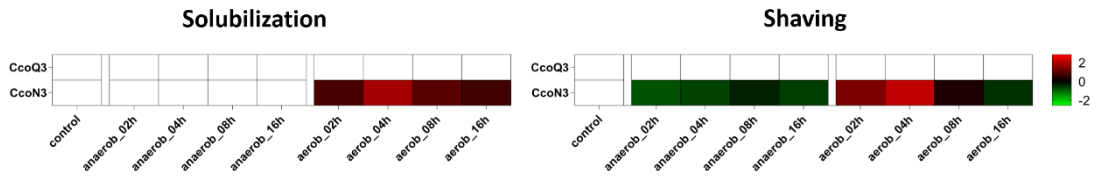

Figure 26 Kinetic profiles of the orphan subunits of the *cbb*$_3$ oxidase CcoNQ3.
Z scores of normalized protein intensities ranging from 2.826 (red) to -2.563 (green), the baseline was set to 0 (black) and proteins that were not identified were displayed as an empty cell (white). Only the CcoN3 subunit was identified while the CcoQ3 subunit was not identified neither with the solubilization nor the shaving approach. CcoN3 was low abundant during cultivation under denitrifying conditions and increased in amount after shifting back to aerobic conditions.

A similar kinetic was observed for CcoN4, with increased amounts eight hours after shifting back to aerobic conditions (Figure 27). The kinetic profiles of CcoN3 and CcoN4 further confirmed the by Hirai *et al.,* (2016) reported expression conditions, as cells were in the stationary phase after shifting to aerobic conditions. Whether *ccoN3* was expressed due to non-metabolized nitrite or due to the influence of the stationary phase remains unclear and further experiments need to confirm the assumed expression conditions.

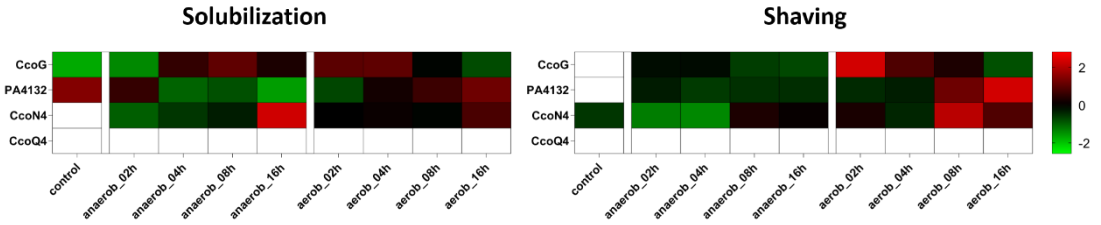

Figure 27 Kinetic profiles of the orphan subunits of the *cbb*$_3$ oxidase CcoNQ4 and adjacent proteins.
Z scores of normalized protein intensities ranging from 2.826 (red) to -2.563 (green), the baseline was set to 0 (black) and proteins that were not identified were displayed as an empty cell (white). Only the CcoN4 subunit was identified while the CcoQ4 subunit was not identified neither with the solubilization nor the shaving approach. CcoN4 was low abundant during cultivation under denitrifying conditions and directly after shifting back to aerobic conditions while the amount increased eight hours after the shift. In addition, proteins encoded by genes adjacent of the *ccoNQ4* operon displayed similar kinetics as CcoN4.

In addition to these findings, the proteins downstream of *ccoNQ4* encoded by the genes PA4131 and PA4132 increased in amount after shifting to aerobic conditions. Moreover, the kinetic profile of the protein encoded by PA4132 was similar to the kinetic profile observed for CcoN4 leading to the assumption that these proteins might be also involved in respiration during stationary phase.

PA4131 encodes a putative iron-sulfur protein and shows high sequence similarity to PA1551 that encodes a ccoG-like protein important for the assembly of cbb_3-type oxidases. CcoG is organized in the *ccoGHIS* operon (PA1551 - PA1548), which is known to be localized in close proximity to the cbb_3-type oxidase encoding operon (Pawlik, *et al.*, 2010). While the exact function of the four corresponding proteins is unclear, it can be assumed that they are involved in either cofactor insertion or assembly of the cbb_3-type oxidases (Koch, *et al.*, 2000).

The GntR family transcriptional regulator also known as HTH-type transcriptional regulator NorG, encoded by the gene PA4132 showed the same kinetic profile as CcoN4 indicating some involvement in the expression of cbb_3 isoforms. Moreover, the sequence of PA4132 appears highly conserved among various Pseudomonas species. However, there is nothing known about the physiological role of this regulatory protein though the description NorG is hinting towards some involvement in denitrification.

The obtained results confirm the presence of two additional pairs of CcoNQ subunits and the involvement of these during aerobic respiration, as reported by Hirai *et al.,* (2016). Furthermore, it seemed reasonable that these subunits are involved in respiration during stationary phase and thus enable *P. aeruginosa* to switch terminal oxidases depending on oxygen availability and growth phase. In addition, with a variety of CcoNQ-containing gene clusters, it also appears comprehensible to encode additional proteins that might be involved in the assembly of varying cbb_3-type oxidases. These findings making the genes PA41311 and PA4132 promising candidates for further studies of the respiratory system of *P. aeruginosa*.

3.4 Analyses of proteins of the denitrification apparatus

The four complexes important for anaerobic denitrification in *P. aeruginosa* consist of 29 proteins of which 26 were identified using both the solubilization and shaving approach. Only one of the six subunits of the periplasmic nitrate reductase Nap, which is primarily used for denitrification under aerobic conditions, was identified. As observed previously, the residual nitrate concentration in the medium remained constant after shifting back to aerobic conditions indicating that nitrate was not further used anymore as nitrogen source. One had also to consider that neither the solubilization nor the shaving approach was suitable for the preparation of periplasmic proteins.

As denitrification is primarily used for energy generation under anaerobic conditions it was expected that most of the reductases involved in denitrification were highly abundant during cultivation under anaerobic conditions. The corresponding proteins of each reductase were highly abundant under anaerobic conditions (Figure 28). However, proteins that are involved in maturation or assembly of the corresponding enzymes were also found to be present in higher amounts after shifting back to aerobic conditions.

Proteins encoded in the *narK$_1$K$_2$GHJI* operon were observed highly abundant under anaerobic conditions and their amount decreased significantly after shifting back to aerobic conditions. These observed kinetic profiles further indicated that nitrate was reduced under anaerobic conditions and after shifting to aerobic conditions, cells relied on aerobic respiration instead of the reduction of nitrate correlating with the previously determined nitrate concentrations (Figure 15).

Altogether, proteins of the nitrite reductase Nir, the nitric oxide reductase cNor and the nitrous oxide reductase Nos showed similar kinetic profiles. All three reductases were low abundant or not present during control conditions. Under anaerobic conditions however, proteins of all three reductase were identified and also present in higher amounts. After shifting back to aerobic conditions, the amount of the corresponding proteins decreased.

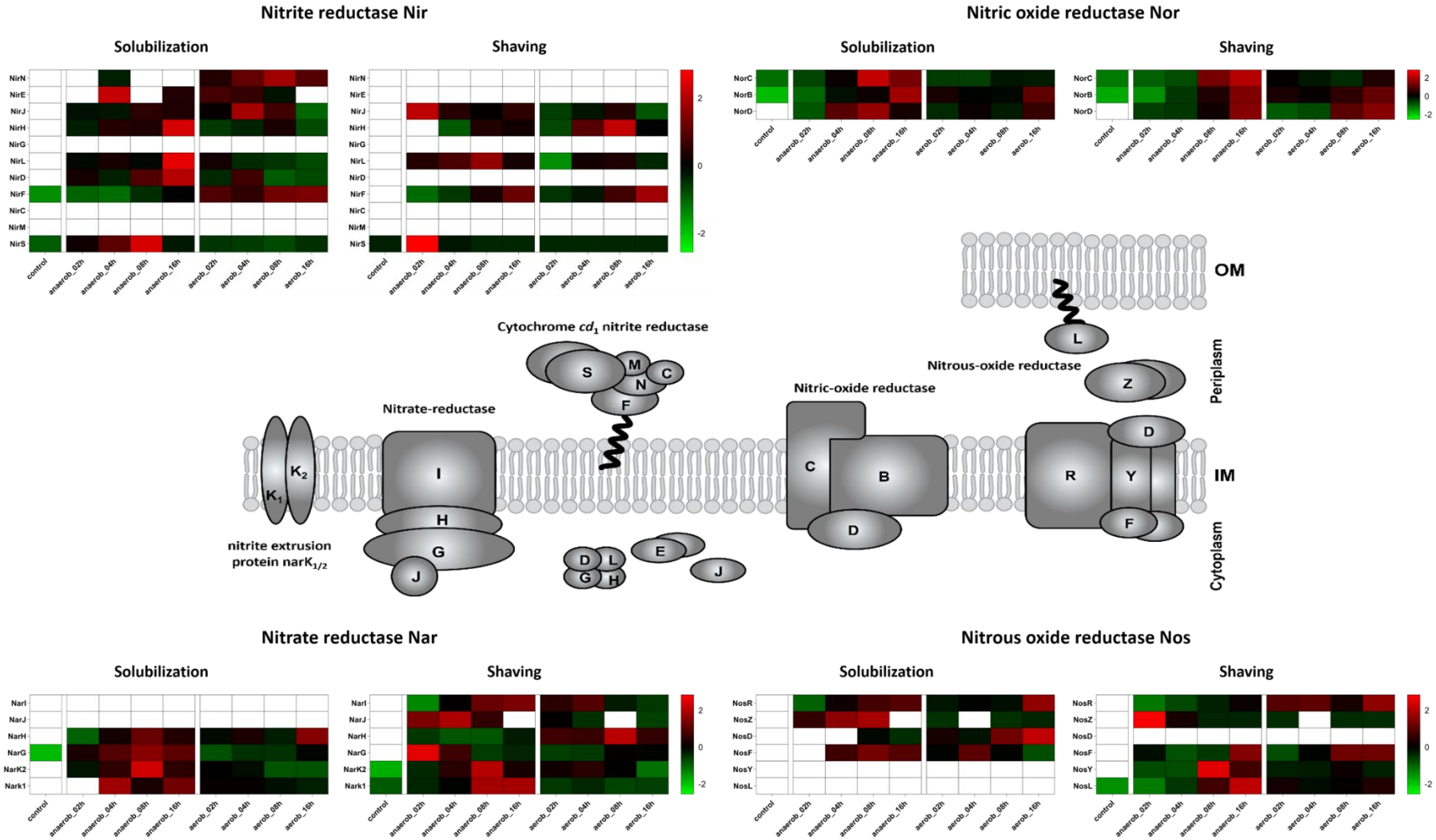

Figure 28 Kinetic profiles of proteins involved in denitrification of *P. aeruginosa* under aerobic and anaerobic conditions.
Z scores of normalized protein intensities ranging from 2.826 (red) to -2.563 (green), the baseline was set to 0 (black) and proteins that were not identified were displayed as an empty cell (white).

3.4.1 Additional roles of NirN and NirF

As expected, the nitrite reductase NirS was highly abundant during cultivation under denitrifying anaerobic conditions, while most of the heme d_1 biosynthesis proteins were present in higher amounts after shifting to aerobic conditions. In particular NirF and NirN displayed different kinetic profiles and their amount increased after shifting back to aerobic conditions. Furthermore, the observed kinetic profile of NirF implied additional function for this protein, in agreement with recent studies that also imply a currently unknown enzymatic activity of NirF (Klünemann, *et al.*, 2020). Regarding NirN, it is known that the protein is involved in the last step of heme d_1 biosynthesis. Cluster analyses comparing kinetic profiles of identified proteins revealed that NirN displayed a similar protein kinetic to the orphan CcoN3 subunit encoded by the gene PA1856, as shown in Figure 29. One possibility might be that the interaction between NirN and the cbb_3 oxidase isoform serve a joined role during respiration in stationary phase. However, it is also possible that the similarities are mere coincidental. Yet, further studies need to be performed to elucidate the physiological role of the new identified cbb_3 oxidase isoforms.

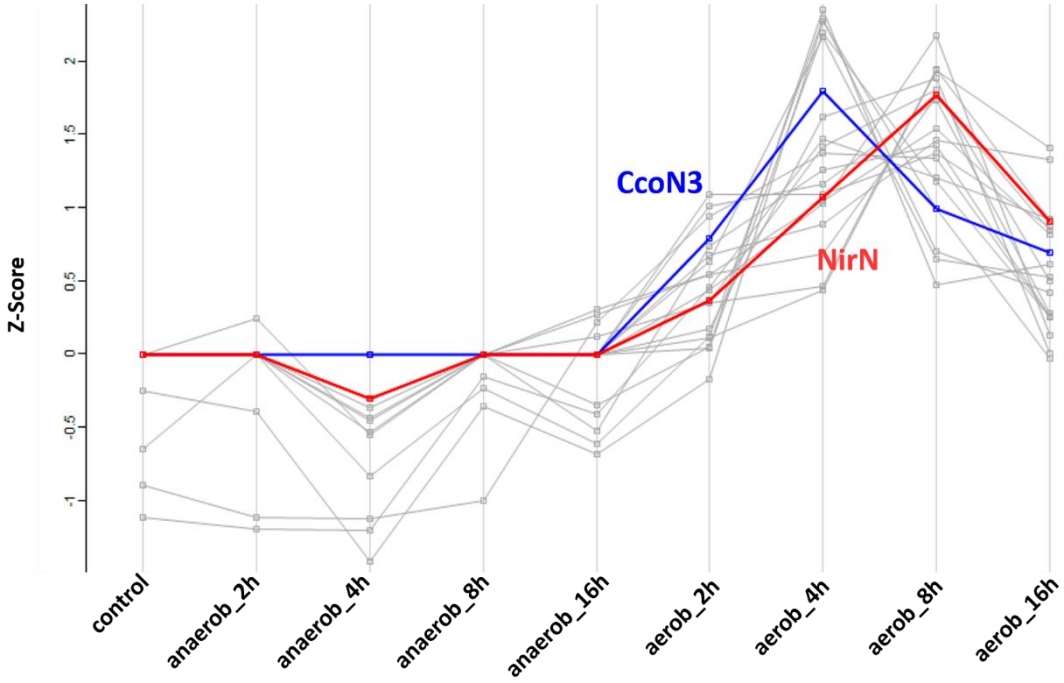

Figure 29 Cluster analysis of NirN and CcoN3 during anaerobic and aerobic cultivation.
K means clustering of the 20 most similar proteins determined via Spearman correlation distances using the kinetic profile of NirN as reference. Among the proteins with similar kinetic profile, CcoN3 (dark blue) was found to also cluster together with NirN (red).

3.4.2 Correlation between NirQOP and the nitric oxide reductase cNor

Similar to proteins of the nitrate reductase complex, the membrane-bound subunits NorC, NorB and the maturation protein NorD of the nitric oxide reductase complex were highly abundant during cultivation under anaerobic conditions. Surprisingly, NorD was also identified highly abundant eight and sixteen hours after shifting back to aerobic conditions with the shaving approach. Both proteins NirQ and NirO displayed a similar kinetic profile and interestingly, the *nirQOP* operon is located upstream of the *norCBD* operon. It was predicted that the corresponding NirQ protein is involved in cNor maturation while little is known about the proteins NirO and NirP (Hayashi, *et al.*, 1998). It was assumed that all three proteins were important only under anaerobic conditions, however as depicted in Figure 30, all three corresponding proteins of the *nirQOP* operon were highly abundant in samples after shifting back to aerobic conditions.

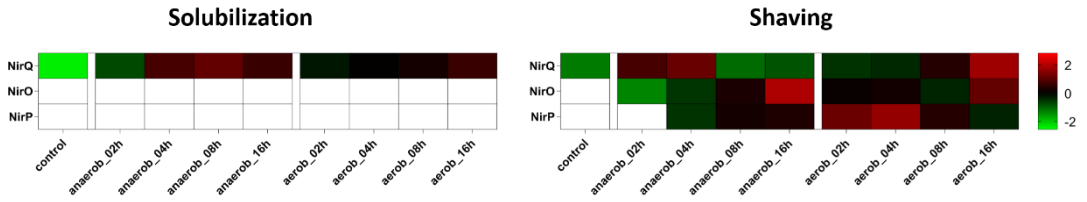

Figure 30 Kinetic profiles of proteins of the *nirQOP* operon.
Z scores of normalized protein intensities ranging from 2.826 (red) to -2.563 (green), the baseline was set to 0 (black) and proteins that were not identified were displayed as an empty cell (white). All three proteins were almost solely identified using the shaving approach. NirQ was higher abundant during early denitrification, while NirO and NirP were present in higher amounts in later stages of cultivation under denitrifying conditions. Interestingly, NirQ and NirO remained at a constant level after the return to aerobic conditions but increased after sixteen hours. In contrast, NirP was high abundant two and four hours after the shift and then decreased.

It is predicted that NirQ is localized in the cytoplasm while NirO and NirP were predicted as integral membrane proteins containing five and three TMHs, respectively. Proteins of both the *norCBD* and the *nirQOP* operon displayed quite similar protein kinetics and cluster analyses further supported a possible correlation between these proteins. Unsurprisingly as displayed in Figure 31, kinetic profiles of proteins of the *norCBD* operon clustered together and additionally, NirQ and NirO were also part of the determined clusters.

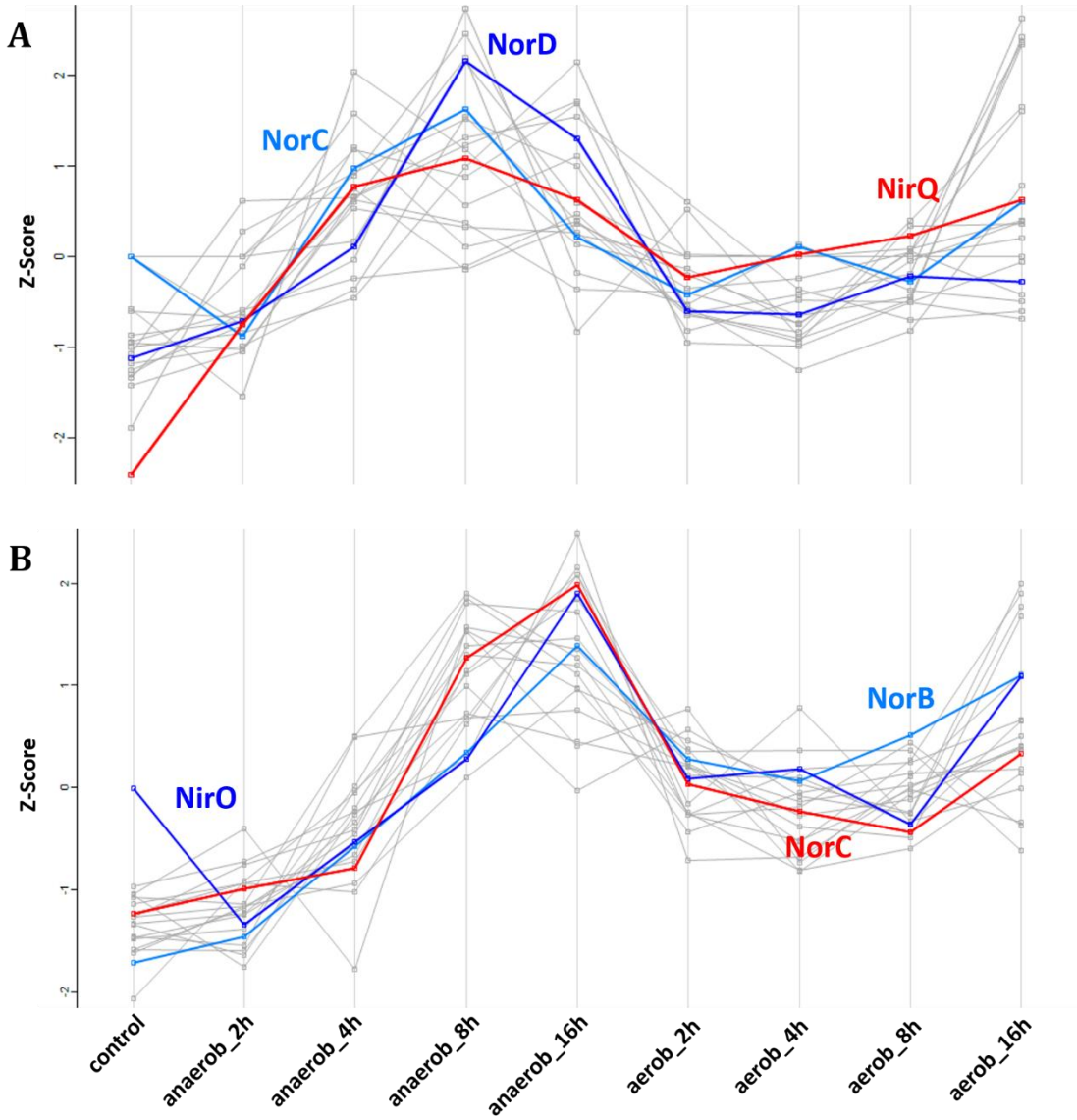

Figure 31 Cluster analyses of NirQ and NorC during anaerobic and aerobic cultivation.
K means clustering of the 20 most similar proteins determined via Spearman correlation distances using the kinetic profiles of **A**) NirQ (red) as reference. Among the proteins with similar kinetic profile, NorC (light blue) and NorD (dark blue) were found to also cluster together with NirQ. Using the kinetic profiles of **B**) NorC (red) as reference resulted in a common cluster together with NirO (dark blue) and NorB (light blue).

As observed in the denitrifying, Gram-negative bacterium *Paracoccus (Pc.) denitrificans*, the genes encoding for the nitric oxide reductase are organized in the *norCBQDEF* operon and similar to *P. aeruginosa* only NorC and NorB build the active cNor complex. Both NorQ and NorD are accessory proteins that were recently reported to be essential for cNor catalysis and to be involved in non-heme Fe cofactor insertion (Kahle, *et al.*, 2018). Furthermore, sequence analyses comparing the NorD protein of *P. aeruginosa* with the NorD protein of *Pc. denitrificans* showed that both proteins shared over 50%. These findings suggest that, on an evolutionary basis, the *norCBQDEF* operon of *Pc. denitrificans*

are equivalent to the *nirQOP* and *norCBD* operon of *P. aeruginosa*. Furthermore, comparing the sequences of NirQ, NirO and NirP with NorQ, NorE and NorF, respectively, showed also high sequence similarities between the orthologous proteins, as shown in Figure 32.

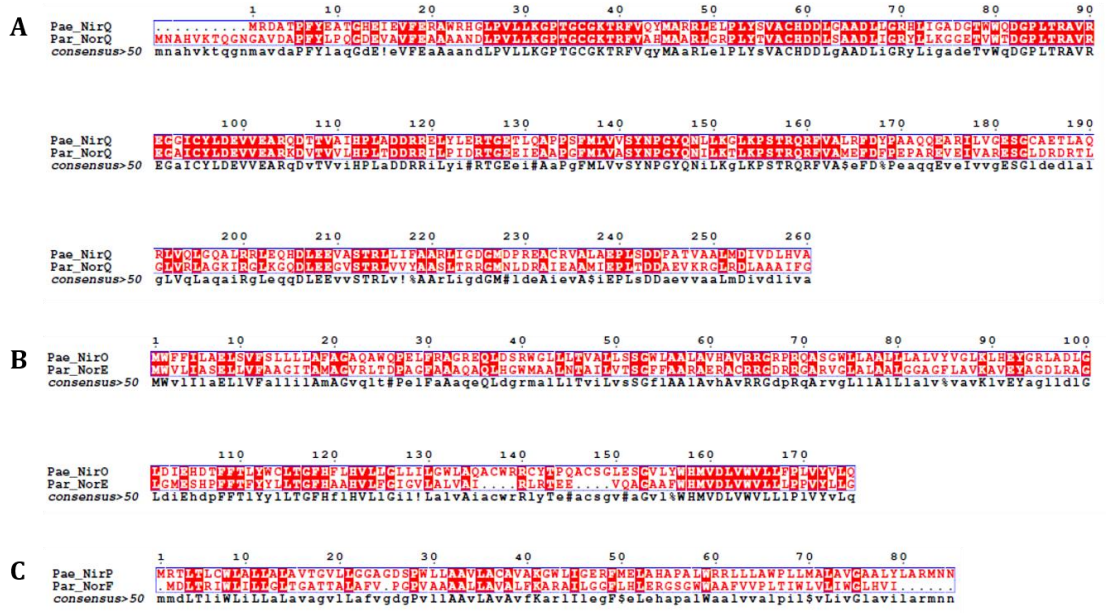

Figure 32 Sequence alignment of NirQOP of *P. aeruginosa* and NorQEF of *Pc. denitrificans*.
Sequences were analyzed using the MultAlin website followed by alignment visualization vie ESPrint 3.0. Pae = *P.* aeruginosa, Par = *Pc. denitrificans* **A**) Sequence alignment of NirQ and NorQ; **B**) Sequence alignment of NirO and NorE; **C**) Sequence alignment of NirP and NorF

In *Pc. denitrificans*, NorQ is a MoxR family protein that belongs to the AAA+ ATPases and is assumed to have chaperone-like functions primarily mediating metal cofactor insertion (Snider, *et al.*, 2006). Furthermore, the NorD protein carries a von Willebrand Factor Type A (VWA) that was shown to be involved in metal ion-dependent protein-protein interaction (Whittaker, *et al.*, 2002). Both proteins are also most likely cytoplasmic proteins like their orthologues in *P. aeruginosa.* Interestingly, both NorE of *Pc. denitrificans* and NirO of *P. aeruginosa* display similarities to the cytochrome c oxidase subunit III while both NorF and NirP show partial similarities to the cytochrome c oxidase subunit IV. Furthermore, NorF and NirP are both small proteins and predicted with two and three TMHs, respectively.

Altogether, the observed protein kinetics as well as the sequence homologies to the Nor proteins of *Pc. denitrificans* suggest that both NirQ and NorD are involved in the maturation of the nitric oxide reductase of *P. aeruginosa.* Furthermore, NirO

and NirP also seem to be involved in respiration either in the stationary phase or in response to oxygen availability. However, previous studies of the cytochrome *c* oxidase-like proteins of *P. aeruginosa* and *Pc. denitrificans* displayed contradictory results highlighting the importance of the characterization of small proteins and their role in bacteria.

3.4.3 Additional role of NosR in the regulation of NQR expression

As described previously, reductases involved in the stepwise reduction of nitrate to nitrogen were predicted to be highly abundant during cultivation under anaerobic conditions and the observed kinetic profile of the nitrous oxide reductase NosZ confirmed this. Interestingly, NosR and NosF were also found in high amounts after shifting back to aerobic conditions indicating some additional roles beyond denitrification. Furthermore, it might also be possible that these proteins remained inactive in the membrane after complex disassembly. As cytoplasmic proteins are easier degradable than integral membrane proteins, integral membrane proteins that are part of a larger protein complex might remain in the membrane or are degraded at a later timepoint than the corresponding cytoplasmic proteins.

Overall, the expression of the *nosRZDFYL* genes is Dnr dependent in the presence of NO. Furthermore, the regulatory function of NosR depends on the arrangement of the *nosR* gene and its promotor (Arai, *et al.*, 2003). Such a case was also reported for the NosR-homologue NirI of *P. denitrificans* where *nirI* is located upstream of *nirS*. Disruption of the *nirI* gene resulted in accumulation of nitrite due to the lack of Nir activity and only reintegration of *nirI* restored the effect (Saunders, *et al.*, 1999). Similar effects were observed in *P.* stutzeri, where interruption of the *nosR* gene resulted in the inability to transcribe the *nosZ* gene (Cuypers, *et al.*, 1992). Moreover, NosR, together with NorC and NorB, forms the central assembly platform for the denitrification complex giving further evidence that this protein complex is still present in the membrane even after oxygen availability has changed (Borrero-de Acuña, *et al.*, 2016).

The periplasmic part of NosR also contains an FMN binding domain like NqrC of the Na^+-translocating NADH dehydrogenase NQR. The three proteins, PA2993,

NqrF and NqrD displayed quite similar kinetic profiles compared with NosR (Figure 33). The gene PA2993 encodes a possible lipoprotein related to ApbE from *Salmonella typhimurium* that acts as a FAD:protein FMN transferase that is responsible for the FMN attachment to the corresponding protein (Beck, *et al.*, 1998). Overall, these findings might suggest that NosR is also involved in the regulation of the transcription of NQR.

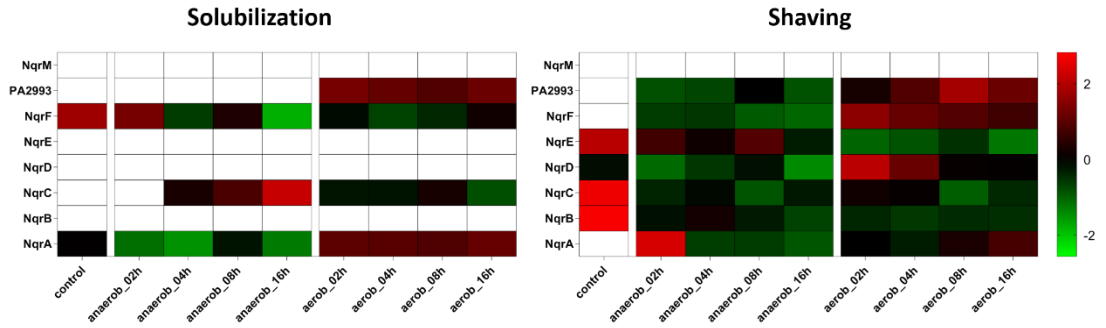

Figure 33 Kinetic profiles of proteins of the Na^+-translocating NADH dehydrogenase.
Z scores of normalized protein intensities ranging from 2.826 (red) to -2.563 (green), the baseline was set to 0 (black) and proteins that were not identified were displayed as an empty cell (white). The NqrM subunit was neither identified using the solubilization nor the shaving approach. The remaining subunits were almost exclusively identified via the shaving approach of which all proteins but NqrA contain one or more TMHs. While four of the six subunits were highly abundant under control conditions, all subunits displayed low amounts during cultivation under denitrifying conditions. Interestingly, the amount of PA2993, NqrF and NqrD increased after shifting to aerobic conditions.

3.5 Proteases and chaperones during and post denitrification

As described prefatory, proteases are important for the processing, quality control and turnover of proteins and thus might be also involved in the assembly and disassembly of protein complexes. Using both the solubilization and shaving approach a total of 43 proteins with annotated or predicted protease activity were identified. Six of these, namely PA0372, PA1327, PA2725, PA3535, PA3913 and PA5474 were annotated as putative proteases.

3.5.1 Membrane-bound proteases FtsH and HtpX

Both the FtsH and the HtpX proteases are two of the few currently known membrane-bound proteases and thus were of particular interest in this work. FtsH is a zinc-containing membrane-bound AAA^+ protease and degrades both membrane embedded and soluble substrates. Furthermore, it was reported in *E. coli*, that FtsH interacts with the HflK/HflC complex (Saikawa, *et al.*, 2004). In addition, disruption of both *ftsH* and *htpX* in *E. coli* resulted in a synthetic growth defect leading to the assumption that HtpX in conjunction with FtsH is involved in the quality control of membrane proteins (Shimohata, *et al.*, 2002).

Using both the solubilization and shaving approach, FtsH and HtpX were identified in all observed samples, as depicted in Figure 34. Here, results of both the solubilization and the shaving approach reported an increase of both FtsH and HtpX during anaerobic denitrifying conditions. After shifting back to aerobic conditions, results of the shaving approach displayed an accumulation of both proteases in the membrane and the amount of both proteases decreases eight hours after the shift. These results corroborate the previously assumed cooperation of FtsH and HtpX. Furthermore, HflK and HflC both increased in their amount after shifting back to aerobic conditions.

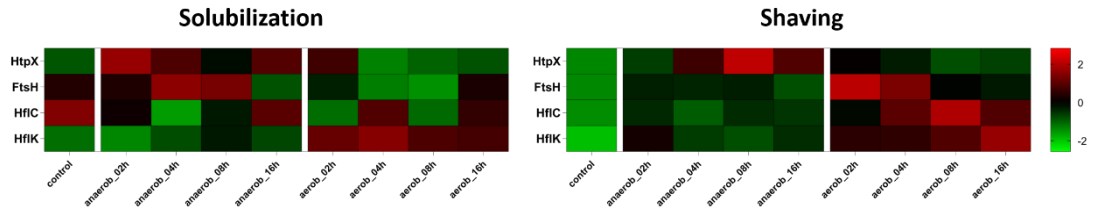

Figure 34 Kinetic profiles of the membrane-bound proteases FtsH and HtpX and protease modulators.
Z scores of normalized protein intensities ranging from 2.826 (red) to -2.563 (green) and the baseline was set to 0 (black). Results of the solubilization approach displayed similar high amounts of FtsH and HtpX under anaerobic conditions and the amount of both decreased after shifting back to aerobic conditions. However, results of the shaving approach displayed a higher amount of FtsH after shifting to aerobic conditions while HtpX displayed a similar kinetic profile to results of the solubilization approach. The protease modulators HflK and HflC displayed a similar protein kinetic and were low abundant during cultivation under anaerobic conditions. However, after shifting back to aerobic conditions, the amounts of both proteins increased.

Recently, a model for the assembly of the *cbb*$_3$ cytochrome *c* oxidase Cco was proposed reporting about the involvement of the FtsH protease during Cco biogenesis in *Rubrivivax gelatinosus* (Durand, *et al.*, 2018). In this model, FtsH degrades the CcoQ subunit after full assembly of the Cco complex, highlighting the involvement of FtsH and possibly other proteases in respiration. Furthermore, the amounts of the protease modulators HflK and HflC increased after shifting back to aerobic conditions whereas the amount of FtsH decreased over time, indicating that HflK and HflC might indeed regulate the activity of FtsH. In addition to this, the reported protein kinetics of NarK$_1$ and NarK$_2$ that displayed both proteins in high amounts during late stages of cultivation under denitrifying conditions followed by a decrease after shifting to aerobic conditions, might also be a hint that both NarK$_1$ and NarK$_2$ may be substrates for FtsH, as the contrary kinetic profiles shown in Figure 35 imply.

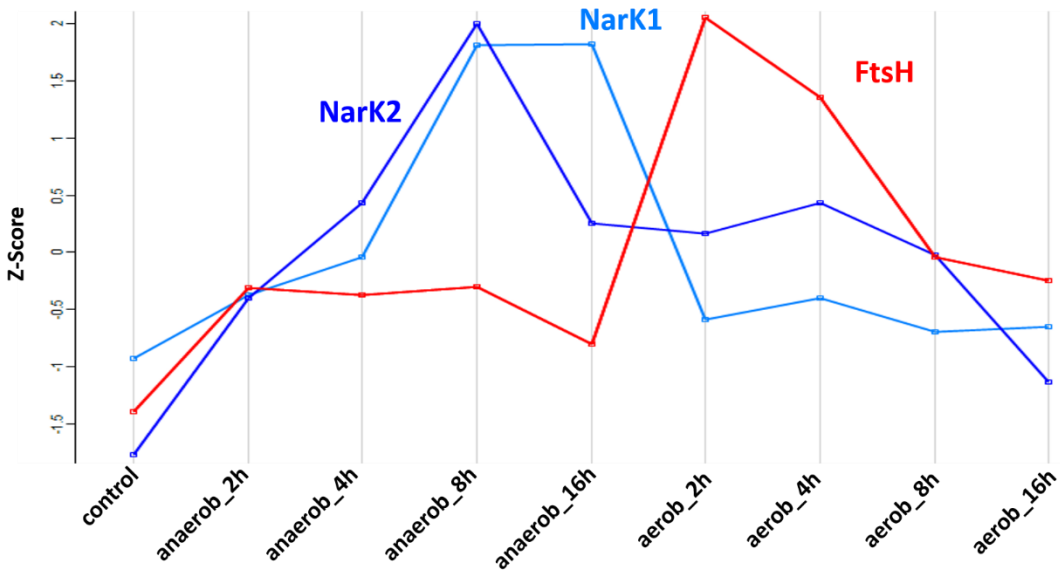

Figure 35 Kinetic profiles of FtsH, $NarK_1$ and $NarK_2$ under anaerobic and aerobic conditions.
Displayed are the Z Scores of the FtsH protease (red) and the nitrite extrusion proteins NarK1 (light blue) and NarK2 (dark blue). The amount of both $NarK_1$ and $NarK_2$ decreased after shifting to aerobic conditions at which point FtsH was high abundant. The contrary kinetic profiles might indicate a FtsH-dependent degradation of $NarK_1$ and $NarK_2$.

Altogether, the observed kinetic profiles of the HtpX and FtsH proteases indicate some involvement in respiration under aerobic and anaerobic conditions. $NarK_1$ and $NarK_2$ might also be substrates of FtsH as the CcoQ subunit of the cytochrome *c* oxidase Cco. It was currently hypothesized that HtpX cleaves within the cytoplasmic loop of a membrane protein thus generating a new cytoplasmic tail. This cytoplasmic tail could then serve as an initiation point for FtsH to further degrade the remaining polypeptide. Some further analyses need to be performed to clarify whether HtpX and FtsH cooperate or just perform similar tasks (Sakoh, *et al.*, 2005).

3.5.2 Involvement of ClpXP proteases in denitrification

Among the identified proteases, various Clp proteins were identified including ClpP, ClpX and ClpP2. ClpX is the ATP-binding subunit of Clp proteases. ClpP is a serine protease and belongs also to the AAA^+ proteases. The ClpP protease is composed of 14 subunits that oligomerize into two heptameric rings (Wang, *et al.*, 1997) (Hasnon, *et al.*, 2005). While ClpX by itself functions as a molecular chaperone, ClpX in cooperation with ClpP forms one of the most characterized proteases that degrades proteins involved in DNA damage repair, gene expression in stationary phase and protein quality control (Levchenko, *et al.*, 1995) (Schirmer,

et al., 1996). In total eight Clp proteins were identified using both the solubilization and the shaving approach (Figure 36). Interestingly, all Clp proteins were highly abundant during early stages of cultivation under anaerobic conditions. Only ClpC and ClpV3 were also identified in larger amounts after shifting back to aerobic conditions.

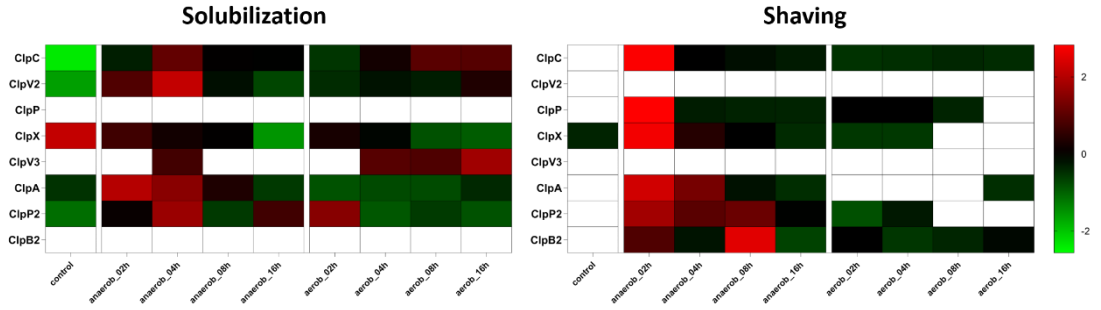

Figure 36 Kinetic profiles of various Clp proteins.
Z scores of normalized protein intensities ranging from 2.826 (red) to -2.563 (green), the baseline was set to 0 (black) and proteins that were not identified were displayed as an empty cell (white). All Clp proteins were present in high amounts during early stages of cultivation under anaerobic conditions while only ClpC and ClpV3 were also identified in higher amounts after shifting back to aerobic conditions.

Interestingly, *P. aeruginosa* besides ClpP possesses two additional ClpP isoforms named ClpP2 and ClpP3 encoded by the genes PA3326 and PA2189, respectively. It was suggested that ClpP2, together with ClpXP is part of the regulatory network of alginate biosynthesis. Furthermore, ClpP2 degrades MucA proteins however, the exact physiological role of ClpP2 is still unclear. Regarding ClpP3, the expression of the corresponding gene was observed to be induced by AlgR, which is a global regulator of virulence including alginate biosynthesis, indicating that both ClpP2 and ClpP3 might be additional regulatory proteins for alginate production (Qui, *et al.*, 2008) (Kong, *et al.*, 2015). ClpP3 was not identified in this work whereas ClpP2 was solely identified using the shaving approach. There, ClpP2 was highly abundant during cultivation under denitrifying conditions. ClpP and ClpP2 seem to have distinct roles. It is assumed that ClpP2 is involved in the modulation of protein composition in the stationary phase and associates with another yet unknown ATP-binding subunit similar to ClpX or ClpA (Hall, *et al.*, 2016).

Furthermore, the *tig* gene encoding the trigger factor (TF) protein is located upstream of the genes encoding ClpX and ClpP. TF promotes co-translational protein folding and interestingly, proteins encoded by *tig*, *clpP* and *clpX* displayed

a similar protein kinetic (Deuerling, *et al.*, 1999). These three proteins were highly abundant in samples taken two hours after cultivation under denitrifying conditions and interestingly, the Lon protease, whose gene is located downstream to *clpX* showed a similar kinetic profile, as displayed in Figure 37.

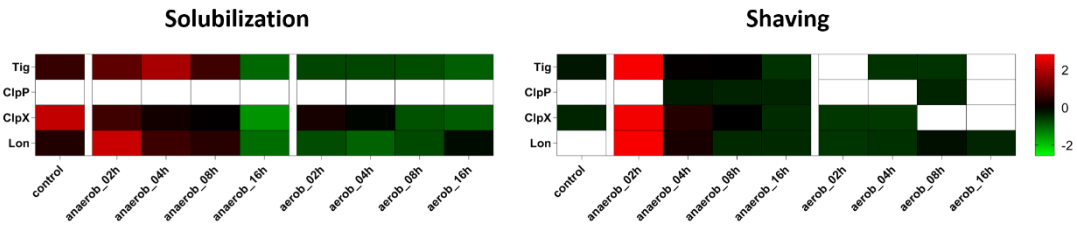

Figure 37 Kinetic profiles of the Tig protein, ClpXP and the adjacent Lon protease.
Z scores of normalized protein intensities ranging from 2.826 (red) to -2.563 (green), the baseline was set to 0 (black) and proteins that were not identified were displayed as an empty cell (white). All three corresponding proteins of the *tig-clpXP* operon were present in higher amounts during cultivation under anaerobic conditions. The Lon protease, whose gene is located downstream of *clpX* showed a similar kinetic profile.

Previous studies in *E. coli* reported a direct interaction between TF and ClpX proposing a combined TF-ClpXP degradation complex. The observed kinetic profiles of the homologous proteins in *P. aeruginosa* suggest that TF, ClpP and ClpX also could act together in *Pseudomonas* and might facilitate the degradation of newly synthesized proteins under denitrifying conditions (Hsiung Yu, 2013). To investigate a possible TF-ClpXP complex, a Strep-tagged ClpP protein can be generated. Subsequently, protein complexes are crosslinked *in-vivo* and purified via affinity chromatography. Resulting protein complexes containing ClpP are then digested and analyzed mass spectrometrically to identify possible interaction partners.

Altogether, Clp proteins and in particular ClpP2 might be involved during denitrification, but the role of ClpP2 remains still unclear. Whether ClpP2 interacts with ClpX or a ClpX-like protein to secure the quality control of denitrifying proteins remains unsolved. Further research needs to be done to elucidate the physiological role of ClpP2 during respiration.

3.6 Identification of SP100 within the membrane proteome

Of particular interest in this work were small proteins that were both annotated or predicted using databases generated in this work. Overall, 69 SP100 were identified of which 14 were currently not annotated in the genome of *P. aeruginosa* PAO1. 40 small proteins were solely identified using the shaving approach and 15 small proteins were exclusively identified using the solubilization approach, as displayed in Figure 38. Both methods shared a total of 14 identified SP100. Surprisingly, the shaving approach was more efficient regarding the identification of small proteins.

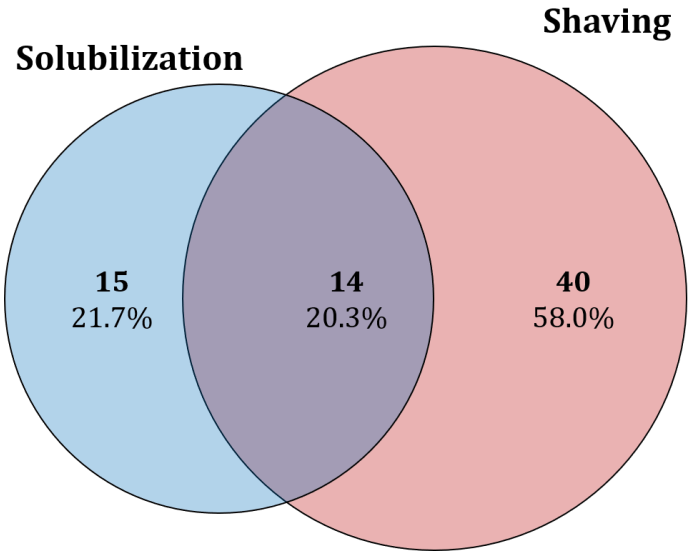

Figure 38 Number of identified SP100 using the solubilization and membrane shaving approach.
Altogether, 69 small proteins were identified of which 40 (58%) proteins were solely identified using the shaving approach. Contrary, 15 (22%) proteins were only identified via the solubilization approach and both approaches shared 14 (20%) identified SP100.

One possible explanation might be that samples of the shaving approach are less complex due to the first unspecific digestion step and the subsequent washing steps. Thereby most of the peripheral and cytoplasmic proteins are removed. Small proteins are supposed to be less abundant than proteins with more than 100 amino acids.

Furthermore, samples of the shaving approach were analyzed in the Orbitrap Fusion using the top-speed mode and thus as much signals as possible were acquired during one cycle and further used for MS/MS analyses. In contrast, samples of the solubilization approach were analyzed at the Orbitrap VelosPro with top20 mode that selected only the 20 most abundant signals per cycle for

MS/MS acquisition. Moreover, it could also be possible that the three different digestion methods chosen for database analyses simply covered more generated peptides compared to database searches using trypsin that were performed for samples of the solubilization approach.

Overall, choosing a more sensitive mass spectrometer in combination with the removal of highly abundant proteins and thereby an enrichment of small proteins resulted in the identification of more small proteins. Of course, the applied methods need to be optimized to enrich further small proteins. Furthermore, MS analyses also need to be performed considering the different used digestion enzymes as trypsin usually generates peptides with charges of +2 and +3. Contrary, using chymotrypsin charges of up to +7 are still possible. In these cases, using HCD-type fragmentation instead of CID-type fragmentation might yield the identification of more multiple-charged peptides as it was shown recently (Tu, *et al.*, 2016).

The length of the identified SP100 ranged from 11 to 100 amino acids and interestingly, already annotated SP100 possessed a length of at least 46 amino acids. Furthermore, 46 of the 69 identified SP100 were predicted with no TMH. More SP100 smaller than 25 aa were identified using the solubilization approach, while the number of SP100 that were identified using the shaving approach increased with the total length of the small proteins (Figure 39 A). Moreover, over 50% of the identified SP100 that were identified with both approaches were longer than 75 aa. Overall, the number of small proteins that contained at least one TMH was higher using the shaving approach compared to the solubilization approach, as shown in Figure 39 B. These findings appear reasonable, as the number of TMHs correlates with the protein length. Usually, transmembrane helices are around 23 aa in size (Saidijam, *et al.*, 2018). Therefore, integral inner membrane proteins need to be at least 23 aa long and it is unsurprising that few integral membrane proteins that are smaller than 25 aa were identified. The obtained results further corroborate the suitability of the shaving approach for the preparation of integral membrane proteins. The smallest, TMH-containing protein that was identified in this work was 55 aa long and possessed a 20 aa long TMH.

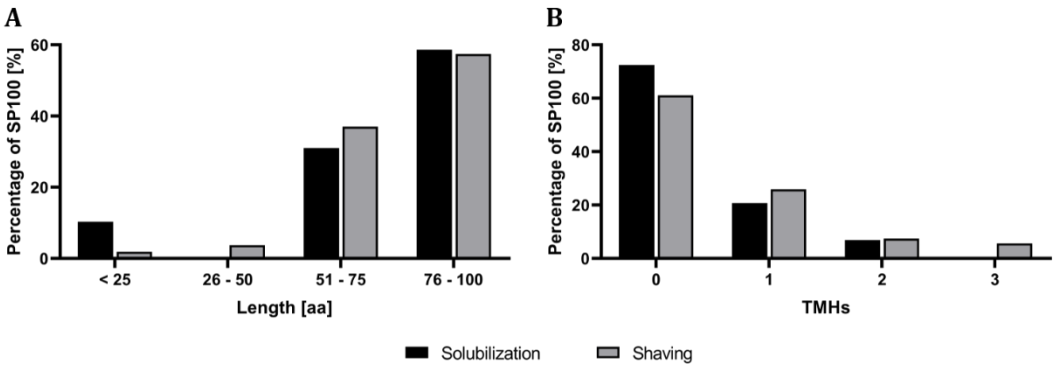

Figure 39 Length distribution and number of TMHs of identified SP100.
A) Length distribution of identified SP100 using the solubilization (black) and shaving (grey) approach. Six SP100 (9%) were smaller or equal than 50 aa while the remaining 63 SP100 (91%) had a length of 51 aa or larger. Most SP100 smaller than 25 aa were identified using the solubilization approach. The larger the length of SP100 was the more SP100 were identified. 58% and 57% of the identified SP100 were larger than 75 aa and were identified using the solubilization and shaving approach, respectively. **B**) Number of TMHs of identified SP100 using the solubilization (black) and shaving (grey) approach. The portion of proteins that contained no TMH was slightly higher using the solubilization approach in comparison to the shaving approach. SP100 with three TMHs where SP100 were exclusively identified with the shaving approach.

In the following, the isoelectric point (pI) of the identified SP100 as well as their GRAVY scores were predicted. Here, 46 identified SP100, contributing 65% (solubilization approach) and 55% (shaving approach) of all identified SP100, displayed a pI larger than 7.6 and thus were weak to strong alkaline proteins. In contrast, 2 (7%) and 17 (32%) SP100 that were identified using the solubilization and shaving approach, respectively, showed pIs smaller than 6.5 indicating an overall more acidic character, as shown in Figure 40. Moreover, six SP100 were identified with a neutral charge ranging from 6.5 to 7.5. Altogether, most identified SP100 were determined as basic proteins. It was observed in prokaryotes that acidic proteins are about 73 residues longer than basic proteins which might explain the higher amount of small proteins with a basic pI (Nandi, *et al.*, 2005). Subsequent, the basic pI might give insight into their physiological role, as ribosomal proteins are also small, basic proteins that are able to interact with nucleic acids. Twelve of the 69 identified SP100 were ribosomal proteins were identified with a pI ranging from 8.9 to 11.7. Furthermore, it is proposed that basic proteins might be better suited to interact with nucleic acids and might thus be regulatory proteins, transcriptional factors or signaling proteins, functions that were previously attributed to new identified small proteins (Kiraga, *et al.*, 2007).

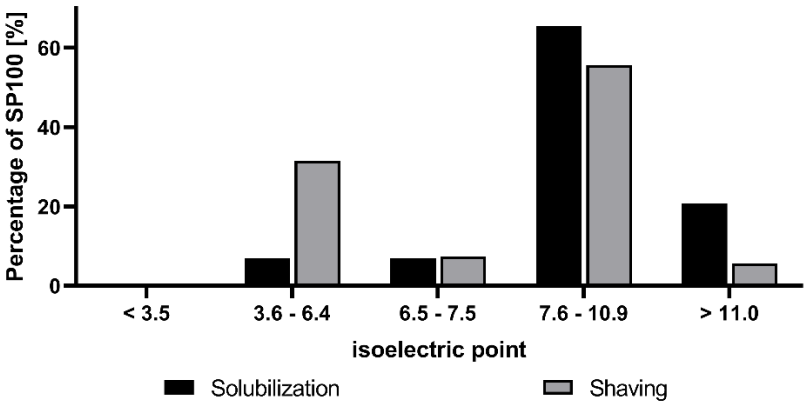

Figure 40 Distribution of the isoelectric point of the identified SP100.
Isoelectric point distribution of all identified SP100 using the solubilization (black) and shaving (grey) approach. Few SP100, 7% of the identified proteins of each approach, displayed a neutral pI. The majority, 65% and 55% of identified SP100 using the solubilization and shaving approach, respectively, showed pIs greater than 7.5 and thus where alkaline while 21% of the via the solubilization approach identified SP100 were strong alkalic displaying values greater 11. Contrary, 32% of SP100 that were identified with the shaving approach displayed values smaller than 6.4 and had thus an acidic character.

In addition, hydrophobicity of the identified SP100 was determined by determining the GRAVY scores (grand average of hydropathy). Here, positive GRAVY values representing greater hydrophobicity, while negative GRAVY values portray hydrophilic properties (Kyte, *et al.*, 1982). Overall, negative GRAVY values were determined for 40 SP100 that were predicted to contain no TMH. Here, small proteins that were predicted to contain at least one TMH showed an equal distribution of positive and negative GRAVY values, with 10 and 13 SP100, respectively. Moreover, the majority of proteins are characterized by negative GRAVY scores around -0.4 regardless of the applied preparation method (Figure 41). Overall, 21 proteins (72.4%) of the SP100 that were identified with the solubilization approach had a negative GRAVY value and thus were hydrophilic. Similar results were observed for SP100, identified using the shaving, where 40 proteins (74.1%) also displayed a negative GRAVY value. Eight (27.6%) and 14 (25.9%) proteins that were identified using the solubilization and shaving approach, respectively had positive GRAVY values. Overall, the percentage of hydrophilic proteins was slightly higher using the shaving approach in contrast to the solubilization approach. While previously, newly identified small proteins where hydrophobic, most small proteins identified in this work were hydrophilic (Storz, *et al.*, 2014). In total, 45 SP100 (65%) were predicted as cytoplasmic proteins corelating with the observed hydrophobicity distribution of the identified small proteins.

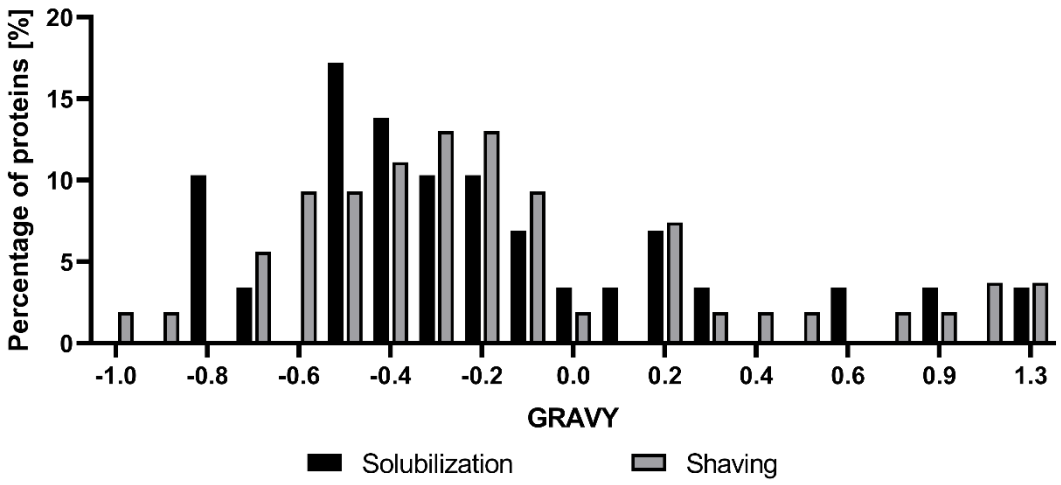

Figure 41 GRAVY distribution of identified SP100.
GRAVY values of all identified proteins using the solubilization and shaving approach. Using the solubilization approach, 21 (72.4%) proteins displayed a negative GRAVY value and were thus hydrophilic. The remaining eight (27.6%) proteins showed positive GRAVY values and thus a hydrophobic character. Like proteins that were identified using the solubilization approach, 40 (74.1%) proteins that were identified with the shaving approach were distributed around a GRAVY value of -0.2 showing a more hydrophilic character. Contrary to proteins that were identified using the solubilization approach, the number of proteins with a positive GRAVY value was higher where 14 (25.9%) proteins were hydrophobic.

Additionally, start codons were predicted via the *Pepper* algorithm showcasing that 55 of the 69 identified SP100 used ATG as a start codon. 51 of the 55 annotated SP100 begin with ATG and only three and one SP100 start with GTG or TTG, respectively (Figure 42). Only four of the 14 currently non-annotated SP100 were predicted to use ATG as a start codon while three were predicted with TTG. The remaining seven non-annotated SP100 were predicted to use either GTG, CTG, ATT, CGC, ATC, ACT or ATA as start codon, respectively. As reported previously, that ATG, GTG and TTG are the three standard initiation codons used throughout all bacteria (Villegas, *et al.*, 2008). However, recent studies analyzing the translation initiation in *E. coli* detected also initiation of translation for 47 of the remaining 61 codons revealing also a possible usage of non-canonical start codons in bacteria (Hecht, *et al.*, 2017). As observed previously, the alternative start codons GTG and TTG were used by small ORFs encoding for non-annotated small proteins offering the possibility that other uncommon start codons might also be used for non-annotated small proteins (Storz, *et al.*, 2014).

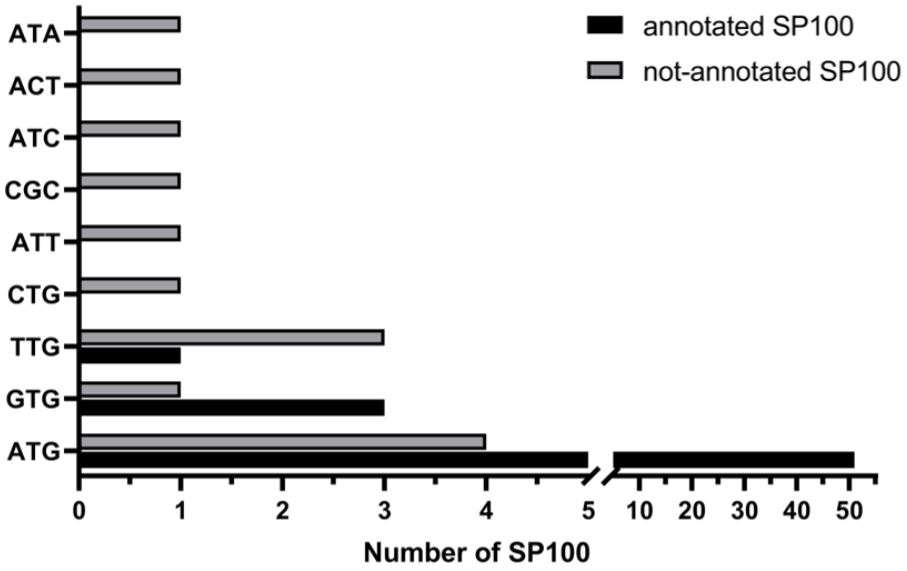

Figure 42 Distribution of start codon usage of annotated and non-annotated small proteins.
51 of the 55 annotated SP100 (black) were determined with ATG as a start codon whereas three and one of these SP100 used GTG and TTG, respectively. Of the 14 identified, non-annotated SP100 only four were predicted to use ATG. Three non-annotated SP100 were determined with TTG as a start codon whereas the remaining seven were predicted to use either GTG, CTG, ATT, CGC, ATC, ACT or ATA as start codon, respectively.

3.6.1 Characterization of non-annotated SP100

Overall, 14 SP100 were identified using both the solubilization and the shaving approach that were not present in the current annotation of *P. aeruginosa* PAO1. The predicted length of the non-annotated SP100 varied between 11 and 100 aa and nine of the 14 non-annotated SP100 were larger than 50 aa, as depicted in Table 14. Interestingly, none of the non-annotated SP100 was identified via both preparation methods as eight and six SP100 were exclusively identified with the shaving or solubilization approach, respectively. Furthermore, localization predictions revealed that eight of the 14 identified SP100 were predicted as cytoplasmic proteins, five were predicted with a periplasmic localization and only one SP100 was predicted as an integral inner membrane protein. Furthermore, the used start codons and possible RBS were determined via the *Pepper* revealing that only four SP100 were determined with ATG as a start codon. Contrary, the remaining ten were determined with the alternative start codons GTG and CTG, while uncommon non-canonical start codons like ACT were also found. Additionally, potential RBSs were determined for eleven non-annotated SP100. Regarding the conservation on amino acid level, eleven SP100 were conserved in at least 50% of the 233 observed genomes of various *P. aeruginosa* strains.

However, conservation of the amino acid sequence on species level showed conservation in roughly one fifth of the observed *Pseudomonas* species indicating that these small proteins were mostly *P. aeruginosa* specific. Moreover, determinations of the physicochemical properties of the identified, non-annotated SP100 showed that ten out of 14 SP100 had high pIs and were determined as basic proteins. In contrast, of the remaining four SP100 two SP100 were predicted as acidic and neutral proteins, respectively. Furthermore, determinations of the hydrophobicity reported negative GRAVY values for ten SP100 and thus were hydrophilic proteins correlating with the predicted cytoplasmic localization. Four of the 14 non-annotated SP100 displayed GRAVY values larger zero and were thus predicted as hydrophobic proteins. Three of the 14 identified, non-annotated small proteins were of further interest due to their localization in the genome and their possible function. Therefore, transcriptional analyses were performed to analyze transcriptional activity for these three predicted ORFs under anaerobic and denitrifying conditions.

Table 14 List and properties of identified, non-annotated SP100.

Overall, 14 SP100 were identified that were not present in the current annotation of *P. aeruginosa* PAO1. Their length varied between 11 and 100 aa and most non-annotated SP100 were larger than 50 aa. Eight SP100 were identified solely with the shaving approach while the remaining six were exclusively identified using the solubilization approach. Most of the SP100, eight in total, were predicted as cytoplasmic proteins, five were predicted with a periplasmic localization and only one SP100 was predicted to be integrated in the IM. Furthermore, only four SP100 were determined with ATG as a start codon whereas the remaining ten were determined with alternative start codons. A potential RBS was determined for eleven non-annotated SP100. Regarding the conservation on amino acid level, eleven SP100 were highly conserved in various *P. aeruginosa* strains while their conservation in different *Pseudomonas* species decreased. Ten of the non-annotated SP100 were determined as basic proteins, while two SP100 were predicted as acidic and neutral proteins, respectively. Again, ten SP100 were predicted with a negative GRAVY value and thus were hydrophilic proteins while the remaining four displayed values larger zero and were thus predicted as hydrophobic proteins.

protein ID	length [aa]	method	subcellular localization	pred. TMH	start codon	potential RBS	Conservation strains (233)	Conservation species (686)	pred. pI	pred. GRAVY
6frt_+1_12309	71	Solubilization	Periplasmic protein	0	TTG	GGTGC	102	104	11.7	-0.1
6frt_+1_26594	94	Shaving	Intracellular Protein	1	TTG	CGAGC	126	128	10.6	-0.4
6frt_+1_4007	14	Shaving	Periplasmic protein	0	ATT	GGTGT	28	28	10.8	-0.9
6frt_+1_6282	79	Shaving	Intracellular Protein	0	CTG	AGAGG	1	1	5.7	-0.2
6frt_+2_26135	81	Shaving	Intracellular Protein	0	TTG	GGAGG	110	112	5.8	0.2
6frt_+2_7442	45	Shaving	Intracellular Protein	0	ATG	-	114	116	11.8	-0.1
6frt_+3_4602	100	Solubilization	Intracellular Protein	0	GTG	GGTGC	195	196	9.3	-0.2
6frt_-1_14346	19	Solubilization	Intracellular Protein	0	ACT	-	195	197	12.2	-0.4
6frt_-1_14524	98	Solubilization	Integral IM Protein	2	ATG	GGAGT	19	19	11.5	0.9
6frt_-1_27422	61	Shaving	Periplasmic protein	0	ATA	CGAGG	149	150	9.3	-0.3
6frt_-2_5445	68	Shaving	Intracellular protein	0	ATC	CGAGG	128	128	7.0	-0.4
6frt_-2_6068	11	Solubilization	Intracellular Protein	0	CGC	GGTGA	180	182	10.4	-0.8
igr1531	18	Solubilization	Periplasmic protein	0	ATG	-	176	178	6.5	0.1
igr2243	60	Shaving	Periplasmic protein	1	ATG	AGAGG	195	197	8.1	0.3

3.6.1.1 HimD is co-transcribed with a currently non-annotated small protein

Of particular interest was the small protein 6frt_14524, which is predicted to possess two TMHs. Furthermore, sequence analyses revealed similarities to the LapA protein (lipopolysaccharide assembly protein A). In E. coli, lapA was reported as a heat shock gene that is also predicted to be involved in the assembly of lipopolysaccharides (LPS) (Klein, *et al.*, 2014). While the predicted SP100 was also observed in a previous study regarding the description and variation of O-antigen serotypes in P. aeruginosa, no further steps towards the characterization of the small protein were done (Raymond, *et al.*, 2002). Here, the small protein 6frt_14524 was identified in higher amounts during later stages of cultivation under denitrifying conditions while the amount drastically decreased after four hours under aerobic conditions. The corresponding sORF is located on the -1 reverse strand at position 3,547,658 - 3,547,362 and is predicted to start with an ATG (Figure 43). Furthermore, a possible ribosomal binding site (RBS) 4 bp upfront the ORF with the sequence AGAGT was determined. The predicted sORF is localized between the 30 bp upstream-located himD gene and the 434 bp downstream-located wzz gene, which encode the integration host factor beta subunit and for the O-antigen chain length regulator, respectively.

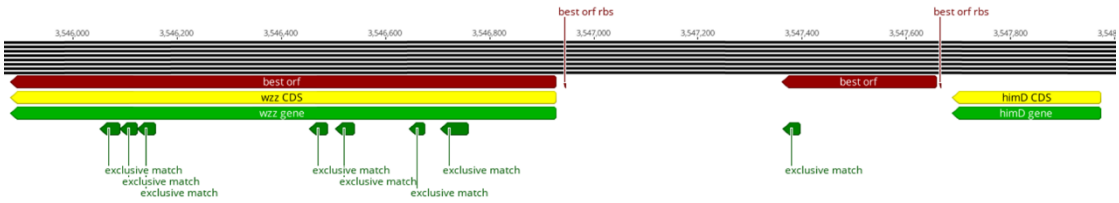

Figure 43 Localization of the predicted small ORF 6frt_14524.
Localization and RBS were predicted using the *Pepper* algorithm showing that the gene of 6frt_14524 was predicted to be downstream of the *himD* and upstream of the *wzz* gene. The predicted RBS sequence was AGAGT and was located 4 bp upstream. Furthermore, the corresponding small protein was identified by one unique peptide.

Based on the localization of the gene close to the gene encoding the O-antigen chain length regulator and the sequence similarities to the LPS assembly protein imply some involvement of the SP100 in the LPS machinery of *P. aeruginosa*. Moreover, transcriptional analyses for the predicted sORF revealed a transcript with a corresponding size of around 600 bp, as depicted in Figure 44.

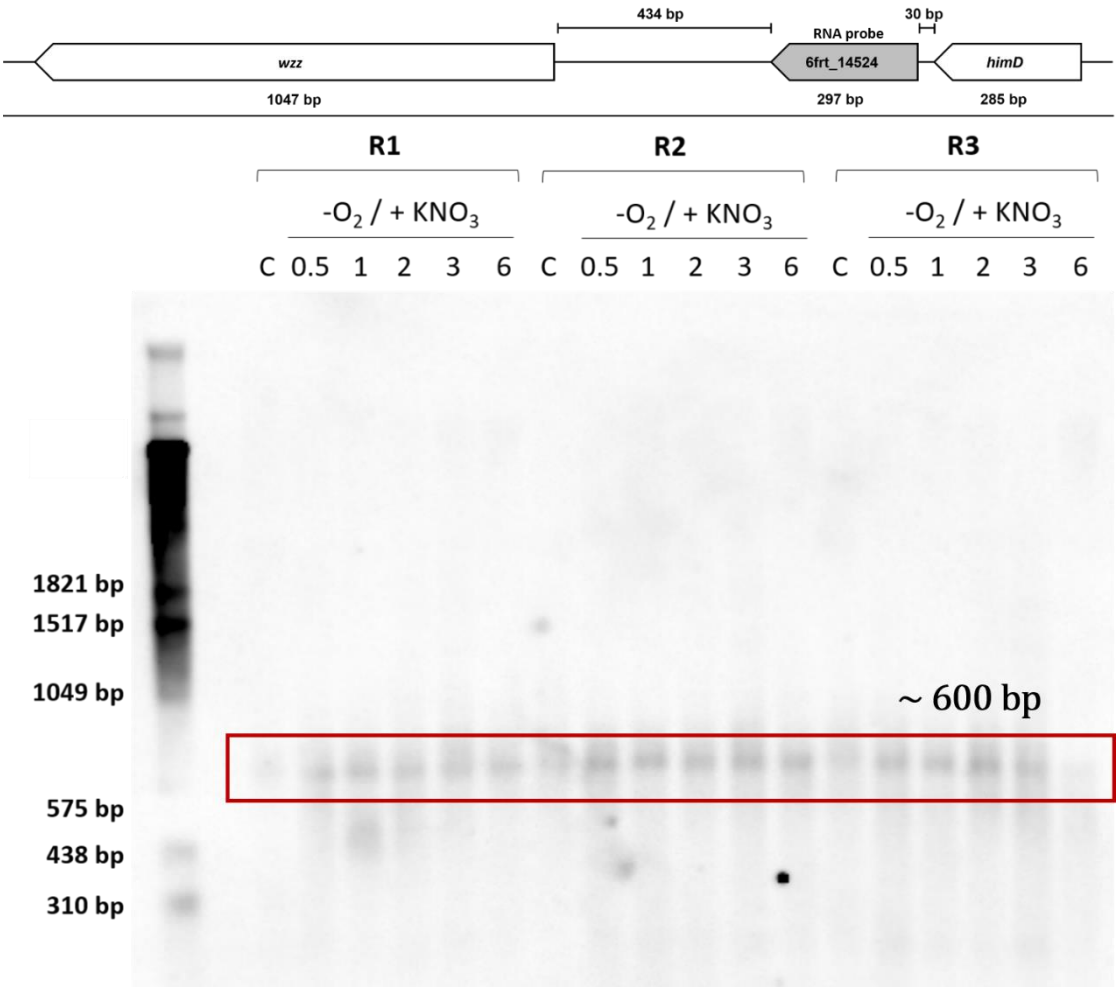

Figure 44 Northern blot analysis of the small ORF corresponding to 6frt_14524.
R1, R2, R3 = replicate 1, 2 and 3 respectively; $-O_2/+KNO_3$ = anaerobic conditions plus 50 mM KNO_3; C = aerobic control OD_{540} = 0.05; 0.5, 1, 2, 3 and 6 = corresponding time point of cell harvest in h; marker = RNA Molecular Weight Marker I, DIG-labeled (Roche); schematic representation of the genetic arrangement is displayed on top with the used RNA probe marked in grey. *P. aeruginosa* PAO1 cells were cultivated in LB under aerobic conditions until OD_{540} of 0.05 followed by shifting to cultivation under anaerobic conditions in the presence of 50 mM KNO_3. Each time point was cultured separately and after selected time point of 0.5, 1, 2, 3 and 6 hours cultivation under denitrifying conditions cells were harvested followed by RNA preparation. Transcriptional analyses were performed by separating RNA samples on a denaturing 2% formaldehyde-agarose gel and subsequent transfer onto a positively charged nylon membrane via vacuum blotting for four hours. Transcripts were visualized by hybridization with corresponding DIG-labeled RNA probes followed by incubation with AP-coupled anti-DIG antibody and CDP-Star and chemiluminescence signals were visualized using the Luminescent Image Analyzer LAS-3000. The observed transcript (red box) had a size of around 600 bp thus was larger than the selected ORF, which was 297 bp. Therefore, the observed transcript might be a bicistronic transcript of *himD* and 6frt_14524, which would be 612 bp long.

This transcript size, while much larger than the actual size of 297 bp of the predicted sORF, indicates a bicistronic transcript with a size of 612 bp as a result of the co-transcription of the *himD* gene and the putative sORF 6frt_14524. For further validation, transcriptional analysis was also performed using RNA probes against *himD* and *wzz,* respectively. Transcriptional analyses of *himD* revealed two transcripts, as depicted in Figure 45. However, analyses of the *wzz* gene displayed no signals (App. 8.11).

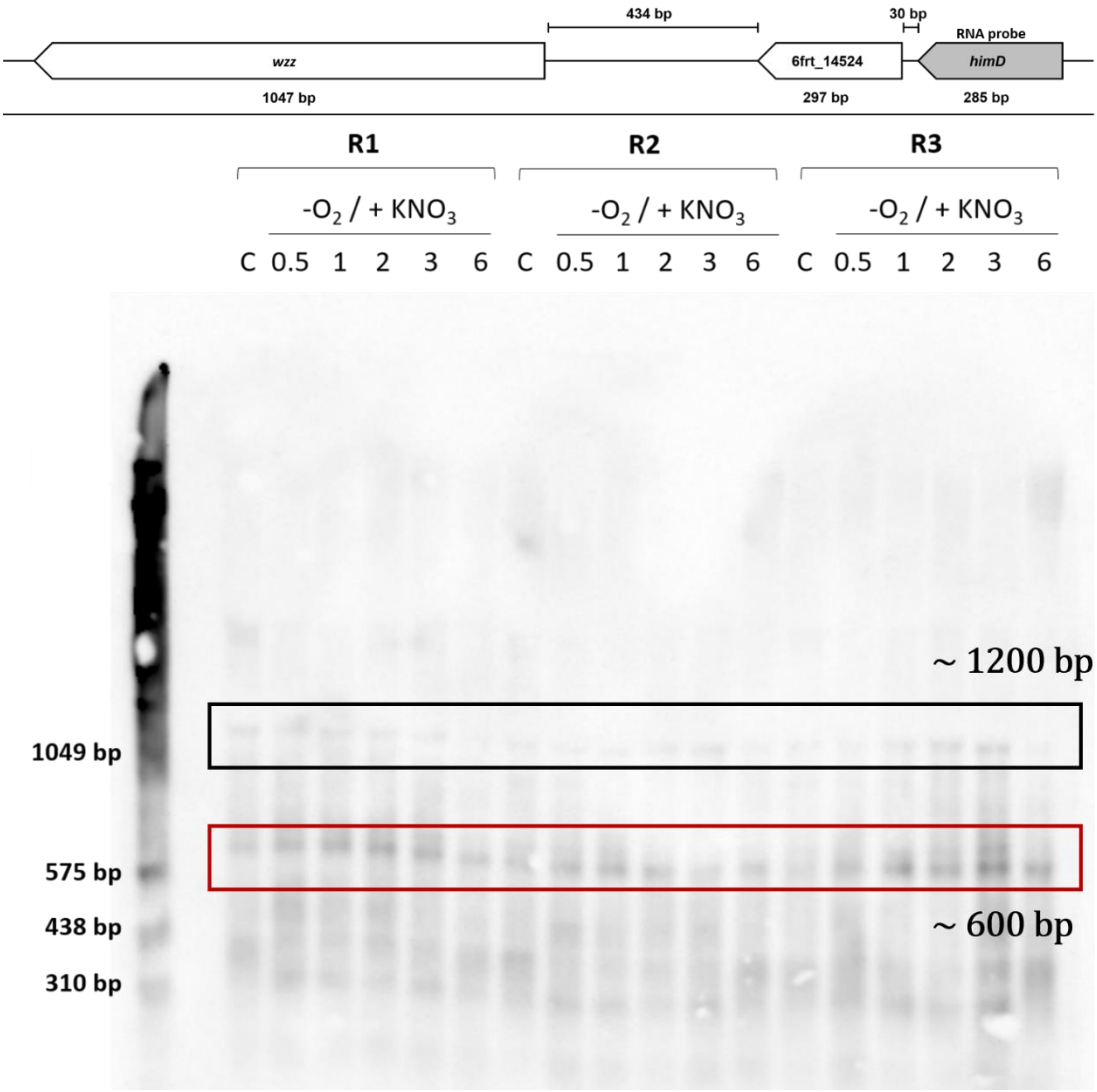

Figure 45 Northern blot analysis of the *himD* gene.
R1, R2, R3 = replicate 1, 2 and 3 respectively; $-O_2/+KNO_3$ = anaerobic conditions plus 50 mM KNO_3; C = aerobic control OD_{540} = 0.05; 0.5, 1, 2, 3 and 6 = corresponding time point of cell harvest in h; marker = RNA Molecular Weight Marker I, DIG-labeled (Roche); schematic representation of the genetic arrangement is displayed on top with the used RNA probe marked in grey. *P. aeruginosa* PAO1 cells were cultivated in LB under aerobic conditions until OD_{540} of 0.05 followed by shifting to cultivation under anaerobic conditions in the presence of 50 mM KNO_3. Each time point was cultured separately and after selected time point of 0.5, 1, 2, 3 and 6 hours cultivation under denitrifying conditions cells were harvested followed by RNA preparation. Transcriptional analyses were performed by separating RNA samples on a denaturing 2% formaldehyde-agarose gel and subsequent transfer onto a positively charged nylon membrane via vacuum blotting for four hours. Transcripts were visualized by hybridization with corresponding DIG-labeled RNA probes followed by incubation with AP-coupled anti-DIG antibody and CDP-Star and chemiluminescence signals were visualized using the Luminescent Image Analyzer LAS-3000. Two transcripts, corresponding with a size around 1200 bp and 600 bp, respectively were detected. The transcript (red box) might be a bicistronic transcript of *himD* and 6frt_14524, which would be 612 bp long while the larger transcript (black box) could not be reliable assigned.

The transcript around 600 bp matches the previously observed transcript size of the analysis of 6frt_14524 substantiating the assumed co-transcription of 6frt_14524 and *himD*. Furthermore, the larger transcript corresponding to a size of roughly 1200 bp could not be assigned reliably. As this transcript was only detected with the *himD* RNA probe, it might be possible that the transcription of

himD begins further upstream of the gene. However, 136 bp upstream of *himD* is the *rpsA* gene located that encodes the 30S ribosomal protein S1.

Altogether, the observed results of the transcriptional analyses of both 6frt_14524 and *himD* showed that both genes were co-transcribed resulting in a transcript with a size of 612 bp. Interestingly, the SP100 6frt_14524 is highly conserved among various *P. aeruginosa* strains but seems to be unknown in the PAO1 strain. There, the ORF was previously identified by whole genome sequencing in the *P. aeruginosa* PAO1 strain and assumed to encode a hypothetical protein. In this work, the small protein was identified and highly abundant during denitrification. Furthermore, the corresponding sORF of the small protein 6frt_14524 is co-transcribed with the *himD* gene. As the small protein shows similarities to the LapA protein of *E. coli* it appears reasonable to assume that the SP100 6frt_14524 of *P. aeruginosa* performs a similar role to the LapA protein of *E. coli.*

3.6.1.2 P. aeruginosa PAO1 encodes the cobalt transporter CbtBA

Another interesting SP100 was the protein igr2243 that was predicted to be 60 aa long possessing one TMH. The protein contained a probable cobalt transporter subunit (CbtB) domain and while the sequence was highly conserved in different *P. aeruginosa* strains, the small protein was previously only found in the alginate-overproducing variant *P. aeruginosa* PAO1-VE2 (Yin, *et al.*, 2013). In *P. aeruginosa* PAO1, this SP100 was solely identified after shifting to aerobic conditions during stationary phase. The corresponding sORF of igr2243 is predicted to be located between *CobW* and *CbtA* that encode the cobalamin biosynthesis protein and a probable cobalt transporter subunit, respectively (Figure 46).

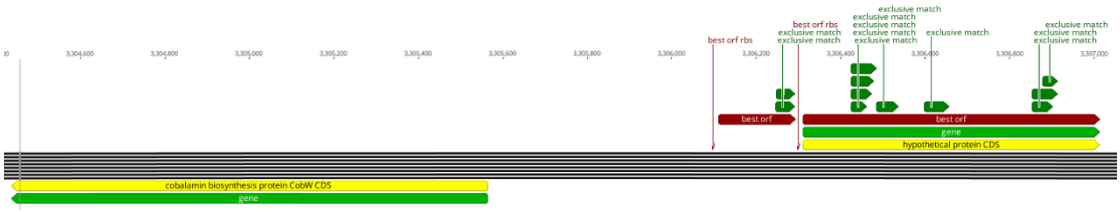

Figure 46 Localization of the predicted small ORF igr2243.
Localization and RBS were predicted using the *Pepper* algorithm showing that the sORF of igr2243 was localized downstream of *CobW* and upstream of *CbtA*. The predicted RBS sequence was AGAGG and was located nine bp upstream. Furthermore, the corresponding small protein was identified by two unique peptides.

The corresponding gene of igr2243 is located on the +1 leading strand at position 3,306,112 - 3,306,294 and is localized 547 bp downstream of *CobW* and only 17 bp upstream of *CbtA*. Furthermore, ATG was determined as the possible start codon and a nine bp upstream located RBS with the sequence AGAGG was detected. Furthermore, transcriptional analyses for the corresponding sORF of igr2243 revealed two smaller transcripts with around 300 bp and 400 bp, respectively and one larger transcript with roughly 900 bp in size, as shown in Figure 47.

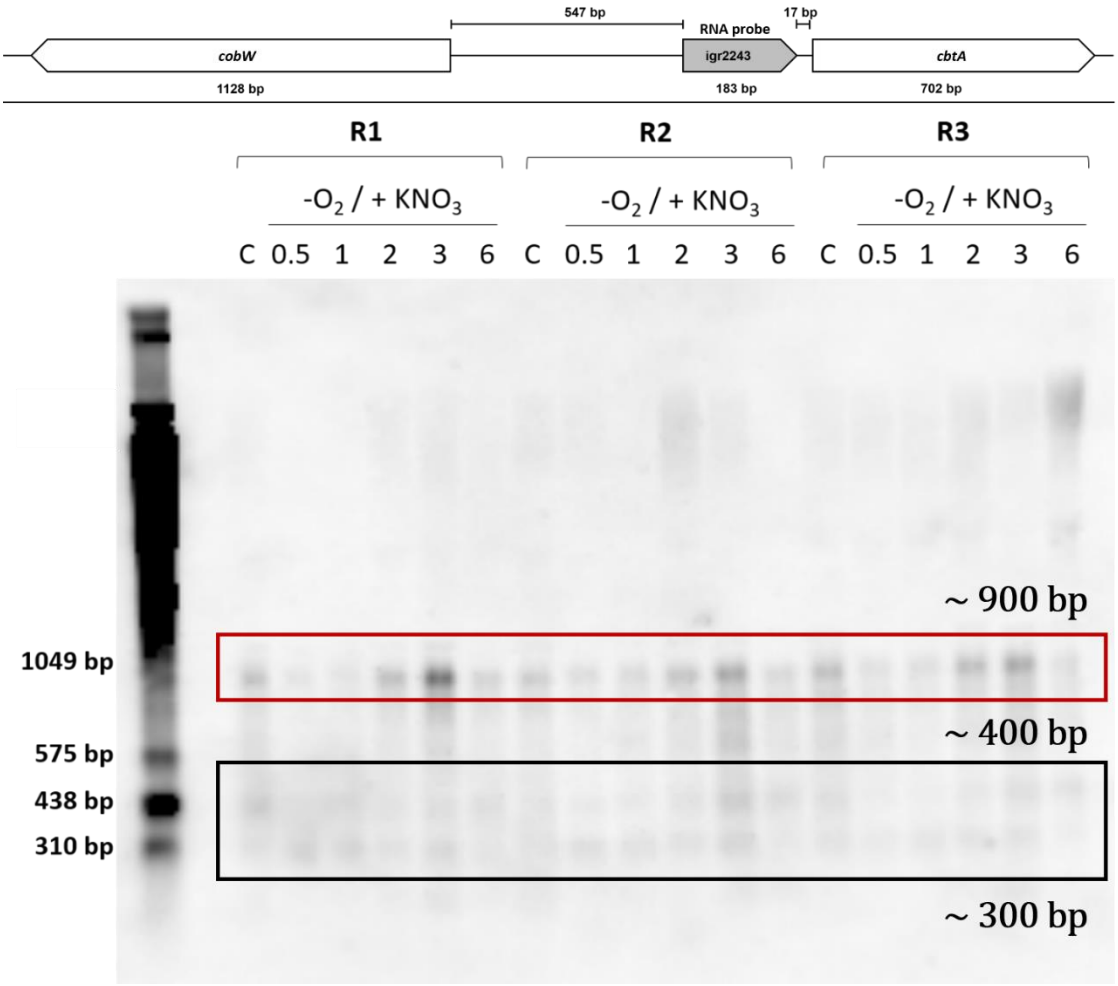

Figure 47 Northern blot analysis of the small ORF corresponding to igr2243.
R1, R2, R3 = replicate 1, 2 and 3 respectively; $-O_2/+KNO_3$ = anaerobic conditions plus 50 mM KNO_3; C = aerobic control OD_{540} = 0.05; 0.5, 1, 2, 3 and 6 = corresponding time point of cell harvest in h; marker = RNA Molecular Weight Marker I, DIG-labeled (Roche); schematic representation of the genetic arrangement is displayed on top with the used RNA probe marked in grey. *P. aeruginosa* PAO1 cells were cultivated in LB under aerobic conditions until OD_{540} of 0.05 followed by shifting to cultivation under anaerobic conditions in the presence of 50 mM KNO_3. Each time point was cultured separately and after selected time point of 0.5, 1, 2, 3 and 6 hours cultivation under denitrifying conditions cells were harvested followed by RNA preparation. Transcriptional analyses were performed by separating RNA samples on a denaturing 2% formaldehyde-agarose gel and subsequent transfer onto a positively charged nylon membrane via vacuum blotting for four hours. Transcripts were visualized by hybridization with corresponding DIG-labeled RNA probes followed by incubation with AP-coupled anti-DIG antibody and CDP-Star and chemiluminescence signals were visualized using the Luminescent Image Analyzer LAS-3000. Three transcripts with a size of around 300 bp, 400 bp and 900 bp were identified, respectively. While the two smaller transcripts (black box) could not be reliable assigned, the transcript (red box) with a size around 900 bp could be the bicistronic product of co-transcription of igr2243 and *CbtA*.

With an expected transcript size of 183 bp, all observed transcripts were larger than anticipated. Here, the smaller transcripts of 300 and 400 bp could not be assigned to a possible transcript. However, it might be possible that the actual transcription starts further upstream of igr2243. To verify an earlier transcription start, a primer extension assay can be performed to determine the transcription start site for the gene by identifying the 5' end of the corresponding mRNA (Carey, *et al.*, 2013). Furthermore, additional small ORF(s) might be located upstream of

igr2243. Additional sequence analyses using the iTerm-PseKNC web-server revealed putative transcriptional terminators between igr2243 and *cbtA* (Feng, *et al.*, 2019). Thus, it might be possible that igr2243 is also co-transcribed with a currently unknown small ORF in front of the gene.

In contrast, the larger transcript around 900 bp might be the result of a possible bicistronic transcript due to co-transcription of igr2243 and *cbtA*. Furthermore, it might also be possible that additional yet unknown ORFs are located upstream of igr2243. In such a case, the unknown larger ORF would likely overlap with the ORF of *cobW.* Interestingly, in *P. putida cbtA* is co-localized with *cbtB* and both are reported to be involved in cobalt transport and cobalamin biosynthesis (Rodionov, *et al.*, 2003) (Zhang, *et al.*, 2009). Comparing the annotated CbtB protein of *P. putida* with the identified, non-annotated igr2243 revealed 50% sequence similarities, as shown in Figure 48.

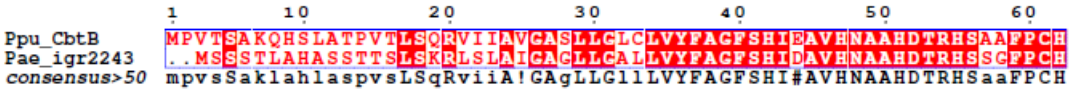

Figure 48 Sequence alignment of igr2243 identified in *P. aeruginosa* and CbtB of *P. putitda*.
Sequences were analyzed using the MultAlin website followed by alignment visualization vie ESPrint 3.0. Ppu = *P. putitda;* Pae = *P.* aeruginosa

Concluding, while *cbtA* and *cbtB* are annotated and localized together in the operon *cbtAB* in *P. putida*, the annotation of the corresponding *cbtB* gene in *P. aeruginosa* is missing. In this work, the identified igr2243 displays similarities to the CbtB protein of *P. putida* and genome analyses of the corresponding sORF of igr2243 showed that the gene is localized near *CbtA* in *P. aeruginosa* PAO1. Furthermore, transcriptional analyses for this sORF displayed a possible co-transcription together with *cbtA* substantiating that this small protein indeed is the CbtB subunit of a cobalt transporter in *P. aeruginosa*.

3.6.1.3 Zinc finger-containing small protein with possible regulatory function

The third SP100 that was of interest was the protein 6frt_26594, which is 94 aa long and is predicted to contain one TMH. As observed previously, the protein sequence is highly conserved among various *P. aeruginosa* strains and *Pseudomonas* species. However, the small protein was previously also found in the *P. aeruginosa* PAO1-VE2 strain (Yin, *et al.*, 2013). In this work, the small protein 6frt_26594 was identified in higher amounts under control conditions, while the amount rapidly decreased during cultivation under denitrifying conditions followed by an increase in the abundance after shifting to aerobic conditions. Moreover, the sORF that encodes 6frt_26594 is located on the +1 leading strand at 5,093,104 - 5,093,388 downstream of PA4545 and upstream of PA4546 (Figure 49). PA4545 encodes the outer membrane protein assembly factor BamD, which is involved in assembly and insertion of beta-barrel proteins into the outer membrane. The gene PA4546 encodes the protein PilS, the sensor kinase of the two-component system PilSR that is required for the regulation of the expression of type 4 fimbriae required for twitching and swimming motility (Hobbs, *et al.*, 1993). In addition, the alternative start codon TTG and a possible, seven bp upstream located RBS with the sequence CGAGC were predicted and interestingly, the sORF of 6frt_26594 showed an overlap of eleven nucleotides with pilS. Furthermore, no RBS for the pilS gene was determined raising the question whether or not both the genes of 6frt_26594 and pilS were co-transcribed.

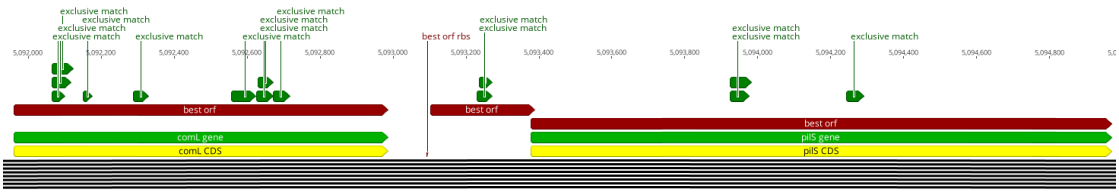

Figure 49 Localization of the predicted small ORF 6frt_26594.
Localization and RBS were predicted using the *Pepper* algorithm showing that the sORF of 6frt_26594 was localized between *comL* and *pilS*. The predicted RBS sequence was CGAGC and was located seven bp upstream. Furthermore, the sORF overlapped seven nucleotides to the adjacent *pilS* gene and the corresponding small protein was identified by two unique peptides.

Performing transcriptional analyses using RNA probe against the predicted 6frt_26594 ORF resulted in a possible transcript with a size of approximately 300 bp that roughly corresponds to the expected transcript size of 285 bp, as shown in Figure 50. Moreover, transcriptional analyses for 6frt_26594 were

particular tricky as the amount of transcript was low in every attempt to detect signals with the corresponding RNA probe. Also, raising the amount of separated RNA in combination with using higher amount of RNA probe subsequently resulted in fairly clear transcriptional signals.

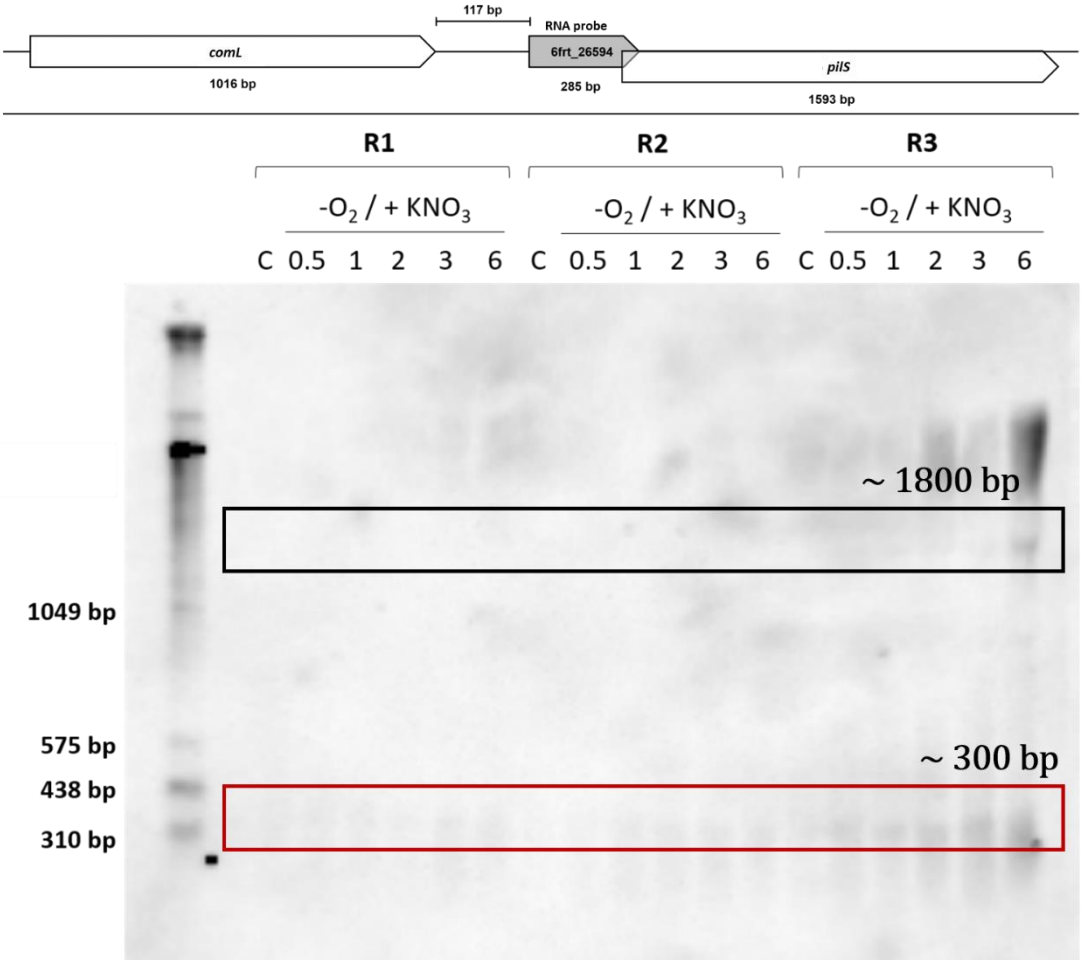

Figure 50 Northern blot analysis of the small ORF corresponding to 6frt_26594.
R1, R2, R3 = replicate 1, 2 and 3 respectively; $-O_2/+KNO_3$ = anaerobic conditions plus 50 mM KNO_3; C = aerobic control OD_{540} = 0.05; 0.5, 1, 2, 3 and 6 = corresponding time point of cell harvest in h; marker = RNA Molecular Weight Marker I, DIG-labeled (Roche); schematic representation of the genetic arrangement is displayed on top with the used RNA probe marked in grey. *P. aeruginosa* PAO1 cells were cultivated in LB under aerobic conditions until OD_{540} of 0.05 followed by shifting to cultivation under anaerobic conditions in the presence of 50 mM KNO_3. Each time point was cultured separately and after selected time point of 0.5, 1, 2, 3 and 6 hours cultivation under denitrifying conditions cells were harvested followed by RNA preparation. Transcriptional analyses were performed by separating RNA samples on a denaturing 2% formaldehyde-agarose gel and subsequent transfer onto a positively charged nylon membrane via vacuum blotting for four hours. Transcripts were visualized by hybridization with corresponding DIG-labeled RNA probes followed by incubation with AP-coupled anti-DIG antibody and CDP-Star and chemiluminescence signals were visualized using the Luminescent Image Analyzer LAS-3000. Slight bands corresponding to a transcript with a size of roughly 300 bp (red box) and approximately of 1800 bp (black box) were visualized. The smaller transcript indicated a monocistronic transcript for 6frt_26594 while the larger transcript could be the result of a possible co-transcription of 6frt_26594 and *pilS*, which would result in an 1878 bp large transcript.

Overall, two possible transcripts were observed each with a size of around 300 bp and 1800 bp, though the larger transcript was only vaguely visible. While the smaller transcript would correspond to a monocistronic transcription of the sORF of 6frt_26594, the larger transcript could be the result of a co-transcription of *pilS* together with 6frt_26594 resulting in a transcript of 1878 bp. Furthermore, sequence analyses of 6frt_26594 using the iTerm-PseKNC web-server revealed a putative transcriptional terminator immediately downstream of 6frt_26594 further corroborating a monocistronic transcription of 6frt_26594.

In addition, the observed protein kinetics of 6frt_26594 and PilS were quite contradictory. 6frt_26594 was abundant during control conditions while PilS was comparable low, as shown in Figure 51. These contrasting kinetic profiles might indicate an antitermination of the transcription of *pilS* by 6frt_26594. It would be expected that *pilsS* and *pilR* are co-transcribed however, *pilS* is located on the +2 strand while *pilR* is localized on the +1 strand. Moreover, analyzing the sequences of both *pilS* and *pilR* utilizing the iTerm-PseKNC web-server revealed a possible terminator sequence 75 bp downstream of *pilS.* The sensor kinase PilS and the response regulator PilR form the PilSR two-component system that regulates the expression of type 4 fimbriae required for twitching and swimming motility. Furthermore, PilR displayed a contrary protein kinetic as the protein was abundant during cultivation under denitrifying conditions though PilR was exclusively identified with the solubilization approach and thus kinetic profiles might not be comparable with each other.

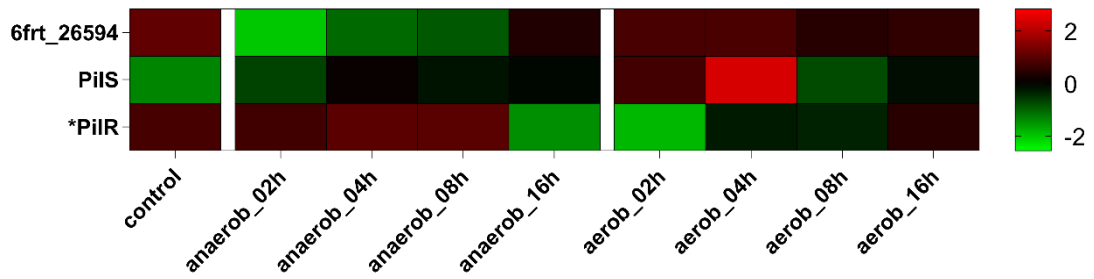

Figure 51 Kinetic profiles of the SP100 6frt_26594 and PilSR.
*PilR = PilR was solely identified with the solubilization approach while both 6frt_26594 and PilS were exclusive to the shaving approach. Z scores of normalized protein intensities ranging from 2.826 (red) to -2.563 (green), the baseline was set to 0 (black). 6frt_26594 and PilS were present in low amounts during cultivation under denitrifying conditions while their amount increased after shifting back to aerobic conditions; however, 6frt_26594 was abundant during control conditions while PilS was comparable low. PilR displayed quite the contrary kinetic profile and was abundant during cultivation under anaerobic conditions while decreasing in amount at the point bacteria entered the stationary phase.

Further analyses regarding the genetic organization of *pilS*, *pilR* and the sORF of 6frt_26594 revealed a similar arrangement of these genes in the genomes of both *P. aeruginosa* PA7 and *P. stutzeri* A1501. In *P. aeruginosa* PA7, the homologous SP100 is encoded by the gene PSPA7_5185, which is 81 aa long and contains one TMH. In contrast, the homologous protein of *P. stutzeri* A1501 is 106 aa long and also contains one TMH. While all three ORFs are located upstream of the *pilS* and *pilR* genes, the corresponding proteins displayed different length while all contained one TMH. Furthermore, comparing the amino acid sequences of all three proteins revealed high sequence similarities highlighting conserved residues among all three proteins, as displayed in Figure 52.

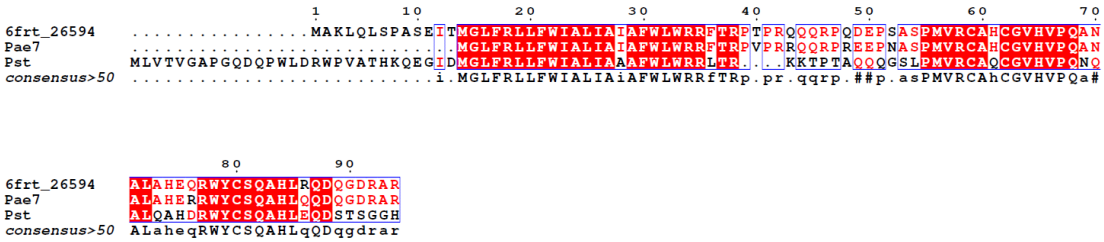

Figure 52 Sequence alignment comparing 6frt_26594 identified in *P. aeruginosa* PAO1 with PSPA7_5185 of *P. aeruginosa* PA7 and PST_3644 of *P. stutzeri*.
Sequences were analyzed using the MultAlin website followed by alignment visualization vie ESPrint 3.0. Pae7 = PSPA7_5185 of *P. aeruginosa* PA7; Pst = PST_3644 of *P. stutzeri*. Overall, all three proteins were highly similar indicating in consequence also similar physiological roles.

Interestingly, while the proteins were annotated in the genomes of *P. aeruginosa* PA7 and *P. stutzeri* A1501, nothing was known about their physiological role. Furthermore, all three proteins displayed characteristics of a MYND-zinc finger-containing protein while a MYND domain (**my**eloid, **N**ervy and **D**EAF-1) was not identified. The MYND domain is primarily present in mammalian and eukaryotic proteins and consists of a cluster of histidine and cysteine residues (Feinstein, *et al.*, 1995). Further analyses of these proteins revealed that the MYND domain might be involved in protein-protein interactions and the present evidence suggests that the MYND domain functions as co-repressor-recruiting interface (Gross, *et al.*, 1996) (Melnick, *et al.*, 2000). As 6frt_26594 was high abundant during control conditions and PilS was only low abundant, these results might indicate a similar role for 6frt_26594.

Altogether, a monocistronic as well as a possible bicistronic transcript was observed using a specific RNA probe against 6frt_26594. Additional

transcriptional analyses against *pilS* might reveal further evidence for the actual transcription of these genes. Nonetheless, analyses of the kinetic profiles and sequence analyses point in the direction that the small protein 6frt_26594 might be a regulatory protein with either repressing or co-repressor-recruiting function. Further characterizations of the small protein are required to understand its influence in *P. aeruginosa* and other pseudomonads. However, the obtained results give direction for further analyses.

3.6.2 Kinetic profile analyses of SP100

Following quantification of identified proteins, kinetic profiles of annotated SP100 were compared to profiles of proteins that are known or predicted to be involved in respiration. For this, *k*-means clustering was performed using the Perseus software to determine the 20 most similar protein profiles.

Thus, cluster analyses of the OM lipoprotein encoded by PA2453 revealed a cluster together with NirD and NosF (Figure 53 A). Furthermore, results of the shaving approach displayed PA2453 also clustered with NirO and NorC (Figure 53 B). In addition to NirD and NosF, the nitrite extrusion protein $NarK_1$ was also identified in a cluster with NosF.

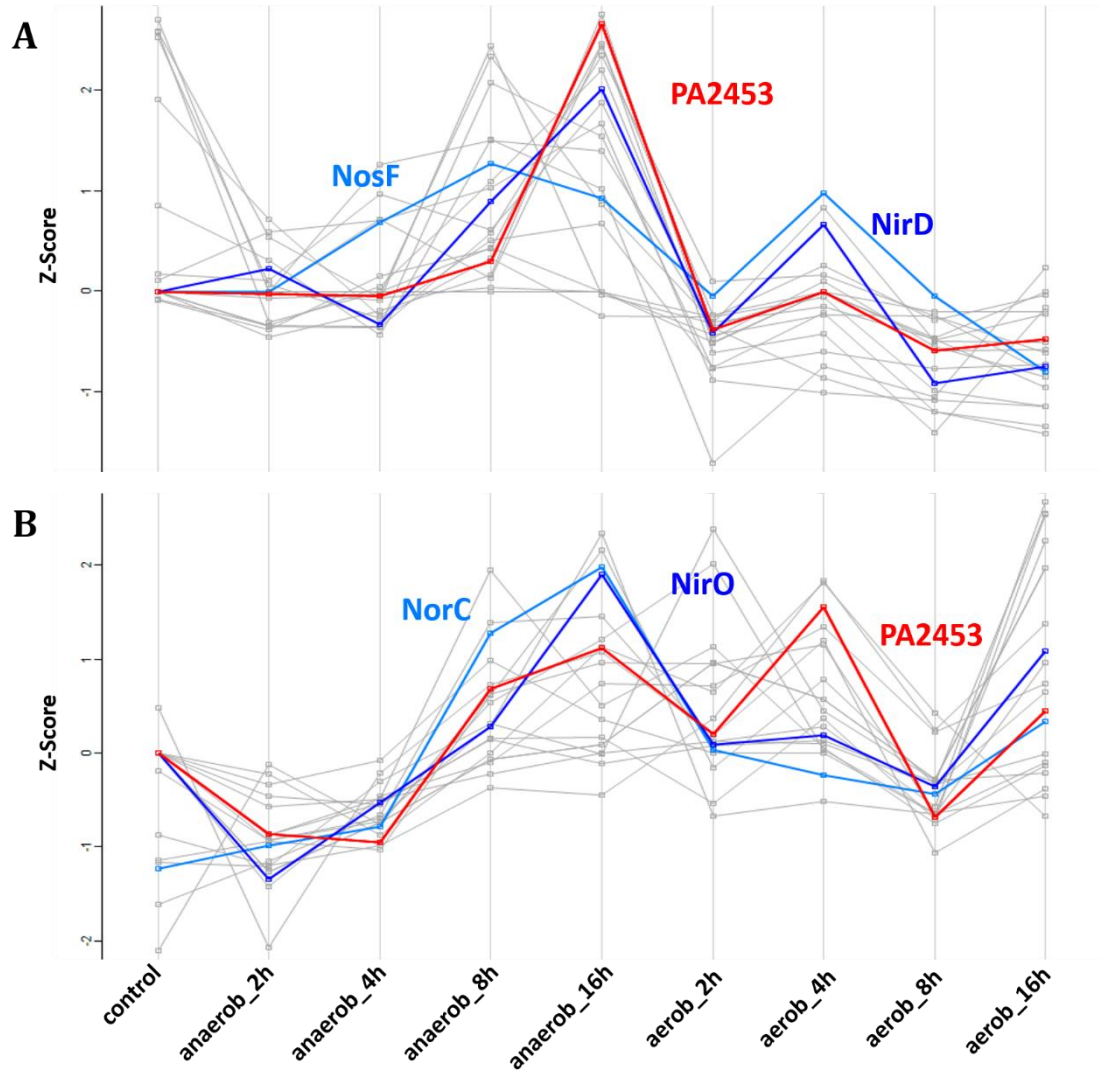

Figure 53 Cluster analyses of PA2453 during anaerobic and aerobic cultivation.
K means clustering of the 20 most similar proteins determined via Spearman correlation distances of PA2453 (red). Results of the **A**) solubilization approach displayed PA2453 high abundant during later stages of cultivation under anaerobic conditions clustering with the proteins NirD (dark blue) and NosF (light blue) while results of the **B**) shaving approach showed PA2453 abundant during and post cultivation under anaerobic conditions in a cluster with NirO (dark blue) and NorC (light blue).

The hypothetical protein PA2453 is predicted to belong to the YgdI/YgdR lipoprotein family and *P. aeruginosa* carries a paralogous protein encoded by PA3031. YgdI/YgdR-like lipoproteins were also identified in other Gram-negative bacteria like *E. coli* and *Salmonella enterica*. However, little is known about the physiological role of these proteins. In *E. coli*, transcriptional analyses of the putative lipoprotein encoding gene observed 4.8-fold and 1.2-fold higher mRNA amounts under anaerobic and denitrifying conditions for YgdI and YgdR, respectively (Brokx, *et al.*, 2004). Further studies predicted that *ygdI* expression is RpoS-mediated under nutrient starvation, stress or at the beginning of the

stationary phase whereas the *ygdR* gene is induced by the regulator of capsular synthesis (Rcs) in response to cell wall damage (Laubacher, *et al.*, 2008). Similar to *E.* coli, *P. aeruginosa* also possesses two YgdI/YgdR-like proteins indicating that these proteins serve a similar function as presumed for *E. coli.*

While the exact function of the YgdI-like lipoprotein is still unclear, the observed kinetic profile correlates with previous reports made in *E. coli* concluding that *P. aeruginosa* also harbors at least one YgdI-like lipoproteins that is somewhat involved in respiration under denitrifying conditions. Furthermore, cluster analyses revealed the protein PA2453 lays in a cluster with NirD, NirO, NorC and NosF, further substantiating a possible role of the small proteins during denitrification.

Following this, the protein PA0522 or NirP was the only integral small membrane protein that clustered with a protein predicted to be involved in respiration, namely the CcoN3 subunit of the orphan cbb_3-type cytochrome *c* oxidase. Interestingly, NirP was the only small protein that clustered with a protein of a terminal oxidase as all other observed SP100 were in a cluster with proteins involved in the reduction of nitrate. Moreover, the obtained cluster showed both NirP and CcoN3 high abundant after shifting to aerobic conditions (Figure 54).

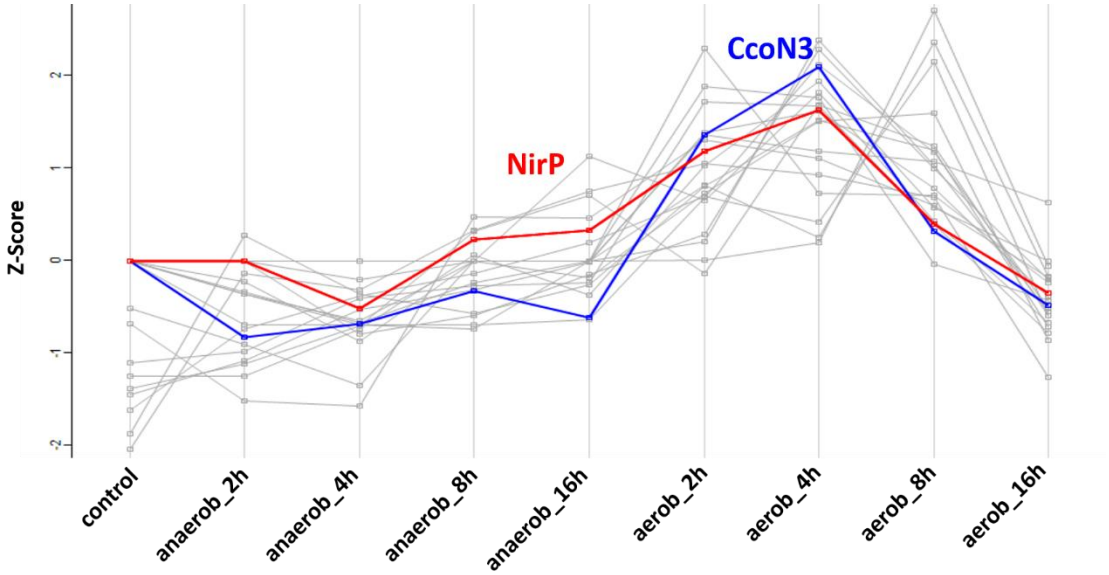

Figure 54 Cluster analysis of NirP during anaerobic and aerobic cultivation.
K means clustering of the 20 most similar proteins determined via Pearson correlation distances of NirP (red). Among the proteins with similar kinetic profile, NirP was found to cluster together with CcoN3 (dark blue) as both proteins were high abundant after shifting to aerobic conditions.

As described previously, the orphan cytochrome oxidase Cco3 and Cco4 might offer a new mechanism for *P. aeruginosa* to handle varying oxygen availability in different growth phases. Additionally, NirO and NirP displayed similarities to subunit III and subunit IV of the bo_3 oxidase indicating that these proteins might be paralogues to CyoC and CyoD of *P. aeruginosa*, which encode subunit III and subunit IV of Cyo, respectively. In *P. aeruginosa*, NirO is predicted to contain five TMHs like CyoC and while CyoC was present in early phases of cultivation under denitrifying conditions NirO was high abundant in later stages of anaerobic cultivation. Similarly, NirP is predicted with three TMHs similar to CyoD while NirP was high abundant after shifting back to aerobic conditions.

Until now, *P. aeruginosa* possesses five annotated terminal oxidases and while the identified orphan cbb_3 oxidases are no independent oxidases, they offer a new mechanism for the adaptation to oxygen. In case of NirOP, they are indeed CyoCD paralogues. The presence of these 'orphan' bo_3-oxidase subunits would further amplify the amount of possible terminal oxidases in *P. aeruginosa* adding an additional component to the respiratory system. To fully understand the physiological role of terminal oxidases and their orphan subunits, deficiency mutants of the genes of the corresponding oxidases can be generated. Subsequently, possible changes in the growth of these mutants under different oxygenic conditions might allude conditions under which these genes are important. Furthermore, generating Strep-tagged versions of the corresponding subunits in combination with mutants deficient in one or more terminal oxidase might contribute to the understanding of the modularity of these oxidases.

Of all identified SP100, the hypothetical protein encoded by PA0526 clustered with the highest number of proteins important for denitrification, namely NorC, NorB and NosL, respectively. This gene is predicted to be located in an operon together with the *dnr* gene, which encodes the corresponding transcriptional regulator. Furthermore, the protein of PA0526 displayed 50% sequence homology to the DnrP protein of *P. stutzeri*, which was also reported in previous studies (Arai, *et al.*, 1995). Interestingly, both *dnrP* and *dnrD* (corresponding to *dnr* of *P. aeruginosa*) of *P. stutzeri* were reported with an Anr binding motif upstream of the corresponding gene and transcriptional analyses revealed monocistronic

transcripts for both genes as well as a bicistronic transcript as a result of the co-transcription of *dnrD* with *dnrP* (Vollack, *et al.*, 2001). In this work, the protein of PA0526 was solely identified via the shaving approach indicating that this SP100 is indeed membrane integrated and as displayed in Figure 55, its kinetic profile clustered together with NorC and NorB of the nitric oxide reductase and the lipoprotein NosL.

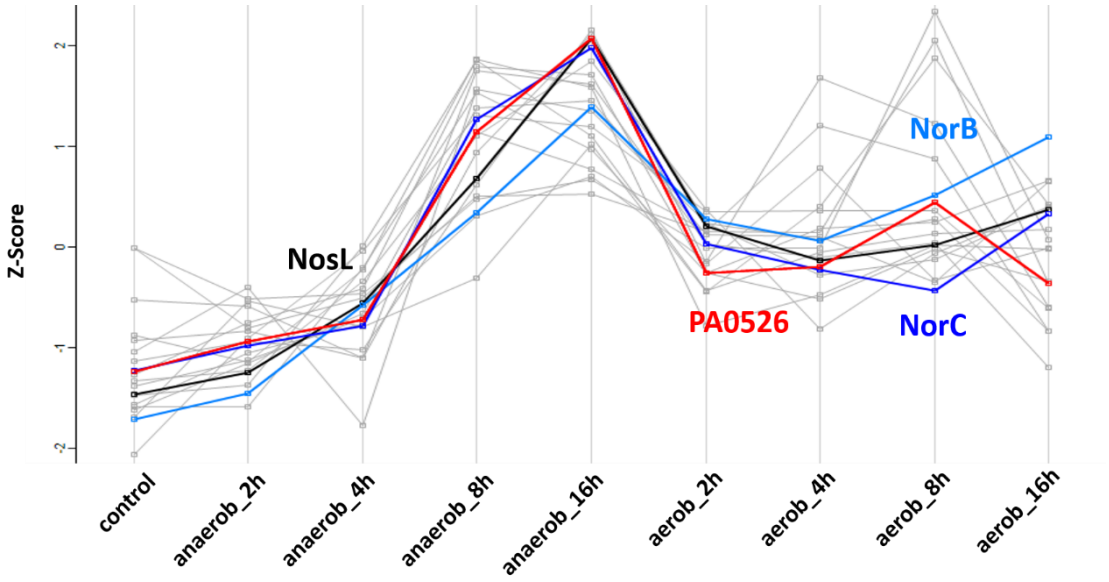

Figure 55 Cluster analysis of PA0526 during anaerobic and aerobic cultivation.
K means clustering of the 20 most similar proteins determined via Pearson correlation distances of PA0526 (red). The small protein was exclusively identified via the shaving approach and among the proteins with similar kinetic profile that clustered together were NorC (dark blue), NorB (light blues) and NosL (black) as all proteins were high abundant during eight and sixteen hours cultivation under anaerobic conditions.

Based on the resulting kinetic profile of PA0526, the protein seems to be involved in denitrification. In addition to this, the proteins NorC and NorB displayed a similar kinetic profile. Interestingly, the *norCBD* operon is located adjacent to the gene PA0526 further emphasizing some involvement of the protein of PA0526 in denitrification. Moreover, the PA0526 gene of *P. aeruginosa* showed similarities to the *dnrP* gene of *P. stutzeri*. Here, *dnrP* is located downstream of *dnrD,* which is homologue to the *dnr* gene of *P. aeruginosa.* In *P. putida*, both *dnrD* and *dnrP* were reported with an upstream Anr binding motif. Similarly, both *dnr* and PA0526 of *P. aeruginosa* were also reported with an upstream Anr binding motif further emphasizing a relevant role of both corresponding proteins during anaerobic conditions. Altogether, the observed protein kinetics also imply a connection between PA0526 and proteins of the nitric oxide reductase. However, the

physiological role of this small, integral membrane protein has yet to be analyzed by further studies.

In addition to these SP100, the small proteins encoded by PA1052a clustered with the proteins NirH and NorC. While this protein seemed to be highly conserved among various *Pseudomonas* species, little to nothing is known about its functionality. The protein is annotated as a hypothetical protein and sequence analyses revealed no conserved domain or known structure. The protein was identified with both the solubilization and the shaving approach and cluster analyses with kinetic profiles of the solubilization approach revealed similarities to the kinetic profiles of NirH and NorC, as shown in Figure 56.

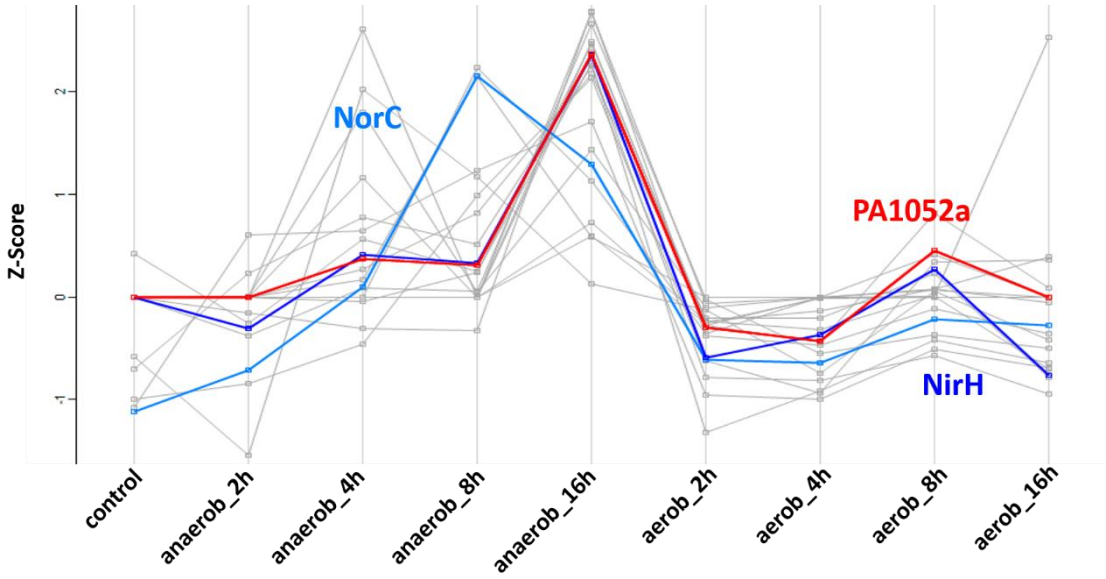

Figure 56 Cluster analysis of PA1052a during anaerobic and aerobic cultivation.
K means clustering of the 20 most similar proteins determined via Pearson correlation distances of PA1052a (red). The small protein was identified with both the solubilization and the shaving approach and among the proteins with similar kinetic profile that clustered together were NirH (dark blue) and NorC (light blues) were identified in high amounts after sixteen hours cultivation under anaerobic conditions.

Again, NorC was among the proteins that clustered together with a small protein which might be an indication that NorC is indeed part of the central assembly platform for the denitrification complex as stated previously. While nothing is known about the physiological role of the small protein encoded by PA1052a, the obtained results imply an involvement during denitrification.

This way, four annotated SP100 were determined that displayed kinetic profiles similar to one or more proteins that are involved in respiration, as listed in Table

15. Interestingly, all SP100 were annotated as hypothetical proteins and one SP100 was predicted to be integral membrane proteins resident in the IM. Furthermore, two SP100 were predicted with one TMH and a possible localization in the cytoplasm where the other one carried an N-terminal signal and was predicted to be an OM lipoprotein.

Table 15 Properties of identified SP100 with kinetic profiles like proteins involved in respiration.
In total, four SP100 were identified that similar expression profiles to proteins, which were known or predicted to be involved in respiration. The Number of TMHs was predicted using TMHMM Server v. 2.0 and localizations were predicted using LocateP v.2. Proteins that were known or predicted to be involved in respiration showing a similar kinetic profile like the SP100 were listed in column 'in Cluster'. Subsequently, related proteins or putative functions were determined using homologue proteins reported in previous studies.

Locus tag	Length [aa]	TMHs	Localization	in Cluster:	Relation/ Function
PA0522	85	3	IM integrated	CcoN3	similar to NorF of *Pc. denitrificans*
PA0526	64	1	cytoplasm	NorC, NorB, NosL	similar to DnrP of *P. stutzeri*
PA1052a	88	1	cytoplasm	NirH, NorC	unknown
PA2453	73	N-term. signal	OM lipoprotein	NirD, NirO, NorC, NosF	OM integrity under stress, stationary phase

Altogether, analyses of the membrane proteome of *P. aeruginosa* in combination with cluster analyses revealed several promising small proteins that might be involved in denitrification or respiration under varying oxygen conditions. Furthermore, these findings draw further emphasis on the importance of the complete characterization of small proteins to elucidate their impact in bacteria and for a complete understanding of physiological important processes like denitrification.

4 Summary and outlook

4.1 Summary

P. aeruginosa is a facultatively anaerobically living bacterium using oxygen or N-oxides as terminal electron acceptors. Previous studies used this bacterium to define the anaerobic respiration complex and surprisingly, interactions and dynamics of proteins that are involved in the electron transport chain under aerobic and anaerobic conditions are little understood and were focused on in the recent ten years. Thus, proteogenomic analyses contributed greatly to the understanding of protein complex formation and assembly. However, proteins smaller than 101 aa (SP100) were neglected so far.

In this work, inner membrane associated proteins from cells shifted from aerobic to anaerobic and back to aerobic conditions were analyzed using two complementary approaches followed by LC-MS/MS analyses to get insight in the dynamics of proteins that are known and predicted to be involved in respiration. Moreover, for the identification of SP100, two different databases were developed covering intergenic regions and all possible six reading frames, respectively.

This way, 76 of 91 proteins known to be involved in aerobic and anaerobic respiration of *P. aeruginosa* were identified. Furthermore, changes in the composition of the terminal oxidases comprising complex IV of the respiratory chain were observed. Here, the cbb_3 oxidases Cco1 and Cco2 diminished under denitrifying conditions and the aa_3 and bo_3 oxidases Cox and Cyo were present. Furthermore, shifting back to aerobic conditions resulted in an increase of different cbb_3 oxidase subunits than before. These findings supported the modular setup of the cbb_3 oxidases in *P. aeruginosa.*

Additionally, 69 SP100 were identified of which the four proteins namely PA0522, PA0526, PA1052a and PA2453 displayed similar expression profiles to proteins involved in anaerobic respiration and thus might be associated with respiratory complexes. Among the 69 SP100 were 14 that were not present in the current annotation of *P. aeruginosa*. Here, transcriptional analyses for three SP100 were performed. Overall, one might be involved in the LPS synthesis of *P. aeruginosa*, one showed involvement in cobalt transport and one displayed strong evidence for a regulatory protein involved in expression of type 4 fimbriae.

4.2 Outlook

P. aeruginosa is able to handle different oxygen concentrations by adapting the composition of the electron transport chain and denitrification is one of the major alternatives. As previously reported and also observed in this work, terminal oxidases play a crucial role during respiration in dependence of oxygen availability. To further assess the roles of different terminal oxidases, mutants deficient in the genes of the corresponding oxidase can be generated, which are then used for growth experiments under different conditions. Furthermore, proteogenomic studies similar to the one performed in this work might reveal possible changes in the composition of respiratory complexes and to clarify whether some oxidases are interchangeable. For analyses of the different cbb_3-type oxidase Cco isoforms, generating Strep-tagged versions of the corresponding subunits in combination with mutants deficient in one or more Cco subunit could contribute to the understanding of the modularity of these oxidases.

In addition, the involvement of proteases like HtpX, ClpP2 and FtsH in denitrification during anaerobic conditions needs to be further addressed. As FtsH was reported to be involved in cbb_3 oxidase maturation, other proteins of respiratory and denitrifying complexes might also be targets for this protease. To clarify this, Strep-tagged, proteolytic inactive forms of FtsH and ClpP2 that retain but not degrade the captured proteins can be generated. Following this, protease-substrate complexes can be analyzed by MS to reveal additional substrates. In addition, as small proteins might be also involved in this degradation process, crosslinking experiments with Strep-tagged proteases followed by MS analyses could contribute to the identification of new interaction partners.

Altogether, four annotated small proteins were identified that might be involved in denitrification or respiration; however, their physiological role needs to be further characterized. This could be achieved by the generation of mutant strains defective in the respective genes and studies regarding their survival under various oxygen depleted conditions as well as proteome analyses of the generated mutant strains. Furthermore, the localization of these small proteins associated with different respiratory complexes can be investigated by generating Strep-

tagged version of these small proteins and applying a PINE-strep based interaction assay.

Furthermore, 14 currently non-annotated small proteins were identified of which three were further analyzed using transcriptional analyses. There, two small proteins were identified, which are homologous to proteins annotated in other *Pseudomonas* strains but not present in the annotation of *P. aeruginosa* PAO1. Of these, the corresponding genes are missing in the current annotation of *P. aeruginosa* PAO1, thus need to be further characterized and subsequently added to the annotation. The third small protein might be involved in the LPS biosynthesis of *P. aeruginosa* and generating a mutant deficient of this gene followed by proteome analyses and additional LPS profiling could contribute to the understanding of the physiological role. Furthermore, the remaining identified, non-annotated small proteins provide additional information for further experiments for the characterization of these proteins.

5 Zusammenfassung

P. aeruginosa ist ein fakultativ anaerobes Bakterium, das Sauerstoff oder N-Oxide als terminale Elektronenakzeptoren verwendet. Dieses Bakterium wurde zur Definition des anaeroben Atmungskomplexes verwendet. Die Wechselwirkungen und die Dynamik der Proteine, die an der Elektronentransportkette unter aeroben und anaeroben Bedingungen beteiligt sind, sind bisher wenig verstanden und wurden in den letzten zehn Jahren schwerpunktmäßig untersucht. In der Vergangenheit durchgeführte proteogenomische Analysen trugen wesentlich zum Verständnis von Proteinkomplexen bei, wobei jedoch Proteine die kleiner als 101 aa (SP100) sind, bisher vernachlässigt wurden.

In dieser Arbeit wurden periphere und integrale Proteine der inneren Membran aus Zellen, die unter verschiedenen Sauerstoffkonzentrationen kultiviert wurden, mit zwei komplementären Ansätzen präpariert, enzymatisch verdaut und massenspektrometrisch analysiert. Dabei sollte insbesondere die Dynamik von Membranproteinen untersucht werden, die mit den verschiedenen Komplexen der Atmungskette assoziiert sind. Des Weiteren wurden zwei verschiedene Datenbanken erstellt, um bisher nicht annotierte kleine Proteine vorherzusagen und zu identifizieren. Mittels des *Pepper* Algorithmus wurden offene Leserahmen für die identifizierten, nicht annotierten kleinen Proteinen ermittelt und charakterisiert.

Insgesamt wurden 76 Proteine identifiziert, die an der aeroben und anaeroben Atmung von *P. aeruginosa* beteiligt sind. Unter anaeroben Bedingungen war eine deutliche Zunahme der Menge der Proteine, die für die Denitrifikation erforderlich sind, zu beobachten. Darüber hinaus wurden Veränderungen in der Zusammensetzung der terminalen Oxidasen, die zum Komplex IV der Atmungskette gehören, beobachtet. Hier nahmen die c*bb*$_3$-Oxidasen Cco1 und Cco2 unter anaeroben, denitrifizierenden Bedingungen ab, gleichzeitig wurde eine deutliche Zunahme der *aa*$_3$- und *bo*$_3$-Oxidasen Cox und Cyo unter diesen Bedingungen beobachtet. Ein Wechsel zu aeroben Bedingungen führte zu einem Anstieg von *cbb*$_3$-Oxidase Untereinheiten, welche unter anaeroben Bedingungen wenig abundant waren. Diese Beobachtungen weisen auf einen modularen Aufbau der *cbb*$_3$-Oxidasen in *P. aeruginosa* hin.

Darüber hinaus wurden 69 SP100 identifiziert, von denen die vier Proteine PA0522, PA0526, PA1052a und PA2453 ähnliche Expressionsprofile wie Proteine aufweisen, die an der anaeroben Atmung beteiligt sind. Das lässt die Vermutung zu, dass die Aktivität dieser Proteine in Verbindung zur Atmungskette steht. Unter den 69 SP100 waren 14, die in der aktuellen Annotation des Genoms von *P. aeruginosa* nicht berücksichtigt wurden. Erste Analysen der Proteine 6frt_14524, igr2243 und 6frt_26594 geben erste Hinweise auf eine Beteiligung an der LPS-Synthese, am Kobalttransport bzw. an der Regulation der Typ 4 Fimbrien in *P. aeruginosa*.

6 References

Adamczack, J., *et al.* 2014. NirN protein from Pseudomonas aeruginosa is a novel electron-bifurcating dehydrogenase catalyzing the last step of heme d1 biosynthesis. *The Journal of Biological Chemistry.* 2014, 289 (44), pp. 30753 - 30762.

Akiyama, Y., *et al.* 1996. FtsH (HflB) is an ATP-dependent protease selectively acting on SecY and some other membrane proteins. *The Journal of biological chemistry.* 1996, 271 (49), pp. 31196 - 31201.

Akiyama, Y., Kihara, A. and Ito, K. 1996. Subunit a of proton ATPase F0 sector is a substrate of the FtsH protease in Escherichia coli. *FEBS letters.* 1996, 399 (1-2), pp. 26 - 28.

Almén, M.S., *et al.* 2009. Mapping the human membrane proteome: a majority of the human membrane proteins can be classified according to function and evolutionary origin. *BMC Biology.* 2009, 7, p. 50.

Andreeva, A., *et al.* 2014. SCOP2 prototype: a new approach to protein structure mining. *Nucleic Acids Research.* 2014, 42, pp. D310 - 314.

Arai, H. 2011. Regulation and function of versatile aerobic and anaerobic respiratory metabolism in Pseudomonas aeruginosa. *Frontiers in Microbiology.* 2011, 2, Article 103.

Arai, H., Igarashi, Y. and Kodama, T. 1995. Expression of the nir and nor genes for denitrification of Pseudomonas aeruginosa requires a novel CRP/FNR-related transcriptional regulator, DNR, in addition to ANR. *FEBS Letters.* 1995, 371 (1), pp. 73 - 76.

Arai, H., Igarashi, Y. and Kodama, T. 1995. The structural genes for nitric oxide reductase from Pseudomonas aeruginosa. *Biochimica et biophysica Acta.* 1995, 1261 (2), pp. 279 - 284.

Arai, H., Mizutani, M. and Igarashi, Y. 2003. Transcriptional regulation of the nos genes for nitrous oxide reductase in Pseudomonas aeruginosa. *Microbiology.* 2003, 149 (Pt 1), pp. 29 - 36.

Bagshaw, R.D., Callahan, J.W. and Mahuran, D.J. 2000. Desalting of In-Gel-Digested Protein Sample with Mini-C18 Columns for Matrix-Assisted Laser Desorption Ionization Time of Flight Peptide Mass Fingerprinting. *Analytical Biochemistry.* 2000, 284 (2), pp. 432 - 435.

Baker, T.A. and Sauer, R.T. 2006. ATP-dependent proteases of bacteria: recognition logic and operating principles. *Trends in biochemical Sciences.* 2006, 31 (12), pp. 647 - 653.

Bali, S., *et al.* 2011. Molecular hijacking of siroheme for the synthesis of heme and d1 heme. *Proceedings of the National Academy of Sciences of the United States of America.* 2011, 108 (45), pp. 18260 - 18265.

Bartnikas, T.B., *et al.* 1997. Characterization of the Nitric Oxide Reductase-Encoding Region in Rhodobacter sphaeroides 2.4.3. *Journal of Bacteriology.* 1997, 179 (11), pp. 3534 - 3540.

Bayer, M.E. 1991. Zones of membrane adhesion in the cryofixed envelope of Escherichia coli. *Joumal of Structural Biology.* 1991, 107 (3), pp. 268 - 280.

Beck, B.J. and Downs, D.M. 1998. The abpE gene encodes a lipoproteins involved in the thiamine synthesis in Salmonella typhimurium. *Journal of Bacteriology.* 1998, 180 (4), pp. 885 - 891.

Benkert, B., *et al.* 2008. Nitrate-responsive NarX-NarL represses arginine-mediated induction of the Pseudomonas aeruginosa arginine fermentation arcDABC operon. *Microbiology.* 2008, 154 (Pt 10), pp. 3053 - 3060.

Berks, B.C., Sargent, F. and Palmer, T. 2000. The Tat protein export pathway. *Molecular Microbiology.* 2000, 35 (2), pp. 260 - 274.

Berry, A.E., *et al.* 2000. Structure and function of cytochrome bc complexes. *Annual Review of Biochemistry*. 2000, 69, pp. 1005 - 1075.

Berry, E.A., *et al.* 2009. Structural and Mutational Studies of the Cytochrome bc1 Complex. [book auth.] C.N. Hunter, *et al. The Purple Phototrophic Bacteria. Advances in Photosynthesis and Respiration.* s.l. : Springer, 2009, pp. 425 - 450.

Beveridge, T.J. 1995. The periplasmic space and the periplasm in Gram-positive and Gram-negative bacteria. *American Society for Microbiology News.* 1995, 61, pp. 125 - 130.

Beveridge, T.J. 1999. Structures of Gram-Negative Cell Walls and Their Derived Membrane Vesicles. *Journal of Bacteriology.* 1999, 181 (16), pp. 4725 - 4733.

Blackler, A.R., *et al.* 2008. A Shotgun Proteomic Method for the Identification of Membrane-Embedded Proteins and Peptides. *Journal of Proteome Research.* 2008, 7 (7), pp. 3028 - 3034.

Blasco, F., *et al.* 1992. Involvement of the narJ or narW gene product in the formation of active nitrate reductase in Escherichia coli. *Molecular Microbiology.* 1992, 6 (2), pp. 221 - 230.

Borrero-de Acuña, J.M., *et al.* 2017. Protein complex formation during denitrification by Pseudomonas aeruginosa. *Microbial biotechnology.* 2017, 10 (6), pp. 1523 - 1534.

Borrero-de Acuña, J.M., *et al.* 2016. Protein network of the Pseudomonas aeruginosa denitrification apparatus. *Journal of Bacteriology.* 2016, 198, pp. 1401 - 1413.

Botzenhart, K. and Döring, G. 1993. Ecology and Epidemiology of Pseudomonas aeruginosa. [book auth.] M. Campa, M. Bendinelli and H. Friedman. *Pseudomonas aeruginosa as an Opportunistic Pathogen. Infectious Agents and Pathogenesis. .* Boston : Springer, 1993, pp. 1 - 18.

Brackenbury, R., Rutishauser, U. and Edelman, G.M. 1981. Distinct calcium-independent and calcium-dependent adhesion systems of chicken embryo cells. *Proceedings of the National Academy of Sciences of the United States of America.* 1981, 78 (1), pp. 387 - 391.

Brandt, U. 2006. Energy converting NADH:quinone oxidoreductase (complex I). *Annual Review of Biochemistry*. 2006, 75, pp. 69 - 92.

Braun, V. 1975. Covalent lipoprotein from the outer membrane of Escherichia coli. *Biochimica et Biophysica Acta.* 1975, 415 (3), pp. 335 - 377.

Brokx, S.J., *et al.* 2004. Genome-wide analysis of lipoprotein expression in Escherichia coli MG1655. *Journal of Bacteriology.* 2004, 186 (10), pp. 3254 - 3258.

Brown, K., *et al.* 2000. A novel type of catalytic copper cluster in nitrous oxide reductase. *Nature Structural Biology*. 2000, 7 (3), pp. 191 - 195.

Bunai, K. and Yamane, K. 2005. Effectiveness and limitation of two-dimensional gel electrophoresis in bacterial membrane protein proteomics and perspectives. *Journal of Chromatography. B, Analytical technologies in the biomedical and life sciences.* 2005, 815 (1-2), pp. 227 - 236.

Burrel, M.M. 1993. *Enzymes of Molecular Biology.* 1993, 16, pp. 277 - 281.

Candiano, G., *et al.* 2004. Blue silver: A very sensitive colloidal Coomassie G-250 staining for proteome analysis. *Electrophoresis.* 2004, 25 (9), pp. 1327 - 1333.

Carey, M.E., Peterson, C.L. and Smale, S.T. 2013. The primer extension assay. *Cold Spring Harbor protocols.* 2013, 2013 (2), pp. 164 - 173.

Carlson, C.A. and Ingraham, J.L. 1983. Comparison of denitrification by Pseudomonas stutzeri, Pseudomonas aeruginosa, and Paracoccus denitrificans. *Applied and Environmental Microbiology.* 1983, 45 (4), pp. 1247 - 1253.

Carlson, C.A., Ferguson, L.P. and Ingraham, J.L. 1982. Properties of dissimilatory nitrate reductase purified from the denitrifier Pseudomonas aeruginosa. *Journal of Bacteriology.* 1982, 151 (1), pp. 162 - 171.

Cascales, E., *et al.* 2002. Pal lipoprotein of Escherichia coli plays a major role in outer membrane integrity. *Journal of bacteriology.* 2002, 184 (3), pp. 754 - 759.

Cecchini, G., *et al.* 2002. Succinate dehydrogenase and fumarate reductase from Escherichia coli. *Biochimica et Biophysica Acta.* 2002, 1553 (1-2), pp. 140 - 157.

Charnock, J.M., *et al.* 2000. Structural investigations of the CuA centre of nitrous oxide reductase from Pseudomonas stutzeri by site-directed mutagenesis and X-ray absorption spectroscopy. *European Journal of Biochemistry.* 2000, 267 (5), pp. 1368 - 1381.

Chen, J. and Strous, M. 2013. Denitrification and aerobic respiration, hybrid electron transport chains and co-evolution. *Biochimica et Biophysica Acta.* 2013, 1827 (2), pp. 136 - 144.

Chiba, S., Akiyama, Y. and Ito, K. 2002. Membrane Protein Degradation by FtsH Can Be Initiated from Either End. *Journal of Bacteriology.* 2002, 184 (17), pp. 4775 - 4782.

Comolli, J.C. and Donohue, T.J. 2004. Differences in two Pseudomonas aeruginosa cbb3 cytochrome oxidases. *Molecular Microbiology.* 2004, 51 (4), pp. 1193 - 1203.

Comolli, J.C. and Donohue, T.J. 2002. Pseudomonas aeruginosa RoxR, a response regulator related to Rhodobacter sphaeroides PrrA, activates expression of the cyanide-insensitive terminal oxidase. *Molecular Microbiology.* 2002, 45 (3), S. 755 - 768.

Compton, S.J. and Jones, C.G. 1985. Mechanism of dye response and interference in the Bradford protein assay. *Analytical biochemistry.* 1985, 151 (2), pp. 369 - 374.

Cooper, M., Tavankar, G.R. and Williams, H.D. 2003. Regulation of expression of the cyanide-insensitive terminal oxidase in Pseudomonas aeruginosa. *Microbiology.* 2003, 149 (Pt 5), pp. 1275 - 1284.

Corpet, F. 1988. Multiple sequence alignment with hierarchical clustering. *Nucleic Acids Research.* 1988, 16 (22), pp. 10881 - 10890.

Cox, J. and Mann, M. 2008. MaxQuant enables high peptide identification rates, individualized p.p.b. - range mass accuracies and proteome-wide protein quantification. *Nature Biotechnology.* 2008, 26, pp. 1367 - 1372.

Cunningham, L., Pitt, M. and Williams, H.D. 1997. The cioAB genes from Pseudomonas aeruginosa code for a novel cyanide-insensitive terminal oxidase related to the cytochrome bd quinol oxidases. *Molecular Microbiology.* 1997, 24 (3), pp. 579 - 591.

Cuypers, H., Viebrock-Sambale, A. and Zumft, W.G. 1992. NosR, a membrane-bound regulatory component necessary for expression of nitrous oxide reductase in denitrifying Pseudomonas stutzeri. *Journal of Bacteriology.* 1992, 174 (16), pp. 5532 - 5539.

Daniel, W.W. 1990. Spearman rank correlation coefficient. *Applied Nonparametric Statistics.* Boston : PWS-Kent, 1990, pp. 358 - 365.

Dasgupta, N., *et al.* 2003. A four-tiered transcriptional regulatory circuit controls flagellar biogenesis in Pseudomonas aeruginosa. *Molecular Microbiology.* 2003, 50 (3), pp. 809 - 8024.

Deuerling, E., *et al.* 1999. Trigger factor and DnaK cooperate in folding of newly synthesized proteins. *Nature.* 1999, 400, pp. 693 - 696.

Diez, D., Çetinkaya-Rundel, M. and Barr, C. 2019. *OpenIntro Statistics: Fourth Edition.* s.l. : OpenIntro, Inc., 2019.

Dubbs, J.M. and Tabita, F.R. 2006. Regulators of nonsulfur purple phototrophic bacteria and the interactive control of CO2 assimilation, nitrogen fixation, hydrogen metabolism and energy generation. *FEMS Microbiology Reviews.* 2006, 28 (3), pp. 353 - 376.

Dubes, R. and Jain, A.K. 1980. Clustering Methodologies in Exploratory Data Analysis. *Advances in Computers.* 1980, 19, pp. 113 - 228.

Dunn, O.J. 1961. Multiple Comparisons among Means. *Journal of the American Statistical Association.* 1961, 56 (293), pp. 52 - 64.

Durand, A., *et al.* 2018. Biogenesis of the bacterial cbb3 cytochrome c oxidase: Active subcomplexes support a sequential assembly model. *The Journal of biological Chemistry.* 2018, 293 (3), pp. 808 - 818.

Eschbach, M., *et al.* 2004. Long-term anaerobic survival of the opportunistic pathogen Pseudomonas aeruginosa via pyruvate fermentation. *Journal of Bacteriology.* 2004, 186 (14), pp. 4596 - 4604.

Esko, J.D., Doering, T.L. and Raetz, C.R.H. 2017. Eubacteria and Archaea. [book auth.] A. Carki, *et al. Essentials of Glycobiology.* Third. Cold Spring Harbor (NY) : Cold Spring Harbor Laboratory Press, 2017, 20.

Feinstein, P.G., *et al.* 1995. Identification of Homeotic Target Genes in Drosophila Melanogaster Including Nervy, a Proto-Oncogene Homologue. *Genetics.* 1995, 140 (2), pp. 573 - 586.

Feng, C.Q., *et al.* 2019. iTerm-PseKNC: a sequence-based tool for predicting bacterial transcriptional terminators. *Bioinformatics.* 2019, 35 (9), pp. 1469 - 1477.

Fernández-Piñar, R., *et al.* 2008. A Two-Component Regulatory System Integrates Redox State and Population Density Sensing in Pseudomonas putida. *Journal of Bacteriology.* 2008, 190 (23), S. 7666 - 7674.

Fick, R. 1993. Pseudomonas aeruginosa—the Microbial Hyena and Its Role in Disease: An Introduciton. *Pseudomonas aeruginosa, the opportunist : pathogenesis and disease.* s.l. : Boca Raton: CRC Press, 1993, pp. 1 - 6.

Filloux, A., Michel, G. and Bally, M. 1998. GSP-dependent protein secretion in gram-negative bacteria: the Xcp system of Pseudomonas aeruginosa. *FEMS Microbiology Reviews.* 1998, 22 (3), pp. 177 - 198.

Fischer, F., *et al.* 2006. Toward the complete membrane proteome: high coverage of integral membrane proteins through transmembrane peptide detection. *Molecular & Cellular Proteomics : MCP.* 2006, 5 (3), pp. 444 - 453.

Freschi, L., *et al.* 2015. Clinical utilization of genomics data produced by the international Pseudomonas aeruginosa consortium. *Frontiers in Microbiology.* 2015, 6:1036.

Frith, M.C., *et al.* 2006. The abundance of short proteins in the mammalian proteome. *PLoS Genetics.* 2006, 2 (4): e52.

Fuchs, S., *et al.* 2007. Anaerobic Gene Expression in Staphylococcus aureus. *Journal of Bacteriology.* 2007, 189 (11), pp. 4275 - 4289.

Fujiki, Y., *et al.* 1982. Isolation of intracellular membranes by means of sodium carbonate treatment: application to endoplasmic reticulum. *The Journal of cell biology.* 1982, 93 (1), pp. 91 - 102.

Fung, J., MacAlister, T.J. and Rothfield, L.I. 1978. Role of murein lipoprotein in morphogenesis of the bacterial division septum: phenotypic similarity of lkyD and lpo mutants. *Journal of bacteriology.* 1978, 133 (3), pp. 1467 - 1471.

Galindo, M.I., *et al.* 2007. Peptides encoded by short ORFs control development and define a new eukaryotic gene family. *PLoS biology.* 2007, 5 (5): e106.

Gamper, M., Zimmermann, A. and Haas, D. 1991. Anaerobic regulation of transcription initiation in the arcDABC operon of Pseudomonas aeruginosa. *Journal of Bacteriology.* 1991, 173 (15), pp. 4742 - 4750.

Garret, R.H. and Grisham, C.M. 2010. *Biochemistry.* (4th ed.). Boston : Brooks/Cole, Cengage Learning, 2010.

Gassel, M., *et al.* 1999. The KdpF subunit is part of the K(+)-translocating Kdp complex of Escherichia coli and is responsible for stabilization of the complex in vitro. *The Journal of biological Chemistry.* 1999, 274 (53), pp. 37901 - 37907.

Giardina, G., *et al.* 2008. NO sensing in Pseudomonas aeruginosa: structure of the transcriptional regulator DNR. *Journal of Molecular Biology.* 2008, 378 (5), pp. 1002 - 1015.

Gohlke, U., *et al.* 2005. The TatA component of the twin-arginine protein transport system forms channel complexes of variable diameter. *Preoceedings of the National Academy of Sciences of the United States of America.* 2005, 102 (30), pp. 10482 - 10486.

Gosset 'Student', W.S. 1908. The Probable Error of a Mean. *Biometrika.* 1908, 6 (1), pp. 1 - 25.

Gottesmann, S., *et al.* 1998. The ClpXP and ClpAP proteases degrade proteins with carboxy-terminal peptide tails added by the SsrA-tagging system. *Genes & Development.* 1998, 12 (9), pp. 1338 - 1347.

Gross, C.T. and McGinnis, W. 1996. DEAF-1, a novel protein that binds an essential region in a Deformed response element. *The EMBO Journal.* 1996, 15 (8), pp. 1961 - 1970.

Gur, E., Biran, D. and Ron, E.Z. 2011. Regulated proteolysis in Gram-negative bacteria: how and when? *Nature Reviews: Microbiology.* 2011, 9 (12), pp. 839 - 848.

Hall, B.M., *et al.* 2016. Two Isoforms of Clp Peptidase in Pseudomonas aeruginosa Control Distinct Aspects of Cellular Physiology. *Journal of Bacteriology.* 2016, 199 (3), pp. pii: e00568-16.

Hanada, K., *et al.* 2007. A large number of novel coding small open reading frames in the intergenic regions of the Arabidopsis thaliana genome are transcribed and/or under purifying selection. *Genome research.* 2007, 17 (5), pp. 632 - 640.

Hanada, K., *et al.* 2010. sORF finder: a program package to identify small open reading frames with high coding potential. *Bioinformatics.* 2010, 26 (3), pp. 399 - 400.

Hardjasa, A., *et al.* 2010. Investigating the Effects of DMSO on PCR Fidelity Using a Restriction Digest-Based Method. *Journal of Experimental Microbiology and Immunology.* 2010, 14, pp. 161 - 164.

Hasegawa, N., Arai, H. and Igarashi, Y. 2003. Need for Cytochrome bc1 Complex for Dissimilatory Nitrite Reduction of Pseudomonas aeruginosa. *Bioscience, Biotechnology, and Biochemistry.* 2003, 67 (1), pp. 121 - 126.

Hasnon, P.I. and Whiteheart, S.W. 2005. AAA+ proteins: have engine, will work. *Nature Reviwes. Molecular cell biology.* 2005, 6 (7), pp. 519 - 529.

Hayashi, N.R., *et al.* 1998. The nirQ gene, which is required for denitrification of Pseudomonas aeruginosa, can activate the RubisCO from Pseudomonas hydrogenothermophila. *Biochimica et Biophysica Acta.* 1998, 1381 (3), pp. 347 - 350.

Hazan, R., *et al.* 2016. Auto Poisoning of the Respiratory Chain by a Quorum Sensing Regulated Molecule Favors Biofilm Formation and Antibiotic Tolerance. *Current Biology.* 2016, 26 (2), S. 195 - 206.

Hecht, A., *et al.* 2017. Measurements of translation initiation from all 64 codons in E. coli. *Nucleic Acids Research.* 2017, 45 (7), pp. 3615 - 3626.

Hederstedt, L. 2002. Succinate:quinone oxidoreductase in the bacteria Paracoccus denitrificans and Bacillus subtilis. *Biochimica et Biophysica Acta.* 2002, 1553 (1-2), pp. 74 - 83.

Heikkilä, M.P., *et al.* 2001. Role of the Tat Transport System in Nitrous Oxide Reductase Translocation and Cytochrome cd1 Biosynthesis in Pseudomonas stutzeri. *Journal of Bacteriology.* 2001, 183 (5), pp. 1663 - 1671.

Heilmann, H.D. 1972. On the Peptidoglycan of the Cell Walls of Pseudomonas aeruginosa. *European Journal of Biochemistry.* 1972, 31 (3), pp. 456 - 463.

Heinrichs, D.E., Yethon, J.A. and Whitfield, C. 1998. Molecular basis for structural diversity in the core regions of the lipopolysaccharides of Escherichia coli and Salmonella enterica. *Molecular Microbiology.* 1998, 30 (2), pp. 221 - 232.

Hino, T., *et al.* 2010. Structural basis of biological N2O generation by bacterial nitric oxide reductase. *Science.* 2010, 330, pp. 1666 - 1670.

Hirai, T., *et al.* 2016. Expression of multiple cbb3 cytochrome c oxidase isoforms by combinations of multiple isosubunits in Pseudomonas aeruginosa. *Proceedings of the National Academy of Sciences of the United States of America.* 2016, 113 (45), pp. 12815 - 12819.

Hobbs, M., *et al.* 1993. PilS and PilR, a two-component transcriptional regulatory system controlling expression of type 4 fimbriae in Pseudomonas aeruginosa. *Molecular Microbiology.* 1993, 7 (5), pp. 669 - 682.

Holloway, B.W. 1955. Genetic recombination in Pseudomonas aeruginosa. *Journal of general Microbiology.* 1955, 13 (3), pp. 572 - 581.

Holm, S. 1979. A Simple Sequentially Rejective Multiple Test Procedure. *Scandinavian Journal of Statistics.* 1979, 6 (2), pp. 65 - 70.

Holst, O. and Seltmann, G. 1982. *The Bacterial Cell Wall.* Berlin : Springer, 1982.

Hsiung Yu, A.Y. 2013. Investigation of ClpXP Protease Mechanism of Function and its Interaction with the Folding Chaperone Trigger Factor. *Biology.* 2013.

Hueck, C.J. 1998. Type III protein secretion systems in bacterial pathogens of animals and plants. *Microbiology an Molecular Biology Reviews: MMBR.* 1998, 62 (2), pp. 379 - 433.

Hunte, C., Zickermann, V. and Brandt, U. 2010. Functional modules and structural basis of confromational coupling in mitochonrial complex I. *Science.* 2010, 329 (5990), pp. 448 - 451.

Hwang, C.-S., Shemorry, A. and Varshavsky, A. 2010. N-Terminal Acetylation of Cellular Proteins Creates Specific Degradation Signals. *Science.* 2010, 327 (5968), pp. 937 - 977.

Inouye, M. 1974. A Three-Dimensional Molecular Assembly Model of a Lipoprotein from the Escherichia coli Outer Membrane. *Proceedings of the National Academy of Sciences of the United States of America.* 1974, 71 (6), pp. 2396 - 2400.

Johnson, J.E. and Cornell, R.B. 1999. Amphitropic proteins: regulation by reversible membrane interactions. *Molecular Membrane Biology.* 1999, 16 (3), pp. 217 - 235.

Kadurugamuwa, J.L. and Beveridge, T.J. 1995. Virulence factors are released from Pseudomonas aeruginosa in association with membrane vesicles during normal growth and exposure to gentamicin: a novel mechanism of enzyme secretion. *Journal of Bacteriology.* 1995, 177 (14), pp. 3998 - 4008.

Kagawa, Y. and Racker, E. 1966. Partial resolution of the enzymes catalyzing oxidative phosphorylation. 8. Properties of a factor conferring oligomycin sensitivity on mitochondrial adenosine triphosphatase. *The Journal of Biological Chemistry.* 1966, 241 (10), pp. 2461 - 2466.

Kahle, M., *et al.* 2018. The insertion of the non-heme FeB cofactor into nitric oxide reductase from P. denitrificans depends on NorQ and NorD accessory proteins. *Biochimica ae Biophysica Acta - Bioenergetics.* 2018, 1859 (10), pp. 1051 - 1058.

Kamath, K.S., *et al.* 2016. Pseudomonas aeruginosa Cell Membrane Protein Expression from Phenotypically Diverse Cystic Fibrosis Isolates Demonstrates Host-Specific Adaptations. *Journal of Proteome Research.* 2016, 15 (7), pp. 2152 - 2163.

Kastenmayer, J.P., *et al.* 2006. Functional genomics of genes with small open reading frames (sORFs) in S. cerevisiae. *Genome research.* 2006, 16 (3), pp. 365 - 373.

Kawakami, T., *et al.* 2010. Differential expression of multiple terminal oxidases for aerobic respiration in Pseudomonas aeruginosa. *Environmental Microbiology.* 2010, 12 (6), pp. 1339 - 1412.

Kawasaki, S., *et al.* 1997. Gene Cluster for Dissimilatory Nitrite Reductase (nir) from Pseudomonas aeruginosa: Sequencing and Identification of a Locus for Heme d1 Biosynthesis. *Journal of Bacteriology.* 1997, 179 (1), p. 235 . 242.

Kihara, A., Akiyama, Y. and Ito, K. 1996. A protease complex in the Escherichia coli plasma membrane: HflKC (HflA) forms a complex with FtsH (HflB), regulating its proteolytic activity against SecY. *The EMBO Journal.* 1996, 15 (22), pp. 6122 - 6131.

Kihara, A., Akiyama, Y. and Ito, K. 1998. Different pathways for protein degradation by the FtsH/HflKC membrane-embedded protease complex: an implication from the interference by a mutant form of a new substrate protein, YccA. *Journal of molecular Biology.* 1998, 279 (1), pp. 175 - 188.

Kihara, A., Akiyama, Y. and Ito, K. 1999. Dislocation of membrane proteins in FtsH-mediated proteolysis. *The EMBO journal.* 1999, 18 (11), pp. 2970 - 2981.

Kihara, A., Akiyama, Y. and Ito, K. 1995. FtsH is required for proteolytic elimination of uncomplexed forms of SecY, an essential protein translocase subunit. *Proceedings of the National Academy of Sciences of the United States of America.* 1995, 92 (10), pp. 4532 - 4536.

Kiraga, J., *et al.* 2007. The relationships between the isoelectric point and: length of proteins, taxonomy and ecology of organisms. *BMC Genomics.* 2007, 8: 163.

Klein, G., *et al.* 2014. Assembly of Lipopolysaccharide in Escherichia coli Requires the Essential LapB Heat Shock Protein. *The Journal of biological Chemistry.* 2014, 289 (21), pp. 14829 - 14853.

Klünemann, T., *et al.* 2020. Crystal structure of NirF: Insights into its role in heme d1 biosynthesis. *bioRvix.* 2020.

Knirel, Y.A., *et al.* 2006. Conserved and variable structural features in the lipopolysaccharide of Pseudomonas aeruginosa. *Journal of Endotoxin Research.* 2006, 12 (6), pp. 324 - 336.

Knowles, M.R. and Boucher, R.C. 2002. Mucus clearance as a primary innate defense mechanism for mammalian airways. *The Journal of Clinical Investigation.* 2002, 109 (5), pp. 571 - 577.

Koch, H.G., *et al.* 2000. Roles of the ccoGHIS gene products in the biogenesis of the cbb(3)-type cytochrome c oxidase. *Journal of molecular Biology.* 2000, 297 (1), pp. 49 - 65.

Kong, W., *et al.* 2015. ChIP-seq reveals the global regulator AlgR mediating cyclic di-GMP synthesis in Pseudomonas aeruginosa. *Nucleic Acids Research.* 2015, 43 (17), pp. 8268 - 8282.

Krey, J.F., *et al.* 2014. Accurate Label-Free Protein Quantitation with High- and Low-Resolution Mass Spectrometers. *Journal of Proteome Research.* 2014, 13 (2), pp. 1034 - 1044.

Krieger, R., *et al.* 2002. The Pseudomonas aeruginosa hemA promoter is regulated by Anr, Dnr, NarL and Integration Host Factor. *Molecular Genetics and Genomics.* 2002, 267 (3), pp. 409 - 417.

Krogh, A., *et al.* 2001. Predicting transmembrane protein topology with a hidden Markov model: application to complete genomes. *Journal of Molecular Biology.* 2001, 305 (3), pp. 567 - 580.

Kruskal, W.H. and Wallis, W.A. 1952. Use of Ranks in One-Criterion Variance Analysis. *Journal of the American Statistical Association.* 1952, 47 (260), pp. 583 - 621.

Kyte, J. and Doolittle, R.F. 1982. A simple method for displaying the hydropathic character of a protein. *Journal of molecular Biology.* 1982, 157 (1), pp. 105 - 132.

Lambert, P.A. 2002. Mechanisms of antibiotic resistance in Pseudomonas aeruginosa. *Journal of the Royal Society of Medicine.* 2002, 95, pp. 22 - 26.

Lancaster, C.R.D. 2002. Succinate:quinone oxidoreductases: an overview. *Biochimica et Biophysica Acta.* 2002, 1553 (1-2), pp. 1 - 6.

Lassek, C., *et al.* 2015. A metaproteomics approach to elucidate host and pathogen protein expression during catheter-associated urinary tract infections (CAUTIs). *Molecular and Cellular Proteomics.* April 2015, 14 (4), pp. 989 - 1008.

Laubacher, M.E. and Ades, S.E. 2008. The Rcs phosphorelay is a cell envelope stress response activated by peptidoglycan stress and contributes to intrinsic antibiotic resistance. *Journal of Bacteriology.* 2008, 190 (6), pp. 2065 - 2074.

le Maire, M., Champeil, P. and Moller, J.V. 2000. Interaction of membrane proteins and lipids with solubilizing detergents. *Biochimica et Biophysica Acta.* 2000, 1508 (1-2), pp. 86 - 111.

Lecoutere, E., *et al.* 2012. A theoretical and experimental proteome map of Pseudomonas aeruginosa PAO1. *Microbiology Open.* 2012, 1 (2), pp. 169 - 181.

Levchenko, I., Luo, L. and Baker, T.A. 1995. Disassembly of the Mu transposase tetramer by the ClpX chaperone. *Genes & Development.* 1995, 9 (19), pp. 2399 - 2408.

Liu, J., Hicks, D.B. and Krulwich, T.A. 2012. Roles of AtpI and Two YidC-Type Proteins from Alkaliphilic Bacillus pseudofirmus OF4 in ATP Synthase Assembly and Nonfermentative Growth. *Journal of Bacteriology.* 2012, 195 (2), pp. 220 - 230.

Lloyd, S.P. 1982. Least squares quantization in PCM. *IEEE Transactions on Information Theory.* 1982, 28 (2), pp. 129 - 137.

Loo, R.R., Dales, N. and Andrews, P.C. 1994. Surfactant effects on protein structure examined by electrospray ionization mass spectrometry. *Protein Science.* 1994, 3 (11), pp. 1975 - 1983.

Low, T.Y., *et al.* 2013. Quantitative and qualitative proteome characteristics extracted from in-depth integrated genomics and proteomics analysis. *Cell Reports.* 2013, 5 (5), pp. 1469 - 1478.

Lüthi, E., *et al.* 1990. The arc operon for anaerobic arginine catabolism in Pseudomonas aeruginosa contains an additional gene, arcD, encoding a membrane protein. *Gene.* 1990, 87 (1), pp. 37 - 43.

Magnowska, Z., *et al.* 2014. Membrane proteomics of Pseudomonas aeruginosa. *Methods in Molecular Biology.* 2014, 1149, pp. 213 - 224.

Majumdar, D., Avissar, Y.J. and Wxche, J.H. 1991. Simultaneous and rapid isolation of bacterial and eukaryotic DNA and RNA: a new approach for isolating DNA. *Biotechniques.* 1991, 11 (1), pp. 94 - 101.

Makhatadze, G.I. and Privalov, P.L. 1992. Protein interactions with urea and guanidinium chloride. A calorimetric study. *Journal of Molecular Biology.* 1992, 226 (2), pp. 491 - 505.

Marshall, A.G., Hendrickson, C.L. and Jackson, G.S. 1998. Fourier transform ion cyclotron resonance mass spectrometry: a primer. *Mass Spectrometry Reviews.* 1998, 17 (1), pp. 1 - 35.

Matos, E.C.O., *et al.* 2018. Mortality in patients with multidrug-resistant Pseudomonas aeruginosa infections: a meta-analysis. *Revista de Sociedade Brasileira de Medicina Tropical.* 2018, 51 (4), pp. 415 - 420.

Matsushita, K., *et al.* 1980. Membrane-bound respiratory chain of Pseudomonas aeruginosa grown aerobically. *Journal of Bacteriology.* 1980, 141 (1), pp. 389 - 392.

Matsushita, K., *et al.* 1983. Membrane-bound respiratory chain of Pseudomonas aeruginosa grown aerobically. A KCN-insensitive alternate oxidase chain and its energetics. *Journal of Biochemistry.* 1983, 93 (4), pp. 1137 - 1144.

Matticks, J.S. 2002. Type IV pili and twitching motility. *Annual Review of Microbiology.* 2002, 56, pp. 289 - 314.

McGuirl, M.A., *et al.* 2001. Expression, purification, and characterization of NosL, a novel Cu(I) protein of the nitrous oxide reductase (nos) gene cluster. *Journal of Biological Inorganic Chemistry.* 2001, 6, pp. 189 - 195.

Melnick, A.M., *et al.* 2000. The ETO Protein Disrupted in t(8;21)-Associated Acute Myeloid Leukemia Is a Corepressor for the Promyelocytic Leukemia Zinc Finger Protein. *Molecular and Cellular Biology.* 2000, 20 (6), pp. 2075 - 2086.

Mercenier, A., *et al.* 1980. Regulation of enzyme synthesis in the arginine deiminase pathway of Pseudomonas aeruginosa. *Journal of Bacteriology.* 1980, 144 (1), pp. 159 - 163.

Meylan, S., *et al.* 2017. Carbon Sources Tune Antibiotic Susceptibility in Pseudomonas aeruginosa via Tricarboxylic Acid Cycle Control. *Cell chemical biology.* 2017, 24 (2), pp. 195 - 206.

Mizuno, T. and Kageyama, M. 1979. Isolation and characterization of major outer membrane proteins of Pseudomonas aeruginosa strain PAO with special reference to peptidoglycan-associated protein. *Journal of biochemistry.* 1979, 86 (4), pp. 979 - 989.

Mogi, T., *et al.* 2009. Biochemical and spectroscopic properties of cyanide-insensitive quinol oxidase from Gluconobacter oxydans. *Journal of Biochemistry.* 2009, 146 (2), pp. 263 - 271.

Möglich, A., Krieger, F. and Kiefhaber, T. 2005. Molecular basis for the effect of urea and guanidinium chloride on the dynamics of unfolded polypeptide chains. *Journal of Molecular Biology.* 2005, 345 (1), pp. 153 - 162.

Moller, S., Croning, M.D.R. and Apweiler, R. 2001. Evaluation of methods for the prediction of membrane spanning regions. *Bioinformatics.* 2001, 17 (7), pp. 646 - 653.

Moore, S.D. and Sauer, R.T. 2005. Ribosome rescue: tmRNA tagging activity and capacity in Escherichia coli. *Molecular Microbiology.* 2005, 58 (2), pp. 456 - 466.

Morand, K., Talbo, G. and Mann, M. 1993. Oxidation of peptides during electrospray ionization. *Rapid communications in mass spectrometry: RCM.* 1993, 7 (8), pp. 738 - 743.

Morein, S., Henricson, D. and Rilfors, L. 1994. Separation of Inner and Outer Membrane Vesicles from Escherichia Coli in Self-Generating Percoll Gradients. *Analytical Biochemistry.* 1994, 216, pp. 47 - 51.

Morihara, K. and Tsuzuki, H. 1975. Specificity of proteinase K from Tritirachium album Limber for synthetic peptides. *Agricultural and Biological Chemistry.* 1975, 39, pp. 1489 - 1492.

Nandi, S., *et al.* 2005. Comparison of theoretical proteomes: identification of COGs with conserved and variable pI within the multimodal pI distribution. *BMC Genomics.* 2005, 6, p. 116.

Navare, A.T., *et al.* 2015. Probing the protein interaction network of Pseudomonas aeruginosa cells by chemical cross-linking mass spectrometry. *Structure.* 2015, 23 (4), pp. 762 - 773.

Nicke, T., *et al.* 2013. Maturation of the cytochrome cd1 nitrite reductase NirS from Pseudomonas aeruginosa requires transient interactions between the three proteins NirS, NirN and NirF. *Bioscience Reports.* 2013, 33 (3), p. e00048.

Noinaj, N., Gumbart, J.C. and Buchanan, S.K. 2017. The β-barrel assembly machinery in motion. *Nature Reviews. Microbiology.* 2017, 15 (4), pp. 197 - 204.

Nouwens, A.S., *et al.* 2000. Complementing genomics with proteomics: the membrane subproteome of Pseudomonas aeruginosa PAO1. *Electrophoresis.* 2000, 21 (17), pp. 3797 - 3809.

Nouwens, A.S., *et al.* 2002. Proteomic comparison of membrane and extracellular proteins from invasive (PAO1) and cytotoxic (6206) strains of Pseudomonas aeruginosa. *Proteomics.* 2002, 2 (9), pp. 1325 - 1346.

Ochsner, U.A., *et al.* 2002. Effects of the twin-arginine translocase on secretion of virulence factors, stress response, and pathogenesis. *Proceedings of the National Academy of Sciences of the United States of America.* 2002, 99 (12), pp. 8312 - 8317.

Ochsner, U.A., *et al.* 2002. GeneChip expression analysis of the iron starvation response in Pseudomonas aeruginosa: identification of novel pyoverdine biosynthesis genes. *Molecular Microbiology.* 2002, 45 (5), pp. 1277 - 1287.

Oda, K. 2012. New families of carboxyl peptidases: serine-carboxyl peptidases and glutamic peptidases. *The Journal of Biochemistry.* 2012, 151 (1), pp. 13 - 25.

Ogura, T., *et al.* 1999. Balanced biosynthesis of major membrane components through regulated degradation of the committed enzyme of lipid A biosynthesis by the AAA protease FtsH (HflB) in Escherichia coli. *Molecular Microbiology.* 1999, 31 (3), pp. 833 - 844.

Okamoto, T., *et al.* 2001. Analysis of the association of proteins with membranes. *Current protocols in cell biology.* June 2001, 5.4, pp. 1 - 17.

Olsen, J. V., Ong, S.-E. and Mann, M. 2004. Trypsin Cleaves Exclusively C-terminal to Arginine and Lysine Residues. *Molecular & Cellular Proteomics.* 2004, 3 (6), pp. 606 - 614.

O'Sullivan, B.P. and Freedman, S.D. 2009. Cystic fibrosis. *Lancet.* 2009, 373, pp. 1891 - 1904.

Ott, C.M. and Lingappa, V.R. 2002. Integral membrane protein biosynthesis: why topology is hard to predict. *Journal of Cell Science.* 2002, 115, pp. 2003 - 2009.

Oyedotun, K.S. and Lemire, B.D. 2004. The quaternary structure of the Saccharomyces cerevisiae succinate dehydrogenase. Homology modeling, cofactor docking, and molecular dynamics simulation studies. *The Journal of biological Chemistry.* 2004, 279 (10), pp. 9424 - 9431.

Palmer, T. and Berks, B.C. 2012. The twin-arginine translocation (Tat) protein export pathway. *Nature Reviews: Microbiology.* 2012, 10 (7), pp. 483 - 496.

Park, S.J., Tseng, C.P. and Gunsalus, R.P. 1995. Regulation of succinate dehydrogenase (sdhCDAB)operon expression in Escherichia coii in response to carbon supply and anaerobiosis: role of ArcA and Fnr. *Molecular Microbiology.* 1995, 15 (3), pp. 473 - 782.

Passador, L., *et al.* 1993. Expression of Pseudomonas aeruginosa virulence genes requires cell-to-cell communication. *Science.* 1993, 260 (5111), pp. 1127 - 1130.

Pawlik, G., *et al.* 2010. The Putative Assembly Factor CcoH Is Stably Associated with the cbb3-Type Cytochrome Oxidase. *Journal of Bacteriology.* 2010, 192 (24), pp. 6378 - 6389.

Peng, M., *et al.* 2012. Protease bias in absolute protein quantitation. *Nature Methods.* 2012, 9 (6), pp. 524 - 525.

Peters, A., *et al.* 2008. Stability of the cbb3-Type Cytochrome Oxidase Requires Specific CcoQ-CcoP Interactions. *Journal of Bacteriology.* 2008, 190, pp. 5576 - 5586.

Petrova, O.E., *et al.* 2012. Microcolony formation by the opportunistic pathogen Pseudomonas aeruginosa requires pyruvate and pyruvate fermentation. *Molecular Microbiology.* 2012, 86 (4), pp. 819 - 835.

Poole, K. 2001. Multidrug efflux pumps and antimicrobial resistance in Pseudomonas aeruginosa and related organisms. *Journal of Molecular Microbiology and Biotechnology.* 2001, 3 (2), pp. 255 - 264.

Qui, D., *et al.* 2008. ClpXP proteases positively regulate alginate overexpression and mucoid conversion in Pseudomonas aeruginosa. *Microbiology.* 2008, 154 (Pt 7), pp. 2119 - 2130.

Raba, D.A., *et al.* 2018. Characterization of the Pseudomonas aeruginosa NQR complex, a bacterial proton pump with roles in autopoisoning resistance. *Journal of biological Chemistry.* 2018, 293 (40), pp. 15664 - 15677.

Raetz, C.R. and Whitfield, C. 2002. Lipopolysaccharide endotoxins. *Annual Reviwes of Biochemistry.* 2002, 71, pp. 635 - 700.

Raetz, C.R.H., *et al.* 2009. Discovery of new biosynthetic pathways: the lipid A story. *Journal of Lipid Research.* 2009, 50, pp. 103 - 108.

Rainey, S. and Repka, J. 2006. Quantitative sequence and open reading frame analysis based on codon bias. *Systemics, Cybernetics and Informatica.* 2006, 4 (1), pp. 65 - 72.

Ramamurthi, K.S., *et al.* 2009. Geometric cue for protein localization in a bacterium. *Science.* 2009, 323 (5919), pp. 1354 - 1357.

Raymond, C.K., *et al.* 2002. Genetic Variation at the O-Antigen Biosynthetic Locus in Pseudomonas aeruginosa. *Journal of Bacteriology.* 2002, 184 (13), pp. 3614 - 3622.

Reimann, J., *et al.* 2007. A pathway for protons in nitric oxide reductase from Paracoccus denitrificans. *Biochimica et Biophysica Acta.* 2007, 1767 (5), pp. 362 - 373.

Reynolds, J.A. and Tanford, C. 1970. The gross conformation of protein-sodium dodecyl sulfate complexes. *The journal of biological Chemistry.* 1970, 245 (19), pp. 5161 - 5165.

Riordan, J.R., *et al.* 1989. Identification of the cystic fibrosis gene: cloning and characterization of complementary DNA. *Science.* 1989, 245, pp. 1066 - 1073.

Rizvi, M., *et al.* 2011. Rising prevalence of antimicrobial resistance in urinary tract infections during pregnancy: necessity for exploring newer treatment options. *Journal of Laboratory Physicians.* 2011, 3 (2), pp. 98 - 103.

Robert, X. and Gouet, P. 2014. Deciphering key features in protein structures with the new ENDscript server. *Nucleic Acids Research.* 2014, 42 (W1), pp. W320 - W324.

Rodionov, D.A., *et al.* 2003. Comparative genomics of the vitamin B12 metabolism and regulation in prokaryotes. *The Journal of biological Chemistry.* 2003, 278 (42), pp. 41148 - 41159.

Roels, S., Driks, A. and Losick, R. 1992. Characterization of spoIVA, a sporulation gene involved in coat morphogenesis in Bacillus subtilis. *Journal of bacteriology.* 1992, 174 (2), pp. 575 - 585.

Sabarth, N., *et al.* 2002. Identification of surface proteins of Helicobacter pylori by selective biotinylation, affinity purification, and two-dimensional gel electrophoresis. *The Journal of biological Chemistry.* 2002, 277 (31), pp. 27896 - 27902.

Saghatelian, A. and Couso, J.P. 2015. Discovery and characterization of smORF-encoded bioactive polypeptides. *Nature chemical biology.* 2015, 11 (12), pp. 909 - 916.

Saidijam, M., Azizpour, S. and Patching, S.G. 2018. Comprehensive analysis of the numbers, lengths and amino acid compositions of transmembrane helices in prokaryotic, eukaryotic and viral integral membrane proteins of high-resolution structure. *Journal of Biomolecular Structure and Dynamics.* 2018, 36 (2), pp. 443 - 464.

Saikawa, N., Akiyama, Y. and Ito, K. 2004. FtsH exists as an exceptionally large complex containing HflKC in the plasma membrane of Escherichia coli. *Journal of structural Biology.* 2004, 146 (1-2), pp. 123 - 129.

Saiki, K., *et al.* 1996. Probing a role of subunit IV of the Escherichia coli bo-type ubiquinol oxidase by deletion and cross-linking analyses. *The Journal of biological Chemistry.* 1996, 271 (26), pp. 15336 - 15340.

Saiki, K., Mogi, T. and Anraku, Y. 1992. Heme O biosynthesis in Escherichia coli: the cyoE gene in the cytochrome bo operon encodes a protoheme IX farnesyltransferase. *Biochemical and biophysical research communications.* 1992, 189 (3), pp. 1491 - 1497.

Sakoh, M., Ito, K. and Akiyama, Y. 2005. Proteolytic activity of HtpX, a membrane-bound and stress-controlled protease from Escherichia coli. *The Journal of biological Chemistry.* 2005, 280 (39), pp. 33305 - 33310.

Sandman, K., Losick, R. and Youngman, P. 1987. Genetic analysis of Bacillus subtilis spo mutations generated by Tn917-mediated insertional mutagenesis. *Genetics.* 1987, 117 (4), pp. 603 - 617.

Santini, S., *et al.* 2014. Binding of azurin to cytochrome c 551 as investigated by surface plasmon resonance and fluorescence. *Journal of Molecular Recognition.* 2014, 27 (3), pp. 124 - 130.

Sargent, F. 2007. The twin-arginine transport system: moving folded proteins across membranes. *Biochemical Society Transactions.* 2007, 35 (Pt 5), pp. 835 - 847.

Sauer, R.T. and Baker, T.A. 2011. AAA+ proteases: ATP-fueled machines of protein destruction. *Annual Review of Biochemistry.* 2011, 80, pp. 587 - 612.

Saunders, N.F.W., *et al.* 1999. Transcription regulation of the nir gene cluster encoding nitrite reductase of Paracoccus denitrificans involves NNR and NirI, a novel type of membrane protein. *Molecular Microbiology.* 1999, 34 (1), pp. 24 - 36.

Sawers, R.G. 1991. Identification and molecular characterization of a transcriptional regulator from Pseudomonas aeruginosa PAO1 exhibiting structural and functional similarity to the FNR protein of Escherichia coli. *Molecular Microbiolgy.* 1991, 5 (6), pp. 1469 - 1481.

Schirmer, E.C., *et al.* 1996. HSP100/Clp proteins: a common mechanism explains diverse functions. *Trends in biochemical Sciences.* 1996, 21 (8), pp. 289 - 296.

Schleifer, K.H. and Kandler, O. 1972. Peptidoglycan types of bacterial cell walls and their taxonomic implications. *Bacteriology Reviews.* 1972, 36 (4), pp. 407 - 477.

Schobert, M. and Jahn, D. 2010. Anaerobic physiology of Pseudomonas aeruginosa in the cystic fibrosis lung. *International Journal of Medical Microbiology.* 2010, 300 (8), pp. 549 - 556.

Schreiber, K., *et al.* 2006. Anaerobic survival of Pseudomonas aeruginosa by pyruvate fermentation requires an Usp-type stress protein. *Journal of Bacteriology.* 2006, 188 (2), pp. 659 - 668.

Schreiber, K., *et al.* 2007. The Anaerobic Regulatory Network Required for Pseudomonas aeruginosa Nitrate Respiration. *Journal of Bacteriology.* 2007, 189 (11), pp. 4310 - 4314.

Schuster, M., *et al.* 2004. The Pseudomonas aeruginosa RpoS regulon and its relationship to quorum sensing. *Molecular Microbiology.* 2004, 51 (4), pp. 973 - 985.

Schwanhäusser, B., *et al.* 2011. Global quantification of mammalian gene expression control. *Nature.* 2011, 473 (7347), pp. 337 - 342.

Selkrig, J., *et al.* 2014. Assembly of β-barrel proteins into bacterial outer membranes. *Biochimica et Biophysica Acta.* 2014, 1843 (8), pp. 1542 - 1550.

Shimohata, N., *et al.* 2002. The Cpx stress response system of Escherichia coli senses plasma membrane proteins and controls HtpX, a membrane protease with a cytosolic active site. *Genes to cells: devoted to molecular & cellular mechanisms.* 2002, 7 (7), pp. 653 - 662.

Shin, J.-B., *et al.* 2013. Molecular Architecture of the Chick Vestibular Hair Bundle. *Nature Neuroscience.* 2013, 16 (3), pp. 365 - 374.

Sievers, S. 2018. Membrane Proteomics in Gram-Positive Bacteria: Two Complementary Approaches to Target the Hydrophobic Species of Proteins. *Methods in molecular Biology.* 2018, 1841, pp. 21 - 33.

Silby, M.W., *et al.* 2011. Pseudomonas genomes: diverse and adaptable. *FEMS Microbiology Reviews.* 2011, 35 (4), pp. 652 - 680.

Silhavy, T.J., Kahne, D. and Walker, S. 2010. The bacterial cell envelope. *Cold Spring Harbor perspectives in Biology.* 2010, 2 (5).

Silvestrini, M.C., *et al.* 1981. The electron transfer system of Pseudomonas aeruginosa: a study of the pH-dependent transitions between redox forms of azurin and cytochrome c551. *Journal of Inorganic Biochemistry.* 1981, 14 (4), pp. 327 - 338.

Silvestrini, M.C., *et al.* 1982. The kinetics of electron transfer between pseudomonas aeruginosa cytochrome c-551 and its oxidase. *Biochemical Journal.* 1982, 203 (2), pp. 445 - 451.

Simon, L.S., *et al.* 2009. Efficacy and safety of topical diclofenac containing dimethyl sulfoxide (DMSO) compared with those of topical placebo, DMSO vehicle and oral diclofenac for knee osteoarthritis. *Pain.* 2009, 143 (3), pp. 238 - 245.

Snider, J. and Houry, W.A. 2006. MoxR AAA+ ATPases: A novel family of molecular chaperones? *Journal of Structural Biology.* 2006, 156 (1), pp. 200 - 209.

Spearman, C. 1904. The proof and measurement of association between two things. *American Joumal of Psychology.* 1904, 15 (1), pp. 72 - 101.

Speers, A.E. and Wu, C.C. 2007. Proteomics of integral membrane proteins--theory and application. *Chemical Reviews.* 2007, 107 (8), pp. 3687 - 3714.

Sriramulu, D.D., Nimtz, M. and Romling, U. 2005. Proteome analysis reveals adaptation of Pseudomonas aeruginosa to the cystic fibrosis lung environment. *Proteomics.* 2005, 5 (14), pp. 3712 - 3721.

Stasyk, T. and Huber, L.A. 2004. Zooming in: fractionation strategies in proteomics. *Proteomics.* 2004, 4 (12), pp. 3704 - 3716.

Storz, G., Wolf, Y.I. and Ramamurthi, K.S. 2014. Small Proteins Can No Longer Be Ignored. *Annual Reviews of Biochemistry.* 2014, 83, pp. 753 - 777.

Stover, C.K., *et al.* 2000. Complete genome sequence of Pseudomonas aeruginosa PA01, an opportunistic pathogen. *Nature.* 2000, 406, pp. 959 - 964.

Thöny-Meyer, L. and Künzler, P. 1997. Translocation to the periplasm and signal sequence cleavage of preapocytochrome c depend on sec and lep, but not on the ccm gene products. *European Joumal of Biochemistry.* 1997, 246 (3), pp. 794 - 799.

Tomoyasu, T., *et al.* 1993. Topology and subcellular localization of FtsH protein in Escherichia coli. *Journal of Bacteriology.* 1993, 175 (5), pp. 1352 - 1357.

Torres, A., *et al.* 2019. NADH Dehydrogenases in Pseudomonas aeruginosa Growth and Virulence. *Frontiers in Microbiology.* 2019, 10, p. 75.

Trunk, K., *et al.* 2010. Anaerobic adaptation in Pseudomonas aeruginosa: definition of the Anr and Dnr regulons. *Environmental Microbiology.* 2010, 12 (6), pp. 1719 - 1733.

Tu, C., *et al.* 2016. Performance Investigation of Proteomic Identification by HCD/CID Fragmentations in Combination with High/Low-Resolution Detectors on a Tribrid, High-Field Orbitrap Instrument. *PLoS One.* 2016, 11 (7), p. e0160160.

Tyanova, S., *et al.* 2016. The Perseus computational platform for comprehensive analysis of (prote)omics data. *Nature Methods.* 2016, 13 (9), pp. 731 - 740.

Typas, A., *et al.* 2011. From the regulation of peptidoglycan synthesis to bacterial growth and morphology. *Nature Reviews. Microbiology.* 2011, 10 (2), pp. 123 - 136.

Van Alst, N.E., *et al.* 2010. Compensatory periplasmic nitrate reductase activity supports anaerobic growth of Pseudomonas aeruginosa PAO1 in the absence of membrane nitrate reductase. *Canadian Journal of Microbiology.* 2010, 55 (10), pp. 1133 - 1144.

van Bloois, E., *et al.* 2008. Detection of cross-links between FtsH, YidC, HflK/C suggests a linked role for these proteins in quality control upon insertion of bacterial inner membrane proteins. *FEBS Letters.* 2008, 528 (10), pp. 1419 - 1424.

Vasil, M.L. and Ochsner, U.A. 1999. The response of Pseudomonas aeruginosa to iron: genetics, biochemistry and virulence. *Molecular Microbiology.* 1999, 34 (3), pp. 399 - 413.

Villegas, A. and Kropinski, A.M. 2008. An analysis of initiation codon utilization in the Domain Bacteria - concerns about the quality of bacterial genome annotation. *Microbiology.* 2008, 154 (Pt 9), pp. 2559 - 2661.

Vollack, K.U. and Zumft, W.G. 2001. Nitric oxide signaling and transcriptional control of denitrification genes in Pseudomonas stutzeri. *Journal of Bacteriology.* 2001, 183 (8), pp. 2516 - 2526.

Wang, J., Hartling, J.A. and Flanagan, J.M. 1997. The structure of ClpP at 2.3 A resolution suggests a model for ATP-dependent proteolysis. *Cell.* 1997, 91 (4), pp. 447 - 456.

Wasserstein, R.L. and Lazar, N.A. 2016. The ASA Statement on p-Values: Context, Process, and Purpose. *The American Statistician.* 2016, 70 (2), pp. 129 - 133.

Waterman, M.R. 1976. Effect of carbamidomethylation of cysteine residues G11(104)alpha on the properties of hemoglobin A. *Biochimica et biophysica acta.* 1976, 439 (1), pp. 167 - 174.

Weingarten, R.A., Taveirne, M.E. and Olson, J.W. 2009. The Dual-Functioning Fumarate Reductase Is the Sole Succinate:Quinone Reductase in Campylobacter jejuni and Is Required for Full Host Colonization. *Journal of Bacteriology.* 2009, 191 (16), pp. 5293 - 5300.

Wetzstein, M., *et al.* 1992. Cloning, sequencing, and molecular analysis of the dnaK locus from Bacillus subtilis. *Jourbal of Bacteriology.* 1992, 174 (10), pp. 3300 - 3310.

Whittaker, C.A. and Hynes, R.O. 2002. Distribution and evolution of von Willebrand/integrin A domains: Widely dispersed domains with roles in cell adhesion and elsewhere. *Molecular Biology of the Cell.* 2002, 13 (10), pp. 3369 - 3387.

Williams, H.D., Zlosnik, J.E. and Ryall, B. 2007. Oxygen, cyanide and energy generation in the cystic fibrosis pathogen Pseudomonas aeruginosa. *Advances in Microbial Physiology.* 2007, 52, pp. 1 - 71.

Williams, M.D., Ouyang, T.X. and Flickinger, M.C. 1994. Starvation-induced expression of SspA and SspB: the effects of a null mutation in sspA on Escherichia coli protein synthesis and survival during growth and prolonged starvation. *Molecular Microbiology.* 1994, 11 (6), pp. 1029 - 1043.

Winsor, G.L., *et al.* 2016. Enhanced annotations and features for comparing thousands of Pseudomonas genomes in the Pseudomonas genome database. *Nucleic Acids Research.* 2016, 44 (D1), pp. 646 - 653.

Worlitzsch, D., *et al.* 2002. Effects of reduced mucus oxygen concentration in airway Pseudomonas infections of cystic fibrosis patients. *The Journal of Clinical Investigation.* 2002, 109, pp. 317 - 325.

Wunsch, P. and Zumft, W.G. 2005. Functional domains of NosR, a novel transmembrane iron-sulfur flavoprotein necessary for nitrous oxide respiration. *Journal of Bacteriology.* 2005, 187 (6), pp. 1992 - 2001.

Xue, T., *et al.* 2011. The Staphylococcus aureus KdpDE two-component system couples extracellular K+ sensing and Agr signaling to infection programming. *Infection and Immunity.* 2011, 79 (6), pp. 2154 - 2167.

Yagi, T., *et al.* 2001. NADH dehydrogenases: from basic science to biomedicine. *Journal of Bioenergetics and Biomembranes.* 2001, 33 (3), pp. 233 - 242.

Yang, X., *et al.* 2011. Discovery and annotation of small proteins using genomics, proteomics, and computational approaches. *Genome research.* 2011, 21 (4), pp. 634 - 641.

Yasid, N.A., *et al.* 2016. Homeostasis of metabolites in Escherichia coli on transition from anaerobic to aerobic conditions and the transient secretion of pyruvate. *Royal Society Open Science.* 2016, 3 (8).

Yin, Y., *et al.* 2013. Draft Genome Sequences of Two Alginate-Overproducing Variants of Pseudomonas aeruginosa, PAO1-VE2 and PAO1-VE13. *Genome Announcements.* 2013, 1 (6), pp. pii: e01031-13.

Yokota, S., *et al.* 1987. Characterization of a polysaccharide component of lipopolysaccharide from Pseudomonas aeruginosa IID 1008 (ATCC 27584) as D-rhamnan. *European Journal of Biochemistry.* 1987, 167 (2), pp. 203 - 209.

Yu, Y.Q., *et al.* 2003. Enzyme-friendly, mass spectrometry-compatible surfactant for in-solution enzymatic digestion of proteins. *Analytical Chemistry.* November 2003, 75 (21), pp. 6023 - 6028.

Yu, Y.Q., Gilar, M. and Gebler, J.C. 2004. A complete peptide mapping of membrane proteins: a novel surfactant aiding the enzymatic digestion of bacteriorhodopsin. *Rapid Communications in Mass Spectrometry.* 2004, 18 (6), pp. 711 - 715.

Zhang, Y., *et al.* 2009. Comparative genomic analyses of nickel, cobalt and vitamin B12 utilization. *BMC Genomics.* 2009, 10:78.

Zhou, M., *et al.* 2008. LocateP: genome-scale subcellular-location predictor for bacterial proteins. *BMC Bioinformatics.* 2008, 9 (173).

Ziebandt, A.K., *et al.* 2001. Extracellular proteins of Staphylococcus aureus and the role of SarA and sigma B. *Proteomics.* 2001, 1 (4), pp. 480 - 493.

Zufferey, R., *et al.* 1996. Assembly and function of the cytochrome cbb3 oxidase subunits in Bradyrhizobium japonicum. *The Journal of biological Chemistry.* 1996, 271 (15), pp. 9114 - 9119.

Zumft, W.G. 1997. Cell biology and molecular basis of denitrification. *Microbiology and Molecular Biology Reviews: MMBR.* 1997, 61 (4), pp. 533 - 616.

Zumft, W.G., Viebrock-Sambale, A. and Braun, C. 1990. Nitrous oxide reductase from denitrifying Pseudomonas stutzeri. Genes for copper-processing and properties of the deduced products, including a new member of the family of ATP/GTP-binding proteins. *European Journal of Biochemistry.* 1990, 192 (3), pp. 591 - 599.

7 Acknowledgement

At this point I would like to thank all the people that helped me throughout the time of my PhD in one or another manner.

First, I would like to thank Prof. Dr. Susanne Engelmann for the excellent supervision and advice throughout my work, also entrusting me with this project and, hence succeeding. I would like to thank Prof. Dr. Ralf-Rainer Mendel for funding via the DFG and the possibility to participate in the PROCOMPAS graduate school as well as Dr. Dagmar Zwerschke for the scientific, administrative support and a friendly ear.

Furthermore, I direct my thank to Prof. Dr. Michael Steinert for supporting my work at the Institute of Microbiology. I also thank Prof. Dr. Dieter Jahn for the scientific expertise and taking over the second examiner as well as Prof. Dr. André Fleißner for the acceptance of the chairmanship of the examination commission.

Next, I profoundly appreciate the support by Prof. Dr. Lothar Jänsch and Dr. Josef Wissing regarding mass spectrometric analyses at the Orbitrap Fusion and scientific discussions. Furthermore, I thank Dr. Stephan Fuchs from the Robert-Koch Institute in Wernigerode for the excellent support during bioinformatic analyses, the cooperation, and the development of the *Pepper* without whom I would still evaluate all data manually.

Special thanks go to Dr. Martin Kucklick for the support regarding mass spectrometric analyses and troubleshooting as well as all members of the research group Birgit Jung, Nicole Beier, Julia Bosselmann, Martin Weinert, Alexander Beckmann, Ayten Mustafayeva and all bachelor and master students for the friendly environment, and also for the cake.

Special thanks go to Christina Nitzsche and Gunhild Voß for administrative support throughout my work.

Last but not least, I would like to thank my family, my friends and Nils for all the personal support and patience they had all this time.

8 Appendix

8.1 Determined optical densities for growth curve and absorbances of nitrate concentration determination

Table 16 Determined optical densities and nitrate concentrations.
R1, R2, R3 and R4 = replicate 1, 2, 3 and 4, respectively. Cell densities were determined via optical density measurements at a wavelength of 540 nm. Nitrate concentrations were determined by photometrically measuring the amount of nitrate-nitrogen (NO3-N) at a wavelength of 375 nm using the Nitrate Spectroquant® Analytical Test Kit.

	WT R1			WT R2			WT R3			WT R4		
time [h]	OD_{540}	OD_{375}	NO_3^- [g/l]	OD_{540}	OD_{375}	NO_3^- [g/l]	OD_{540}	OD_{375}	NO_3^- [g/l]	OD_{540}	OD_{375}	NO_3^- [g/l]
0	0.062			0.062			0.065			0.064		
2	0.380			0.470			0.460			0.400		
2.08	0.550			0.550			0.525			0.525		
4.08	0.450	0.398	7.79	0.580	0.352	6.81	0.560	0.386	7.54	0.460	0.352	6.81
6.08	0.560	0.367	7.13	0.450	0.341	6.58	0.630	0.361	7.01	0.410	0.342	6.60
8.08	0.800	0.362	7.03	0.560	0.341	6.58	0.640	0.358	6.94	0.630	0.340	6.56
10.08	0.610	0.362	7.03	0.570	0.346	6.69	0.570	0.352	6.81	0.590	0.351	6.79
12.08	0.700	0.342	6.60	0.620	0.348	6.73	0.780	0.376	7.33	0.640	0.341	6.58
14.08	0.800	0.311	5.94	0.780	0.337	6.50	0.750	0.328	6.30	0.700	0.325	6.24
16.08	0.990	0.222	4.05	0.780	0.263	4.92	0.850	0.295	5.60	0.870	0.293	5.56
18.08	1.830	0.183	3.22	1.590	0.221	4.03	1.970	0.243	4.50	1.640	0.267	5.01
19.08	1.240			1.140			1.230			0.990		
20.08	2.240	0.182	3.20	1.830	0.206	3.71	2.490	0.243	4.50	1.850	0.211	3.81
21.08	1.930			1.990			2.140			1.870		
22.08	2.090	0.188	3.33	2.400	0.210	3.79	2.580	0.214	3.88	2.110	0.205	3.69
23.08	2.410			2.080			2.330			2.240		
24.08	2.400	0.211	3.81	2.450	0.192	3.41	2.450	0.212	3.84	2.520	0.193	3.43
25.08	2.370			2.360			2.570			2.540		
26.08	2.720	0.162	2.77	2.730	0.228	4.18	2.660	0.235	4.33	2.700	0.207	3.73
27.08	2.570			2.520			2.740			2.680		
28.08	2.790	0.164	2.81	2.930	0.193	3.43	3.170	0.229	4.20	3.160	0.217	3.94
29.08	2.450			2.360			2.390			2.510		
30.08	2.500	0.172	2.99	2.450	0.210	3.79	2.650	0.230	4.22	2.710	0.206	3.71
31.08	2.610			2.630			2.830			2.830		
32.08	2.530	0.180	3.16	2.700	0.231	4.24	2.930	0.235	4.33	2.900	0.191	3.39
33.08	2.810			2.730			3.080			2.950		
34.08	2.740	0.180	3.16	2.870	0.219	3.99	3.070	0.250	4.64	3.040	0.193	3.43

8.2 Regression curves for growth rate determination

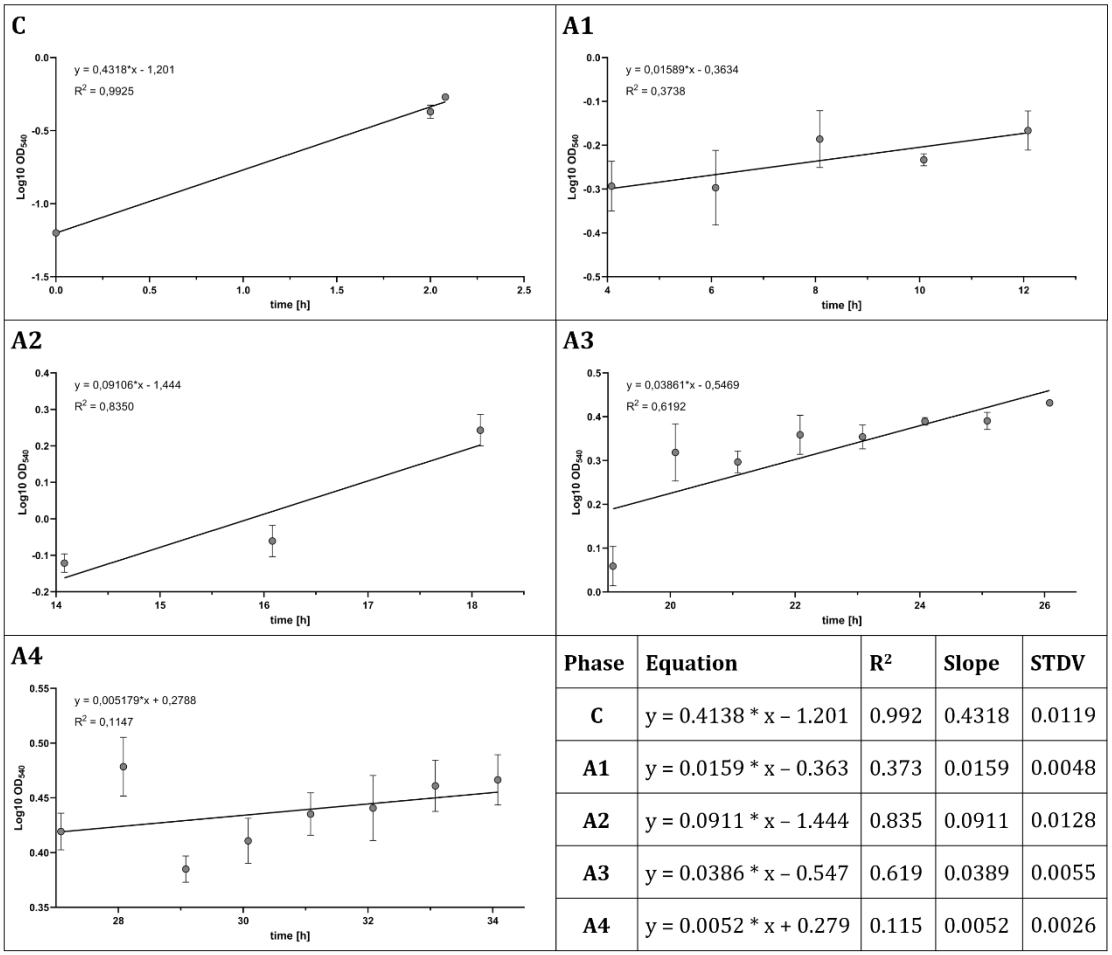

Phase	Equation	R^2	Slope	STDV
C	y = 0.4138 * x – 1.201	0.992	0.4318	0.0119
A1	y = 0.0159 * x – 0.363	0.373	0.0159	0.0048
A2	y = 0.0911 * x – 1.444	0.835	0.0911	0.0128
A3	y = 0.0386 * x – 0.547	0.619	0.0389	0.0055
A4	y = 0.0052 * x + 0.279	0.115	0.0052	0.0026

Figure 57 Determined regression curves of observed growth phases of cultivation of *P. aeruginosa* under aerobic and anaerobic conditions.
R2 = coefficient of determination; slope = slope of the equation of the determined regression curve; STDV = standard deviation of the determined slope. The *P. aeruginosa* strain PA01 was cultivated in complex medium to determine its growth behavior before and after shifting the cells from aerobic to anaerobic conditions and vice versa. Therefore, four biological replicates were used and the bacterial culture density started at an OD_{540} around 0.06. Regression curves were determined for each of the five observed phase.

8.3 SDS-PAGEs of membrane protein extracts of *P. aeruginosa* PAO1 WT

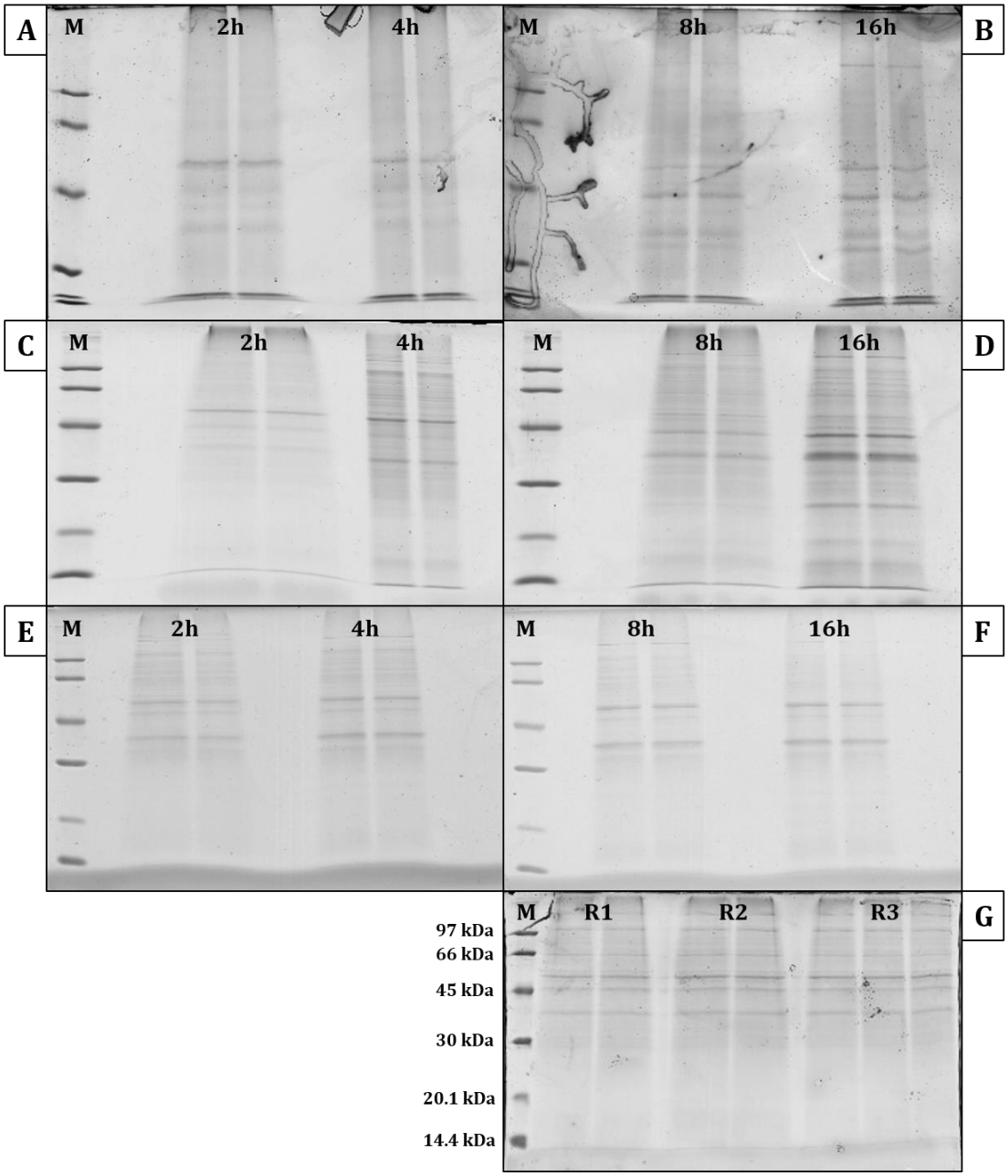

Figure 58 SDS-PAGEs of the inner membrane protein extracts of *P. aeruginosa* PAO1 WT in 1.3 L LB medium under aerobic and anaerobic conditions.

A, C + E = anaerobic cultivation, harvest after 2 h or 4 h of replicates 1, 2 and 3 respectively; B, D + F = anaerobic cultivation, harvest after 8 h or 16 h of replicates 1, 2 and 3 respectively; G = aerobic cultivation until OD_{450} = 0.5 of replicates 1, 2 and 3; M = Marker (Low Molecular Weight Marker, GE Healthcare). *P. aeruginosa* PAO1 WT was cultivated under aerobic conditions until an OD_{450} of 0.5. Controls were harvested in triplicates and the remaining cultures were shifted to anaerobic cultivation with 50 mM KNO_3. After the indicated time points, cultures were harvested via centrifugation followed by cell lysis using the FastPrep™. The cell lysate was subjected to a three-step sucrose gradient and the inner membrane fraction was selected and washed. Following, the membrane proteins were prepared and the protein concentration was determined. Of each sample, 20 µg protein were mixed with one volume loading dye and separated on a 12% SDS-gel. 10 µl of LMW marker were loaded as a size standard. The gel ran for about two hours at 150 V until the running front was close to the gel border. The gels were fixed for one hour in 40% ethanol/ 10% acetic acid, shortly washed in ddH_2O and stained for one hour in Coomassie G-250 solution. Afterwards, the gels were washed in ddH_2O until the background was sufficiently destained.

8.4 Amount of protein in fractions of samples of the solubilization approach

Table 17 Protein amount of each fraction of all samples of the solubilization approach.
R1 = replicate 1, R2 = replicate 2, R3 = replicate 3, C = aerobic control, 2h = 2 h anaerobic cultivation, 4h = 4 h anaerobic cultivation, 8h = 8 h anaerobic cultivation, 16h = 16 h anaerobic cultivation. Trypsin was added to the samples in a ratio of 1 : 20.

Sample	Fraction	Integral-Bkg.	Protein [µg]	Trypsin [µg]
C_R1	1	592944.0	3.33	0.17
	2	450739.3	2.53	0.13
	3	523526.8	0.49	0.02
	4	432301.6	2.43	0.12
	5	421649.4	2.37	0.12
	6	407818.4	2.29	0.11
	7	331841.4	1.86	0.09
	8	299349.3	1.68	0.08
2h_R1	1	102394085.0	7.23	0.36
	2	77745147.9	5.49	0.27
	3	62244986.4	4.39	0.22
	4	26274472.8	0.31	0.02
	5	38503997.6	2.72	0.14
	6	50884397.0	3.59	0.18
	7	51624981.4	3.64	0.18
	8	53358915.5	3.77	0.19
4h_R1	1	114591492.0	8.09	0.40
	2	95703106.3	6.76	0.34
	3	72711326.8	5.13	0.26
	4	22722262.0	0.27	0.01
	5	50809985.0	3.59	0.18
	6	47986651.0	3.39	0.17
	7	58559818.1	4.13	0.21
	8	54612193.4	3.85	0.19
8h_R1	1	70917575.2	2.89	0.14
	2	35367484.5	1.44	0.07
	3	51504602.8	2.10	0.10
	4	11347968.6	0.08	0.00
	5	32118793.5	1.31	0.07
	6	39007368.5	1.59	0.08

Sample	Fraction	Integral-Bkg.	Protein [µg]	Trypsin [µg]
	7	23774297.3	0.97	0.05
	8	21610219.7	0.88	0.04
16h_R1	1	75409968.6	3.07	0.15
	2	66744795.6	2.72	0.14
	3	52618307.6	2.14	0.11
	4	14895800.9	0.10	0.01
	5	34180542.6	1.39	0.07
	6	36887689.7	1.50	0.08
	7	27314803.6	1.11	0.06
	8	36725104.9	1.50	0.07
C_R2	1	616586.4	3.46	0.17
	2	480485.6	2.70	0.13
	3	617312.9	0.58	0.03
	4	501657.3	2.82	0.14
	5	502119.8	2.82	0.14
	6	458260.6	2.57	0.13
	7	350823.8	1.97	0.10
	8	313898.2	1.76	0.09
2h_R2	1	47189975.5	4.37	0.22
	2	26161365.9	2.42	0.12
	3	27275829.1	2.53	0.13
	4	12795401.8	0.20	0.01
	5	22984769.4	2.13	0.11
	6	19567398.3	1.81	0.09
	7	33222609.8	3.08	0.15
	8	42487588.6	3.93	0.20
4h_R2	1	29621485.2	2.74	0.14
	2	21337043.2	1.98	0.10
	3	35953333.0	3.33	0.17
	4	11399991.4	0.18	0.01
	5	20040915.6	1.86	0.09
	6	23313673.9	2.16	0.11
	7	58711793.6	5.44	0.27
	8	50062190.2	4.63	0.23
8h_R2	1	36162514.0	2.52	0.13

Sample	Fraction	Integral-Bkg.	Protein [µg]	Trypsin [µg]
	2	25534326.3	1.78	0.09
	3	41726503.0	2.91	0.15
	4	9957147.4	0.12	0.01
	5	33328141.4	2.33	0.12
	6	34025946.0	2.37	0.12
	7	35288153.1	2.46	0.12
	8	33888672.1	2.37	0.12
16h_R2	1	35309095.2	2.46	0.12
	2	27801081.3	1.94	0.10
	3	36379925.0	2.54	0.13
	4	9766663.8	0.11	0.01
	5	41770216.5	2.92	0.15
	6	51261977.9	3.58	0.18
	7	49740743.4	3.47	0.17
	8	55544727.3	3.88	0.19
C_R3	1	769801.5	4.32	0.22
	2	616200.8	3.46	0.17
	3	786324.0	0.74	0.04
	4	674429.3	3.79	0.19
	5	666496.9	3.74	0.19
	6	595067.8	3.34	0.17
	7	481760.6	2.70	0.14
	8	424493.6	2.38	0.12
2h_R3	1	39918036.6	6.33	0.32
	2	30970647.8	4.91	0.25
	3	29388256.9	4.66	0.23
	4	9427656.6	0.25	0.01
	5	25451090.5	4.04	0.20
	6	21753230.1	3.45	0.17
	7	48349748.5	7.67	0.38
	8	41529739.6	6.59	0.33
4h_R3	1	49155185.4	7.80	0.39
	2	22960871.6	3.64	0.18
	3	37158013.3	5.90	0.29
	4	11671882.3	0.31	0.02

Sample	Fraction	Integral-Bkg.	Protein [µg]	Trypsin [µg]
	5	29098559.8	4.62	0.23
	6	27913107.0	4.43	0.22
	7	50288736.9	7.98	0.40
	8	47839129.6	7.59	0.38
8h_R3	1	25398848.2	5.02	0.25
	2	13654393.0	2.70	0.13
	3	16073260.2	3.17	0.16
	4	7137647.5	0.23	0.01
	5	14005715.0	2.77	0.14
	6	17152921.3	3.39	0.17
	7	26195365.3	5.17	0.26
	8	25001837.4	4.94	0.25
16h_R3	1	21872747.2	4.32	0.22
	2	7084793.3	1.40	0.07
	3	17087731.1	3.38	0.17
	4	6247257.9	0.21	0.01
	5	15438338.0	3.05	0.15
	6	18082681.6	3.57	0.18
	7	22015901.6	4.35	0.22
	8	26540240.7	5.24	0.26

8.5 Determined OD_{590}/OD_{450} ratios and resulting protein concentrations of samples of the shaving approach before chymotrypsin digestion

Table 18 Determined OD590/OD450 ratios and resulting protein concentrations of samples of the shaving approach before chymotrypsin digestion.
R1 = replicate 1, R2 = replicate 2, R3 = replicate 3, C = aerobic control, 2h = 2 h anaerobic cultivation, 4h = 4 h anaerobic cultivation, 8h = 8 h anaerobic cultivation, 16h = 16 h anaerobic cultivation

sample	dilution	volume [µl]	OD_{590}	OD_{450}	OD_{590}/OD_{450}	protein concentration [µg/µl]
C_R1	5	15	0.524	0.834	0.628	0.24
2h_R1	5	10	0.502	0.797	0.630	0.38
4h_R1	5	5	0.500	0.796	0.628	0.70
8h_R1	10	9	0.489	0.774	0.632	0.91
16h_R1	10	12	0.498	0.792	0.629	0.60
C_R2	5	10	0.511	0.813	0.629	0.36
2h_R2	5	9	0.526	0.837	0.628	0.40
4h_R2	5	5	0.532	0.844	0.630	0.77
8h_R2	10	9	0.533	0.844	0.632	0.90
16h_R2	5	7	0.531	0.845	0.628	0.51
C_R3	5	15	0.504	0.797	0.632	0.28
2h_R3	10	7	0.521	0.825	0.632	1.16
4h_R3	10	5	0.523	0.827	0.632	1.67
8h_R3	10	5	0.507	0.807	0.628	1.41
16h_R3	15	5	0.504	0.801	0.629	2.21

8.6 Scoring matrix of the *Pepper* algorithm for ranking predicted ORFs

Table 19 Scoring matrix for the ranking of predicted open reading frames.

Predicted ORFs were ranked based on the resulting scores of their used start codon as well as the presence of an RBS and the length of the RBS spacer. In case different ORFs share the same ORF class, the longer predicted ORF is preferred.

ORF class	Start codon class	RBS class	RBS spacer class
1	1	1	1
2	1	2	1
3	1	3	1
4	2	1	1
5	2	2	1
6	2	3	1
7	3	1	1
8	3	2	1
9	3	3	1
10	1	1	2
11	1	2	2
12	1	3	2
13	2	1	2
14	2	2	2
15	2	3	2
16	3	1	2
17	3	2	2
18	3	3	2
19	3	-	-
20	3	-	-
21	3	-	-
21	3	-	-

8.7 Possible false predicted cytoplasmic proteins

Table 20 List of possible false predicted cytoplasmic proteins with one or more TMHs.
The localization of the proteins was predicted as cytoplasmic proteins using LocateP v.2; TMHs were predicted using TMHMM Server v. 2.0. Overall, 76 proteins were predicted with at least one TMH indicating a possible false prediction of either the localization or the number of TMHs.

pred. TMH	length [aa]	protein ID	function
1	94	6frt_+1_26594	hypothetical protein
1	178	6frt_-3_7539	hypothetical protein
1	1101	PA0077	type VI secretion protein IcmF
1	449	PA0078	TssL1
1	329	PA0319	hypothetical protein
1	319	PA0406	transporter TonB3
1	323	PA0471	transmembrane sensor
1	146	PA0523	nitric oxide reductase subunit C
1	64	PA0526	hypothetical protein
1	665	PA0548	transketolase
1	239	PA0663	hypothetical protein
1	1041	PA0788	hypothetical protein
1	255	PA0807	protein AmpDh3
1	80	PA1052a	hypothetical protein
1	415	PA1155	ribonucleotide-diphosphate reductase subunit NrdB
1	270	PA1164	hypothetical protein
1	264	PA1344	short-chain dehydrogenase
1	296	PA1461	flagellar motor protein MotD
1	69	PA1548	hypothetical protein
1	179	PA1550	hypothetical protein
1	61	PA1552.1	cytochrome C oxidase cbb3-type subunit CcoQ
1	203	PA1553	cbb3-type cytochrome C oxidase subunit II
1	61	PA1555.1	cytochrome C oxidase cbb3-type subunit CcoQ
1	113	PA1615	lipase
1	289	PA1668	DotU2
1	259	PA1679	hypothetical protein
1	315	PA1752	2-dehydropantoate 2-reductase
1	443	PA1791	hypothetical protein
1	341	PA1832	protease
1	411	PA2345	hypothetical protein
1	448	PA2393	dipeptidase
1	179	PA2404	FpvH
1	257	PA2820	hypothetical protein
1	55	PA2883	hypothetical protein
1	326	PA2973	peptidase
1	146	PA2982	hypothetical protein
1	107	PA3042	hypothetical protein
1	174	PA3095	type II secretion system protein M
1	237	PA3098	type II secretion system protein J
1	219	PA3110	hypothetical protein
1	436	PA3159	UDP-N-acetyl-d-glucosamine 6-dehydrogenase
1	312	PA3242	temperature-regulated acyltransferase HtrB1

pred. TMH	length [aa]	protein ID	function
1	323	PA3402	hypothetical protein
1	94	PA3634	cell division protein FtsB
1	107	PA3694	hypothetical protein
1	231	PA3712	hypothetical protein
1	688	PA3729	hypothetical protein
1	401	PA3734	hypothetical protein
1	347	PA3804	hypothetical protein
1	646	PA4003	penicillin-binding protein 2
1	310	PA4170	hypothetical protein
1	547	PA4180	acetolactate synthase
1	190	PA4369	hypothetical protein
1	480	PA4411	UDP-N-acetylmuramate--L-alanine ligase
1	579	PA4418	penicillin-binding protein 3
1	56	PA4537	hypothetical protein
1	185	PA4551	type 4 fimbrial biogenesis protein PilV
1	372	PA4565	gamma-glutamyl kinase
1	187	PA4600	transcriptional regulator NfxB
1	252	PA4663	molybdopterin biosynthesis protein MoeB
1	297	PA4717	hypothetical protein
1	356	PA4842	hypothetical protein
1	421	PA4851	hypothetical protein
1	289	PA4941	protease subunit HflC
1	400	PA4942	protease subunit HflK
1	207	PA5042	type 4 fimbrial biogenesis protein PilO
1	198	PA5043	type 4 fimbrial biogenesis protein PilN
1	231	PA5052	hypothetical protein
1	82	PA5068	twin-arginine translocation protein TatA
1	139	PA5130	hypothetical protein
1	237	PA5273	hypothetical protein
1	166	PA5515	hypothetical protein
1	156	PA5558	ATP synthase subunit B
4	663	PA2390	pyoverdine biosynthesis protein PvdT
5	570	PA4223	ABC transporter ATP-binding protein
6	588	PA1113	ABC transporter ATP-binding protein/permease

8.8 DNA fragments for template generation for RNA probes

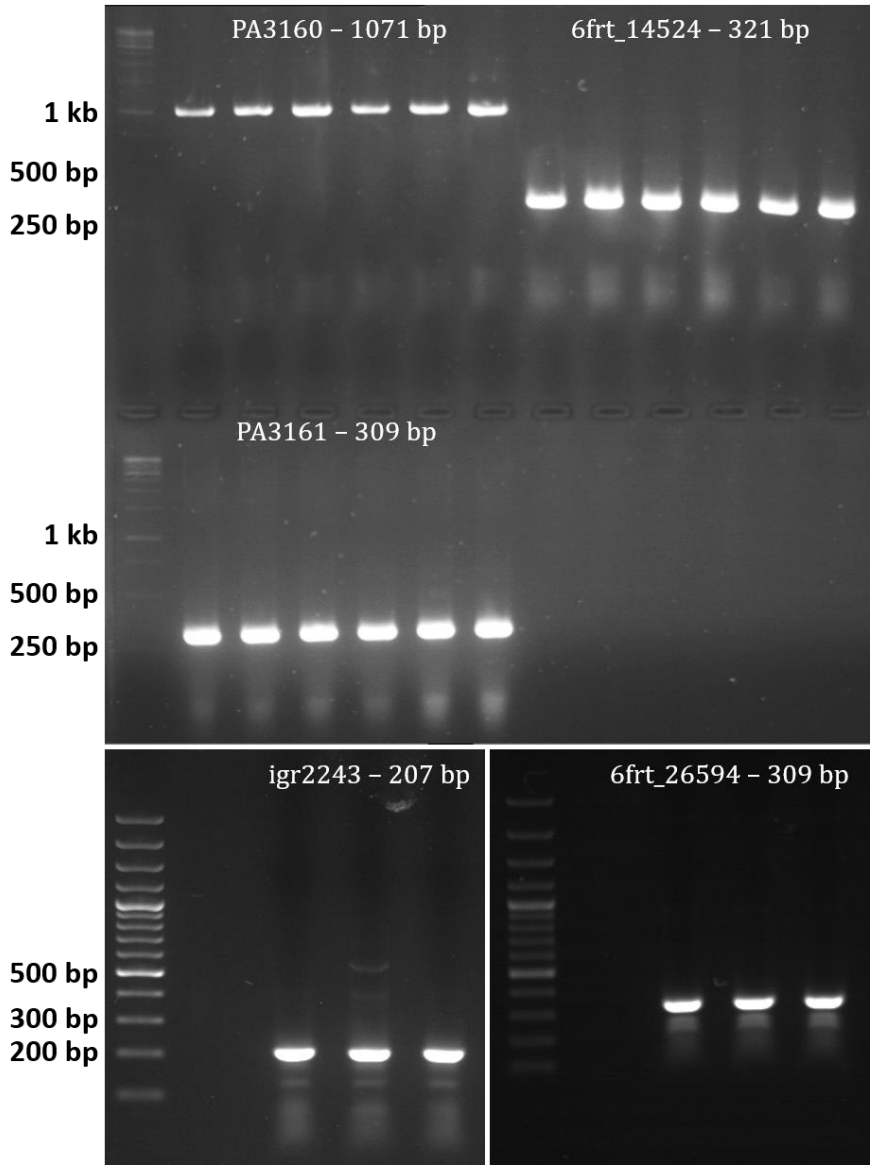

Figure 59 DNA fragments of PCR reactions for template generation for RNA probes.
Visualized PCR fragments using corresponding primers for generation of RNA probe templates. Six or three reactions each 20 µl were separated on a 1.5% agarose gel for roughly 45 min at 120 V and 350 mA. As markers, 6 µl of GeneRuler™ 1kb DNA ladder and GeneRuler™ 100bp DNA ladder (Thermo Fisher Scientific) were used for the top and bottoms gels, respectively. Bands were visualized under the illuminator at 320 nm. The detected signals matched the expected sizes of 1071 bp for the gene PA3160, 32 bp for 6frt_14524m 309 bp for the gene PA3161, 207 bp for igr2243 and 309 bp for 6frt_26594.

8.9 Results of the labeling efficiency test of DIG-labeled RNA probes

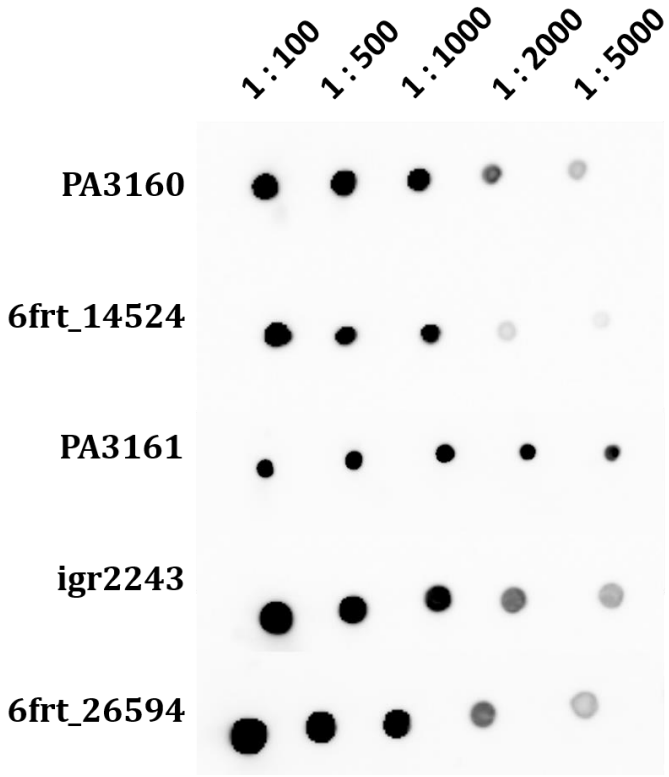

Figure 60 Results of the labeling efficiency test of DIG-labeled RNA probes.
RNA probes were generated using 500 ng of the corresponding DNA template, 1x DIG RNA Labeling Mix, 1x transcription buffer, 40 U T7 RNA polymerase and 40 U rRNasin®. After incubation, the reaction was stopped and the RNA probes were precipitated. Following, probes were washed and stored until further use at -80 °C. To test the labeling efficiency, RNA probes were diluted in DEPC-water, covalently bound to the nylon membrane via UV cross-linking (120 J/ cm^2) and the membrane was equilibrated for 30 minutes in buffer II at RT. Subsequently, the membrane was incubated with anti-Digoxigenin-AP1 : 10,000 in buffer II for 30 minutes at RT. Afterwards, the membrane was washed two times for 15 minutes each with buffer I followed by equilibration for one minute in buffer III. After incubating the membrane for five minutes in CDP-Star 1:200 in buffer III at RT in the dark, chemiluminescence signals were detected using the Luminescent Image Analyzer LAS 3000. The results obtained from the labeling efficiency test displayed that the RNA probes for PA3160 and 6frt_14524 were effective up to a dilution of 1:1000 whereas the RNA probe for PA3161 displayed signals up to a dilution of 1:5000. Both probes for igr2243 and 6frt_26594 showed sufficient signals up to a dilution of 1:2000, respectively.

8.10 Methylene blue staining of northern blots

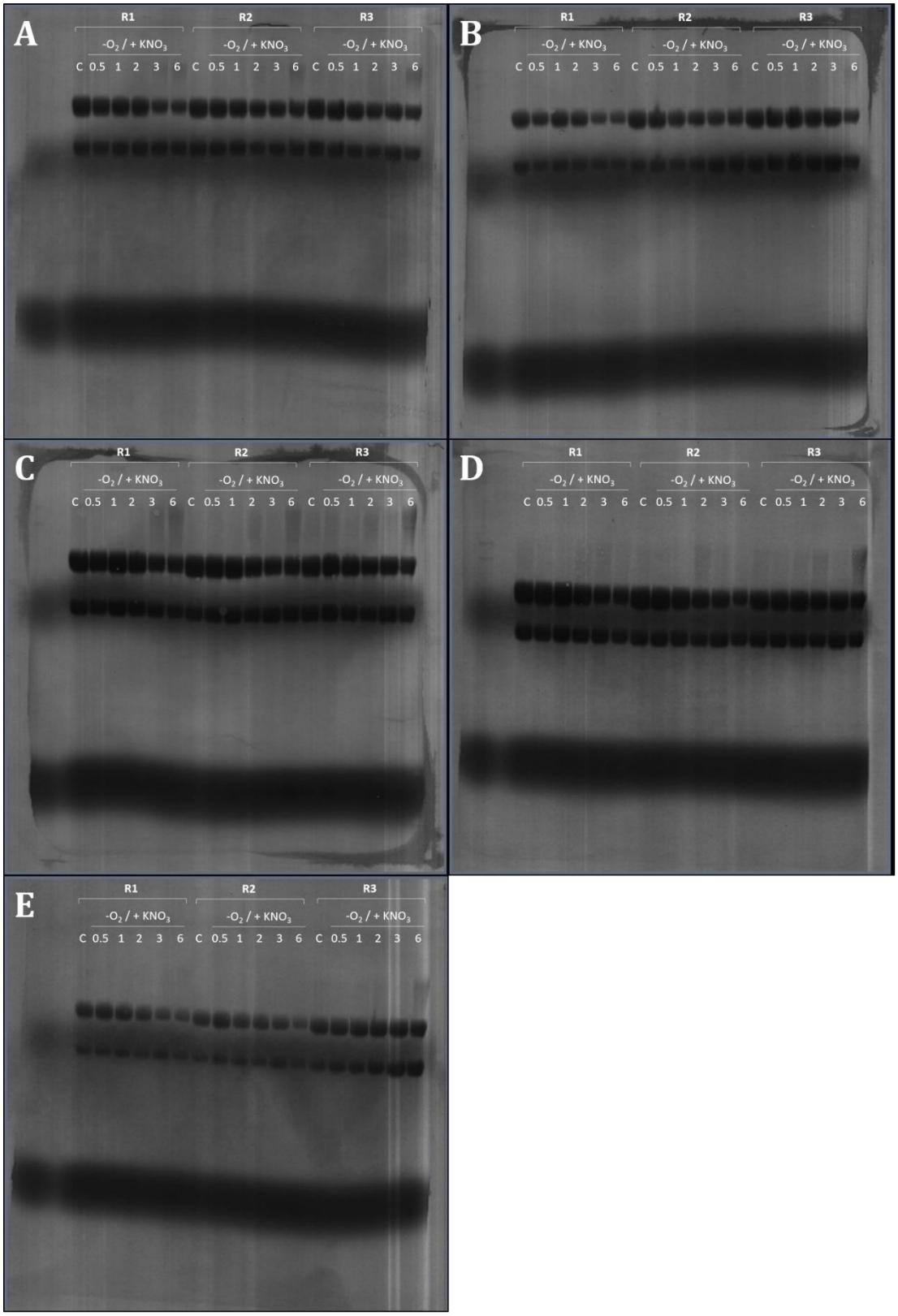

Figure 61 Methylene blue staining of northern blots.
Depicted are northern blots after staining in methylene blue for five minutes followed by destaining with ddH_2O. R1, R2, R3 = replicate 1, 2 and 3 respectively; $-O_2/+KNO_3$ = anaerobic conditions plus 50 mM KNO_3; C = aerobic control OD_{540} = 0.05; 0.5, 1, 2, 3 and 6 = corresponding time point of cell harvest in h.

8.11 Northern Blot analysis of the *wzz* gene (PA3160)

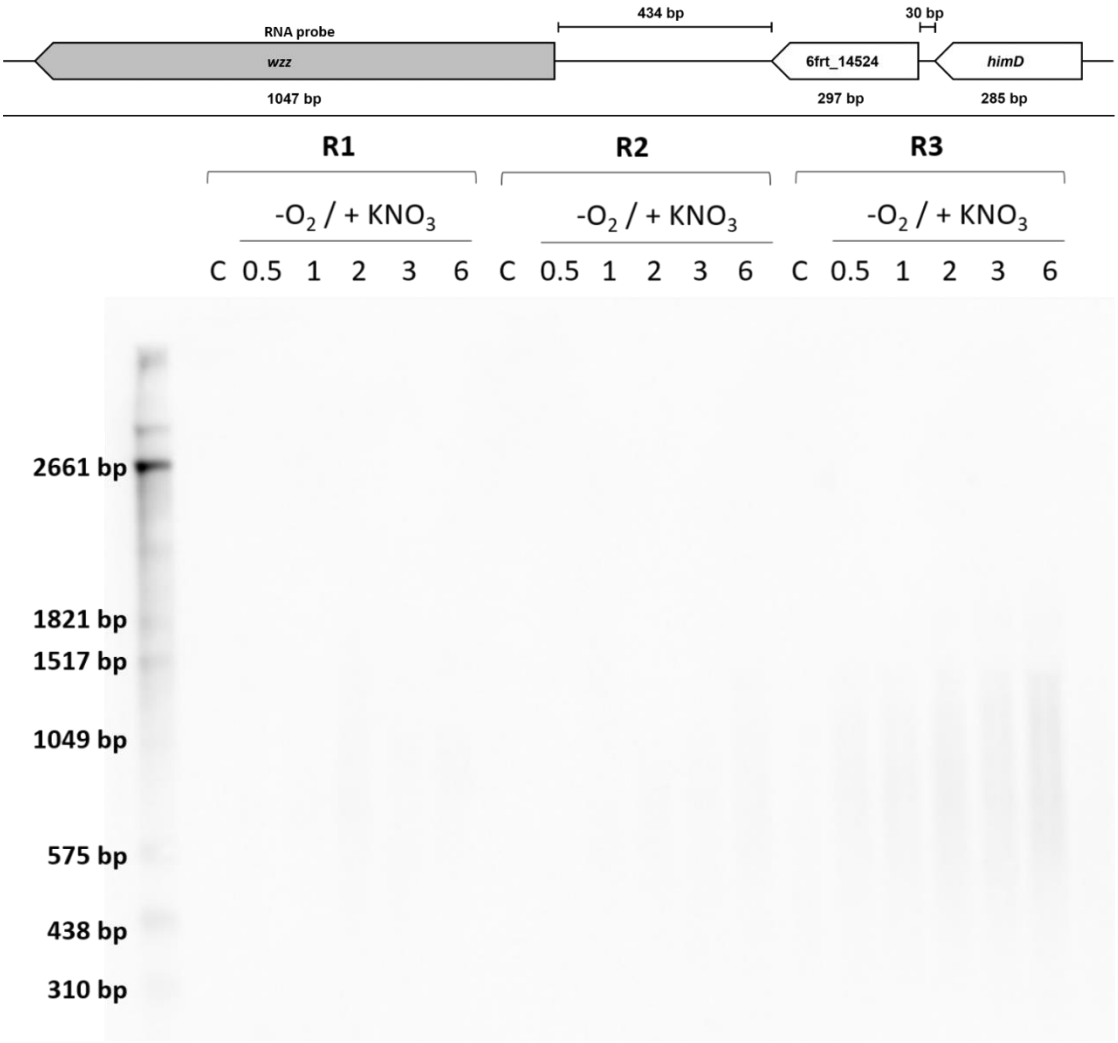

Figure 62 Northern blot analysis of the *wzz* gene of *P. aeruginosa* (PA3160).
R1, R2, R3 = replicate 1, 2 and 3 respectively; $-O_2/+KNO_3$ = anaerobic conditions plus 50 mM KNO_3; C = aerobic control OD_{540} = 0.05; 0.5, 1, 2, 3 and 6 = corresponding time point of cell harvest in h; marker = RNA Molecular Weight Marker I, DIG-labeled (Roche); schematic representation of the genetic arrangement is displayed on top with the used RNA probe marked in grey. *P. aeruginosa* PAO1 cells were cultivated in LB under aerobic conditions until OD_{540} of 0.05 followed by shifting to cultivation under anaerobic conditions in the presence of 50 mM KNO_3. Each time point was cultured separately and after selected time point of 0.5, 1, 2, 3 and 6 hours cultivation under denitrifying conditions cells were harvested followed by RNA preparation. Transcriptional analyses were performed by separating RNA samples on a denaturing 2% formaldehyde-agarose gel and subsequent transfer onto a positively charged nylon membrane via vacuum blotting for four hours. Transcripts were visualized by hybridization with corresponding DIG-labeled RNA probes followed by incubation with AP-coupled anti-DIG antibody and CDP-Star and chemiluminescence signals were visualized using the Luminescent Image Analyzer LAS-3000. In total, 10 µg RNA per lane were separated and signals were detected for one hour, but no signals were detected.

8.12 List of all identified proteins

Table 21 List of all proteins identified in this work and their physicochemical properties.
List of all 2461 identified proteins in this work using both the solubilization and shaving approach. Subcellular localizations were predicted using LocateP v.2 and TMHs were predicted suing TMHMM v.2. Start codons, RBS as well as isoelectric point (pI) and hydrophobicity indices (GRAVY) were determined via the *Pepper* algorithm.

protein ID	(predicted) function	length [aa]	TMH	start	RBS	pI	GRAVY
6frt_+1_12309	unknown	71	0	TTG	GGTGC	11.7	-0.1
6frt_+1_15981	putative DNA helicase	1260	0	CTG	CGAGC	10.1	-0.7
6frt_+1_23634	putative lipoprotein	152	0	ATG	GGAGC	10.5	0.1
6frt_+1_26594	hypothetical protein	94	1	TTG	CGAGC	10.6	-0.4
6frt_+1_4007	unknown	14	0	ATT	GGTGT	10.8	-0.9
6frt_+1_6282	possible polypeptide deformylase	79	0	CTG	AGAGG	5.7	-0.2
6frt_+2_16490	hypothetical protein PA2727	1006	0	GTG	GGAGG	9.0	-0.3
6frt_+2_26135	unknown	81	0	TTG	GGAGG	5.8	0.2
6frt_+2_7442	unknown	45	0	ATG	-	11.8	-0.1
6frt_+3_24393	hypothetical protein PA4059	304	0	TTG	AGAGG	11.7	-0.6
6frt_+3_4602	possible helix-turn-helix transcriptional regulator	100	0	GTG	GGTGC	9.3	-0.2
6frt_-1_14346	unknown	19	0	ACT	-	12.2	-0.4
6frt_-1_14492	probable 3-phosphoshikimate 1-carboxyvinyltransferase AroA	709	0	TTG	GGAGC	5.6	0.1
6frt_-1_14524	LapA family protein	98	2	ATG	GGAGT	11.5	0.9
6frt_-1_27422	unknown	61	0	ATA	CGAGG	9.3	-0.3
6frt_-2_14050	hypothetical protein	231	0	TTG	GGTGC	11.0	-0.6
6frt_-2_5445	possible plasmid maintenance system killer protein	68	0	ATC	CGAGG	7.0	-0.4
6frt_-2_6068	unknown	11	0	CGC	GGTGA	10.4	-0.8
6frt_-2_7521	hypothetical protein PA4360	208	0	GTG	GGTGG	10.6	-1.0
6frt_-3_14007	hypothetical protein	143	0	ATG	CGAGG	10.5	0.2
6frt_-3_29662	hypothetical protein	203	0	CTG	-	8.2	-0.4
6frt_-3_657	hypothetical protein	217	0	GTG	CGAGG	10.1	-0.3
6frt_-3_7539	hypothetical protein	178	1	TTG	GGAGC	6.1	-0.6
igr1531	unknown	18	0	ATG	-	6.5	0.1
igr2243	possible cobalt transporter subunit CbtB	60	1	ATG	AGAGG	8.1	0.3
PA0001	chromosome replication initiator DnaA	514	0	GTG	-	8.6	-0.3
PA0002	DNA polymerase III subunit beta	367	0	ATG	CGAGG	5.1	-0.2
PA0003	DNA replication and repair protein RecF	369	0	ATG	-	8.2	-0.3
PA0004	DNA gyrase subunit B	806	0	ATG	GGAGT	5.6	-0.4
PA0005	lysophosphatidic acid acyltransferase LptA	257	1	ATG	-	9.7	0.2
PA0008	glycine--tRNA ligase subunit beta	684	0	ATG	GGAGG	5.1	0.0
PA0009	glycine--tRNA ligase subunit alpha	315	0	GTG	GGTGA	5.0	-0.2
PA0011	acyltransferase HtrB1	295	0	GTG	CGAGG	9.4	-0.1
PA0013	hypothetical protein	217	6	ATG	-	10.2	0.8
PA0016	potassium transporter inner membrane associated	457	0	ATG	CGAGC	5.2	0.0
PA0017	Ribosomal RNA small subunit methyltransferase B	434	0	ATG	GGTGC	8.3	-0.2
PA0020	T4P secretin-associated protein TsaP	341	0	ATG	-	8.9	-0.3
PA0024	coproporphyrinogen III oxidase	305	0	GTG	GGTGA	5.6	-0.5
PA0025	shikimate dehydrogenase	274	0	ATG	-	5.6	0.0

protein ID	(predicted) function	length [aa]	TMH	start	RBS	pI	GRAVY
PA0035	tryptophan synthase subunit alpha	268	0	ATG	GGAGT	5.2	0.1
PA0036	tryptophan synthase subunit beta	402	0	ATG	GGAGC	5.9	-0.2
PA0040	hypothetical protein	562	0	GTG	-	8.4	-0.6
PA0041	hemagglutinin	3535	1	ATG	GGAGT	5.3	-0.2
PA0043	hypothetical protein	460	13	ATG	GGAGA	10.2	0.7
PA0045	hypothetical protein	228	0	ATG	GGAGA	9.2	-0.2
PA0061	hypothetical protein	145	0	ATG	GGAGC	8.6	-0.3
PA0063	hypothetical protein	375	0	GTG	-	9.6	-0.3
PA0064	hypothetical protein	327	8	ATG	-	8.8	0.9
PA0065	5'-nucleotidase	221	0	ATG	CGAGG	5.7	-0.3
PA0067	oligopeptidase A	681	0	GTG	-	5.1	-0.3
PA0070	TagQ1	304	0	ATG	GGAGT	8.9	-0.5
PA0071	TagR1	570	0	ATG	AGAGG	5.8	-0.3
PA0072	TagS1	399	5	ATG	CGAGG	9.4	0.4
PA0073	ABC transporter ATP-binding protein TagT1	239	0	ATG	-	9.0	-0.1
PA0074	serine/threonine protein kinase PpkA	1032	0	ATG	TGAGA	5.3	-0.2
PA0075	serine/threonine phosphatase PppA	242	0	ATG	-	5.8	0.0
PA0076	TagF1	226	0	TTG	GGAGC	4.7	0.2
PA0077	type VI secretion protein IcmF	1101	1	ATG	-	6.0	-0.2
PA0078	TssL1	449	1	ATG	CGAGG	7.8	-0.3
PA0079	TssK1	444	0	ATG	GGAGT	5.7	0.0
PA0080	TssJ1	154	0	ATG	TGAGG	6.1	-0.2
PA0081	Fha domain-containing protein	497	0	ATG	GGAGT	5.2	-0.4
PA0082	TssA1	344	0	GTG	GGAGA	4.4	0.0
PA0083	TssB1	172	0	ATG	CGAGG	5.1	-0.3
PA0084	TssC1	498	0	ATG	AGAGG	5.2	-0.4
PA0085	protein secretion apparatus assembly protein Hcp1	162	0	ATG	GGAGG	6.3	-0.4
PA0086	TagJ1	281	0	ATG	-	4.7	0.0
PA0088	TssF1	619	0	ATG	GGAGG	7.0	-0.3
PA0090	secretion protein ClpV1	902	0	ATG	GGAGA	5.4	-0.2
PA0100	hypothetical protein	306	0	ATG	GGAGA	4.3	-0.2
PA0101	hypothetical protein	415	0	ATG	-	4.9	-0.1
PA0102	carbonic anhydrase	242	0	ATG	CGAGG	6.2	-0.2
PA0105	cytochrome C oxidase subunit II	374	3	ATG	-	6.1	-0.1
PA0106	cytochrome C oxidase subunit I	530	12	ATG	GGAGA	6.6	0.8
PA0109	hypothetical protein	69	2	ATG	GGAGT	9.7	1.1
PA0111	hypothetical protein	192	1	ATG	GGAGA	9.7	-0.1
PA0114	cytochrome c oxidase assembly protein SenC	211	1	ATG	AGAGC	7.8	0.0
PA0118	hypothetical protein	195	0	ATG	AGAGC	6.3	0.0
PA0126	hypothetical protein	206	0	ATG	-	7.7	-0.3
PA0127	hypothetical protein	166	0	ATG	GGAGG	8.7	0.0
PA0129	gamma-aminobutyrate permease	475	12	ATG	-	9.7	0.8
PA0130	3-oxopropanoate dehydrogenase	497	0	ATG	AGAGA	5.7	0.0
PA0139	alkyl hydroperoxide reductase subunit C	187	0	ATG	AGAGG	5.9	-0.2
PA0141	hypothetical protein	298	0	GTG	-	8.4	-0.6
PA0155	transcriptional regulator PcaR	279	0	ATG	CGAGC	7.2	0.1

protein ID	(predicted) function	length [aa]	TMH	start	RBS	pI	GRAVY
PA0156	resistance-nodulation-cell division (RND) efflux TriA	383	0	ATG	-	6.1	-0.1
PA0157	resistance-nodulation-cell division (RND) efflux TriB	356	0	ATG	GGAGG	8.7	-0.2
PA0158	resistance-nodulation-cell division (RND) efflux TriC	1015	11	ATG	CGAGG	5.8	0.2
PA0159	transcriptional regulator	312	0	GTG	CGAGG	5.7	-0.2
PA0162	histidine porin OpdC	444	0	ATG	GGAGC	5.0	-0.5
PA0163	transcriptional regulator	265	0	ATG	-	9.0	-0.2
PA0165	hypothetical protein	278	0	ATG	GGAGC	5.1	-0.4
PA0167	transcriptional regulator	221	0	ATG	-	8.6	-0.1
PA0169	SiaD	235	0	GTG	GGAGC	9.3	-0.5
PA0171	hypothetical protein	180	0	ATG	-	6.5	-0.3
PA0172	SiaA	663	2	ATG	-	6.5	-0.2
PA0173	chemotaxis response regulator protein-glutamate	349	0	ATG	GGAGA	8.5	0.0
PA0174	hypothetical protein	200	0	ATG	-	8.5	-0.1
PA0175	chemotaxis protein methyltransferase	280	0	ATG	-	9.2	-0.2
PA0176	aerotaxis transducer Aer2	679	0	ATG	-	5.1	-0.3
PA0177	purine-binding chemotaxis protein	161	0	ATG	GGAGG	4.5	0.3
PA0178	two-component sensor	639	0	ATG	GGAGG	4.8	-0.1
PA0180	trichloroethylene chemotactic transducer CttP	390	1	ATG	GGAGT	5.7	-0.1
PA0182	3-ketoacyl-ACP reductase FabG	250	0	ATG	GGAGA	5.0	0.3
PA0195	NAD(P) transhydrogenase subunit alpha part1	372	0	GTG	GGAGA	5.7	0.2
PA0196	pyridine nucleotide transhydrogenase subunit	478	8	ATG	-	6.7	0.7
PA0212	malonate decarboxylase subunit gamma	268	0	ATG	GGAGA	6.5	0.0
PA0236	transcriptional regulator	259	0	ATG	-	8.0	-0.1
PA0246	major facilitator superfamily transporter	501	14	TTG	GGTGC	9.3	0.9
PA0255	hypothetical protein	228	6	ATG	-	11.5	0.8
PA0259	Type 6 lipase adaptor, Tla3	480	0	ATG	GGAGG	5.2	-0.3
PA0265	glutarate-semialdehyde dehydrogenase DavD	483	0	ATG	GGAGA	5.6	0.0
PA0266	5-aminovalerate aminotransferase DavT	426	0	ATG	TGAGG	6.1	0.1
PA0267	hypothetical protein	399	0	ATG	AGAGG	5.5	0.0
PA0268	transcriptional regulator	473	0	ATG	-	9.0	-0.3
PA0277	hypothetical protein	252	0	ATG	GGAGC	6.1	-0.2
PA0278	hypothetical protein	250	8	ATG	CGAGA	9.7	1.1
PA0280	sulfate.thiosulfate ABC transporter ATP-binding	329	0	ATG	CGAGG	5.8	-0.2
PA0281	sulfate transporter CysW	289	6	ATG	GGAGG	5.8	0.8
PA0285	hypothetical protein	760	2	ATG	-	5.9	-0.3
PA0291	anaerobically-induced outer membrane porin OprE	460	1	ATG	-	8.7	-0.4
PA0294	transcriptional regulator AguR	221	0	ATG	GGAGA	6.0	0.0
PA0295	polyamine binding protein	353	0	ATG	CGAGA	5.7	-0.2
PA0296	glutamine synthetase	458	0	ATG	GGTGT	4.8	-0.2
PA0298	glutamine synthetase	452	0	ATG	TGAGG	5.2	-0.3
PA0299	aminotransferase	456	0	ATG	AGAGG	5.7	-0.2
PA0300	putrescine ABC transporter substrate-binding	367	0	ATG	GGAGC	7.0	-0.3
PA0301	spermidine ABC transporter substrate-binding	365	0	ATG	GGAGT	5.5	-0.2
PA0302	polyamine transporter PotG	384	0	ATG	GGAGT	6.0	-0.1
PA0303	polyamine transporter PotH	293	6	ATG	-	5.2	0.9

protein ID	(predicted) function	length [aa]	TMH	start	RBS	pI	GRAVY
PA0304	polyamine transporter PotI	289	6	ATG	GGAGG	9.3	0.7
PA0305	acylhomoserine lactone acylase B	795	1	ATG	GGAGA	5.5	-0.4
PA0306a	transcriptional regulator	167	0	ATG	GGAGT	5.4	-0.6
PA0307	hypothetical protein	203	1	ATG	-	6.9	0.1
PA0308	hypothetical protein	339	0	ATG	GGTGC	6.3	-0.3
PA0316	D-3-phosphoglycerate dehydrogenase	409	0	ATG	-	6.1	0.0
PA0317	hypothetical protein	464	0	ATG	TGAGA	5.1	-0.1
PA0318	hypothetical protein	221	0	ATG	GGAGT	5.4	-0.1
PA0319	hypothetical protein	329	1	ATG	-	5.1	-0.2
PA0327	calcium-regulated beta-propeller protein CarP	321	1	ATG	-	5.2	-0.2
PA0328	arginine-specific autotransporter of Pseudomonas aeruginosa, AaaA	647	0	GTG	AGAGG	4.8	-0.4
PA0329	hypothetical protein	110	0	ATG	GGAGC	9.3	-0.5
PA0331	threonine dehydratase	504	0	ATG	-	6.1	-0.2
PA0333	hypothetical protein	423	4	ATG	-	9.7	0.4
PA0335	hypothetical protein	217	0	GTG	GGAGT	4.8	-0.2
PA0336	RNA pyrophosphohydrolase	159	0	GTG	CGAGG	9.3	-0.5
PA0337	phosphoenolpyruvate-protein phosphotransferase	759	0	ATG	GGAGA	5.5	-0.1
PA0338	hypothetical protein	376	0	GTG	-	6.2	-0.6
PA0340	hypothetical protein	267	7	ATG	-	10.3	1.0
PA0341	prolipoprotein diacylglyceryl transferase	266	7	ATG	GGAGT	9.6	0.5
PA0344	hypothetical protein	459	0	ATG	GGAGA	6.3	-0.2
PA0345	hypothetical protein	461	4	TTG	GGAGG	6.9	0.2
PA0352	transporter	461	10	ATG	-	8.7	0.9
PA0353	dihydroxy-acid dehydratase	612	0	ATG	-	5.7	-0.1
PA0354	hypothetical protein	398	0	ATG	GGAGC	6.5	-0.1
PA0356	hypothetical protein	274	0	GTG	-	5.3	-0.1
PA0357	formamidopyrimidine-DNA glycosylase	270	0	ATG	-	9.4	-0.2
PA0359	hypothetical protein	114	1	ATG	-	4.6	0.6
PA0363	phosphopantetheine adenylyltransferase	159	0	ATG	-	8.0	0.0
PA0364	oxidoreductase	531	0	ATG	TGAGA	6.5	-0.2
PA0365	hypothetical protein	182	0	ATG	GGTGA	6.8	0.1
PA0366	coniferyl aldehyde dehydrogenase	476	0	ATG	CGAGG	8.9	-0.1
PA0370	hypothetical protein	198	0	ATG	GGAGC	9.1	-0.3
PA0371	hypothetical protein	495	1	ATG	GGAGG	5.7	-0.2
PA0372	zinc protease	465	0	GTG	TGAGA	6.2	-0.3
PA0373	signal recognition particle receptor FtsY	455	0	ATG	TGAGA	4.8	-0.3
PA0374	cell division protein FtsE	223	0	ATG	GGAGA	10.2	-0.1
PA0375	cell division protein FtsX	335	3	ATG	TGAGG	5.4	0.1
PA0377	hypothetical protein	201	1	ATG	GGAGG	5.3	-0.1
PA0378	monofunctional biosynthetic peptidoglycan	243	1	ATG	-	10.3	-0.2
PA0379	hypothetical protein	125	4	ATG	GGAGT	10.0	1.1
PA0381	thiazole synthase	265	0	ATG	GGAGT	5.0	0.2
PA0382	tRNA (guanine-N(7)-)-methyltransferase	223	0	ATG	-	7.9	-0.4
PA0385	hypothetical protein	107	3	ATG	-	9.0	1.1
PA0386	coproporphyrinogen III oxidase	384	0	GTG	-	5.3	-0.3
PA0389	hypothetical protein	206	0	ATG	TGAGG	6.1	-0.2

protein ID	(predicted) function	length [aa]	TMH	start	RBS	pI	GRAVY
PA0390	homoserine O-acetyltransferase	379	0	ATG	CGAGA	5.6	-0.1
PA0391	hypothetical protein	655	0	ATG	GGAGC	9.6	-0.5
PA0392	conserved hypothetical protein	197	4	ATG	GGAGT	9.7	1.3
PA0393	pyrroline-5-carboxylate reductase	273	0	ATG	-	4.8	0.2
PA0395	twitching motility protein PilT	344	0	ATG	GGAGT	6.4	-0.1
PA0396	twitching motility protein PilU	382	0	ATG	TGAGT	6.3	-0.2
PA0397	cation efflux system protein	299	5	ATG	GGAGC	5.5	0.6
PA0398	hypothetical protein	134	4	ATG	CGAGG	9.1	0.3
PA0399	cystathionine beta-synthase	457	0	ATG	GGAGA	5.5	-0.1
PA0400	probable cystathionine gamma-lyase	394	0	ATG	GGAGA	6.2	-0.1
PA0401	noncatalytic dihydroorotase-like protein	423	0	ATG	GGAGG	5.6	0.1
PA0402	aspartate carbamoyltransferase	334	0	ATG	-	6.3	-0.1
PA0403	bifunctional pyrimidine regulatory protein PyrR/uracil phosphoribosyltransferase	170	0	ATG	CGAGG	5.6	0.0
PA0406	transporter TonB3	319	1	GTG	-	10.0	-0.6
PA0408	pilus biosynthesis/twitching motility protein PilG	135	0	ATG	CGAGT	6.7	0.0
PA0411	twitching motility protein PilJ	682	2	ATG	-	4.7	-0.1
PA0413	chemotactic signal transduction system protein	2472	0	ATG	GGAGT	4.4	-0.2
PA0414	methylesterase	343	0	ATG	-	5.1	-0.2
PA0421	hypothetical protein	496	0	ATG	GGAGT	9.8	-0.2
PA0422	hypothetical protein	189	4	ATG	-	9.6	0.4
PA0423	protease PasP	191	0	ATG	GGAGA	6.1	-0.4
PA0425	multidrug resistance protein MexA	383	0	ATG	TGAGG	8.8	-0.2
PA0426	multidrug resistance protein MexB	1046	11	ATG	-	5.5	0.3
PA0427	outer membrane protein OprM	485	0	ATG	-	5.5	-0.2
PA0428	ATP-dependent RNA helicase	639	0	ATG	-	10.0	-0.8
PA0429	hypothetical protein	356	0	ATG	-	6.5	-0.3
PA0430	5,10-methylenetetrahydrofolate reductase	290	0	GTG	AGAGG	6.1	-0.2
PA0432	adenosylhomocysteinase	469	0	ATG	GGAGA	5.7	-0.2
PA0434	hypothetical protein	730	0	ATG	-	5.7	-0.5
PA0435	hypothetical protein	492	4	ATG	TGAGG	10.0	-0.1
PA0436	transcriptional regulator	206	0	ATG	-	6.2	-0.3
PA0438	cytosine permease	416	11	ATG	GGAGA	9.0	0.9
PA0446	hypothetical protein	407	0	ATG	CGAGA	5.4	-0.1
PA0447	glutaryl-CoA dehydrogenase	393	0	ATG	CGAGG	5.8	-0.2
PA0451	hypothetical protein	443	6	ATG	GGAGG	8.2	0.6
PA0452	hypothetical protein	264	1	ATG	GGAGG	6.9	0.0
PA0454	hypothetical protein	733	9	ATG	-	8.6	0.1
PA0455	ATP-dependent RNA helicase DbpA	458	0	GTG	CGAGC	8.6	0.0
PA0456	cold-shock protein	69	0	ATG	GGAGA	8.1	-0.5
PA0458	major facilitator superfamily transporter	477	14	ATG	CGAGG	8.7	0.8
PA0459	probable ClpA/B protease ATP binding subunit	932	0	ATG	GGAGT	6.4	-0.4
PA0461	acyltransferase	295	1	ATG	-	9.2	-0.1
PA0462	hypothetical protein	169	0	GTG	GGAGA	6.2	-0.4
PA0463	DNA-binding response regulator CreB	229	0	ATG	-	5.5	-0.2
PA0464	sensory histidine kinase CreC	474	2	ATG	-	5.9	-0.2
PA0469	hypothetical protein	285	0	ATG	GGAGG	4.9	-0.3

protein ID	(predicted) function	length [aa]	TMH	start	RBS	pI	GRAVY
PA0470	ferrichrome receptor FiuA	802	0	ATG	GGAGC	5.5	-0.5
PA0471	transmembrane sensor	323	1	GTG	GGAGA	8.3	-0.2
PA0482	malate synthase G	725	0	ATG	TGAGG	5.5	-0.3
PA0485	hypothetical protein	298	10	ATG	-	9.8	0.8
PA0486	serine/threonine protein kinase	324	0	ATG	CGAGC	5.0	-0.2
PA0487	molybdenum transport regulator	252	0	ATG	-	8.8	0.0
PA0494	acetyl-CoA carboxylase biotin carboxylase	458	0	ATG	GGAGG	5.6	-0.2
PA0496	hypothetical protein	325	0	ATG	GGAGG	7.0	0.0
PA0501	8-amino-7-oxononanoate synthase	401	0	ATG	CGAGC	5.7	0.1
PA0502	biotin biosynthesis protein BioH	240	0	ATG	GGAGG	4.5	-0.1
PA0506	acyl-CoA dehydrogenase	601	0	ATG	AGAGG	5.6	-0.2
PA0509	cytochrome C NirN	493	0	ATG	CGAGG	7.0	-0.2
PA0510	uroporphyrin-III C-methyltransferase	279	0	ATG	-	6.6	0.2
PA0511	heme d1 biosynthesis protein NirJ	387	0	ATG	GGAGG	6.9	-0.4
PA0512	heme d1 biosynthesis protein NirH	171	0	ATG	GGAGG	9.8	-0.2
PA0514	heme d1 biosynthesis protein NirL	174	0	ATG	GGAGG	9.2	-0.5
PA0515	heme d1 biosynthesis protein NirD	150	0	ATG	GGAGG	6.0	-0.4
PA0516	heme d1 biosynthesis protein NirF	392	0	ATG	GGAGA	6.1	-0.3
PA0519	nitrite reductase	568	0	ATG	TGAGG	7.8	-0.4
PA0520	denitrification regulatory protein NirQ	260	0	ATG	GGAGT	5.3	-0.2
PA0521	cytochrome C oxidase subunit	175	5	ATG	-	7.0	0.8
PA0522	hypothetical protein	85	3	ATG	TGAGG	9.5	1.1
PA0523	nitric oxide reductase subunit C	146	1	ATG	GGAGG	5.9	-0.3
PA0524	nitric oxide reductase subunit B	466	12	ATG	GGAGG	9.3	0.8
PA0525	denitrification protein NorD	612	0	ATG	-	8.5	-0.5
PA0526	hypothetical protein	64	1	ATG	CGAGC	7.6	-0.1
PA0527	transcriptional regulator Dnr	227	0	ATG	CGAGC	6.2	-0.2
PA0533	transcriptional regulator	496	0	ATG	AGAGG	5.0	-0.3
PA0534	FAD-dependent oxidoreductase	429	0	ATG	GGAGG	6.3	-0.3
PA0535	transcriptional regulator	184	0	ATG	AGAGG	5.2	-0.2
PA0536	hypothetical protein	341	3	ATG	-	5.4	0.2
PA0537	hypothetical protein	202	0	ATG	TGAGT	8.6	-0.2
PA0538	disulfide bond formation protein	169	4	TTG	-	8.7	1.0
PA0541	hypothetical protein	152	0	ATG	AGAGC	8.5	-0.7
PA0545	hypothetical protein	434	6	ATG	GGAGT	9.3	0.2
PA0546	S-adenosylmethionine synthetase	396	0	ATG	-	5.3	-0.1
PA0547	transcriptional regulator	333	0	ATG	-	5.6	-0.1
PA0548	transketolase	665	1	ATG	GGAGA	5.2	-0.2
PA0549	hypothetical protein	354	0	ATG	CGAGG	7.7	-0.4
PA0551	D-erythrose 4-phosphate dehydrogenase	353	0	ATG	GGAGC	5.6	-0.2
PA0552	phosphoglycerate kinase	387	0	ATG	-	5.3	0.2
PA0553	hypothetical protein	66	0	ATG	GGAGG	5.1	-0.3
PA0554	hypothetical protein	113	0	ATG	GGAGG	5.1	-0.3
PA0555	fructose-1,6-bisphosphate aldolase	354	0	ATG	GGAGA	5.3	-0.2
PA0558	hypothetical protein	255	0	ATG	GGAGG	5.9	-0.1
PA0561	hypothetical protein	384	7	ATG	-	9.2	0.5
PA0563	hypothetical protein	117	3	ATG	GGAGG	9.3	0.4

protein ID	(predicted) function	length [aa]	TMH	start	RBS	pI	GRAVY
PA0566	hypothetical protein	171	5	ATG	-	8.6	0.9
PA0568	hypothetical protein	152	0	ATG	GGAGA	4.5	-0.5
PA0571	hypothetical protein	204	0	ATG	-	5.1	-0.4
PA0575	hypothetical protein	1245	1	ATG	CGAGA	5.5	-0.2
PA0576	RNA polymerase sigma factor RpoD	617	0	ATG	AGTGG	4.9	-0.6
PA0577	DNA primase	664	0	ATG	CGAGA	6.8	-0.6
PA0580	tRNA N6-adenosine threonylcarbamoyltransferase	341	0	ATG	-	5.8	0.1
PA0581	glycerol-3-phosphate acyltransferase PlsY	189	5	ATG	GGTGG	11.0	0.7
PA0585	hypothetical protein	168	0	ATG	GGAGC	8.7	0.0
PA0586	hypothetical protein	517	0	ATG	GGAGG	5.2	-0.6
PA0587	hypothetical protein	423	0	ATG	TGAGG	7.2	-0.5
PA0588	hypothetical protein	640	0	ATG	CGAGG	5.6	-0.5
PA0590	bis(5'-nucleosyl)-tetraphosphatase	283	0	ATG	GGAGC	6.7	-0.4
PA0592	ribosomal RNA small subunit methyltransferase A	268	0	ATG	-	6.8	-0.2
PA0594	chaperone SurA	430	0	GTG	-	5.7	-0.5
PA0595	organic solvent tolerance protein OstA	924	0	ATG	-	5.4	-0.6
PA0596	hypothetical protein	338	0	ATG	GGAGA	5.3	-0.1
PA0600	two-component sensor AgtS	797	0	ATG	GGAGT	5.6	-0.2
PA0601	two-component response regulator AgtR	210	0	GTG	TGAGG	6.1	0.1
PA0602	ABC transporter	344	0	ATG	GGAGA	6.9	-0.2
PA0603	ABC transporter ATP-binding protein AgtA	369	0	ATG	GGTGC	6.0	-0.2
PA0604	ABC transporter AgtB	348	0	ATG	GGAGA	5.9	-0.3
PA0605	ABC transporter permease AgtC	415	6	ATG	GGAGT	9.5	0.5
PA0606	ABC transporter permease AgtD	276	6	ATG	GGAGA	9.7	1.0
PA0609	anthranilate synthase component I	492	0	ATG	TGAGG	5.0	-0.1
PA0614	hypothetical protein	149	2	GTG	GGAGG	8.5	0.4
PA0615	hypothetical protein	171	0	ATG	GGAGT	4.5	-0.2
PA0617	bacteriophage protein	108	0	ATG	GGAGG	9.5	-0.1
PA0618	bacteriophage protein	295	0	GTG	GGAGG	4.6	0.0
PA0620	bacteriophage protein	691	0	ATG	-	8.4	-0.1
PA0622	bacteriophage protein	386	0	ATG	GGAGA	5.3	0.0
PA0623	bacteriophage protein	167	0	ATG	GGAGC	5.1	-0.1
PA0625	hypothetical protein	745	0	ATG	CGAGA	9.5	-0.2
PA0626	hypothetical protein	290	0	ATG	GGAGT	9.7	-0.2
PA0628	hypothetical protein	329	0	GTG	GGAGA	8.8	-0.4
PA0629	hypothetical protein	209	0	ATG	GGAGG	10.1	-0.4
PA0630	hypothetical protein	120	1	ATG	GGTGC	5.1	0.1
PA0633	hypothetical protein	164	0	ATG	GGAGA	4.9	-0.3
PA0634	hypothetical protein	115	0	ATG	TGAGG	5.1	-0.4
PA0636	hypothetical protein	611	0	ATG	-	8.9	-0.2
PA0638	bacteriophage protein	231	0	ATG	TGAGG	4.7	-0.4
PA0640	bacteriophage protein	200	0	ATG	AGAGG	10.1	0.1
PA0641	bacteriophage protein	1204	0	ATG	-	5.8	-0.4
PA0643	hypothetical protein	363	0	ATG	GGAGA	8.5	-0.2
PA0646	hypothetical protein	350	0	ATG	GGAGA	8.5	-0.1
PA0647	hypothetical protein	100	0	ATG	GGAGG	4.4	0.2

protein ID	(predicted) function	length [aa]	TMH	start	RBS	pI	GRAVY
PA0651	indole-3-glycerol phosphate synthase	278	0	GTG	AGAGG	4.9	0.1
PA0652	cAMP-regulatory protein	214	0	ATG	-	8.3	-0.3
PA0655	hypothetical protein	215	0	ATG	GGAGG	5.4	-0.3
PA0657	ATPase	493	0	GTG	GGAGC	5.8	-0.1
PA0658	short-chain dehydrogenase	266	0	ATG	GGAGA	10.0	0.0
PA0659	hypothetical protein	358	4	ATG	-	4.5	0.2
PA0660	hypothetical protein	322	0	ATG	GGAGT	5.9	0.0
PA0661	hypothetical protein	140	4	ATG	AGAGG	9.8	0.7
PA0662	N-acetyl-gamma-glutamyl-phosphate reductase	344	0	ATG	GGAGT	6.2	0.1
PA0663	hypothetical protein	239	1	ATG	-	9.7	-0.6
PA0665	iron-sulfur cluster insertion protein ErpA	116	0	ATG	GGAGA	4.2	-0.1
PA0668	tyrosine--tRNA ligase	399	0	ATG	-	5.6	-0.2
PA0701a	AraC family transcriptional regulator	221	0	ATG	-	10.5	-0.1
PA0705	alpha-1,6-rhamnosyltransferase MigA	299	0	ATG	CGAGT	8.3	-0.4
PA0715	hypothetical protein	318	0	ATG	TGAGA	9.5	-0.2
PA0716	hypothetical protein	441	0	ATG	-	5.2	-0.1
PA0732	hypothetical protein	347	0	ATG	GGAGC	9.2	-0.2
PA0735	hypothetical protein	271	1	ATG	CGAGG	9.7	-0.6
PA0736	hypothetical protein	358	8	ATG	GGAGC	8.7	0.7
PA0739	transcriptional regulator	304	0	ATG	GGAGT	7.2	0.0
PA0744	enoyl-CoA hydratase	367	0	ATG	CGAGC	5.3	-0.1
PA0745	enoyl-CoA hydratase	272	0	ATG	TGAGG	6.0	-0.2
PA0746	acyl-CoA dehydrogenase	387	0	ATG	CGAGG	5.4	-0.2
PA0747	methylmalonate-semialdehyde dehydrogenase	502	0	ATG	GGAGG	5.8	-0.1
PA0752	hypothetical protein	505	13	ATG	TGAGG	8.9	1.0
PA0753	hypothetical protein	156	4	ATG	CGAGG	7.7	1.0
PA0754	hypothetical protein	327	0	ATG	GGAGC	5.6	0.0
PA0755	cis-aconitate porin OpdH	427	0	ATG	GGAGA	7.8	-0.5
PA0756	two-component response regulator	223	0	ATG	GGTGG	5.4	0.0
PA0757	two-component sensor	460	2	GTG	GGAGG	5.2	0.0
PA0758	hypothetical protein	278	0	ATG	-	5.0	-0.1
PA0759	hypothetical protein	314	0	ATG	-	5.4	0.1
PA0760	hypothetical protein	84	0	ATG	CGAGG	4.6	-0.6
PA0761	L-aspartate oxidase	538	0	ATG	-	5.9	-0.3
PA0762	RNA polymerase sigma factor AlgU	193	0	ATG	AGAGG	5.4	-0.4
PA0763	anti-sigma factor MucA	194	0	ATG	AGAGG	5.7	-0.3
PA0764	sigma factor AlgU regulator MucB	316	0	ATG	TGAGG	5.8	-0.2
PA0766	serine protease MucD	474	0	ATG	GGAGC	7.0	-0.1
PA0767	elongation factor 4	599	0	GTG	CGAGT	5.4	-0.1
PA0768	signal peptidase I	284	1	ATG	AGTGG	8.5	-0.1
PA0769	hypothetical protein	125	1	ATG	TGAGG	8.0	-0.1
PA0770	ribonuclease III	229	0	GTG	-	6.2	-0.3
PA0771	GTPase Era	305	0	ATG	GGAGA	6.2	-0.3
PA0774	tRNA (mo5U34)-methyltransferase	322	0	ATG	-	6.0	-0.2
PA0775	tRNA (cmo5U34)-methyltransferase	246	0	GTG	CGAGG	5.4	0.0
PA0778	inhibitor of cysteine peptidase	134	0	ATG	CGAGG	4.9	-0.3
PA0779	ATP-dependent protease AsrA	799	0	ATG	GGTGC	6.4	-0.2

protein ID	(predicted) function	length [aa]	TMH	start	RBS	pI	GRAVY
PA0782	bifunctional proline dehydrogenase/pyrroline-5-carboxylate dehydrogenase	1060	0	ATG	GGAGG	5.8	-0.1
PA0783	sodium/proline symporter PutP	506	13	ATG	GGAGT	7.7	0.8
PA0787	hypothetical protein	387	0	ATG	CGAGA	6.8	-0.2
PA0788	hypothetical protein	1041	1	ATG	GGTGC	9.5	-0.3
PA0789	probable amino acid permease	471	12	ATG	TGAGG	9.4	0.8
PA0794	aconitate hydratase	868	0	ATG	TGAGT	5.4	-0.2
PA0795	methylcitrate synthase	375	0	ATG	GGAGA	6.0	-0.2
PA0796	2-methylisocitrate lyase	298	0	ATG	AGAGG	5.3	0.0
PA0798	phospholipid methyltransferase	216	0	ATG	-	6.8	0.1
PA0799	helicase	663	0	ATG	CGAGG	5.9	-0.3
PA0801	hypothetical protein	506	8	ATG	GGAGC	9.5	0.2
PA0807	protein AmpDh3	255	1	ATG	GGTGA	5.9	-0.4
PA0825	hypothetical protein	111	2	ATG	AGTGG	6.8	0.4
PA0833	hypothetical protein	237	0	ATG	CGAGG	8.9	-0.4
PA0834	acyltransferase	304	1	ATG	-	9.5	-0.1
PA0835	phosphate acetyltransferase	704	0	ATG	GGAGC	5.2	0.0
PA0836	acetate kinase	394	0	ATG	GGAGC	6.6	-0.1
PA0840	oxidoreductase	370	0	ATG	GGAGT	5.5	-0.1
PA0846	sulfate transporter CysZ	246	4	ATG	GGAGA	9.1	0.8
PA0847	diguanylate cyclase	735	2	ATG	-	5.7	-0.3
PA0850	hypothetical protein	139	2	ATG	GGAGC	9.7	1.2
PA0852	chitin-binding protein CbpD precursor	389	0	ATG	-	6.4	-0.4
PA0853	oxidoreductase	207	0	ATG	GGAGG	8.4	-0.4
PA0856	hypothetical protein	182	0	ATG	-	9.4	-0.3
PA0859	hypothetical protein	200	0	ATG	-	4.9	0.0
PA0860	ABC transporter ATP-binding protein/permease	596	3	ATG	-	8.6	0.2
PA0861	RbDA	818	2	ATG	-	5.2	-0.1
PA0865	4-hydroxyphenylpyruvate dioxygenase	357	0	ATG	GGAGG	5.1	-0.3
PA0866	aromatic amino acid transporter AroP 2	472	12	ATG	TGAGA	9.4	0.7
PA0867	lysozyme inhibitor MliC	127	0	ATG	AGAGG	5.1	-0.2
PA0869	D-alanyl-D-alanine endopeptidase	310	1	GTG	TGAGC	10.6	-0.1
PA0870	aromatic amino acid aminotransferase	399	0	ATG	CGAGG	5.9	0.0
PA0871	pterin-4-alpha-carbinolamine dehydratase	118	0	ATG	-	5.9	-0.3
PA0872	phenylalanine 4-monooxygenase	262	0	ATG	GGAGT	5.5	-0.2
PA0873	transcriptional regulator PhhR	519	0	ATG	-	6.4	-0.1
PA0876	transcriptional regulator	314	0	ATG	AGAGG	5.9	0.1
PA0877	transcriptional regulator	298	0	ATG	GGAGT	6.8	0.0
PA0886	C4-dicarboxylate transporter	427	13	ATG	AGAGG	9.3	1.3
PA0887	acetyl-CoA synthetase	651	0	ATG	CGAGG	5.9	-0.2
PA0888	arginine/ornithine binding protein AotJ	259	0	ATG	GGAGT	6.4	-0.2
PA0889	arginine/ornithine transport protein AotQ	229	5	ATG	AGAGG	9.0	0.7
PA0890	arginine/ornithine transport protein AotM	232	5	GTG	TGAGT	9.5	0.7
PA0892	arginine/ornithine transport protein AotP	254	0	ATG	CGAGA	7.2	-0.2
PA0893	transcriptional regulator ArgR	329	0	ATG	-	8.4	-0.2
PA0895	acetylornithine aminotransferase	406	0	ATG	GGAGA	5.6	-0.1
PA0897	arginine N-succinyltransferase subunit beta	340	0	ATG	GGAGC	6.1	-0.1

protein ID	(predicted) function	length [aa]	TMH	start	RBS	pI	GRAVY
PA0898	N-succinylglutamate 5-semialdehyde	488	0	ATG	CGAGG	5.9	0.1
PA0902	hypothetical protein	334	0	GTG	CGAGG	6.0	0.1
PA0903	alanine--tRNA ligase	874	0	ATG	CGTGG	5.3	-0.3
PA0904	aspartokinase	412	0	ATG	-	5.2	0.0
PA0907	lysis phenotype activator, AlpA	176	0	ATG	GGAGG	9.8	-0.3
PA0910	AlpD	167	0	ATG	GGAGT	5.9	0.0
PA0913	Mg transporter MgtE	482	3	ATG	GGTGG	4.7	0.0
PA0916	ribosomal protein S12 methylthiotransferase	440	0	ATG	CGAGG	4.9	-0.2
PA0917	potassium transport system protein kup	634	12	ATG	-	7.0	0.6
PA0918	cytochrome b561	182	4	ATG	AGAGA	9.7	0.3
PA0919	alanyl-phosphatidylglycerol hydrolase	427	1	ATG	GGTGA	5.2	-0.3
PA0920	alanyl-phosphatidylglycerol synthase	881	14	ATG	TGAGG	9.6	0.5
PA0925	hypothetical protein	135	0	ATG	-	4.8	-0.2
PA0927	D-lactate dehydrogenase	329	0	ATG	-	5.7	0.0
PA0928	sensor/response regulator hybrid protein	925	2	GTG	GGAGA	5.0	-0.2
PA0933	23S rRNA (uracil(1939)-C(5))-methyltransferase RlmD	450	0	ATG	TGAGC	7.7	-0.2
PA0934	GTP pyrophosphokinase	747	0	ATG	CGTGG	7.1	-0.3
PA0936	lipopolysaccharide biosynthetic protein LpxO2	312	2	ATG	-	9.9	-0.1
PA0938	Wzz2	442	2	ATG	-	9.0	-0.3
PA0945	phosphoribosylformylglycinamidine cyclo-ligase	353	0	ATG	-	4.8	0.1
PA0946	hypothetical protein	345	1	ATG	CGAGA	4.9	-0.2
PA0947	DNA replication initiation factor	234	0	ATG	-	5.8	-0.2
PA0951	hypothetical protein	411	6	ATG	GGAGA	8.9	0.4
PA0953	thioredoxin	154	0	ATG	AGAGG	5.1	-0.2
PA0955	hypothetical protein	318	0	ATG	TGAGC	5.2	-0.4
PA0956	proline--tRNA ligase	571	0	ATG	-	5.3	-0.2
PA0958	porin D	443	0	ATG	GGAGC	5.0	-0.5
PA0961	cold-shock protein	204	4	ATG	GGTGA	9.9	0.5
PA0962	DNA-binding stress protein	156	0	ATG	GGAGA	5.0	-0.1
PA0963	aspartate--tRNA ligase	591	0	ATG	CGAGA	5.4	-0.3
PA0964	pqsR-mediated PQS regulator, PmpR	248	0	ATG	GGAGT	4.6	-0.2
PA0965	crossover junction endodeoxyribonuclease RuvC	174	0	ATG	-	9.9	0.1
PA0967	Holliday junction ATP-dependent DNA helicase	352	0	ATG	GGTGG	5.3	-0.1
PA0968	hypothetical protein	148	0	ATG	AGAGT	8.6	-0.3
PA0969	translocation protein TolQ	231	3	GTG	GGAGA	6.0	0.2
PA0970	translocation protein TolR	146	1	ATG	AGAGG	5.8	0.1
PA0971	translocation protein TolA	347	1	TTG	CGAGG	9.6	-0.7
PA0972	translocation protein TolB	432	0	GTG	GGAGG	8.9	-0.3
PA0973	peptidoglycan associated lipoprotein OprL	168	0	ATG	GGAGT	6.0	-0.4
PA0974	conserved hypothetical protein	274	0	ATG	-	7.8	-0.5
PA0981	hypothetical protein	207	0	ATG	GGAGA	6.3	0.0
PA0985	pyocin S5	498	1	ATG	GGAGA	8.5	-0.5
PA0995	methylated-DNA--protein-cysteine	173	0	ATG	AGAGG	6.9	-0.3
PA0996	anthranilate--CoA ligase	517	0	ATG	AGAGG	5.8	-0.1
PA0997	PqsB	283	0	ATG	GGAGG	4.9	-0.1
PA0998	PqsC	348	0	ATG	GGAGA	5.1	-0.1

protein ID	(predicted) function	length [aa]	TMH	start	RBS	pI	GRAVY
PA0999	3-oxoacyl-ACP synthase	337	0	ATG	GGAGG	5.3	0.1
PA1001	anthranilate synthase component I	530	0	ATG	-	5.7	-0.2
PA1003	transcriptional regulator MvfR	332	0	ATG	-	7.1	-0.1
PA1004	quinolinate synthetase A	352	0	ATG	GGTGT	5.4	0.0
PA1005	hypothetical protein	477	0	ATG	TGAGC	7.8	-0.4
PA1007	hypothetical protein	357	8	ATG	-	7.0	1.0
PA1009	hypothetical protein	185	0	ATG	-	5.5	0.0
PA1011	hypothetical protein	396	0	ATG	GGAGC	4.9	-0.5
PA1013	phosphoribosylaminoimidazole-succinocarboxamide synthase	236	0	ATG	GGAGC	5.3	-0.3
PA1014	glycosyl transferase family protein	330	0	GTG	-	8.5	-0.3
PA1015	transcriptional regulator	266	0	ATG	AGAGG	6.5	-0.2
PA1017	pimeloyl-CoA synthetase	715	0	ATG	GGTGA	5.4	0.2
PA1031	DNA recombination protein RmuC	453	0	TTG	GGAGC	5.5	-0.7
PA1032	acyl-homoserine lactone acylase QuiP	847	0	ATG	GGAGC	7.3	-0.4
PA1035	hypothetical protein	164	0	ATG	-	6.5	-0.2
PA1040	hypothetical protein	165	0	ATG	GGAGA	5.7	-0.2
PA1041	probable outer membrane protein precursor	210	0	ATG	CGAGG	5.3	-0.1
PA1043	hypothetical protein	269	0	ATG	GGAGG	7.8	-0.1
PA1044	hypothetical protein	154	4	ATG	GGAGA	11.4	0.9
PA1045	ATP-dependent DNA helicase DinG	714	0	ATG	-	5.7	-0.2
PA1047	esterase	392	0	ATG	CGAGG	5.8	-0.2
PA1048	probable outer membrane protein precursor	293	0	ATG	-	9.3	-0.4
PA1049	pyridoxine 5'-phosphate oxidase	215	0	ATG	GGAGA	6.4	-0.7
PA1050	hypothetical protein	370	0	ATG	-	6.9	-0.2
PA1051	transporter	452	13	ATG	GGAGG	8.3	1.0
PA1052	hypothetical protein	381	0	ATG	CGAGG	5.1	0.2
PA1052a	hypothetical protein[	80	1	ATG	-	9.5	-0.4
PA1053	hypothetical protein	154	0	ATG	GGAGA	9.6	0.1
PA1054	monovalent cation/H+ antiporter subunit A	933	25	ATG	AGAGG	7.1	0.9
PA1056	monovalent cation/H+ antiporter subunit D	499	14	ATG	GGAGG	9.5	1.0
PA1057	monovalent cation/H+ antiporter subunit E	174	3	ATG	GGAGG	6.4	0.8
PA1058	monovalent cation/H+ antiporter subunit F	89	3	ATG	GGAGA	5.1	1.3
PA1060	hypothetical protein	301	9	TTG	GGTGG	9.1	0.9
PA1064	hypothetical protein	221	0	ATG	GGAGT	5.4	-0.4
PA1068	heat shock protein (hsp90 family)	636	0	GTG	-	5.6	-0.3
PA1069	hypothetical protein	764	0	ATG	GGAGA	4.6	-0.4
PA1070	ABC transporter ATP-binding protein BraG	233	0	ATG	TGAGC	6.2	0.0
PA1071	ABC transporter ATP-binding protein BraF	255	0	ATG	GGAGC	7.8	-0.1
PA1072	branched-chain amino acid ABC transporter BraE	417	11	ATG	GGAGG	9.9	0.9
PA1073	branched-chain amino acid ABC transporter BraD	307	9	ATG	CGAGA	7.7	1.0
PA1074	branched-chain amino acid ABC transporter BraC	373	0	ATG	GGAGC	5.6	-0.2
PA1080	flagellar hook protein FlgE	462	0	ATG	GGAGC	4.6	-0.3
PA1084	flagellar basal body P-ring protein	369	0	ATG	TGAGG	6.9	0.1
PA1086	flagellar hook-associated protein FlgK	683	0	ATG	GGAGG	4.6	-0.3
PA1087	flagellar hook-associated protein FlgL	439	0	ATG	CGAGA	4.6	-0.4
PA1088	hypothetical protein	253	0	ATG	-	5.1	-0.3

protein ID	(predicted) function	length [aa]	TMH	start	RBS	pI	GRAVY
PA1090	hypothetical protein	220	0	GTG	GGAGA	5.4	-0.1
PA1091	flagellar glycosyl transferase FgtA	1694	0	ATG	-	5.3	-0.1
PA1092	B-type flagellin	488	0	ATG	GGAGG	5.4	-0.1
PA1094	B-type flagellar hook-associated protein FliD	474	0	ATG	GGAGA	6.5	-0.2
PA1097	transcriptional regulator FleQ	490	0	ATG	-	5.3	-0.4
PA1098	two-component sensor	402	0	ATG	CGAGA	6.4	-0.1
PA1099	two-component response regulator	473	0	ATG	GGAGT	6.0	0.0
PA1101	flagellar MS-ring protein	598	2	ATG	CGAGG	5.0	-0.3
PA1102	flagellar motor switch protein FliG	338	0	ATG	TGAGT	4.9	-0.1
PA1104	flagellum-specific ATP synthase	451	0	ATG	GGAGA	6.3	-0.1
PA1112	conserved hypothetical protein	382	0	ATG	GGAGA	6.2	-0.3
PA1113	ABC transporter ATP-binding protein/permease	588	6	ATG	CGAGC	9.9	0.3
PA1115	hypothetical protein	774	5	GTG	GGAGC	7.8	-0.2
PA1116	hypothetical protein	279	0	ATG	GGAGA	9.0	-0.2
PA1119	YfiB	168	0	GTG	GGAGA	8.1	-0.3
PA1120	diguanylate cyclase	435	2	ATG	-	5.9	-0.1
PA1125	NAD-dependent protein deacylase	250	0	ATG	GGAGG	7.1	0.0
PA1126	hypothetical protein	195	2	ATG	-	9.5	0.3
PA1127	oxidoreductase	329	0	ATG	GGAGT	5.4	-0.3
PA1130	rhamnosyltransferase	325	0	ATG	GGAGA	10.5	-0.2
PA1131	major facilitator superfamily transporter	422	10	GTG	GGAGG	10.2	0.9
PA1135	molecular chaperone Hsp31/glyoxalase	291	0	ATG	CGAGC	6.0	-0.3
PA1136	transcriptional regulator	243	0	ATG	-	5.7	-0.1
PA1137	oxidoreductase	328	0	ATG	-	5.7	0.0
PA1141	transcriptional regulator	300	0	ATG	-	8.4	-0.1
PA1142	transcriptional regulator	238	0	ATG	GGAGA	8.6	-0.3
PA1150	pyocin-S2	689	0	ATG	-	9.1	-0.4
PA1155	ribonucleotide-diphosphate reductase subunit NrdB	415	1	ATG	GGAGA	4.8	-0.4
PA1156	ribonucleotide-diphosphate reductase subunit NrdA	963	0	ATG	GGAGA	5.6	-0.3
PA1157	two-component response regulator	236	0	GTG	GGAGG	5.0	-0.2
PA1158	probable two-component sensor	798	2	CTG	GGAGC	11.0	-0.5
PA1159	cold-shock protein	69	0	ATG	GGAGA	6.7	-0.6
PA1161	rRNA methyltransferase	267	0	ATG	TGAGG	7.7	-0.2
PA1163	glycosyl transferase	869	9	ATG	-	9.0	0.2
PA1164	hypothetical protein	270	1	ATG	AGAGG	8.9	0.0
PA1165	4'-phosphopantetheinyl transferase	242	0	ATG	-	6.5	0.0
PA1169	arachidonate 15-lipoxygenase	685	0	ATG	GGAGT	6.3	0.0
PA1170	hypothetical protein	244	5	TTG	GGAGT	6.7	0.9
PA1171	transglycosylase SltB2	398	0	ATG	-	9.0	-0.2
PA1174	nitrate reductase catalytic subunit NapA	829	0	GTG	-	8.6	-0.4
PA1178	PhoP/Q and low Mg2+ inducible outer membrane protein H1 precursor	200	0	ATG	GGAGA	9.0	-0.5
PA1179	two-component response regulator PhoP	225	0	ATG	GGAGG	5.3	-0.3
PA1180	two-component sensor PhoQ	448	2	GTG	CGAGC	5.9	-0.2
PA1181	sensor protein	1120	8	ATG	CGAGC	5.5	0.1
PA1182	transcriptional regulator	333	0	ATG	-	8.9	-0.4
PA1183	C4-dicarboxylate transport protein	436	9	ATG	TGAGG	8.2	0.8

protein ID	(predicted) function	length [aa]	TMH	start	RBS	pI	GRAVY
PA1190	hypothetical protein	199	5	ATG	GGAGG	5.4	0.8
PA1192	tRNA 2-thiocytidine biosynthesis protein TtcA	274	0	ATG	AGAGC	6.2	-0.2
PA1193	hypothetical protein	223	0	ATG	-	8.9	-0.2
PA1196	transcriptional regulator DdaR	466	0	ATG	CGAGG	6.3	0.0
PA1197	NAD-dependent protein deacylase	256	0	ATG	GGAGC	5.8	-0.1
PA1200	hypothetical protein	220	0	ATG	GGAGG	5.4	-0.1
PA1207	glutathione-regulated potassium-efflux system	613	12	GTG	GGAGT	6.4	0.5
PA1216	hypothetical protein	248	0	ATG	GGAGA	5.8	-0.3
PA1222	membrane-bound lytic murein transglycosylase A	385	0	GTG	-	5.7	-0.3
PA1223	transcriptional regulator	297	0	ATG	-	9.8	-0.1
PA1243	sensor/response regulator hybrid protein	858	0	ATG	CGAGC	5.2	-0.1
PA1245	AprX	414	0	ATG	CGAGG	4.3	0.4
PA1246	alkaline protease secretion ATP-binding protein	593	5	ATG	TGAGC	9.4	0.2
PA1247	alkaline protease secretion protein AprE	432	1	ATG	GGAGG	8.0	-0.3
PA1248	alkaline protease secretion protein AprF	481	0	ATG	GGAGA	5.9	-0.5
PA1269	transcriptional regulator	222	0	ATG	-	5.7	-0.2
PA1271	tonB-dependent receptor	616	0	ATG	GGAGC	5.3	-0.5
PA1272	cob(I)alamin adenosyltransferase	203	0	ATG	GGAGT	7.1	-0.3
PA1273	hydrogenobyrinate a,c-diamide synthase	435	0	ATG	GGAGA	5.9	0.0
PA1275	cobalamin biosynthesis protein CobD	312	3	ATG	CGAGC	8.8	0.2
PA1277	cobyric acid synthase	490	0	ATG	GGAGC	6.0	0.0
PA1280	hypothetical protein	194	0	ATG	-	6.3	-0.4
PA1281	adenosylcobinamide-GDP ribazoletransferase	245	4	ATG	-	9.2	0.9
PA1283	transcriptional regulator	186	0	ATG	AGAGG	5.2	-0.2
PA1288	probable outer membrane protein precursor	424	0	ATG	GGAGT	5.7	-0.3
PA1292	3-mercaptopyruvate sulfurtransferase	284	0	ATG	GGAGT	5.4	-0.1
PA1293	hypothetical protein	353	0	ATG	-	5.7	-0.2
PA1294	ribonuclease D	374	0	GTG	GGAGA	5.1	-0.4
PA1301	transmembrane sensor	327	0	ATG	GGAGG	6.4	-0.2
PA1303	signal peptidase	179	0	ATG	-	9.8	-0.2
PA1308	hypothetical protein	174	2	ATG	CGAGG	7.0	-0.2
PA1317	cytochrome o ubiquinol oxidase subunit II	331	3	ATG	-	5.5	0.0
PA1318	cytochrome o ubiquinol oxidase subunit I	658	14	ATG	GGAGT	8.9	0.6
PA1319	cytochrome o ubiquinol oxidase subunit III	209	5	ATG	-	6.1	0.7
PA1320	cytochrome o ubiquinol oxidase subunit IV	111	3	ATG	-	6.2	1.2
PA1324	hypothetical protein	170	0	ATG	-	5.7	-0.4
PA1326	threonine dehydratase	515	0	ATG	GGAGG	6.1	-0.1
PA1327	protease	656	0	ATG	CGAGG	8.5	-0.3
PA1330	short-chain dehydrogenase	259	0	ATG	AGAGG	6.0	-0.3
PA1331	hypothetical protein	515	7	ATG	GGAGG	5.3	0.3
PA1333	hypothetical protein	68	0	ATG	CGAGG	9.0	-0.3
PA1335	two-component response regulator AauR	425	0	TTG	-	6.4	-0.1
PA1336	two-component sensor AauS	633	2	ATG	-	6.9	-0.3
PA1337	glutaminase-asparaginase	362	0	ATG	CGAGA	6.7	0.0
PA1338	gamma-glutamyltranspeptidase precursor	557	0	ATG	-	5.9	-0.1
PA1340	amino acid ABC transporter permease AatM	222	4	ATG	GGAGG	9.5	0.8

protein ID	(predicted) function	length [aa]	TMH	start	RBS	pI	GRAVY
PA1341	amino acid ABC transporter permease AatQ	248	4	ATG	CGAGG	9.1	0.6
PA1342	ABC transporter AatJ	302	0	ATG	CGAGG	8.3	-0.3
PA1343	hypothetical protein	152	0	ATG	GGAGT	8.0	-0.1
PA1344	short-chain dehydrogenase	264	1	ATG	GGAGA	5.2	0.2
PA1361	multidrug resistance protein PmpM (NorM)	477	12	GTG	-	9.8	0.6
PA1365	siderophore receptor	813	0	GTG	CGAGA	5.2	-0.4
PA1372	hypothetical protein	711	0	ATG	-	5.5	-0.3
PA1373	3-oxoacyl-ACP synthase	422	0	ATG	-	6.0	0.1
PA1376	bifunctional isocitrate dehydrogenase kinase/phosphatase	577	0	ATG	-	5.2	-0.3
PA1377	hypothetical protein	177	0	ATG	-	7.0	-0.4
PA1397	two-component response regulator	210	0	ATG	GGAGA	5.4	0.0
PA1398	hypothetical protein	113	0	ATG	-	5.8	-0.4
PA1403	transcriptional regulator	210	0	ATG	GGAGC	5.6	-0.3
PA1407	hypothetical protein	313	0	ATG	-	7.1	-0.3
PA1408	hypothetical protein	807	11	ATG	-	8.8	0.5
PA1410	probable periplasmic spermidine/putrescine-binding protein	363	0	ATG	TGAGG	6.6	-0.3
PA1413	transcriptional regulator	290	0	GTG	GGAGA	6.1	0.1
PA1418	sodium:solute symport protein	463	13	ATG	GGAGA	9.3	0.9
PA1422	protein GbuR	297	0	GTG	GGAGT	8.6	-0.1
PA1429	cation-transporting P-type ATPase	902	10	ATG	CGAGG	5.6	0.3
PA1430	transcriptional regulator LasR	239	0	ATG	-	6.1	0.0
PA1432	acyl-homoserine-lactone synthase LasI	201	0	ATG	GGAGG	6.1	-0.1
PA1433	hypothetical protein	650	2	ATG	GGAGG	6.1	-0.1
PA1437	two-component response regulator	229	0	ATG	AGAGG	6.0	-0.2
PA1438	two-component sensor	481	2	GTG	GGAGA	5.9	-0.2
PA1442	flagellar basal body protein FliL	173	1	ATG	-	9.6	0.1
PA1443	flagellar motor switch protein FliM	323	0	ATG	-	5.2	-0.1
PA1444	flagellar motor switch protein FliN	157	0	ATG	GGAGG	4.2	0.0
PA1445	flagellar protein FliO	150	2	ATG	-	10.2	0.3
PA1446	flagellar biosynthesis protein FliP	255	5	ATG	-	5.4	0.9
PA1450	hypothetical protein	419	6	ATG	TGAGA	7.7	0.5
PA1451	hypothetical protein	447	8	ATG	GGAGA	6.3	0.4
PA1452	flagellar biosynthesis protein FlhA	707	8	GTG	GGAGT	6.2	0.4
PA1454	flagellar synthesis regulator FleN	280	0	ATG	-	8.5	0.2
PA1455	flagellar biosynthesis sigma factor FliA	247	0	ATG	-	5.7	-0.4
PA1457	protein phosphatase CheZ	262	0	ATG	AGAGG	4.9	-0.6
PA1458	two-component sensor	753	0	ATG	GGAGC	4.6	-0.1
PA1459	chemotaxis-specific methylesterase	368	0	ATG	TGAGG	8.7	0.0
PA1460	flagellar motor protein MotC	246	4	ATG	CGAGG	5.0	0.5
PA1461	flagellar motor protein MotD	296	1	ATG	GGAGC	5.4	-0.4
PA1462	plasmid partitioning protein	262	0	ATG	AGAGT	9.6	0.0
PA1464	purine-binding chemotaxis protein	159	0	ATG	AGAGG	4.3	0.0
PA1465	hypothetical protein	135	1	ATG	CGAGG	8.6	-0.1
PA1474	hypothetical protein	492	0	ATG	-	6.1	-0.1
PA1475	cytochrome c biogenesis ATP-binding export	233	0	ATG	-	5.6	0.0
PA1476	heme exporter protein CcmB	223	6	ATG	-	8.0	1.2

protein ID	(predicted) function	length [aa]	TMH	start	RBS	pI	GRAVY
PA1477	heme exporter protein CcmC	252	6	ATG	AGAGC	9.5	0.7
PA1479	cytochrome c-type biogenesis protein CcmE	162	1	GTG	GGAGG	6.4	-0.2
PA1480	cytochrome c-type biogenesis protein CcmF	657	15	ATG	GGAGG	9.4	0.6
PA1481	cytochrome c-type biogenesis protein CcmG	180	1	TTG	GGAGC	5.4	0.1
PA1482	cytochrome c-type biogenesis protein CcmH	155	2	ATG	GGAGG	9.4	-0.2
PA1483	cytochrome c-type biogenesis protein CycH	407	2	ATG	-	5.1	-0.1
PA1483a	hypothetical protein	138	0	GTG	GGAGG	10.0	-0.7
PA1494	mucoidy inhibitor gene A	551	0	GTG	AGAGA	5.7	-0.5
PA1496	probable potassium channel	283	6	ATG	GGAGC	8.5	0.5
PA1504	transcriptional regulator	216	0	ATG	-	7.0	-0.3
PA1505	cyclic pyranopterin monophosphate synthase	331	0	ATG	CGAGT	6.6	-0.3
PA1513	hypothetical protein	425	8	GTG	AGAGG	8.6	0.3
PA1520	transcriptional regulator	259	0	ATG	CGAGA	7.2	-0.4
PA1526	transcriptional regulator	219	0	ATG	-	7.0	-0.1
PA1527	hypothetical protein	1162	0	ATG	GGAGC	5.1	-0.7
PA1528	cell division protein ZipA	289	1	ATG	-	5.6	-0.6
PA1529	NAD-dependent DNA ligase LigA	794	0	ATG	-	5.3	-0.2
PA1530	hypothetical protein	125	1	ATG	GGAGT	8.0	-0.3
PA1531	hypothetical protein	288	0	ATG	-	8.5	-0.1
PA1532	DNA polymerase III subunits gamma/tau	681	0	ATG	-	4.7	-0.1
PA1539	hypothetical protein	282	0	ATG	GGTGG	5.3	-0.3
PA1543	adenine phosphoribosyltransferase	182	0	ATG	-	4.8	0.3
PA1544	transcriptional regulator Anr	244	0	ATG	-	5.4	-0.1
PA1546	oxygen-independent coproporphyrinogen-III	460	0	ATG	-	5.4	-0.4
PA1548	hypothetical protein	69	1	ATG	CGAGG	4.3	0.0
PA1549	cation-transporting P-type ATPase	811	8	ATG	GGAGC	6.1	0.2
PA1550	hypothetical protein	179	1	ATG	TGAGT	5.3	-0.4
PA1551	ferredoxin	471	5	ATG	CGTGG	8.8	0.0
PA1552	cytochrome C oxidase cbb3-type subunit CcoP	318	2	ATG	GGAGT	5.8	-0.2
PA1552.1	cytochrome C oxidase cbb3-type subunit CcoQ	61	1	ATG	AGAGC	8.1	-0.1
PA1553	cbb3-type cytochrome C oxidase subunit II	203	1	ATG	TGAGG	7.8	-0.4
PA1554	cbb3-type cytochrome C oxidase subunit I	475	12	ATG	CGTGG	9.4	0.6
PA1555	cytochrome C oxidase cbb3-type subunit CcoP	308	2	ATG	GGAGT	6.1	-0.2
PA1555.1	cytochrome C oxidase cbb3-type subunit CcoQ	61	1	ATG	GGTGA	8.1	-0.2
PA1556	cbb3-type cytochrome C oxidase subunit II	202	1	ATG	TGAGG	7.7	-0.4
PA1557	cbb3-type cytochrome C oxidase subunit I	475	12	ATG	CGTGG	9.1	0.6
PA1558	hypothetical protein	210	0	TTG	CGAGG	9.5	-0.1
PA1561	aerotaxis receptor Aer	521	2	ATG	-	5.6	-0.3
PA1562	aconitate hydratase	910	0	ATG	TGAGG	5.4	-0.2
PA1563	23S rRNA (cytidine(2498)-2'-O)-methyltransferase RlmM	352	0	ATG	GGAGA	8.7	-0.3
PA1564	sulfurtransferase TusA	79	0	ATG	GGAGT	5.9	-0.2
PA1565	oxidoreductase	436	0	ATG	-	7.3	-0.2
PA1570	transcriptional regulator	293	0	ATG	GGAGT	5.6	0.0
PA1572	hypothetical protein	381	0	ATG	GGAGT	5.2	0.1
PA1578	hypothetical protein	251	1	ATG	-	9.8	-0.3
PA1580	citrate synthase	428	0	ATG	GGAGG	6.5	-0.2

protein ID	(predicted) function	length [aa]	TMH	start	RBS	pI	GRAVY
PA1581	succinate dehydrogenase (C subunit)	128	3	GTG	-	9.8	0.8
PA1582	succinate dehydrogenase subunit D	122	3	ATG	-	9.0	0.9
PA1583	succinate dehydrogenase flavoprotein subunit A	590	0	ATG	-	6.0	-0.2
PA1584	succinate dehydrogenase iron-sulfur subunit B	235	0	ATG	GGTGC	6.6	-0.2
PA1585	2-oxoglutarate dehydrogenase subunit E1	943	0	ATG	CGAGG	6.1	-0.4
PA1586	2-oxoglutarate dehydrogenase complex	409	0	ATG	-	5.4	0.1
PA1587	2-oxoglutarate dehydrogenase complex	478	0	ATG	TGAGA	6.5	0.1
PA1588	succinyl-CoA ligase subunit beta	388	0	ATG	-	5.8	-0.1
PA1589	succinyl-CoA ligase subunit alpha	295	0	ATG	GGAGG	5.8	0.2
PA1590	branched-chain amino acid transporter	437	12	ATG	AGTGG	8.4	1.1
PA1591	hypothetical protein	254	4	ATG	AGAGG	6.4	0.4
PA1592	hypothetical protein	78	0	ATG	GGAGG	4.6	-0.6
PA1595	hypothetical protein	409	3	ATG	TGAGG	7.1	0.0
PA1596	chaperone protein HtpG	634	0	ATG	GGAGC	5.1	-0.5
PA1601	aldehyde dehydrogenase	748	0	ATG	GGAGG	8.8	-0.2
PA1608	chemotaxis transducer	541	2	ATG	-	4.8	-0.1
PA1609	3-oxoacyl-ACP synthase	405	0	ATG	-	5.4	-0.1
PA1610	3-hydroxydecanoyl-ACP dehydratase	171	0	ATG	TGAGG	6.4	0.0
PA1611	sensor/response regulator hybrid protein	651	1	ATG	GGAGA	5.0	-0.2
PA1612	hypothetical protein	252	0	GTG	-	6.0	-0.2
PA1613	hypothetical protein	702	0	GTG	CGAGA	5.5	-0.5
PA1614	glycerol-3-phosphate dehydrogenase	340	0	ATG	-	5.9	0.0
PA1615	lipase	113	1	ATG	CGAGG	5.2	0.2
PA1617	AMP-binding protein	555	0	GTG	GGAGG	6.7	-0.2
PA1623	conserved hypothetical protein	220	0	ATG	GGAGA	5.9	-0.3
PA1624	hypothetical protein	268	0	ATG	TGAGG	6.0	-0.1
PA1626	major facilitator superfamily transporter	424	12	ATG	-	9.4	0.8
PA1633	potassium-transporting ATPase subunit A	564	10	ATG	GGAGG	7.7	0.7
PA1634	potassium-transporting ATPase subunit B	690	7	ATG	-	6.3	0.3
PA1636	two-component sensor KdpD	885	3	ATG	GGAGT	5.8	-0.1
PA1637	two-component response regulator KdpE	230	0	ATG	CGAGT	5.6	-0.1
PA1640	hypothetical protein	345	0	ATG	-	5.1	-0.1
PA1641	hypothetical protein	92	0	ATG	GGAGA	8.8	-0.2
PA1646	chemotaxis transducer	652	2	ATG	GGAGG	5.2	-0.1
PA1647	sulfate transporter	573	11	ATG	-	9.1	0.7
PA1650	transporter	297	9	ATG	GGAGC	9.4	1.1
PA1651	transporter	398	11	ATG	-	8.9	0.8
PA1652	hypothetical protein	211	5	ATG	CGAGG	7.8	0.8
PA1654	aminotransferase	388	0	ATG	GGTGA	5.5	-0.1
PA1656	HsiA2	518	0	ATG	GGTGT	6.3	-0.2
PA1657	HsiB2	168	0	ATG	GGAGA	4.8	-0.3
PA1658	HsiC2	491	0	ATG	-	5.3	-0.4
PA1660	HsiG2	526	0	ATG	-	5.9	-0.2
PA1662	ClpA/B-type protease	877	0	ATG	-	5.5	-0.2
PA1663	transcriptional regulator Sfa2	503	0	ATG	TGAGG	5.8	-0.1
PA1665	Fha2	397	0	ATG	GGAGC	5.3	-0.5

protein ID	(predicted) function	length [aa]	TMH	start	RBS	pI	GRAVY
PA1666	Lip2	168	1	ATG	CGAGC	6.6	-0.1
PA1667	HsiJ2	443	0	ATG	GGTGA	6.1	-0.2
PA1668	DotU2	289	1	ATG	-	5.5	-0.1
PA1669	IcmF2	1175	3	ATG	-	9.2	-0.3
PA1670	serine/threonine phosphoprotein phosphatase Stp1	242	0	ATG	GGTGC	5.9	-0.2
PA1673	bacteriohemerythrin	153	0	ATG	-	5.8	-0.5
PA1678	50S ribosomal protein L3 glutamine	304	0	ATG	CGAGG	4.6	-0.1
PA1679	hypothetical protein	259	1	ATG	AGAGG	8.0	-0.4
PA1680	hypothetical protein	327	0	ATG	-	9.9	-0.1
PA1681	chorismate synthase	363	0	ATG	GGAGC	6.2	-0.3
PA1683	methylthioribulose-1-phosphate dehydratase	205	0	ATG	AGAGG	6.1	-0.3
PA1686	DNA-3-methyladenine glycosidase II	297	0	ATG	-	6.4	0.0
PA1687	polyamine aminopropyltransferase	286	0	ATG	GGAGA	5.1	-0.2
PA1689	hypothetical protein	700	5	ATG	AGAGC	6.1	0.0
PA1713	exoenzyme S transcriptional regulator ExsA	278	0	ATG	-	8.6	-0.1
PA1714	ExsD	276	0	ATG	TGAGG	5.1	-0.3
PA1723	type III export protein PscJ	248	1	ATG	-	9.0	0.0
PA1727	signaling protein MucR	685	7	ATG	-	5.9	0.4
PA1732	hypothetical protein	266	0	ATG	GGAGG	6.2	-0.4
PA1735	hypothetical protein	295	10	GTG	-	9.4	1.0
PA1737	3-hydroxyacyl-CoA dehydrogenase	714	0	ATG	GGAGA	6.3	0.0
PA1738	transcriptional regulator	304	0	ATG	CGAGT	7.2	-0.1
PA1742	amidotransferase	240	0	ATG	AGAGA	5.2	-0.2
PA1745	hypothetical protein	162	0	ATG	-	8.4	-0.3
PA1746	hypothetical protein	168	0	ATG	-	6.2	0.0
PA1750	phospho-2-dehydro-3-deoxyheptonate aldolase	358	0	ATG	TGAGT	6.1	-0.3
PA1752	2-dehydropantoate 2-reductase	315	1	ATG	TGAGG	6.2	0.0
PA1754	transcriptional regulator CysB	324	0	ATG	CGAGG	6.5	0.0
PA1755	hypothetical protein	115	0	ATG	GGAGA	5.9	-0.5
PA1759	transcriptional regulator	901	0	GTG	-	6.0	-0.1
PA1760	transcriptional regulator	907	0	ATG	CGAGC	6.4	-0.1
PA1766	hypothetical protein	327	0	ATG	-	6.5	-0.2
PA1767	hypothetical protein	508	7	ATG	TGAGT	8.8	0.3
PA1768	hypothetical protein	179	0	ATG	-	9.2	-0.3
PA1770	phosphoenolpyruvate synthase	791	0	TTG	GGAGA	5.0	-0.1
PA1773	transporter CmaX	332	2	ATG	-	5.3	-0.2
PA1775	conserved cytoplasmic membrane protein, CmpX protein	274	5	ATG	TGAGT	7.9	1.0
PA1777	outer membrane porin F	350	0	ATG	-	5.0	-0.4
PA1787	aconitate hydratase B	869	0	GTG	TGAGG	5.2	-0.1
PA1789	hypothetical protein	287	0	ATG	GGAGA	5.4	-0.1
PA1790	hypothetical protein	207	0	GTG	-	6.3	-0.1
PA1791	hypothetical protein	443	1	GTG	-	5.8	-0.3
PA1792	UDP-2,3-diacylglucosamine hydrolase	240	0	ATG	-	7.9	-0.3
PA1793	peptidyl-prolyl cis-trans isomerase B	165	0	ATG	-	5.8	-0.4
PA1794	glutamine--tRNA ligase	556	0	ATG	AGAGC	5.6	-0.6
PA1795	cysteine--tRNA ligase	460	0	GTG	TGAGG	5.4	-0.3

protein ID	(predicted) function	length [aa]	TMH	start	RBS	pI	GRAVY
PA1798	two-component sensor ParS	428	2	ATG	GGAGC	5.3	-0.2
PA1799	two-component response regulator ParR	235	0	ATG	-	5.9	-0.1
PA1800	trigger factor	436	0	ATG	CGAGG	4.8	-0.4
PA1801	ATP-dependent Clp protease proteolytic subunit	213	0	ATG	GGAGT	6.0	0.0
PA1802	ATP-dependent protease ATP-binding subunit ClpX	426	0	ATG	-	5.1	-0.3
PA1803	Lon protease	798	0	ATG	AGAGC	5.8	-0.3
PA1804	DNA-binding protein HU	90	0	GTG	-	10.0	0.2
PA1805	peptidyl-prolyl cis-trans isomerase D	621	1	ATG	-	5.0	-0.4
PA1806	NADH-dependent enoyl-ACP reductase	265	0	ATG	-	5.7	0.0
PA1807	ABC transporter ATP-binding protein NppD	536	0	ATG	CGAGG	7.0	-0.1
PA1808	ABC transporter permease NppC	339	6	ATG	GGAGT	9.2	0.4
PA1809	ABC transporter permease NppB	360	6	ATG	GGAGT	6.1	0.7
PA1811	solute-binding protein NppA1	609	0	ATG	-	9.7	-0.4
PA1816	DNA polymerase III subunit epsilon	246	0	ATG	AGAGA	5.2	-0.2
PA1818	lysine-specific pyridoxal 5'-phosphate-dependent	751	0	ATG	-	5.8	-0.1
PA1819	amino acid permease	451	12	ATG	GGTGT	8.8	0.7
PA1820	Na(+)/H(+) antiporter NhaB	500	11	GTG	GGAGT	7.0	0.8
PA1822	hypothetical protein	562	0	ATG	GGAGG	5.2	0.0
PA1824	hypothetical protein	259	6	ATG	-	10.0	0.8
PA1825	hypothetical protein	214	2	ATG	-	7.9	0.3
PA1829	hypothetical protein	356	0	ATG	CGAGA	5.7	-0.4
PA1831	hypothetical protein	236	0	GTG	CGAGG	5.9	-0.2
PA1832	protease	341	1	GTG	AGAGG	8.7	-0.1
PA1833	oxidoreductase	330	0	ATG	GGAGG	5.4	0.3
PA1837a	hypothetical protein[	75	2	ATG	GGAGG	9.7	0.5
PA1843	B12-dependent methionine synthase	1234	0	ATG	-	4.9	-0.2
PA1846	cis/trans isomerase	762	0	ATG	TGAGG	5.8	-0.4
PA1847	NfuA	194	0	ATG	CGAGG	4.5	-0.2
PA1851	hypothetical protein	401	5	ATG	CGAGG	5.8	0.3
PA1853	probable transcriptional regulator	287	0	ATG	TGTGG	5.8	-0.2
PA1856	cbb3-type cytochrome C oxidase subunit I	480	12	ATG	-	9.4	0.5
PA1857	hypothetical protein	307	4	ATG	-	6.6	0.8
PA1861	molybdenum ABC transporter ATP-binding protein ModC	361	0	ATG	-	8.5	-0.1
PA1862	molybdenum ABC transporter permease ModB	228	5	ATG	-	8.1	0.8
PA1868	type II secretion system protein D	776	1	ATG	-	7.3	-0.1
PA1871	protease LasA	418	0	ATG	GGAGC	9.0	-0.3
PA1872	hypothetical protein	263	0	ATG	-	9.6	0.1
PA1880	oxidoreductase	731	0	ATG	-	6.9	-0.1
PA1888	hypothetical protein	469	0	ATG	-	6.2	-0.3
PA1889	hypothetical protein	327	0	GTG	-	7.3	-0.1
PA1890	glutathione S-transferase	207	0	ATG	-	6.4	-0.3
PA1892	hypothetical protein	245	0	ATG	CGAGC	6.5	-0.2
PA1894	hypothetical protein	230	0	ATG	GGAGA	5.3	-0.5
PA1901	phenazine biosynthesis protein PhzC	405	0	ATG	GGTGA	6.9	-0.3
PA1902	phenazine biosynthesis protein PhzD	207	0	ATG	GGAGA	5.6	-0.1
PA1903	phenazine biosynthesis protein PhzE	627	0	ATG	CGAGG	5.5	-0.2

protein ID	(predicted) function	length [aa]	TMH	start	RBS	pI	GRAVY
PA1910	ferric-mycobactin receptor FemA	804	1	ATG	CGAGG	5.9	-0.3
PA1913	hypothetical protein	226	0	ATG	-	7.9	-0.2
PA1919	class III (anaerobic) ribonucleoside-triphosphate reductase activating protein NrdG	232	0	ATG	CGAGA	8.2	0.0
PA1920	anaerobic ribonucleoside triphosphate reductase	675	0	ATG	GGAGA	6.1	-0.4
PA1926	Uncharacterized protein	756	0	GTG	GGTGC	4.7	-0.1
PA1927	5-methyltetrahydropteroyltriglutamate-homocysteine S-methyltransferase	766	0	ATG	GGAGG	5.6	-0.2
PA1930	chemotaxis transducer	431	0	ATG	GGAGT	6.1	-0.2
PA1939	hypothetical protein	665	0	ATG	-	5.8	-0.3
PA1940	hypothetical protein	379	1	ATG	-	8.8	-0.4
PA1941	hypothetical protein	631	1	ATG	-	7.7	-0.5
PA1943	hypothetical protein	365	0	ATG	GGAGA	8.7	-0.5
PA1947	ribose transporter RbsA	510	0	ATG	GGAGC	6.1	0.0
PA1948	ribose ABC transporter permease	332	8	ATG	-	9.4	0.9
PA1949	ribose operon repressor RbsR	337	0	ATG	-	6.7	0.0
PA1950	ribokinase	308	0	ATG	-	5.2	0.2
PA1951	FapF	421	0	ATG	-	4.8	-0.2
PA1959	undecaprenyl-diphosphatase	277	6	ATG	GGAGA	7.8	0.7
PA1960	hypothetical protein	240	3	ATG	GGTGG	10.5	-0.1
PA1961	transcriptional regulator	311	0	ATG	GGAGC	7.1	-0.2
PA1964	ABC-F family ATPase	521	0	ATG	-	5.0	-0.2
PA1965	hypothetical protein	111	0	ATG	-	5.1	0.0
PA1969	hypothetical protein	130	0	ATG	-	9.0	-0.1
PA1971	branched-chain amino acid transport system 3 BraZ	437	12	ATG	-	9.0	1.1
PA1973	coenzyme PQQ synthesis protein F	775	0	ATG	CGAGG	8.4	-0.1
PA1984	aldehyde dehydrogenase ExaC	506	0	ATG	GGAGA	5.4	-0.1
PA1992	sensor histidine kinase	564	0	ATG	CGAGG	5.8	-0.2
PA1998	transcriptional regulator DhcR	306	0	ATG	TGAGA	6.1	0.0
PA2000	dehydrocarnitine CoA transferase subunit B	218	0	ATG	AGAGG	4.8	0.2
PA2001	acetyl-CoA acetyltransferase	393	0	ATG	GGAGA	6.0	0.1
PA2002	hypothetical protein	474	10	ATG	CGAGA	8.7	0.8
PA2003	3-hydroxybutyrate dehydrogenase	256	0	ATG	GGAGA	5.5	0.2
PA2004	hypothetical protein	463	9	ATG	GGAGA	9.3	0.9
PA2006	major facilitator superfamily transporter	450	12	ATG	-	8.9	0.8
PA2007	maleylacetoacetate isomerase	212	0	ATG	-	6.4	-0.3
PA2008	fumarylacetoacetase	432	0	ATG	GGAGA	5.7	-0.2
PA2009	homogentisate 1,2-dioxygenase	432	0	ATG	GGAGG	5.7	-0.3
PA2010	transcriptional regulator	267	0	ATG	-	5.7	0.2
PA2012	methylcrotonyl-CoA carboxylase subunit alpha	655	0	ATG	GGAGA	5.5	-0.2
PA2013	gamma-carboxygeranoyl-CoA hydratase	265	0	ATG	CGAGT	5.4	0.0
PA2015	isovaleryl-CoA dehydrogenase	387	0	ATG	GGTGA	5.5	-0.1
PA2016	liu genes regulator	134	0	ATG	GGTGC	5.6	-0.7
PA2018	multidrug efflux protein MexY	1045	11	ATG	GGAGA	6.0	0.3
PA2019	multidrug efflux lipoprotein MexX	396	0	ATG	CGAGG	6.0	-0.1
PA2020	transcriptional regulator MexZ	210	0	GTG	TGAGG	6.8	-0.4
PA2023	UTP-glucose-1-phosphate uridylyltransferase	279	0	ATG	-	5.3	-0.2
PA2026	hypothetical protein	333	8	ATG	AGAGC	9.5	0.9

protein ID	(predicted) function	length [aa]	TMH	start	RBS	pI	GRAVY
PA2034	hypothetical protein	224	0	ATG	GGTGT	6.0	0.1
PA2039	hypothetical protein	252	6	ATG	-	9.4	0.7
PA2040	glutamine synthetase	458	0	ATG	GGTGT	4.8	-0.2
PA2041	amino acid permease	456	12	ATG	CGAGG	9.4	0.7
PA2042	serine/threonine transporter SstT	409	9	ATG	AGAGT	7.1	1.0
PA2044	hypothetical protein	624	0	ATG	TGAGG	5.9	-0.5
PA2047	transcriptional regulator	329	0	ATG	-	9.2	-0.2
PA2049	hypothetical protein	664	0	ATG	-	6.4	-0.3
PA2056	transcriptional regulator	300	0	ATG	TGAGA	7.6	0.1
PA2062	pyridoxal-phosphate dependent protein	393	0	ATG	-	6.8	-0.1
PA2063	hypothetical protein	407	0	ATG	TGAGC	9.6	-0.5
PA2066	hypothetical protein	212	0	ATG	AGAGG	6.0	0.0
PA2069	carbamoyl transferase	574	0	ATG	AGAGG	5.9	-0.2
PA2071	elongation factor G	702	0	ATG	-	5.1	-0.3
PA2072	hypothetical protein	864	2	ATG	-	5.7	-0.1
PA2080	kynureninase KynU	416	0	ATG	GGAGT	5.4	-0.1
PA2097	flavin-binding monooxygenase	491	0	ATG	GGAGC	9.4	-0.4
PA2108	thiamine pyrophosphate protein	590	0	ATG	GGAGG	6.1	-0.1
PA2110	hypothetical protein	313	0	ATG	GGAGG	7.0	0.0
PA2111	hypothetical protein	237	0	ATG	GGAGG	6.9	-0.1
PA2113	pyroglutatmate porin OpdO	409	0	ATG	CGAGG	5.7	-0.3
PA2114	major facilitator superfamily transporter	423	11	ATG	GGTGC	9.4	0.6
PA2115	transcriptional regulator	317	0	ATG	-	7.8	0.0
PA2116	hypothetical protein	265	0	ATG	GGAGC	6.1	-0.1
PA2118	O6-methylguanine-DNA methyltransferase	358	0	ATG	-	9.3	-0.4
PA2119	alcohol dehydrogenase (Zn-dependent)	366	0	ATG	TGAGG	5.4	0.1
PA2120	hypothetical protein	142	0	ATG	AGAGG	6.1	0.1
PA2123	transcriptional regulator	310	0	ATG	-	6.7	-0.3
PA2126	cupA gene regulator C, CgrC	211	0	ATG	TGAGG	7.1	-0.3
PA2127	cupA gene regulator A, CgrA	408	0	ATG	AGAGG	9.6	-0.5
PA2130	usher CupA3	872	1	ATG	-	8.9	-0.5
PA2176	hypothetical protein	196	0	ATG	GGAGT	5.1	0.2
PA2194	hydrogen cyanide synthase subunit HcnB	464	0	ATG	GGAGG	8.3	-0.1
PA2195	hydrogen cyanide synthase subunit HcnC	417	2	ATG	-	6.2	-0.1
PA2196	transcriptional regulator	194	0	ATG	-	6.1	-0.3
PA2197	hypothetical protein	345	0	ATG	AGAGG	5.9	-0.1
PA2199	dehydrogenase	291	0	ATG	CGAGG	5.5	0.3
PA2222	hypothetical protein	215	0	ATG	AGAGG	5.2	0.0
PA2223	hypothetical protein	339	0	GTG	AGAGG	5.3	-0.4
PA2229	conserved hypothetical protein	239	0	ATG	AGAGA	6.1	-0.4
PA2231	biofilm formation protein PslA	478	5	ATG	AGAGC	9.7	0.2
PA2232	biofilm formation protein PslB	488	0	ATG	-	5.7	-0.1
PA2233	biofilm formation protein PslC	303	0	ATG	CGAGA	8.8	-0.2
PA2234	biofilm formation protein PslD	256	0	ATG	-	8.7	0.0
PA2235	biofilm formation protein PslE	662	2	ATG	TGAGG	6.0	-0.2
PA2236	biofilm formation protein PslF	395	0	ATG	GGAGC	8.6	0.0
PA2237	biofilm formation protein PslG	442	1	ATG	GGTGG	5.7	-0.2

protein ID	(predicted) function	length [aa]	TMH	start	RBS	pI	GRAVY
PA2238	biofilm formation protein PslH	402	0	ATG	GGAGT	6.5	-0.2
PA2239	biofilm formation protein PslI	367	0	ATG	GGAGC	8.5	-0.2
PA2240	biofilm formation protein PslJ	478	11	ATG	CGAGG	10.8	0.7
PA2241	biofilm formation protein PslL	469	12	ATG	CGAGG	10.1	0.9
PA2242	hypothetical protein	355	10	GTG	GGAGT	9.6	0.7
PA2247	2-oxoisovalerate dehydrogenase subunit alpha	410	0	ATG	GGAGG	5.7	-0.3
PA2248	2-oxoisovalerate dehydrogenase subunit beta	350	0	ATG	GGAGC	5.4	-0.1
PA2249	branched-chain alpha-keto acid dehydrogenase	428	0	ATG	GGAGG	5.8	-0.1
PA2250	branched-chain alpha-keto acid dehydrogenase	464	0	ATG	GGAGT	6.2	0.2
PA2252	AGCS sodium/alanine/glycine symporter	481	8	ATG	CGAGG	8.8	0.7
PA2259	transcriptional regulator PtxS	340	0	GTG	AGAGG	6.4	-0.2
PA2261	2-ketogluconate kinase	316	0	ATG	GGAGG	5.6	-0.1
PA2265	gluconate dehydrogenase	591	0	ATG	AGAGG	6.8	-0.3
PA2269	hypothetical protein	401	11	ATG	CGAGG	8.5	0.9
PA2278	arsenite-antimonite efflux pump ArsB	427	11	ATG	CGAGC	9.4	1.1
PA2280	oxidoreductase	230	0	ATG	GGAGG	6.9	-0.3
PA2289	hypothetical protein	710	0	ATG	-	5.5	-0.5
PA2290	glucose dehydrogenase	803	5	ATG	GGAGT	5.9	-0.1
PA2291	glucose-sensitive porin	452	0	GTG	CGAGG	5.5	-0.5
PA2300	chitinase	483	0	ATG	CGAGG	5.2	-0.3
PA2301	hypothetical protein	180	0	ATG	CGAGG	6.1	0.1
PA2302	protein AmbE	2124	0	ATG	CGAGG	5.1	0.0
PA2304	protein AmbC	362	0	ATG	GGAGA	6.3	-0.4
PA2305	protein AmbB	1249	0	ATG	GGAGA	6.0	-0.1
PA2306	AmbA	205	5	ATG	-	9.4	0.8
PA2316	transcriptional regulator	297	0	ATG	GGAGC	8.3	0.0
PA2317	oxidoreductase	432	0	ATG	-	7.3	-0.1
PA2320	GntR family transcriptional regulator	343	0	ATG	-	8.3	-0.1
PA2322	gluconate permease	450	12	ATG	GGAGA	7.2	1.1
PA2323	glyceraldehyde-3-phosphate dehydrogenase	541	0	ATG	CGAGG	6.0	-0.1
PA2325	hypothetical protein	411	0	ATG	GGAGT	6.3	-0.2
PA2327	probable permease of ABC transporter	254	6	GTG	CGAGG	10.0	0.8
PA2329	ABC transporter ATP-binding protein	278	0	ATG	CGAGG	6.5	0.0
PA2330	hypothetical protein	355	0	ATG	GGAGT	6.2	0.1
PA2344	fructokinase	310	0	ATG	GGAGA	5.8	0.1
PA2345	hypothetical protein	411	1	ATG	-	6.6	0.0
PA2353	hypothetical protein	384	0	ATG	GGTGG	5.9	-0.2
PA2366	uricase	494	0	ATG	GGAGA	5.6	-0.3
PA2371	ClpA/B-type protease	849	0	ATG	GGAGG	5.3	-0.1
PA2378	aldehyde dehydrogenase	771	0	ATG	GGAGG	8.4	-0.2
PA2382	L-lactate dehydrogenase	383	0	ATG	GGAGT	9.0	-0.1
PA2386	L-ornithine N5-oxygenase	443	0	ATG	AGAGG	6.0	-0.3
PA2389	pyoverdine biosynthesis protein PvdR	391	1	ATG	-	9.2	-0.3
PA2390	pyoverdine biosynthesis protein PvdT	663	4	ATG	-	6.1	0.1
PA2391	probable outer membrane protein precursor	474	0	ATG	-	5.9	-0.2
PA2392	pyoverdine biosynthesis protein PvdP	544	0	ATG	-	6.2	-0.5
PA2393	dipeptidase	448	1	ATG	-	5.9	-0.3

protein ID	(predicted) function	length [aa]	TMH	start	RBS	pI	GRAVY
PA2397	pyoverdine biosynthesis protein PvdE	549	6	ATG	-	6.9	0.2
PA2398	ferripyoverdine receptor	815	0	ATG	AGAGC	5.4	-0.6
PA2399	pyoverdine synthetase D	2448	0	GTG	AGAGG	5.2	-0.2
PA2400	pyoverdine biosynthesis protein PvdJ	2157	0	ATG	-	5.2	-0.2
PA2402	peptide synthase	5149	0	ATG	-	5.2	-0.2
PA2403	FpvG	403	4	ATG	-	9.7	0.2
PA2404	FpvH	179	1	ATG	GGAGG	9.7	-0.1
PA2407	FpvC	317	1	ATG	-	9.2	0.0
PA2408	ABC transporter ATP-binding protein FpvD	251	0	ATG	GGAGT	8.9	0.0
PA2411	thioesterase	254	0	GTG	-	5.5	-0.1
PA2413	diaminobutyrate--2-oxoglutarate aminotransferase	469	0	ATG	TGAGG	6.0	0.0
PA2424	peptide synthase PvdL	4342	0	ATG	-	5.3	-0.2
PA2430	hypothetical protein	334	1	ATG	GGAGA	9.7	-0.2
PA2431	hypothetical protein	724	10	ATG	GGAGG	7.6	0.5
PA2442	glycine cleavage system protein T2	373	0	ATG	GGAGT	6.0	0.1
PA2443	L-serine dehydratase	458	0	ATG	GGAGA	6.4	0.0
PA2445	glycine dehydrogenase	959	0	ATG	TGAGG	5.7	-0.1
PA2449	transcriptional regulator GcsR	511	0	ATG	-	5.8	0.0
PA2450	hypothetical protein	305	0	ATG	-	6.0	-0.4
PA2453	hypothetical protein	73	0	ATG	-	7.9	-0.3
PA2462	hemagglutinin	5627	1	ATG	GGAGT	5.3	-0.2
PA2463	hypothetical protein	565	1	ATG	-	8.4	-0.6
PA2466	ferrioxamine receptor FoxA	820	0	ATG	-	5.0	-0.4
PA2467	anti-sigma factor FoxR	328	0	GTG	GGAGC	9.8	-0.3
PA2469	transcriptional regulator	304	0	ATG	CGAGG	7.8	-0.2
PA2475	cytochrome P450	444	0	ATG	GGAGC	6.0	-0.3
PA2477	thiol:disulfide interchange protein	278	4	ATG	GGAGC	8.8	0.3
PA2478	thiol:disulfide interchange protein DsbD	587	8	ATG	-	6.7	0.4
PA2479	two-component response regulator	226	0	ATG	-	5.7	-0.2
PA2480	two-component sensor	440	2	ATG	GGAGA	6.3	0.0
PA2483	hypothetical protein	333	0	ATG	GGAGC	5.8	0.0
PA2502	hypothetical protein	499	0	ATG	-	6.1	0.1
PA2503	hypothetical protein	417	0	ATG	AGAGA	4.9	-0.2
PA2523	two-component response regulator CzcR	224	0	ATG	-	7.1	-0.2
PA2525	OpmB	498	0	ATG	GGAGA	5.3	-0.2
PA2526	resistance-nodulation-cell division (RND) efflux MuxC	1036	10	ATG	-	5.9	0.3
PA2527	resistance-nodulation-cell division (RND) efflux MuxB	1043	10	ATG	GGTGG	5.3	0.4
PA2528	resistance-nodulation-cell division (RND) efflux MuxA	426	1	ATG	-	8.9	-0.2
PA2531	probable aminotransferase	374	0	ATG	GGAGG	9.3	-0.2
PA2532	2-Cys peroxiredoxin	165	0	ATG	-	5.2	0.2
PA2533	sodium:alanine symporter	449	10	ATG	-	8.3	0.8
PA2535	oxidoreductase	331	0	ATG	CGAGG	6.4	-0.3
PA2536	phosphatidate cytidylyltransferase	311	8	ATG	GGAGG	9.1	0.8
PA2537	acyltransferase	209	0	ATG	AGAGT	6.9	0.0
PA2539	hypothetical protein	437	8	GTG	-	8.8	0.4
PA2540	hypothetical protein	586	0	ATG	-	8.4	-0.2

protein ID	(predicted) function	length [aa]	TMH	start	RBS	pI	GRAVY
PA2541	CDP-alcohol phosphatidyltransferase	211	3	ATG	-	9.3	0.7
PA2542	hypothetical protein	1221	1	GTG	-	5.5	-0.2
PA2543	hypothetical protein	579	0	ATG	-	6.3	-0.4
PA2544	hypothetical protein	237	0	ATG	TGTGG	8.6	-0.4
PA2551	transcriptional regulator	310	0	ATG	GGAGC	9.5	-0.3
PA2552	acyl-CoA dehydrogenase	375	0	ATG	AGAGG	5.5	-0.1
PA2553	acyl-CoA thiolase	396	0	ATG	GGAGG	5.7	0.1
PA2554	short-chain dehydrogenase	255	0	GTG	GGAGA	6.2	0.2
PA2555	AMP-binding protein	555	0	ATG	CGAGG	5.8	-0.1
PA2559	hypothetical protein	180	0	ATG	CGAGT	5.9	0.0
PA2561	CtpH	568	2	ATG	CGAGC	5.4	-0.2
PA2563	sulfate transporter	495	11	ATG	-	7.1	0.8
PA2564	trans-aconitate 2-methyltransferase	275	0	ATG	GGAGG	6.3	-0.2
PA2567	hypothetical protein	587	0	ATG	GGAGT	5.0	-0.1
PA2568	hypothetical protein	135	3	ATG	GGAGG	7.8	0.7
PA2571	two-component sensor	470	0	ATG	CGAGG	5.4	-0.2
PA2572	two-component response regulator	447	0	ATG	GGTGG	5.4	-0.3
PA2573	probable chemotaxis transducer	535	1	ATG	GGAGC	5.2	-0.1
PA2574	alkane-1 monooxygenase	382	7	ATG	GGAGC	6.8	0.2
PA2575	hypothetical protein	200	0	ATG	GGAGC	6.0	-0.2
PA2577	transcriptional regulator	145	0	ATG	CGAGG	7.7	-0.3
PA2579	tryptophan 2,3-dioxygenase	288	0	ATG	GGAGA	6.1	-0.3
PA2581	hypothetical protein	346	0	ATG	-	8.8	-0.2
PA2582	hypothetical protein	177	0	ATG	-	9.8	-0.7
PA2583	sensor/response regulator hybrid protein	992	1	ATG	-	5.6	-0.1
PA2584	CDP-diacylglycerol--glycerol-3-phosphate	186	3	ATG	-	8.0	0.9
PA2585	excinuclease ABC subunit C	608	0	ATG	-	8.6	-0.3
PA2586	response regulator GacA	214	0	GTG	CGAGG	5.8	0.0
PA2587	2-heptyl-3-hydroxy-4(1H)-quinolone synthase	382	0	ATG	GGAGC	6.7	0.0
PA2592	probable periplasmic spermidine/putrescine-binding protein	367	0	ATG	-	6.3	-0.2
PA2600	hypothetical protein	355	0	ATG	TGAGC	6.2	-0.2
PA2601	transcriptional regulator	298	0	ATG	GGTGC	5.6	0.1
PA2604	conserved hypothetical protein	222	7	ATG	GGAGT	7.9	0.9
PA2611	siroheme synthase	465	0	ATG	CGAGG	5.9	0.1
PA2612	seryl-tRNA synthetase	426	0	ATG	CGAGA	5.4	-0.4
PA2613	recombination factor protein RarA	441	0	GTG	GGAGT	6.0	-0.4
PA2614	outer-membrane lipoprotein carrier protein	208	0	ATG	AGAGG	5.8	-0.2
PA2615	DNA translocase FtsK	811	5	GTG	-	6.4	-0.1
PA2617	leucyl/phenylalanyl-tRNA--protein transferase	226	0	ATG	-	7.1	-0.3
PA2618	arginyl-tRNA--protein transferase	235	0	ATG	GGAGT	8.6	-0.5
PA2619	translation initiation factor IF-1	72	0	ATG	CGAGG	9.2	-0.5
PA2620	ATP-binding protease component ClpA	758	0	ATG	GGAGC	5.7	-0.3
PA2623	isocitrate dehydrogenase	418	0	ATG	GGAGT	5.1	-0.1
PA2624	isocitrate dehydrogenase	741	0	ATG	AGAGA	5.8	-0.3
PA2626	tRNA-specific 2-thiouridylase MnmA	375	0	ATG	-	5.7	-0.4
PA2627	high frequency lysogenization protein HflD	206	0	GTG	GGAGG	10.4	-0.2

protein ID	(predicted) function	length [aa]	TMH	start	RBS	pI	GRAVY
PA2629	adenylosuccinate lyase	456	0	ATG	CGAGA	5.6	-0.1
PA2630	hypothetical protein	389	0	ATG	-	4.4	-0.3
PA2634	isocitrate lyase	531	0	ATG	-	5.7	-0.3
PA2637	NADH-quinone oxidoreductase subunit A	137	3	ATG	GGAGT	10.0	0.6
PA2638	NADH-quinone oxidoreductase subunit B	225	0	ATG	TGAGG	5.3	-0.2
PA2639	NADH:-quinone oxidoreductase subunit C/D	593	0	ATG	CGAGA	6.2	-0.4
PA2641	NADH dehydrogenase I subunit F	448	0	ATG	GGAGG	6.6	-0.2
PA2642	NADH-quinone oxidoreductase subunit G	905	0	ATG	-	5.7	-0.3
PA2643	NADH-quinone oxidoreductase subunit H	331	8	ATG	GGAGG	6.4	0.9
PA2644	NADH-quinone oxidoreductase subunit I	182	0	GTG	GGAGA	6.4	-0.2
PA2645	NADH-quinone oxidoreductase subunit J	166	5	GTG	GGAGA	6.3	1.2
PA2646	NADH-quinone oxidoreductase subunit K	102	3	ATG	-	6.0	1.0
PA2647	NADH-quinone oxidoreductase subunit L	615	16	ATG	CGAGA	8.2	0.8
PA2648	NADH-quinone oxidoreductase subunit M	509	12	ATG	GGAGA	7.2	1.0
PA2649	NADH-quinone oxidoreductase subunit N	486	14	ATG	-	7.8	1.1
PA2651	hypothetical protein	352	7	ATG	-	9.5	0.9
PA2652	methyl-accepting chemotaxis protein	561	2	ATG	GGAGT	5.1	-0.1
PA2653	transporter	441	12	ATG	GGAGT	7.1	1.0
PA2654	probable chemotaxis transducer	714	1	ATG	-	4.9	-0.1
PA2656	two-component sensor CarS	445	2	ATG	GGTGG	6.4	-0.3
PA2660	hypothetical protein	360	0	ATG	GGAGA	9.6	-0.3
PA2662	hypothetical protein	397	12	GTG	GGAGG	11.6	0.8
PA2663	psl and pyoverdine operon regulator PpyR	85	2	ATG	GGAGA	10.1	0.9
PA2664	flavohemoprotein	393	0	ATG	GGAGT	5.2	-0.2
PA2679	hypothetical protein	250	0	ATG	GGAGA	5.3	-0.2
PA2683	serine/threonine dehydratase	320	0	ATG	CGAGG	6.0	0.0
PA2691	hypothetical protein	401	0	ATG	GGAGC	5.1	0.1
PA2692	transcriptional regulator	174	0	ATG	GGAGT	6.2	-0.2
PA2695	hypothetical protein	367	0	ATG	-	9.7	-0.2
PA2701	major facilitator superfamily transporter	529	12	ATG	-	9.8	0.7
PA2705	hypothetical protein	393	0	ATG	CGAGG	6.6	-0.5
PA2707	hypothetical protein	281	0	ATG	CGAGG	5.9	-0.3
PA2708	hypothetical protein	361	1	ATG	GGAGG	5.8	-0.2
PA2709	cysteine synthase A	324	0	ATG	-	6.2	0.0
PA2710	hypothetical protein	204	5	ATG	-	9.9	0.9
PA2725	chaperone	627	0	ATG	CGAGG	5.9	-0.1
PA2729	hypothetical protein	449	0	ATG	GGAGG	5.8	-0.6
PA2732	hypothetical protein	1146	0	ATG	GGAGA	5.9	-0.4
PA2734	hypothetical protein	431	0	GTG	-	5.9	-0.3
PA2735	restriction-modification system protein	792	0	ATG	AGAGT	5.5	-0.5
PA2738	integration host factor, alpha subunit	100	0	ATG	-	9.6	-0.8
PA2739	phenylalanine--tRNA ligase subunit beta	792	0	ATG	GGAGA	5.3	-0.1
PA2740	phenylalanine--tRNA ligase subunit alpha	338	0	ATG	GGAGT	5.6	-0.2
PA2741	50S ribosomal protein L20	118	0	ATG	AGAGG	11.7	-0.4
PA2744	threonine--tRNA ligase	640	0	ATG	GGAGG	6.0	-0.4
PA2745	hydrolase	287	0	ATG	-	5.4	-0.2
PA2756	hypothetical protein	144	0	GTG	CGAGG	6.3	-0.1

protein ID	(predicted) function	length [aa]	TMH	start	RBS	pI	GRAVY
PA2760	OprQ	425	0	ATG	-	5.5	-0.5
PA2770	isomerase	259	0	ATG	GGAGT	5.0	-0.1
PA2771	diguanylate cyclase with a self-blocked I-site, Dcsbis	341	0	ATG	-	5.7	-0.3
PA2774	Tse4	195	4	ATG	-	9.6	0.5
PA2775	Tsi4	145	2	ATG	-	9.0	0.3
PA2776	FAD-dependent oxidoreductase	427	0	ATG	AGAGG	6.8	-0.2
PA2788	probable chemotaxis transducer	531	2	ATG	AGTGG	5.5	0.0
PA2789	hypothetical protein	359	2	GTG	-	6.4	-0.3
PA2790	hypothetical protein	161	0	ATG	TGTGG	9.5	-0.5
PA2793	hypothetical protein	344	0	ATG	-	8.4	-0.4
PA2796	transaldolase B	307	0	ATG	-	5.2	-0.2
PA2797	hypothetical protein	160	0	ATG	GGTGT	4.9	0.1
PA2798	two-component response regulator	394	0	ATG	-	4.9	0.0
PA2800	VacJ	234	0	ATG	GGAGA	5.4	-0.2
PA2805	hypothetical protein	87	0	ATG	CGAGG	4.5	-0.2
PA2809	two-component response regulator CopR	226	0	ATG	CGAGG	4.9	-0.2
PA2810	two-component sensor CopS	443	2	ATG	AGAGC	6.9	-0.2
PA2811	ABC transporter permease	259	6	ATG	CGAGG	9.7	0.9
PA2813	glutathione S-transferase	206	0	ATG	AGAGG	5.1	-0.3
PA2815	acyl-CoA dehydrogenase	815	3	ATG	GGAGG	5.7	0.0
PA2818	aminoglycoside response regulator	525	2	ATG	GGAGC	6.6	0.0
PA2820	hypothetical protein	257	1	GTG	GGAGT	8.6	-0.3
PA2823	hypothetical protein	296	0	GTG	CGAGG	5.6	-0.4
PA2824	sensor/response regulator hybrid protein SagS	786	2	ATG	-	5.6	0.1
PA2828	aminotransferase	403	0	ATG	-	5.8	-0.1
PA2830	protease HtpX	291	4	ATG	TGAGG	7.0	0.4
PA2831	hypothetical protein	375	0	ATG	TGAGG	5.3	-0.6
PA2834	transcriptional regulator	319	0	ATG	-	8.4	-0.2
PA2840	ATP-dependent RNA helicase	567	0	ATG	TGAGC	9.0	-0.2
PA2843	aldolase	448	0	ATG	AGAGT	5.8	-0.3
PA2849	transcriptional regulator OhrR	151	0	ATG	-	5.6	-0.1
PA2851	elongation factor P	188	0	ATG	-	4.8	-0.3
PA2853	outer membrane lipoprotein OprI	83	0	ATG	-	7.9	-0.5
PA2854	conserved hypothetical protein	323	0	ATG	-	5.5	-0.1
PA2857	ABC transporter ATP-binding protein	227	0	ATG	-	5.6	-0.2
PA2858	hypothetical protein	830	10	GTG	-	10.0	0.4
PA2864	hypothetical protein	144	4	ATG	TGAGG	8.1	0.9
PA2867	probable chemotaxis transducer	490	2	ATG	-	4.9	0.1
PA2870	diguanylate cyclase	525	2	ATG	TGAGT	6.4	-0.1
PA2873	protein-glutamine gamma-glutamyltransferase TgpA	668	6	ATG	GGAGC	9.9	0.0
PA2874	hypothetical protein	317	2	ATG	-	10.5	-0.2
PA2875	hypothetical protein	305	0	ATG	CGAGG	5.6	0.2
PA2877	transcriptional regulator	297	0	ATG	AGAGA	6.8	-0.3
PA2883	hypothetical protein	55	1	ATG	TGAGG	6.6	-0.1
PA2895	SbrR	254	0	ATG	GGAGG	9.7	-0.2
PA2897	transcriptional regulator	479	0	ATG	CGAGG	9.3	-0.2

protein ID	(predicted) function	length [aa]	TMH	start	RBS	pI	GRAVY
PA2899	transcriptional regulator	212	0	ATG	AGAGG	7.0	0.0
PA2900	probable outer membrane protein precursor	269	0	ATG	GGAGA	6.2	-0.4
PA2901	hypothetical protein	119	0	GTG	-	5.6	-0.4
PA2902	hypothetical protein	282	0	ATG	GGAGC	5.0	-0.1
PA2903	precorrin-3 methylase CobJ	559	0	GTG	GGAGG	5.8	0.1
PA2904	precorrin-2 C(20)-methyltransferase	250	0	ATG	GGAGC	6.0	0.1
PA2905	precorrin-8X methylmutase	208	0	ATG	-	5.7	0.3
PA2906	oxidoreductase	486	0	GTG	-	8.3	-0.1
PA2911	TonB-dependent receptor	718	0	ATG	TGAGA	6.2	-0.6
PA2912	ABC transporter ATP-binding protein	257	0	ATG	CGAGT	7.1	-0.1
PA2920	probable chemotaxis transducer	545	2	ATG	CGAGG	5.1	-0.1
PA2921	transcriptional regulator	329	0	ATG	GGAGG	8.5	0.1
PA2939	aminopeptidase	536	0	ATG	GGAGT	5.0	-0.3
PA2942	magnesium chelatase	338	0	ATG	-	5.6	-0.2
PA2945	cobalamin biosynthesis protein CobW	375	0	GTG	GGTGA	5.1	-0.2
PA2946	hypothetical protein	233	6	ATG	CGAGG	5.6	0.6
PA2949	lipase	315	1	ATG	-	6.1	0.0
PA2950	proton motive force protein, PMF	398	0	ATG	CGAGG	5.0	-0.2
PA2951	electron transfer flavoprotein subunit alpha	309	0	ATG	CGAGG	5.0	0.3
PA2952	electron transfer flavoprotein subunit beta	249	0	ATG	GGAGA	9.0	0.1
PA2953	electron transfer flavoprotein-ubiquinone	551	0	GTG	GGAGA	5.5	-0.3
PA2954	hypothetical protein	189	0	ATG	CGAGG	5.1	-0.3
PA2955	hypothetical protein	210	0	ATG	GGAGA	5.3	-0.3
PA2956	hypothetical protein	298	0	ATG	GGAGT	5.8	-0.3
PA2962	thymidylate kinase	210	0	GTG	GGAGT	5.1	-0.2
PA2963	hypothetical protein	349	1	ATG	-	8.5	-0.4
PA2965	3-oxoacyl-ACP synthase	414	0	GTG	AGAGG	5.6	0.0
PA2967	3-oxoacyl-[acyl-carrier-protein] reductase FabG	247	0	ATG	GGAGA	6.2	0.2
PA2973	peptidase	326	1	ATG	GGAGT	7.8	-0.3
PA2975	ribosomal large subunit pseudouridine synthase	318	0	ATG	-	9.9	-0.4
PA2976	ribonuclease E	1057	0	ATG	-	4.9	-0.9
PA2979	3-deoxy-manno-octulosonate cytidylyltransferase	254	0	ATG	CGAGC	5.4	0.0
PA2981	tetraacyldisaccharide 4'-kinase	332	0	ATG	-	6.8	-0.1
PA2982	hypothetical protein	146	1	GTG	CGAGG	5.6	0.1
PA2983	translocation protein TolQ	211	3	GTG	-	6.4	0.4
PA2986	lipoprotein localization protein LolC	433	4	GTG	-	9.7	0.4
PA2987	lipoprotein-releasing system ABC transporter	227	0	ATG	GGAGG	6.2	-0.1
PA2988	lipoprotein localization protein LolE	416	4	ATG	-	9.1	0.5
PA2989	hypothetical protein	199	0	ATG	CGTGG	5.8	-0.4
PA2991	soluble pyridine nucleotide transhydrogenase	464	0	ATG	TGAGG	6.2	-0.2
PA2993	hypothetical protein	342	0	GTG	-	5.4	-0.3
PA2994	Na(+)-translocating NADH-quinone reductase	407	1	GTG	GGAGA	5.0	-0.2
PA2995	Na(+)-translocating NADH-quinone reductase	202	6	ATG	GGAGG	4.7	1.0
PA2996	Na(+)-translocating NADH-quinone reductase	224	5	GTG	GGAGG	9.5	0.7
PA2997	Na(+)-translocating NADH-quinone reductase	261	1	ATG	GGAGG	5.7	0.0
PA2998	Na(+)-translocating NADH-quinone reductase	403	8	ATG	GGAGG	6.8	0.6

protein ID	(predicted) function	length [aa]	TMH	start	RBS	pI	GRAVY
PA2999	Na(+)-translocating NADH-quinone reductase	445	0	ATG	-	7.1	0.0
PA3000	aromatic amino acid transporter AroP 1	469	12	ATG	-	9.1	0.8
PA3001	glyceraldehyde-3-phosphate dehydrogenase	461	0	ATG	-	7.7	-0.2
PA3002	transcription-repair coupling factor	1148	0	GTG	GGAGC	5.6	-0.2
PA3005	beta-hexosaminidase	332	0	ATG	-	5.8	-0.1
PA3006	transcriptional regulator PsrA	233	0	ATG	GGAGA	9.4	0.0
PA3007	LexA repressor	204	0	ATG	AGAGC	6.1	-0.2
PA3011	DNA topoisomerase I	868	0	ATG	-	8.7	-0.6
PA3013	3-ketoacyl-CoA thiolase	391	0	ATG	AGAGC	6.3	-0.1
PA3014	fatty acid oxidation complex subunit alpha	715	0	ATG	GGAGA	5.7	0.0
PA3019	ABC transporter ATP-binding protein	640	0	ATG	GGAGG	5.2	-0.3
PA3020	lytic transglycosylase	642	0	ATG	-	9.5	-0.4
PA3021	hypothetical protein	128	0	ATG	-	7.6	-0.5
PA3022	hypothetical protein	268	0	ATG	-	5.9	-0.2
PA3026	hypothetical protein	531	0	ATG	CGAGG	8.5	-0.2
PA3029	molybdopterin biosynthesis protein B2	179	0	ATG	-	5.5	0.0
PA3031	hypothetical protein	73	1	ATG	GGAGA	4.9	-0.2
PA3034	transcriptional regulator	185	0	ATG	GGAGG	8.0	-0.3
PA3038	porin OpdQ	421	0	ATG	CGAGG	6.6	-0.5
PA3041	hypothetical protein	126	2	ATG	TGAGC	5.3	0.5
PA3042	hypothetical protein	107	1	ATG	-	12.4	-0.2
PA3047	D-alanyl-D-alanine carboxypeptidase	476	0	ATG	-	9.7	-0.1
PA3048	ribosomal RNA large subunit methyltransferase	725	0	ATG	-	8.0	-0.4
PA3050	dihydroorotate dehydrogenase	342	0	ATG	-	8.6	0.0
PA3052	hypothetical protein	326	0	ATG	-	9.3	-0.3
PA3066	hypothetical protein	190	0	ATG	AGAGG	6.5	0.1
PA3068	NAD-specific glutamate dehydrogenase	1620	0	ATG	GGAGT	5.8	-0.2
PA3070	hypothetical protein	326	0	ATG	-	5.1	-0.1
PA3073	hypothetical protein	340	1	ATG	-	8.0	0.0
PA3074	hypothetical protein	586	2	ATG	GGAGG	5.4	-0.5
PA3075	hypothetical protein	543	1	ATG	-	5.2	-0.3
PA3077	two-component response regulator CprR	223	0	ATG	-	5.9	-0.1
PA3078	CprS	431	2	ATG	GGAGC	4.8	-0.2
PA3079	hypothetical protein	793	12	ATG	-	6.7	0.4
PA3081	hypothetical protein	455	0	ATG	GGAGA	8.9	-0.5
PA3082	glycine betaine transmethylase	654	0	ATG	GGAGT	4.7	-0.4
PA3083	aminopeptidase	885	0	ATG	TGAGC	5.1	-0.3
PA3084	hypothetical protein	266	0	ATG	TGAGC	7.5	-0.3
PA3085	hypothetical protein	87	0	ATG	GGAGC	4.9	-0.6
PA3086	hypothetical protein	286	6	GTG	GGAGG	9.9	0.4
PA3091	hypothetical protein	479	0	ATG	-	5.6	-0.6
PA3092	2,4-dienoyl-CoA reductase FadH1	679	0	ATG	GGAGA	6.7	-0.1
PA3093	hypothetical protein	372	0	ATG	GGAGA	6.0	-0.2
PA3095	type II secretion system protein M	174	1	ATG	GGAGG	9.4	-0.1
PA3096	type II secretion system protein L	382	0	ATG	CGAGC	5.1	0.0
PA3098	type II secretion system protein J	237	1	ATG	GGAGC	5.3	-0.7
PA3100	type II secretion system protein H	172	1	ATG	-	5.6	-0.2

protein ID	(predicted) function	length [aa]	TMH	start	RBS	pI	GRAVY
PA3101	type II secretion system protein G	148	1	GTG	CGTGG	8.1	-0.4
PA3102	type II secretion system protein F	405	3	ATG	-	10.2	0.3
PA3103	type II secretion system protein E	502	0	ATG	-	5.9	-0.2
PA3104	type II secretion system protein N	235	1	ATG	-	5.5	-0.4
PA3105	type II secretion system protein D	658	0	ATG	-	5.8	-0.1
PA3108	amidophosphoribosyltransferase	501	0	ATG	-	6.3	-0.2
PA3110	hypothetical protein	219	1	ATG	GGAGT	5.7	-0.4
PA3112	acetyl-CoA carboxylase carboxyltransferase	290	0	ATG	GGAGA	6.6	-0.1
PA3115	motility protein FimV	919	1	ATG	-	4.2	-0.4
PA3117	aspartate-semialdehyde dehydrogenase	370	0	ATG	GGTGT	5.5	-0.1
PA3118	3-isopropylmalate dehydrogenase	360	0	ATG	AGAGG	5.0	-0.1
PA3121	3-isopropylmalate dehydratase large subunit	474	0	ATG	TGAGG	5.9	-0.2
PA3122	transcriptional regulator	297	0	ATG	GGAGG	6.0	0.0
PA3126	heat-shock protein IbpA	149	0	ATG	GGAGA	5.8	-0.4
PA3128	short-chain dehydrogenase	248	0	ATG	GGAGC	6.4	-0.1
PA3133	transcriptional regulator	180	0	ATG	GGAGA	6.0	0.0
PA3134	glutamate--tRNA ligase	494	0	ATG	AGAGA	6.2	-0.4
PA3135	transcriptional regulator	306	0	ATG	-	7.7	0.1
PA3138	excinuclease ABC subunit B	670	0	ATG	CGAGG	5.3	-0.4
PA3139	aspartate aminotransferase	398	0	ATG	CGAGC	6.2	-0.1
PA3141	nucleotide sugar epimerase/dehydratase WbpM	665	5	ATG	-	9.3	0.1
PA3145	glycosyltransferase WbpL	339	11	ATG	-	9.0	1.0
PA3146	NAD-dependent epimerase/dehydratase	316	0	ATG	-	8.9	0.2
PA3147	glycosyl transferase WbpJ	413	2	ATG	-	6.5	0.1
PA3148	UDP-N-acetylglucosamine 2-epimerase WbpI	354	0	ATG	TGAGT	5.6	0.1
PA3149	glycosyltransferase WbpH	373	0	ATG	-	8.9	-0.2
PA3150	LPS biosynthesis protein WbpG	377	0	GTG	GGAGG	8.3	-0.4
PA3151	imidazole glycerol phosphate synthase subunit	251	0	ATG	GGAGC	5.6	0.1
PA3153	O-antigen translocase	411	12	ATG	-	8.9	1.0
PA3154	B-band O-antigen polymerase	438	12	ATG	-	9.6	0.8
PA3155	UDP-2-acetamido-2-deoxy-3-oxo-D-glucuronate aminotransferase	359	0	ATG	GGTGG	5.8	0.0
PA3156	UDP-2-acetamido-3-amino-2,3-dideoxy-d-glucuronic acid N-acetyltransferase, WbpD	191	0	ATG	CGAGT	7.6	0.1
PA3158	UDP-2-acetamido-2-deoxy-d-glucuronic acid 3-dehydrogenase, WbpB	316	0	ATG	-	6.1	-0.3
PA3159	UDP-N-acetyl-d-glucosamine 6-dehydrogenase	436	1	ATG	TGAGG	5.4	-0.1
PA3160	O-antigen chain length regulator	348	2	ATG	AGAGT	6.1	-0.1
PA3162	30S ribosomal protein S1	559	0	ATG	-	4.8	-0.3
PA3163	cytidylate kinase	229	0	ATG	GGAGA	5.0	-0.1
PA3165	histidinol-phosphate aminotransferase	369	0	ATG	CGAGG	5.1	0.1
PA3167	3-phosphoserine/phosphohydroxythreonine aminotransferase	361	0	GTG	CGAGA	5.0	-0.2
PA3168	DNA gyrase subunit A	923	0	ATG	-	4.9	-0.3
PA3171	3-demethylubiquinone-9 3-methyltransferase	232	0	ATG	-	5.9	-0.2
PA3172	probable hydrolase	226	0	GTG	GGAGG	5.2	-0.1
PA3173	short-chain dehydrogenase	246	0	ATG	-	5.1	0.0
PA3176	glutamate/sodium ion symporter GltS	404	11	ATG	AGAGC	7.6	0.9
PA3179	ribosomal large subunit pseudouridine synthase	386	0	ATG	GGAGG	10.3	-1.0

protein ID	(predicted) function	length [aa]	TMH	start	RBS	pI	GRAVY
PA3181	2-dehydro-3-deoxy-phosphogluconate aldolase	220	0	ATG	GGAGC	7.0	0.0
PA3182	6-phosphogluconolactonase	238	0	ATG	GGAGG	6.1	0.0
PA3184	HTH-type transcriptional regulator	285	0	ATG	CGAGG	6.3	0.1
PA3186	glucose-sensitive porin	454	1	ATG	CGAGG	5.5	-0.5
PA3187	ABC transporter ATP-binding protein	386	0	ATG	GGAGA	7.0	-0.1
PA3188	sugar ABC transporter permease	281	7	ATG	CGAGG	9.2	0.9
PA3189	sugar ABC transporter permease	310	6	ATG	CGAGA	9.8	0.6
PA3191	two-component sensor GtrS	473	2	GTG	-	6.2	-0.1
PA3195	glyceraldehyde 3-phosphate dehydrogenase	334	0	ATG	AGAGA	6.2	0.0
PA3196	hypothetical protein	176	0	ATG	-	4.2	0.1
PA3199	hypothetical protein	209	0	ATG	-	6.2	-0.2
PA3201	intracellular septation protein A	195	5	ATG	-	8.6	0.6
PA3203	hypothetical protein	120	1	ATG	GGAGT	10.4	-0.5
PA3206	two-component sensor	445	2	ATG	-	9.5	-0.3
PA3208	hypothetical protein	186	0	ATG	GGAGT	6.1	0.0
PA3210	potassium uptake protein TrkH	484	12	ATG	AGAGC	9.5	0.7
PA3211	ABC transporter permease	381	7	ATG	GGTGT	5.4	0.7
PA3212	ABC transporter ATP-binding protein	264	0	GTG	GGAGA	6.0	0.1
PA3213	hypothetical protein	312	1	ATG	GGAGA	6.5	-0.1
PA3214	hypothetical protein	214	0	ATG	GGAGT	10.0	-0.2
PA3217	protein CyaB	463	5	ATG	-	9.2	0.1
PA3225	transcriptional regulator	309	0	ATG	GGAGG	6.9	-0.2
PA3226	hydrolase	275	0	ATG	CGAGT	7.6	-0.2
PA3228	ABC transporter ATP-binding protein/permease	610	5	ATG	AGAGA	7.0	0.2
PA3233	hypothetical protein	599	0	ATG	CGAGA	5.9	-0.1
PA3234	acetate permease	551	14	ATG	GGAGG	9.3	0.8
PA3235	hypothetical protein	103	2	ATG	TGAGG	8.1	0.3
PA3241	hypothetical protein	389	0	GTG	-	10.1	0.0
PA3242	temperature-regulated acyltransferase HtrB1	312	1	ATG	-	9.8	-0.4
PA3243	septum formation inhibitor MinC	263	0	ATG	-	6.1	-0.2
PA3244	cell division inhibitor MinD	271	0	TTG	GGTGA	5.6	-0.1
PA3255	hypothetical protein	192	0	ATG	GGAGC	4.6	-0.1
PA3256	oxidoreductase	320	0	GTG	GGAGG	5.4	0.3
PA3257	tail-specific protease	698	0	ATG	-	6.2	-0.5
PA3259	hypothetical protein	159	0	ATG	CGAGT	10.4	-0.4
PA3262	FkbP-type peptidyl-prolyl cis-trans isomerase	253	0	ATG	-	5.1	-0.4
PA3263	recombination associated protein RdgC	306	0	ATG	GGAGA	5.0	-0.2
PA3264	transporter	311	8	ATG	-	10.7	1.1
PA3266	major cold shock protein CspA	69	0	ATG	GGAGT	8.2	-0.3
PA3267	hypothetical protein	624	11	ATG	-	8.8	0.6
PA3268	TonB-dependent receptor	721	0	ATG	GGAGC	5.1	-0.5
PA3270	hypothetical protein	195	0	ATG	GGAGC	9.5	-0.3
PA3271	two-component sensor	1159	12	ATG	GGAGT	8.3	0.2
PA3272	ATP-dependent DNA helicase	1448	0	ATG	-	6.2	-0.2
PA3289	hypothetical protein	137	0	ATG	GGAGA	6.1	0.0
PA3295	HIT family protein	145	0	ATG	-	5.8	-0.1

protein ID	(predicted) function	length [aa]	TMH	start	RBS	pI	GRAVY
PA3297	ATP-dependent helicase	1326	0	ATG	-	8.4	-0.4
PA3299	long-chain-fatty-acid--CoA ligase	562	0	ATG	GGAGT	7.1	0.0
PA3300	long-chain-fatty-acid--CoA ligase	562	0	ATG	AGAGG	6.7	0.0
PA3304	hypothetical protein	285	1	ATG	GGAGA	8.9	-0.1
PA3306	hypothetical protein	200	0	ATG	-	7.2	-0.6
PA3308	RNA polymerase-associated protein RapA	950	0	GTG	-	5.1	-0.3
PA3309	hypothetical protein	151	0	ATG	GGAGG	5.5	-0.1
PA3310	hypothetical protein	551	5	ATG	GGAGT	6.9	0.1
PA3311	signaling protein NbdA	783	7	ATG	GGAGC	7.6	0.1
PA3314	phosphonates ABC transporter ATP-binding	267	0	GTG	-	9.8	0.1
PA3317	hypothetical protein	242	0	ATG	GGAGA	6.6	-0.4
PA3321	transcriptional regulator	304	0	ATG	-	9.5	-0.1
PA3326	ATP-dependent Clp protease proteolytic subunit	201	0	ATG	GGAGG	5.5	-0.3
PA3327	non-ribosomal peptide synthetase	2352	0	ATG	AGAGG	5.5	-0.1
PA3328	FAD-dependent monooxygenase	388	0	ATG	-	8.4	-0.2
PA3329	hypothetical protein	442	0	ATG	GGAGT	5.8	-0.3
PA3330	short-chain dehydrogenase	304	0	ATG	CGAGG	8.8	0.1
PA3331	cytochrome P450	418	0	GTG	GGAGG	5.5	-0.2
PA3332	hypothetical protein	141	0	ATG	AGAGG	5.4	-0.2
PA3333	3-oxoacyl-ACP synthase III	330	0	ATG	GGAGC	5.1	0.3
PA3335	hypothetical protein	250	0	GTG	GGAGG	5.3	-0.1
PA3336	major facilitator superfamily transporter	388	12	ATG	GGAGC	9.6	1.2
PA3337	ADP-L-glycero-D-mannoheptose-6-epimerase	332	0	GTG	-	6.1	-0.4
PA3339	patatin-like protein, PlpD	728	0	ATG	-	5.3	-0.3
PA3340	hypothetical protein	682	1	ATG	GGAGA	4.8	-0.2
PA3341	transcriptional regulator	144	0	ATG	-	8.0	-0.2
PA3343	diguanylate cyclase HsbD	389	5	GTG	AGAGA	8.1	0.2
PA3344	ATP-dependent DNA helicase RecQ	712	0	ATG	GGAGT	5.7	-0.3
PA3346	two-component response regulator HsbR	571	0	ATG	-	5.5	0.0
PA3348	chemotaxis protein methyltransferase	274	0	GTG	AGAGG	9.3	-0.1
PA3349	chemotaxis protein	310	0	ATG	TGAGG	5.9	-0.1
PA3350	flagellar basal body P-ring biosynthesis protein	232	0	TTG	-	8.5	-0.1
PA3353	hypothetical protein	263	0	GTG	-	6.4	-0.4
PA3354	hypothetical protein	203	0	ATG	GGAGA	5.5	0.0
PA3355	hypothetical protein	434	12	ATG	GGAGG	8.1	0.7
PA3356	Glutamylpolyamine synthetase	413	0	ATG	GGTGC	5.5	-0.1
PA3357	D-serine dehydratase	448	0	TTG	GGAGT	5.7	0.0
PA3363	aliphatic amidase regulator	196	0	ATG	GGAGC	6.1	-0.1
PA3364	aliphatic amidase expression-regulating protein	385	0	ATG	GGAGA	5.6	-0.3
PA3365	chaperone	371	0	ATG	GGAGT	8.6	-0.4
PA3366	aliphatic amidase	346	0	ATG	AGAGG	5.3	-0.3
PA3391	regulatory protein NosR	715	6	ATG	-	6.6	0.1
PA3392	nitrous-oxide reductase	636	1	ATG	TGAGG	6.1	-0.4
PA3393	copper-binding periplasmic protein NosD	428	0	TTG	GGTGG	6.4	-0.3
PA3394	copper ABC transporter ATP-binding protein NosF	304	0	GTG	GGAGC	9.0	-0.1
PA3395	membrane protein NosY	275	6	ATG	GGAGC	7.9	1.1

protein ID	(predicted) function	length [aa]	TMH	start	RBS	pI	GRAVY
PA3396	acessory protein NosL	178	0	ATG	CGAGG	5.4	-0.2
PA3397	ferredoxin-NADP reductase	258	0	ATG	GGAGT	5.7	-0.4
PA3402	hypothetical protein	323	1	ATG	-	6.0	-0.4
PA3409	transmembrane sensor HasS	328	0	GTG	CGAGA	10.2	-0.3
PA3415	branched-chain alpha-keto acid dehydrogenase	370	0	ATG	GGAGA	5.5	-0.1
PA3417	pyruvate dehydrogenase E1 component subunit	365	0	ATG	GGAGG	5.4	-0.3
PA3419	hypothetical protein	270	0	ATG	GGAGG	5.8	-0.3
PA3424	hypothetical protein	468	0	ATG	GGAGC	6.3	-0.3
PA3437	short-chain dehydrogenase	234	0	ATG	TGAGA	6.5	0.0
PA3440	conserved hypothetical protein	103	0	ATG	CGAGA	5.6	-0.6
PA3452	malate:quinone oxidoreductase	523	0	ATG	-	5.7	-0.2
PA3453	hypothetical protein	221	0	ATG	-	5.4	-0.3
PA3455	hypothetical protein	496	0	ATG	GGAGA	8.2	-0.6
PA3456	tRNA 5-methylaminomethyl-2-thiouridine biosynthesis bifunctional protein MnmC	654	0	ATG	-	6.8	-0.1
PA3459	glutamine amidotransferase	589	0	ATG	GGAGA	5.6	-0.3
PA3460	acetyltransferase	585	0	ATG	GGAGC	5.9	-0.4
PA3462	sensor/response regulator hybrid protein	919	6	ATG	GGAGT	6.4	0.1
PA3465	hypothetical protein	571	10	ATG	-	9.2	0.5
PA3466	ATP-dependent RNA helicase	446	0	ATG	-	9.8	-0.3
PA3468	hypothetical protein	442	4	ATG	-	8.4	0.2
PA3471	NAD-dependent malic enzyme	564	0	ATG	CGAGT	5.3	-0.2
PA3474	hypothetical protein	286	10	ATG	GGTGC	9.7	0.7
PA3476	acyl-homoserine-lactone synthase RhlI	201	0	ATG	-	5.4	0.0
PA3477	transcriptional regulator RhlR	241	0	ATG	-	6.7	-0.3
PA3478	rhamnosyltransferase subunit B	426	0	ATG	GGAGT	8.8	0.0
PA3479	rhamnosyltransferase subunit A	295	0	ATG	GGAGG	7.0	-0.2
PA3481	hypothetical protein	364	0	ATG	-	5.3	0.1
PA3482	methionine--tRNA ligase	677	0	ATG	-	5.4	-0.2
PA3483	hypothetical protein	266	1	ATG	GGAGG	6.3	-0.2
PA3484	Tse3	408	0	ATG	GGAGG	8.8	-0.2
PA3485	Tsi3	145	0	ATG	TGAGG	5.1	-0.4
PA3487	phospholipase D	1099	0	ATG	-	6.3	-0.3
PA3488	Tli5	344	0	ATG	GGAGT	6.5	-0.7
PA3491	electron transport complex subunit C	774	0	ATG	GGAGC	6.4	-0.2
PA3493	electron transport complex subunit G	214	1	ATG	-	9.0	0.0
PA3511	short-chain dehydrogenase	253	0	ATG	GGTGT	5.4	0.1
PA3525	argininosuccinate synthase	405	0	ATG	GGAGT	5.4	-0.3
PA3526	MotY	321	0	GTG	GGAGC	9.8	-0.3
PA3529	alkylhydroperoxide reductase C	200	0	ATG	GGAGA	5.4	-0.1
PA3533	GrxD	108	0	ATG	TGAGG	4.8	-0.1
PA3535	serine protease	995	0	ATG	GGAGA	5.3	-0.3
PA3537	ornithine carbamoyltransferase, anabolic	305	0	ATG	-	5.6	-0.2
PA3538	ABC transporter ATP-binding protein	360	0	ATG	TGAGC	6.0	0.0
PA3539	hypothetical protein	259	0	ATG	CGAGG	6.2	-0.4
PA3553	undecaprenyl-phosphate	339	2	ATG	GGAGA	8.3	0.2

protein ID	(predicted) function	length [aa]	TMH	start	RBS	pI	GRAVY
PA3554	bifunctional UDP-glucuronic acid decarboxylase/UDP-4-amino-4-deoxy-L-arabinose formyltransferase	662	0	ATG	CGAGC	6.2	-0.3
PA3560	PTS system fructose-specific transporter subunit	585	8	ATG	GGAGG	8.4	0.7
PA3561	1-phosphofructokinase	314	0	ATG	GGAGG	5.6	0.0
PA3562	PTS system fructose-specific transporter subunit	956	0	ATG	GGAGG	5.1	0.0
PA3563	FruR family transcriptional regulator	329	0	TTG	AGAGA	6.0	-0.1
PA3569	3-hydroxyisobutyrate dehydrogenase	298	0	ATG	GGAGA	5.9	0.2
PA3573	major facilitator superfamily transporter	392	12	ATG	CGAGC	8.8	0.9
PA3575	hypothetical protein	176	4	ATG	CGAGG	10.2	0.6
PA3579	glycerol kinase	494	0	ATG	-	5.6	-0.1
PA3582	glycerol kinase	505	0	ATG	-	5.7	-0.3
PA3583	glycerol-3-phosphate regulon repressor	251	0	ATG	CGAGA	5.4	-0.1
PA3584	glycerol-3-phosphate dehydrogenase	512	0	ATG	-	8.5	-0.3
PA3587	transcriptional regulator MetR	306	0	ATG	AGAGG	5.6	0.1
PA3594	probable transcriptional regulator	295	0	ATG	GGTGC	6.5	0.0
PA3602	hypothetical protein	536	2	ATG	GGAGA	7.6	-0.1
PA3603	diacylglycerol kinase	123	4	GTG	TGAGA	9.5	0.8
PA3604	response regulator ErdR	217	0	ATG	-	5.0	0.1
PA3607	polyamine transporter ATP-binding protein PotA	363	0	GTG	-	5.4	-0.1
PA3608	polyamine transport protein PotB	297	6	ATG	-	9.2	0.7
PA3609	polyamine ABC transporter permease PotC	256	7	ATG	GGAGG	9.0	1.0
PA3610	polyamine ABC transporter substrate-binding potD	354	0	ATG	-	5.6	-0.2
PA3613	hypothetical protein	801	0	ATG	GGAGG	6.0	-0.3
PA3614	hypothetical protein	467	0	ATG	GGAGG	6.5	-0.3
PA3615	hypothetical protein	356	0	ATG	GGAGT	5.7	-0.2
PA3617	recombinase A	346	0	ATG	CGAGG	5.4	-0.1
PA3620	DNA mismatch repair protein MutS	855	0	ATG	-	5.8	-0.2
PA3623	hypothetical protein	297	0	ATG	-	10.4	-0.1
PA3624	L-isoaspartate protein carboxylmethyltransferase type II	211	0	ATG	-	5.8	0.0
PA3625	survival protein SurE	249	0	ATG	-	5.3	0.1
PA3626	tRNA pseudouridine synthase D	355	0	ATG	-	6.3	-0.2
PA3629	alcohol dehydrogenase class III	370	0	ATG	GGAGT	5.5	0.1
PA3631	hypothetical protein	408	10	ATG	-	10.3	0.7
PA3634	cell division protein FtsB	94	1	TTG	GGAGT	6.2	-0.4
PA3635	enolase	429	0	ATG	GGAGT	5.1	-0.1
PA3637	CTP synthetase	542	1	ATG	-	5.4	-0.2
PA3638	tRNA(Ile)-lysidine synthase	442	0	ATG	TGAGG	8.9	-0.2
PA3639	acetyl-CoA carboxylase carboxyltransferase	316	0	ATG	-	5.3	-0.3
PA3640	DNA polymerase III subunit alpha	1173	0	ATG	-	5.3	-0.2
PA3641	amino acid permease	471	9	ATG	GGAGT	8.3	0.8
PA3642	ribonuclease HII	201	0	ATG	GGTGG	6.1	0.1
PA3643	lipid-A-disaccharide synthase	378	0	ATG	TGAGC	9.2	0.1
PA3644	UDP-N-acetylglucosamine acyltransferase	258	0	ATG	-	6.5	-0.1
PA3645	3-hydroxyacyl--[acyl-carrier-protein] dehydratase FabZ	146	0	ATG	-	7.0	-0.1
PA3646	UDP-3-O-[3-hydroxylauroyl] glucosamine N-acyltransferase	353	0	ATG	-	5.8	0.2

protein ID	(predicted) function	length [aa]	TMH	start	RBS	pI	GRAVY
PA3647	probable outer membrane protein precursor	168	1	GTG	GGAGT	9.4	-0.6
PA3648	outer membrane protein Opr86	797	0	ATG	-	5.1	-0.4
PA3649	zinc metalloprotease MucP	450	3	ATG	GGAGG	6.4	0.3
PA3650	1-deoxy-D-xylulose 5-phosphate reductoisomerase	396	0	ATG	GGTGC	5.6	0.2
PA3651	phosphatidate cytidylyltransferase	271	7	ATG	CGAGG	9.9	0.9
PA3653	ribosome recycling factor	185	0	ATG	GGAGG	5.9	-0.5
PA3654	uridylate kinase	245	0	ATG	GGAGA	5.5	0.1
PA3655	elongation factor Ts	289	0	ATG	AGAGG	5.2	0.0
PA3656	30S ribosomal protein S2	246	0	ATG	CGAGG	8.5	-0.3
PA3658	bifunctional uridylyltransferase/uridylyl-removing protein	900	0	ATG	-	5.4	-0.3
PA3659	succinyldiaminopimelate transaminase	402	0	ATG	TGAGA	5.5	-0.1
PA3660	sodium/hydrogen antiporter	581	11	ATG	-	9.2	0.4
PA3666	tetrahydrodipicolinate succinylase	344	0	ATG	CGAGG	5.7	0.2
PA3669	hypothetical protein	326	1	ATG	GGAGG	9.6	-0.2
PA3670	hypothetical protein	615	2	ATG	TGAGG	5.4	-0.2
PA3671	ABC transporter permease	244	6	ATG	GGAGG	5.9	0.9
PA3672	ABC transporter ATP-binding protein	307	0	ATG	-	6.2	-0.1
PA3673	glycerol-3-phosphate acyltransferase	834	0	ATG	-	9.4	-0.1
PA3674	hypothetical protein	132	0	ATG	GGAGG	6.8	-0.2
PA3676	resistance-nodulation-cell division (RND) efflux MexK	1025	11	ATG	GGAGT	6.4	0.2
PA3677	resistance-nodulation-cell division (RND) efflux MexJ	367	0	ATG	GGTGT	9.5	-0.2
PA3678	transcriptional regulator MexL	212	0	ATG	-	5.9	-0.1
PA3680	ribosomal RNA small subunit methyltransferase J	261	0	ATG	-	8.9	-0.2
PA3685	YeaZ	226	0	ATG	-	5.0	0.2
PA3686	adenylate kinase	215	0	ATG	GGAGC	6.0	-0.2
PA3690	metal-transporting P-type ATPase	740	5	ATG	-	5.7	0.2
PA3691	hypothetical protein	134	0	ATG	AGAGG	7.9	-0.6
PA3692	outer membrane porin F, LptF	261	0	ATG	-	9.5	-0.6
PA3694	hypothetical protein	107	1	ATG	-	5.6	0.2
PA3695	hypothetical protein	301	1	ATG	AGAGG	6.5	-0.1
PA3696	hypothetical protein	248	0	ATG	GGAGA	5.4	0.0
PA3697	hypothetical protein	431	0	ATG	TGAGA	6.1	-0.3
PA3699	transcriptional regulator	237	0	GTG	GGAGG	5.5	-0.1
PA3700	lysine--tRNA ligase	501	0	ATG	-	5.2	-0.4
PA3701	peptide chain release factor 2 (prfB)	248	0	ATG	GGAGT	5.4	-0.5
PA3702	two-component response regulator WspR	347	0	ATG	GGAGA	5.6	-0.2
PA3703	chemotaxis-specific methylesterase	335	0	TTG	GGAGA	6.2	0.2
PA3704	chemotaxis sensor/effector fusion protein	769	0	ATG	GGAGC	5.1	-0.2
PA3706	biofilm formation methyltransferase WspC	422	0	ATG	GGAGT	7.7	-0.2
PA3707	hypothetical protein	171	0	GTG	TGAGG	6.9	-0.1
PA3708	chemotaxis transducer	542	2	GTG	CGAGT	4.9	-0.1
PA3709	major facilitator superfamily transporter	539	12	ATG	GGAGA	9.0	0.6
PA3710	GMC-type oxidoreductase	557	0	ATG	CGAGG	7.2	-0.3
PA3712	hypothetical protein	231	1	ATG	GGAGG	5.8	-0.4
PA3713	spermidine dehydrogenase SpdH	620	0	ATG	-	6.3	-0.3

protein ID	(predicted) function	length [aa]	TMH	start	RBS	pI	GRAVY
PA3716	hypothetical protein	568	0	ATG	CGAGA	4.4	-0.3
PA3723	FMN oxidoreductase	368	0	ATG	GGAGT	5.9	-0.2
PA3725	single-stranded-DNA-specific exonuclease RecJ	571	0	ATG	CGAGC	5.6	0.0
PA3727	hypothetical protein	230	0	ATG	TGAGG	5.1	-0.5
PA3728	hypothetical protein	1746	0	ATG	-	5.1	-0.4
PA3729	hypothetical protein	688	1	ATG	GGAGA	5.2	-0.4
PA3730	hypothetical protein	213	3	ATG	AGAGC	5.5	0.7
PA3731	hypothetical protein	231	0	ATG	GGAGG	6.7	-0.4
PA3734	hypothetical protein	401	1	GTG	-	8.3	0.1
PA3735	threonine synthase	469	0	ATG	-	6.2	-0.1
PA3736	homoserine dehydrogenase	434	0	GTG	GGAGT	5.3	0.1
PA3737	thiol:disulfide interchange protein DsbC	242	0	ATG	GGAGT	8.8	-0.2
PA3739	sodium/hydrogen antiporter	611	12	ATG	-	9.0	0.6
PA3742	50S ribosomal protein L19	116	0	ATG	GGAGC	10.4	-0.4
PA3743	tRNA (guanine-N(1)-)-methyltransferase	252	0	ATG	-	5.1	-0.5
PA3745	30S ribosomal protein S16	83	0	ATG	-	10.9	-0.5
PA3746	signal recognition particle protein Ffh	457	0	ATG	CGTGG	9.6	-0.2
PA3748	hypothetical protein	430	4	ATG	-	5.0	0.1
PA3751	phosphoribosylglycinamide formyltransferase 2	393	0	ATG	CGAGG	5.8	-0.1
PA3754	hypothetical protein	203	0	ATG	-	4.7	-0.1
PA3757	transcriptional regulator	247	0	ATG	-	6.9	-0.3
PA3759	aminotransferase	340	0	ATG	GGTGG	5.6	0.1
PA3760	N-acetyl-D-glucosamine phosphotransferase system	842	0	ATG	TGAGC	5.4	0.0
PA3761	N-acetyl-D-glucosamine phosphotransferase system	570	12	ATG	GGAGA	8.2	0.5
PA3763	phosphoribosylformylglycinamidine synthase	1298	0	ATG	AGAGG	5.0	-0.2
PA3764	membrane-bound lytic murein transglycosylase F	452	0	GTG	GGAGC	5.9	-0.6
PA3766	aromatic amino acid transporter	418	11	ATG	GGAGT	8.8	0.8
PA3767	hypothetical protein	182	0	GTG	CGAGG	9.1	-0.2
PA3768	metallo-oxidoreductase	463	1	ATG	GGTGA	6.2	-0.3
PA3769	GMP synthase	525	0	ATG	CGAGA	5.5	0.0
PA3770	inosine 5'-monophosphate dehydrogenase	489	0	ATG	GGAGC	6.2	0.0
PA3776	transcriptional regulator	302	0	ATG	-	9.2	0.0
PA3777	exodeoxyribonuclease VII large subunit	459	0	ATG	-	10.9	-0.3
PA3778	transcriptional regulator	311	0	ATG	TGAGC	9.1	0.0
PA3787	hypothetical protein	282	1	ATG	CGAGT	9.9	-0.2
PA3788	hypothetical protein	131	4	ATG	GGAGA	7.8	1.0
PA3789	hypothetical protein	471	6	ATG	TGAGG	9.6	0.1
PA3790	copper transport outer membrane porin OprC	723	0	ATG	-	6.0	-0.5
PA3792	2-isopropylmalate synthase	592	0	GTG	-	5.5	-0.3
PA3794	hypothetical protein	151	3	ATG	GGAGC	6.7	0.7
PA3798	aminotransferase	382	0	ATG	-	5.8	-0.1
PA3799	GTPase Der	493	0	ATG	GGAGA	9.1	-0.4
PA3800	outer membrane protein assembly factor BamB	380	0	ATG	GGAGA	5.3	0.0
PA3801	hypothetical protein	214	0	GTG	GGAGT	5.0	-0.4
PA3802	histidine--tRNA ligase	429	0	GTG	-	5.3	-0.2

protein ID	(predicted) function	length [aa]	TMH	start	RBS	pI	GRAVY
PA3803	4-hydroxy-3-methylbut-2-en-1-yl diphosphate synthase (flavodoxin)	371	0	ATG	-	6.0	-0.1
PA3804	hypothetical protein	347	1	ATG	-	5.1	-0.2
PA3805	type 4 fimbrial biogenesis protein PilF	252	0	ATG	GGAGG	6.7	-0.5
PA3806	23S rRNA (adenine(2503)-C(2))-methyltransferase RlmN	379	0	ATG	TGAGG	8.6	-0.2
PA3807	nucleoside diphosphate kinase	143	0	ATG	GGAGT	5.5	-0.1
PA3810	chaperone protein HscA	619	0	ATG	AGAGC	4.9	-0.1
PA3812	probable iron-binding protein IscA	107	0	ATG	GGAGT	4.9	-0.1
PA3814	cysteine desulfurase	404	0	ATG	GGAGT	5.7	-0.3
PA3815	HTH-type transcriptional regulator	163	0	ATG	-	6.4	-0.2
PA3816	O-acetylserine synthase	258	0	ATG	GGAGT	6.1	-0.2
PA3817	methyltransferase	257	0	TTG	GGAGA	5.9	-0.1
PA3818	type III secretion system regulator SuhB	271	0	ATG	GGTGA	6.2	-0.1
PA3819	hypothetical protein	182	1	GTG	GGAGG	9.1	-0.2
PA3820	preprotein translocase subunit SecF	306	6	ATG	TGTGG	4.8	0.5
PA3821	preprotein translocase subunit SecD	620	6	ATG	GGTGT	8.9	0.1
PA3822	preprotein translocase subunit YajC	112	1	ATG	GGAGT	9.0	0.4
PA3823	queuine tRNA-ribosyltransferase	372	0	ATG	TGAGC	6.4	-0.2
PA3824	S-adenosylmethionine--tRNA	347	0	ATG	CGAGA	6.0	-0.1
PA3825	Cyclic-guanylate-specific phosphodiesterase	526	1	ATG	CGAGT	5.7	0.0
PA3827	Lipopolysaccharide export system permease protein LptG	355	6	ATG	CGAGG	9.1	0.4
PA3828	Lipopolysaccharide export system permease protein LptF	372	6	TTG	GGAGT	9.5	0.3
PA3831	leucyl aminopeptidase	495	0	ATG	-	8.7	0.0
PA3832	DNA polymerase III subunit chi	142	0	GTG	-	5.6	-0.4
PA3834	valine--tRNA ligase	950	0	ATG	-	5.4	-0.4
PA3837	ABC transporter permease	296	8	ATG	-	9.8	1.1
PA3838	ABC transporter ATP-binding protein	264	0	ATG	GGAGC	6.5	0.0
PA3839	sodium:sulfate symporter	610	11	ATG	-	8.6	0.8
PA3840	SAM-dependent methyltransferase	336	0	ATG	CGAGA	9.0	-0.4
PA3845	transcriptional regulator	298	0	ATG	-	9.2	-0.2
PA3847	hypothetical protein	156	0	ATG	GGAGC	11.6	-0.2
PA3848	hypothetical protein	451	2	ATG	AGAGC	7.9	-0.1
PA3853	transferase	229	0	GTG	-	9.6	-0.2
PA3855	hypothetical protein	233	0	ATG	-	7.7	-0.1
PA3857	phosphatidylcholine synthase	238	7	ATG	AGAGA	6.9	0.9
PA3860	acyl-CoA synthetase	632	0	ATG	-	5.8	-0.1
PA3861	ATP-dependent RNA helicase RhlB	507	0	GTG	CGAGA	9.0	-0.5
PA3862	NAD(P)H-dependent anabolic L-arginine	315	0	ATG	GGAGA	5.6	0.0
PA3870	molybdenum cofactor biosynthesis protein A1	329	0	ATG	GGAGT	8.6	-0.1
PA3872	respiratory nitrate reductase subunit gamma	227	5	ATG	GGAGT	10.1	0.8
PA3873	respiratory nitrate reductase subunit delta	246	0	ATG	GGAGT	4.6	-0.2
PA3874	respiratory nitrate reductase subunit beta	513	0	ATG	TGAGG	5.8	-0.4
PA3875	respiratory nitrate reductase subunit alpha	1261	0	ATG	TGAGG	6.3	-0.5
PA3876	nitrite extrusion protein 2	468	12	ATG	TGAGG	9.5	0.5
PA3877	nitrite extrusion protein 1	431	12	ATG	AGAGA	9.1	0.7
PA3878	two-component sensor NarX	622	2	ATG	-	5.6	-0.3
PA3881	hypothetical protein	154	1	ATG	-	8.7	-0.1

protein ID	(predicted) function	length [aa]	TMH	start	RBS	pI	GRAVY
PA3882	hypothetical protein	249	0	ATG	GGAGG	7.0	-0.3
PA3883	short-chain dehydrogenase	276	0	ATG	-	9.8	0.1
PA3887	Na+/H+ antiporter NhaP	424	13	ATG	GGAGT	6.1	1.0
PA3891	ABC transporter ATP-binding protein	387	0	ATG	GGAGC	5.7	-0.3
PA3901	Fe(III) dicitrate transporter FecA	784	0	ATG	GGAGT	5.5	-0.5
PA3903	peptide chain release factor 3	527	0	ATG	-	5.6	-0.4
PA3905	hypothetical protein	175	0	GTG	-	6.9	-0.3
PA3911	hypothetical protein	171	0	ATG	GGAGG	9.9	-0.2
PA3912	hypothetical protein	296	0	ATG	TGAGG	5.7	-0.1
PA3913	protease	331	0	ATG	AGAGG	8.5	-0.2
PA3914	molybdenum cofactor biosynthesis protein A1	407	0	GTG	GGTGC	5.9	0.1
PA3915	molybdopterin biosynthesis protein B1	185	0	ATG	-	6.4	0.0
PA3918	molybdenum cofactor biosynthesis protein MoaC	160	0	GTG	GGAGC	6.6	-0.1
PA3919	hypothetical protein	463	0	ATG	GGTGA	5.9	-0.2
PA3920	metal transporting P-type ATPase	792	8	ATG	GGAGG	6.4	0.3
PA3921	transcriptional regulator	906	0	ATG	-	5.8	-0.2
PA3922	hypothetical protein	455	0	ATG	CGAGG	8.6	-0.6
PA3923	hypothetical protein	641	1	ATG	GGAGT	4.9	-0.3
PA3924	probable medium-chain acyl-CoA ligase	560	0	ATG	GGTGT	5.7	-0.1
PA3929	cyanide insensitive terminal oxidase	335	8	ATG	AGAGG	6.6	0.9
PA3930	cyanide insensitive terminal oxidase	488	9	ATG	AGAGG	6.5	0.3
PA3933	choline transporter BetT3	653	12	ATG	-	7.0	0.4
PA3934	hypothetical protein	678	18	ATG	CGAGA	5.3	0.9
PA3949	hypothetical protein	391	0	ATG	-	9.5	-0.1
PA3950	ATP-dependent RNA helicase	449	0	ATG	CGAGT	9.9	-0.1
PA3958	hypothetical protein	379	1	ATG	GGTGA	5.7	-0.3
PA3961	ATP-dependent helicase	838	0	ATG	GGAGC	7.0	-0.2
PA3963	transporter	298	6	ATG	-	6.3	0.4
PA3968	pseudouridine synthase	189	0	GTG	-	9.7	-0.5
PA3969	hypothetical protein	361	0	ATG	AGAGC	9.2	-0.5
PA3972	acyl-CoA dehydrogenase	549	0	ATG	CGAGG	6.0	-0.2
PA3974	lost adherence sensor LadS	795	6	ATG	CGAGG	6.3	0.1
PA3976	thiamine-phosphate pyrophosphorylase	209	0	ATG	TGAGA	6.5	0.1
PA3977	glutamate-1-semialdehyde aminotransferase	427	0	ATG	CGAGA	5.5	0.1
PA3980	(dimethylallyl)adenosine tRNA	446	0	ATG	-	5.6	-0.3
PA3981	hypothetical protein	340	0	TTG	CGAGT	6.7	-0.4
PA3984	apolipoprotein N-acyltransferase	511	8	ATG	-	9.2	0.4
PA3985	hypothetical protein	253	2	ATG	GGAGG	9.9	0.1
PA3987	leucine--tRNA ligase	873	0	ATG	-	5.5	-0.3
PA3988	LPS-assembly lipoprotein LptE	207	1	ATG	GGAGT	5.2	-0.5
PA3989	DNA polymerase III subunit delta	345	0	ATG	-	6.5	-0.1
PA3992	SltB3	448	0	ATG	TGAGG	7.8	-0.2
PA3995	transcriptional regulator	297	0	ATG	CGAGA	6.9	0.0
PA3996	lipoyl synthase	327	0	ATG	-	6.4	-0.4
PA3997	lipoate-protein ligase B	217	0	ATG	GGTGC	5.7	0.0
PA3999	D-ala-D-ala-carboxypeptidase	386	0	ATG	AGAGA	6.3	-0.1

protein ID	(predicted) function	length [aa]	TMH	start	RBS	pI	GRAVY
PA4000	RlpA	342	0	TTG	CGAGG	9.7	-0.2
PA4002	rod shape-determining protein	367	8	ATG	-	9.8	0.9
PA4003	penicillin-binding protein 2	646	1	ATG	-	7.9	-0.3
PA4004	23S rRNA (pseudouridine(1915)-N(3))-methyltransferase RlmH	155	0	ATG	AGAGT	9.0	-0.4
PA4007	gamma-glutamyl phosphate reductase	421	0	ATG	CGAGA	5.3	0.0
PA4010	3-methyladenine DNA glycosylase	239	0	ATG	-	8.8	-0.5
PA4011	hypothetical protein	437	12	ATG	-	10.2	0.8
PA4013	hypothetical protein	236	6	ATG	GGAGG	7.0	1.1
PA4015	hypothetical protein	151	0	ATG	GGAGG	5.5	0.1
PA4016	hypothetical protein	579	0	ATG	-	5.7	-0.6
PA4017	hypothetical protein	213	0	ATG	GGAGA	6.5	0.0
PA4022	aldehyde dehydrogenase HdhA	506	0	ATG	GGAGA	5.5	-0.1
PA4023	transporter	482	12	ATG	TGAGG	6.7	0.8
PA4024	ethanolamine ammonia-lyase large subunit	464	0	ATG	GGAGA	5.1	0.0
PA4025	ethanolamine ammonia-lyase small subunit	273	0	ATG	TGAGG	6.2	-0.2
PA4026	acetyltransferase	153	0	ATG	CGAGG	6.4	-0.3
PA4029	hypothetical protein	221	5	ATG	-	9.5	0.6
PA4036	two-component sensor	766	4	ATG	-	5.8	0.0
PA4044	1-deoxy-D-xylulose-5-phosphate synthase	627	0	ATG	-	5.5	-0.1
PA4046	hypothetical protein	139	4	GTG	CGAGG	11.2	0.8
PA4047	GTP cyclohydrolase II	205	0	GTG	GGAGT	6.2	-0.1
PA4048	hypothetical protein	214	1	ATG	GGAGT	9.2	0.0
PA4050	phosphatidylglycerophosphatase A	171	3	GTG	-	5.1	0.5
PA4054	3,4-dihydroxy-2-butanone-4-phosphate synthase	365	0	ATG	GGTGC	5.2	0.0
PA4055	riboflavin synthase subunit alpha	219	0	ATG	GGAGG	6.0	0.0
PA4056	riboflavin-specific deaminase/reductase	373	0	ATG	CGAGC	6.8	0.0
PA4061	thioredoxin	289	0	ATG	CGAGA	4.6	-0.1
PA4064	ABC transporter ATP-binding protein	234	0	ATG	-	6.7	-0.1
PA4065	hypothetical protein	421	4	ATG	TGAGC	9.1	0.4
PA4067	outer membrane protein OprG	232	0	ATG	GGAGC	4.9	-0.1
PA4068	epimerase	309	0	ATG	-	5.6	-0.1
PA4078	nonribosomal peptide synthetase	991	0	ATG	GGAGT	6.5	-0.3
PA4079	short-chain dehydrogenase	229	0	ATG	GGAGA	5.3	0.1
PA4101	protein BfmR	246	0	ATG	GGAGC	5.9	-0.2
PA4102	protein BfmS	434	2	ATG	CGAGG	6.8	-0.1
PA4108	cyclic di-GMP phosphodiesterase	414	0	GTG	CGAGG	7.8	0.0
PA4110	beta-lactamase	397	0	ATG	-	8.7	-0.3
PA4112	sensor/response regulator hybrid protein	1417	1	GTG	-	5.5	-0.1
PA4113	sugar efflux transporter	396	11	ATG	-	9.9	1.0
PA4117	phytochrome BphP	728	0	ATG	GGAGA	5.6	-0.2
PA4129	hypothetical protein	162	0	ATG	GGAGG	5.5	-0.1
PA4130	sulfite/nitrite reductase	557	0	ATG	TGAGG	5.9	-0.3
PA4131	iron-sulfur protein	573	5	GTG	-	9.6	0.0
PA4132	hypothetical protein	500	0	ATG	GGAGG	7.7	-0.2
PA4133	cbb3-type cytochrome C oxidase subunit I	475	12	ATG	-	9.5	0.5
PA4138	tyrosine--tRNA ligase	412	0	GTG	GGAGA	6.3	-0.2

protein ID	(predicted) function	length [aa]	TMH	start	RBS	pI	GRAVY
PA4145	transcriptional regulator	296	0	ATG	CGAGA	6.7	-0.2
PA4154	hypothetical protein	222	1	ATG	-	9.5	-0.3
PA4155	hypothetical protein	435	0	ATG	GGAGA	5.7	-0.2
PA4157	transcriptional regulator	262	0	ATG	-	8.5	-0.1
PA4162	probable short-chain dehydrogenase	238	0	ATG	-	7.7	0.2
PA4165	transcriptional regulator	496	0	TTG	CGAGG	9.7	-0.1
PA4168	second ferric pyoverdine receptor FpvB	802	0	ATG	-	5.6	-0.5
PA4170	hypothetical protein	310	1	ATG	-	7.1	0.1
PA4176	peptidyl-prolyl cis-trans isomerase C2	93	0	ATG	GGAGT	5.9	-0.3
PA4180	acetolactate synthase	547	1	ATG	CGAGG	5.9	-0.1
PA4181	hypothetical protein	239	0	ATG	-	5.1	0.0
PA4182	hypothetical protein	212	0	ATG	CGAGG	6.1	-0.5
PA4190	probable FAD-dependent monooxygenase	398	0	ATG	GGAGA	6.0	-0.2
PA4197	protein BfiS	758	0	ATG	-	6.4	-0.3
PA4199	acyl-CoA dehydrogenase	593	0	ATG	CGAGG	5.2	0.0
PA4201	D-alanine-D-alanine ligase A	346	0	ATG	GGTGG	5.2	0.1
PA4205	hypothetical protein	148	4	ATG	-	8.9	0.7
PA4206	resistance-nodulation-cell division (RND) efflux	370	1	ATG	TGAGG	8.6	0.0
PA4207	resistance-nodulation-cell division (RND) efflux	1029	10	ATG	-	5.9	0.4
PA4208	probable outer membrane protein precursor	487	0	ATG	GGTGA	5.7	-0.3
PA4209	phenazine-specific methyltransferase	334	0	ATG	CGAGA	5.0	0.0
PA4212	phenazine biosynthesis protein PhzC	405	0	ATG	GGTGA	6.9	-0.3
PA4213	phenazine biosynthesis protein PhzD	207	0	ATG	GGAGA	5.6	-0.1
PA4214	phenazine biosynthesis protein PhzE	627	0	ATG	CGAGG	5.5	-0.2
PA4217	flavin-containing monooxygenase	402	0	ATG	CGAGA	5.7	-0.2
PA4218	transporter AmpP	414	10	ATG	GGAGA	9.4	0.7
PA4219	AmpO	501	8	GTG	-	10.3	0.5
PA4220	hypothetical protein	93	3	ATG	-	11.3	0.8
PA4221	Fe(III)-pyochelin outer membrane receptor	720	1	ATG	CGAGG	5.9	-0.6
PA4222	ABC transporter ATP-binding protein	574	5	ATG	GGAGG	9.0	0.3
PA4223	ABC transporter ATP-binding protein	570	5	GTG	GGAGC	6.3	0.4
PA4224	pyochelin biosynthetic protein PchG	349	0	ATG	GGAGG	5.1	0.1
PA4225	pyochelin synthetase	1809	0	ATG	AGAGG	5.7	-0.1
PA4226	dihydroaeruginoic acid synthetase	1438	0	ATG	GGAGC	5.3	0.0
PA4227	transcriptional regulator PchR	296	0	ATG	-	7.0	-0.2
PA4228	2,3-dihydroxybenzoate-AMP ligase	547	0	ATG	GGAGA	6.4	-0.2
PA4229	pyochelin biosynthetic protein PchC	251	0	ATG	GGAGG	5.9	-0.2
PA4230	isochorismate-pyruvate lyase	101	0	ATG	AGAGG	5.4	-0.3
PA4231	salicylate biosynthesis isochorismate synthase	476	0	ATG	GGTGC	6.4	-0.2
PA4232	single-stranded DNA-binding protein	165	0	ATG	GGAGA	5.5	-1.0
PA4233	major facilitator superfamily transporter	462	11	ATG	TGAGG	9.2	0.8
PA4234	excinuclease ABC subunit A	945	0	GTG	CGAGG	6.2	-0.3
PA4235	bacterioferritin	154	0	ATG	GGAGA	5.0	-0.5
PA4236	catalase	482	0	ATG	TGAGG	6.2	-0.7
PA4237	50S ribosomal protein L17	129	0	ATG	-	10.5	-0.5
PA4238	DNA-directed RNA polymerase subunit alpha	333	0	ATG	GGTGC	4.9	-0.3
PA4239	30S ribosomal protein S4	206	0	ATG	GGAGA	9.9	-0.7

protein ID	(predicted) function	length [aa]	TMH	start	RBS	pI	GRAVY
PA4240	30S ribosomal protein S11	129	0	ATG	-	10.8	-0.4
PA4241	30S ribosomal protein S13	118	0	ATG	GGAGT	10.9	-0.7
PA4243	preprotein translocase subunit SecY	442	10	ATG	CGAGG	9.8	0.6
PA4244	50S ribosomal protein L15	144	0	ATG	GGAGG	11.0	-0.5
PA4245	50S ribosomal protein L30	58	0	ATG	CGAGG	10.1	-0.3
PA4246	30S ribosomal protein S5	166	0	ATG	GGAGT	10.0	-0.2
PA4247	50S ribosomal protein L18	116	0	ATG	-	10.2	-0.4
PA4248	50S ribosomal protein L6	177	0	ATG	-	9.9	-0.3
PA4249	30S ribosomal protein S8	130	0	ATG	GGAGC	9.6	-0.1
PA4250	30S ribosomal protein S14	101	0	ATG	GGAGT	11.4	-0.9
PA4251	50S ribosomal protein L5	179	0	ATG	-	9.7	-0.3
PA4252	50S ribosomal protein L24	104	0	ATG	GGAGT	10.2	-0.5
PA4253	50S ribosomal protein L14	122	0	ATG	GGAGA	10.8	-0.1
PA4254	30S ribosomal protein S17	88	0	ATG	-	9.9	-0.4
PA4255	50S ribosomal protein L29	63	0	ATG	GGTGA	10.3	-0.7
PA4256	50S ribosomal protein L16	137	0	ATG	GGAGT	11.2	-0.5
PA4257	30S ribosomal protein S3	228	0	ATG	GGAGT	10.1	-0.5
PA4258	50S ribosomal protein L22	110	0	ATG	-	10.1	-0.3
PA4259	30S ribosomal protein S19	91	0	GTG	AGAGG	10.6	-0.5
PA4260	50S ribosomal protein L2	273	0	ATG	TGAGT	11.2	-0.6
PA4261	50S ribosomal protein L23	99	0	ATG	CGAGG	10.1	-0.4
PA4262	50S ribosomal protein L4	200	0	ATG	-	9.9	-0.2
PA4263	50S ribosomal protein L3	211	0	ATG	AGAGG	9.9	-0.3
PA4264	30S ribosomal protein S10	103	0	ATG	GGAGT	9.8	-0.5
PA4265	elongation factor Tu	397	0	GTG	AGAGG	5.2	-0.2
PA4266	elongation factor G	706	0	GTG	CGAGG	5.1	-0.3
PA4267	30S ribosomal protein S7	156	0	ATG	TGAGG	10.2	-0.5
PA4268	30S ribosomal protein S12	123	0	ATG	GGAGC	11.0	-0.8
PA4269	DNA-directed RNA polymerase subunit beta'	1399	0	TTG	GGAGG	6.7	-0.2
PA4270	DNA-directed RNA polymerase subunit beta	1357	0	ATG	-	5.6	-0.3
PA4271	50S ribosomal protein L7/L12	122	0	ATG	AGAGT	4.7	0.2
PA4272	50S ribosomal protein L10	166	0	GTG	GGAGT	8.9	0.1
PA4273	50S ribosomal protein L1	231	0	ATG	GGAGG	9.6	-0.1
PA4274	50S ribosomal protein L11	143	0	ATG	GGAGT	9.8	-0.1
PA4275	transcription antitermination protein NusG	177	0	GTG	GGTGC	5.8	-0.4
PA4277	elongation factor Tu	397	0	ATG	-	5.2	-0.2
PA4278	hypothetical protein	234	0	ATG	AGAGG	5.9	-0.2
PA4279	pantothenate kinase	248	0	ATG	TGAGG	5.5	0.2
PA4281	exonuclease SbcD	409	0	ATG	CGAGT	5.3	-0.2
PA4282	exonuclease	1211	0	ATG	-	5.6	-0.9
PA4283	exodeoxyribonuclease V subunit alpha	721	0	ATG	GGAGC	6.2	-0.2
PA4286	hypothetical protein	227	0	GTG	AGAGG	5.4	-0.2
PA4290	chemotaxis transducer	538	1	ATG	GGAGG	5.4	-0.2
PA4292	phosphate transporter	489	9	ATG	-	8.9	0.4
PA4293	two-component sensor PprA	922	0	ATG	TGAGG	5.7	-0.3
PA4303	TadZ	394	0	ATG	GGAGG	6.9	0.2
PA4304	type II/III secretion system protein RcpA	416	1	ATG	TGAGG	5.3	0.0

protein ID	(predicted) function	length [aa]	TMH	start	RBS	pI	GRAVY
PA4307	chemotactic transducer PctC	632	2	ATG	-	4.9	0.0
PA4308	hypothetical protein	496	0	ATG	CGAGG	6.1	-0.2
PA4309	chemotactic transducer PctA	629	2	ATG	-	5.2	-0.1
PA4310	chemotactic transducer PctB	629	2	ATG	-	5.0	-0.1
PA4317	hypothetical protein	245	6	ATG	-	8.9	1.0
PA4318	hypothetical protein	265	2	ATG	-	6.5	0.3
PA4319	hypothetical protein	326	5	ATG	GGAGA	9.4	0.3
PA4320	hypothetical protein	523	5	ATG	GGAGC	9.1	0.0
PA4321	hypothetical protein	423	1	ATG	GGAGC	5.5	-0.4
PA4322	hypothetical protein	335	0	ATG	-	5.9	-0.1
PA4323	hypothetical protein	443	2	ATG	-	9.8	-0.3
PA4326	hypothetical protein	127	0	ATG	GGAGG	9.5	-0.2
PA4327	hypothetical protein	268	0	ATG	GGAGA	8.8	-0.5
PA4328	hypothetical protein	304	0	ATG	GGAGC	5.6	-0.2
PA4329	pyruvate kinase II	483	0	ATG	GGAGT	6.2	-0.1
PA4330	enoyl-CoA hydratase	257	0	ATG	GGAGT	6.2	0.1
PA4331	hypothetical protein	308	0	GTG	GGAGG	7.0	0.0
PA4332	SadC	375	6	ATG	GGAGC	9.2	0.2
PA4333	fumarase	507	0	ATG	AGAGG	5.3	0.0
PA4334	probable transport protein	418	9	GTG	-	7.9	0.8
PA4347	hypothetical protein	384	0	ATG	CGAGG	7.1	-0.3
PA4349	hypothetical protein	298	0	ATG	GGAGT	5.8	0.1
PA4352	hypothetical protein	286	0	ATG	GGAGG	5.9	0.1
PA4353	hypothetical protein	190	0	ATG	-	8.0	-0.4
PA4356	xenobiotic reductase	350	0	ATG	GGAGG	5.1	-0.2
PA4358	ferrous iron transporter B	766	9	ATG	-	5.8	0.5
PA4361	oxidoreductase	329	0	ATG	GGAGA	8.2	0.1
PA4362	hypothetical protein	352	0	ATG	GGAGA	8.4	-0.1
PA4363	chromosome replication initiation inhibitor	300	0	ATG	-	6.3	0.1
PA4364	hypothetical protein	133	0	ATG	-	5.8	0.2
PA4366	superoxide dismutase	193	0	ATG	GGAGA	5.3	-0.3
PA4367	protein BifA	687	2	TTG	-	5.7	-0.2
PA4368	hypothetical protein	300	2	ATG	-	6.6	-0.4
PA4369	hypothetical protein	190	1	ATG	GGAGC	7.9	0.1
PA4370	insulin-cleaving metalloproteinase outer membrane protein	446	0	ATG	-	4.7	-0.3
PA4371	hypothetical protein	473	0	ATG	-	5.6	-0.3
PA4372	hypothetical protein	354	0	ATG	TGAGG	5.8	-0.2
PA4373	hypothetical protein	364	1	ATG	TGAGG	6.1	-0.2
PA4374	resistance-nodulation-cell division (RND) efflux MexV	376	1	ATG	-	5.6	0.0
PA4375	multidrug efflux protein MexW	1018	12	ATG	-	5.2	0.4
PA4376	nicotinate phosphoribosyltransferase	398	0	ATG	AGTGG	6.2	-0.1
PA4378	InaA protein	234	0	ATG	-	9.5	-0.6
PA4380	two-component sensor ColS	426	2	ATG	GGAGG	5.1	0.0
PA4381	two-component response regulator ColR	227	0	ATG	GGAGT	5.7	-0.2
PA4383	camphor resistance protein CrcB	127	4	ATG	-	9.5	1.0
PA4385	molecular chaperone GroEL	547	0	ATG	AGAGG	5.0	0.0

protein ID	(predicted) function	length [aa]	TMH	start	RBS	pI	GRAVY
PA4386	co-chaperonin GroES	97	0	ATG	GGAGA	5.2	-0.1
PA4387	phage exclusion suppressor FxsA	155	3	ATG	-	10.6	0.4
PA4388	hypothetical protein	244	0	TTG	GGAGT	5.9	-0.1
PA4389	3-ketoacyl-ACP reductase	252	0	ATG	CGTGG	6.8	0.1
PA4390	hypothetical protein	335	0	GTG	-	5.4	-0.6
PA4393	AmpG protein	594	14	ATG	-	9.3	0.8
PA4394	hypothetical protein	278	3	ATG	GGAGG	6.6	0.5
PA4395	nucleotide-binding protein	159	0	ATG	GGAGA	7.7	-0.5
PA4396	two-component response regulator	366	0	ATG	CGAGC	5.5	0.0
PA4398	two-component sensor	698	2	ATG	AGAGC	5.7	-0.2
PA4399	hypothetical protein	192	0	ATG	AGAGG	5.9	-0.3
PA4400	hypothetical protein	315	0	GTG	CGAGG	5.3	-0.2
PA4402	bifunctional ornithine acetyltransferase/N-acetylglutamate synthase	405	0	ATG	GGAGC	5.4	0.2
PA4403	preprotein translocase subunit SecA	916	0	ATG	TGTGG	5.4	-0.5
PA4406	UDP-3-O-acyl-N-acetylglucosamine deacetylase	303	0	ATG	-	5.2	-0.1
PA4407	cell division protein FtsZ	394	0	ATG	GGAGA	4.9	0.0
PA4408	cell division protein FtsA	417	0	ATG	TGAGG	5.2	0.0
PA4409	cell division protein FtsQ	287	0	ATG	CGAGG	9.9	-0.2
PA4410	D-alanine-D-alanine ligase	319	0	ATG	GGAGG	4.9	0.0
PA4411	UDP-N-acetylmuramate--L-alanine ligase	480	1	GTG	GGAGG	5.8	0.0
PA4412	UDP-N-acetylglucosamine--N-acetylmuramyl-(pentapeptide) pyrophosphoryl-undecaprenol N-acetylglucosamine transferase	357	0	ATG	AGAGG	9.6	0.1
PA4413	cell division protein FtsW	399	10	ATG	AGAGG	6.4	0.7
PA4414	UDP-N-acetylmuramoylalanine--D-glutamate ligase	448	0	ATG	TGAGG	5.6	0.1
PA4415	phospho-N-acetylmuramoyl-pentapeptide-transferase	360	10	ATG	CGAGG	9.5	0.8
PA4416	UDP-N-acetylmuramoylalanyl-D-glutamyl-2, 6-diaminopimelate--D-alanyl-D-alanyl ligase	458	0	ATG	GGAGG	6.1	0.2
PA4417	UDP-N-acetylmuramoylalanyl-D-glutamate-2, 6-diaminopimelate ligase	487	0	ATG	GGAGG	5.2	0.0
PA4418	penicillin-binding protein 3	579	1	ATG	CGAGG	9.6	-0.1
PA4419	cell division protein FtsL	97	1	ATG	GGAGA	9.7	0.2
PA4420	S-adenosyl-methyltransferase MraW	313	0	ATG	-	7.0	-0.4
PA4422	hypothetical protein	282	0	GTG	CGAGG	5.9	0.0
PA4423	hypothetical protein	604	0	ATG	TGAGA	6.7	-0.3
PA4426	hypothetical protein	192	1	ATG	GGAGT	9.2	-0.1
PA4428	stringent starvation protein A	205	0	ATG	GGAGG	5.9	-0.2
PA4429	cytochrome C1	260	2	ATG	GGTGA	7.0	-0.1
PA4430	cytochrome b	403	9	ATG	GGAGA	8.6	0.6
PA4431	iron-sulfur protein	197	1	ATG	GGAGA	6.1	-0.1
PA4432	30S ribosomal protein S9	130	0	ATG	-	11.2	-0.6
PA4433	50S ribosomal protein L13	142	0	ATG	TGAGG	9.8	-0.6
PA4434	probable oxidoreductase	345	0	ATG	CGAGG	5.6	-0.4
PA4438	conserved hypothetical protein	364	0	ATG	-	5.8	-0.3
PA4439	tryptophan--tRNA ligase	448	0	ATG	-	5.7	-0.2
PA4441	hypothetical protein	148	1	GTG	AGAGG	5.9	-0.5
PA4442	bifunctional sulfate adenylyltransferase subunit 1/adenylylsulfate kinase	633	0	ATG	TGAGG	5.6	-0.2
PA4446	AlgW protein	389	1	ATG	-	6.3	0.0

protein ID	(predicted) function	length [aa]	TMH	start	RBS	pI	GRAVY
PA4448	histidinol dehydrogenase	440	0	ATG	AGAGG	5.1	0.0
PA4449	ATP phosphoribosyltransferase	211	0	ATG	GGAGG	9.0	0.0
PA4450	UDP-N-acetylglucosamine 1-carboxyvinyltransferase	421	0	ATG	-	5.5	0.2
PA4452	hypothetical protein	102	0	ATG	AGAGG	5.5	0.2
PA4453	hypothetical protein	215	0	ATG	TGAGG	9.1	-0.3
PA4454	hypothetical protein	157	1	ATG	GGAGA	4.9	0.3
PA4455	ABC transporter permease	265	5	ATG	GGAGA	6.7	0.8
PA4456	ABC transporter ATP-binding protein	269	0	ATG	GGAGT	6.4	0.0
PA4457	arabinose-5-phosphate isomerase KdsD	326	0	TTG	-	5.5	0.3
PA4459	Lipopolysaccharide export system protein LptC	190	1	ATG	AGAGC	6.2	-0.4
PA4460	LptH	175	0	ATG	AGAGG	9.1	-0.4
PA4461	ABC transporter ATP-binding protein LptB	241	0	ATG	-	6.2	-0.1
PA4462	RNA polymerase factor sigma-54	497	0	ATG	-	4.7	-0.4
PA4464	nitrogen regulatory IIA protein	154	0	ATG	-	4.9	0.1
PA4465	hypothetical protein	286	0	ATG	-	5.6	-0.3
PA4474	hypothetical protein	480	0	ATG	GGAGT	5.2	-0.1
PA4476	hypothetical protein	1276	2	ATG	TGAGG	6.6	-0.2
PA4477	cytoplasmic axial filament protein	485	0	ATG	AGTGG	5.3	-0.2
PA4480	rod shape-determining protein MreC	330	0	GTG	-	5.6	-0.1
PA4481	rod shape-determining protein MreB	345	0	ATG	-	5.3	0.0
PA4483	aspartyl/glutamyl-tRNA amidotransferase subunit A	484	0	ATG	-	5.5	-0.1
PA4484	Glu-tRNA(Gln) amidotransferase subunit B	481	0	ATG	TGAGG	5.3	-0.4
PA4487	MagF	263	0	ATG	-	5.1	-0.3
PA4488	MagE	549	0	GTG	-	8.8	-0.4
PA4489	MagD	1516	0	ATG	-	5.5	-0.3
PA4491	MagB	589	1	ATG	-	5.1	-0.2
PA4492	MagA	269	0	ATG	-	5.8	-0.2
PA4493	DNA-binding response regulator RoxR	186	0	ATG	AGAGG	5.4	-0.2
PA4494	sensor histidine kinase RoxS	422	5	ATG	-	6.3	0.2
PA4495	hypothetical protein	236	0	ATG	GGAGT	5.8	-0.2
PA4498	metallopeptidase MdpA	405	0	ATG	CGAGG	5.8	-0.2
PA4500	ABC transporter	533	0	ATG	TGAGG	8.1	-0.4
PA4501	glycine-glutamate dipeptide porin OpdP	484	0	GTG	GGAGC	5.6	-0.5
PA4502	ABC transporter	531	0	ATG	GGAGG	6.2	-0.3
PA4503	ABC transporter permease DppB	336	6	ATG	TGAGG	8.0	0.7
PA4504	ABC transporter permease DppC	303	7	ATG	TGAGG	7.7	0.7
PA4505	ABC transporter ATP-binding protein DppD	324	0	ATG	GGAGA	5.8	0.0
PA4506	peptide ABC transporter ATP-binding protein	323	0	ATG	CGAGG	9.3	-0.4
PA4512	lipopolysaccharide biosynthetic protein LpxO1	299	2	ATG	-	9.7	-0.2
PA4513	oxidoreductase	850	5	GTG	GGTGA	6.8	-0.2
PA4514	iron transport outer membrane receptor	753	0	ATG	GGAGG	5.7	-0.6
PA4515	hydroxylase	226	0	ATG	CGTGG	6.1	-0.3
PA4519	ornithine decarboxylase	387	0	ATG	GGAGT	5.0	-0.2
PA4520	probable chemotaxis transducer	673	2	GTG	GGAGA	5.1	0.0
PA4521	AmpE	278	5	ATG	GGAGG	8.9	0.8
PA4523	hypothetical protein	751	0	ATG	GGTGG	5.5	-0.2

protein ID	(predicted) function	length [aa]	TMH	start	RBS	pI	GRAVY
PA4524	nicotinate-nucleotide pyrophosphorylase	282	0	ATG	GGAGC	5.3	-0.1
PA4525	type 4 fimbrial protein PilA	149	1	ATG	GGAGA	6.2	0.1
PA4526	type 4 fimbrial biogenesis protein PilB	566	0	ATG	-	5.6	-0.3
PA4528	type 4 prepilin peptidase PilD	290	6	ATG	-	7.7	0.6
PA4535	hypothetical protein	209	0	ATG	TGAGC	9.2	-0.6
PA4537	hypothetical protein	56	1	ATG	GGAGG	8.3	0.4
PA4538	NADH dehydrogenase	435	0	ATG	TGAGA	8.4	-0.1
PA4539	hypothetical protein	363	0	GTG	GGAGT	9.0	-0.2
PA4542	chaperone protein ClpB	854	0	ATG	-	5.4	-0.4
PA4544	pseudouridine synthase	320	0	ATG	TGAGC	6.8	-0.1
PA4545	competence protein ComL	341	0	ATG	-	5.0	-0.6
PA4546	two-component sensor PilS	530	6	GTG	-	6.3	0.0
PA4547	two-component response regulator PilR	445	0	ATG	-	5.8	-0.4
PA4548	D-amino acid oxidase	364	0	GTG	GGAGG	6.1	-0.1
PA4550	type 4 fimbrial biogenesis protein FimU	168	1	ATG	GGAGC	9.4	-0.1
PA4551	type 4 fimbrial biogenesis protein PilV	185	1	ATG	-	8.5	-0.1
PA4552	type 4 fimbrial biogenesis protein PilW	274	1	ATG	CGAGC	8.8	-0.3
PA4553	type 4 fimbrial biogenesis protein PilX	195	1	ATG	-	5.9	-0.1
PA4554	type 4 fimbrial biogenesis protein PilY1	1161	0	ATG	CGAGC	6.0	-0.5
PA4556	type 4 fimbrial biogenesis protein PilE	141	1	ATG	GGAGG	9.7	-0.3
PA4557	4-hydroxy-3-methylbut-2-enyl diphosphate reductase	314	0	ATG	CGAGA	5.3	-0.3
PA4559	lipoprotein signal peptidase	169	5	ATG	CGAGG	8.0	0.6
PA4560	isoleucine--tRNA ligase	943	0	ATG	-	5.8	-0.3
PA4562	hypothetical protein	512	13	ATG	-	10.0	0.9
PA4563	30S ribosomal protein S20	91	0	GTG	CGAGG	11.1	-0.5
PA4565	gamma-glutamyl kinase	372	1	ATG	TGAGG	6.7	0.0
PA4566	GTPase ObgE	406	0	ATG	GGAGG	4.8	-0.4
PA4567	50S ribosomal protein L27	85	0	ATG	GGAGG	10.7	-0.3
PA4568	50S ribosomal protein L21	103	0	ATG	GGAGA	9.9	-0.3
PA4569	octaprenyl-diphosphate synthase	322	0	ATG	GGAGC	4.9	0.0
PA4571	cytochrome C	675	0	ATG	TGAGG	6.2	-0.3
PA4572	peptidyl-prolyl cis-trans isomerase FklB	205	0	ATG	GGAGC	4.8	-0.1
PA4576	ATP-dependent protease	817	0	ATG	-	5.0	-0.2
PA4578	hypothetical protein	162	0	ATG	AGAGA	5.9	-0.1
PA4579	hypothetical protein	618	0	ATG	-	5.4	-0.4
PA4583	hypothetical protein	404	0	ATG	GGAGC	8.4	-0.2
PA4585	RNA 3'-terminal-phosphate cyclase	341	0	ATG	-	7.7	-0.1
PA4587	cytochrome C551 peroxidase	346	0	ATG	GGAGA	6.3	-0.3
PA4588	glutamate dehydrogenase	445	0	ATG	GGTGA	5.8	-0.2
PA4591	hypothetical protein	425	1	ATG	GGAGA	8.9	-0.2
PA4592	probable outer membrane protein precursor	493	0	ATG	CGAGG	5.9	-0.3
PA4595	ABC transporter ATP-binding protein	554	0	TTG	TGAGG	5.5	-0.4
PA4597	multidrug efflux outer membrane protein OprJ	479	0	ATG	GGAGT	9.1	-0.3
PA4598	resistance-nodulation-cell division (RND) MexD	1043	12	ATG	CGAGG	5.1	0.4
PA4599	resistance-nodulation-cell division (RND) MexC	387	0	ATG	GGTGT	5.8	-0.1
PA4600	transcriptional regulator NfxB	187	1	ATG	-	6.0	-0.1

protein ID	(predicted) function	length [aa]	TMH	start	RBS	pI	GRAVY
PA4601	motility regulator	1415	2	GTG	-	5.7	-0.3
PA4602	serine hydroxymethyltransferase	417	0	ATG	TGAGG	5.7	-0.1
PA4604	hypothetical protein	334	0	ATG	-	4.7	-0.1
PA4606	hypothetical protein	688	16	ATG	-	7.2	0.8
PA4608	hypothetical protein	125	0	ATG	-	4.8	-0.4
PA4609	DNA repair protein RadA	453	0	ATG	AGAGG	6.4	0.0
PA4610	hypothetical protein	144	4	ATG	GGAGA	11.4	0.8
PA4611	hypothetical protein	84	0	ATG	GGAGG	5.9	-1.0
PA4614	large-conductance mechanosensitive channel	137	2	ATG	GGAGT	4.9	0.7
PA4615	oxidoreductase	258	0	ATG	GGAGC	5.4	-0.2
PA4616	C4-dicarboxylate-binding protein	332	0	ATG	-	8.8	-0.3
PA4617	hypothetical protein	374	0	ATG	-	8.7	0.0
PA4622	major facilitator superfamily transporter	403	10	ATG	-	9.9	0.8
PA4624	cyclic diguanylate-regulated TPS partner B, CdrB	568	0	ATG	CGAGG	5.6	-0.4
PA4628	lysine-specific permease	487	12	ATG	GGAGG	9.2	0.6
PA4631	hypothetical protein	341	0	GTG	-	7.3	-0.1
PA4632	hypothetical protein	273	0	ATG	AGAGG	7.0	-0.2
PA4633	probable chemotaxis transducer	712	2	ATG	-	4.8	-0.1
PA4636	hypothetical protein	386	0	ATG	-	6.9	-0.4
PA4639	hypothetical protein	195	0	ATG	GGAGA	9.5	-0.1
PA4640	malate:quinone oxidoreductase	507	0	ATG	GGAGA	6.5	-0.3
PA4647	uracil permease	427	12	ATG	-	8.5	0.9
PA4651	pili assembly chaperone CupE4	262	1	ATG	GGAGG	9.3	-0.3
PA4655	ferrochelatase	340	0	ATG	-	6.4	-0.2
PA4656	hypothetical protein	305	0	ATG	CGAGG	8.4	-0.3
PA4659	transcriptional regulator	299	0	ATG	-	7.8	-0.1
PA4661	lipid A 3-O-deacylase	173	0	ATG	-	5.9	0.0
PA4662	glutamate racemase	265	0	ATG	-	5.4	0.2
PA4663	molybdopterin biosynthesis protein MoeB	252	1	ATG	-	5.5	0.2
PA4665	peptide chain release factor 1	360	0	ATG	-	5.1	-0.5
PA4666	glutamyl-tRNA reductase	422	0	ATG	-	5.6	0.0
PA4667	hypothetical protein	590	0	ATG	-	5.1	-0.5
PA4668	molecular chaperone LolB	205	0	ATG	CGAGA	6.9	-0.5
PA4669	4-diphosphocytidyl-2C-methyl-D-erythritol kinase	282	0	ATG	-	6.1	-0.1
PA4670	ribose-phosphate pyrophosphokinase	313	0	GTG	-	6.1	0.1
PA4671	50S ribosomal protein L25/general stress protein	204	0	ATG	GGAGA	5.8	0.0
PA4672	peptidyl-tRNA hydrolase	194	0	GTG	AGAGG	9.3	-0.1
PA4673	GTP-dependent nucleic acid-binding protein EngD	366	0	ATG	CGAGG	5.0	-0.1
PA4675	TonB-dependent receptor ChtA	742	0	ATG	-	5.3	-0.4
PA4677	hypothetical protein	412	0	ATG	GGAGC	9.1	-0.5
PA4684	hypothetical protein	432	0	ATG	-	6.8	-0.4
PA4686	hypothetical protein	948	0	ATG	GGAGG	5.4	-0.5
PA4687	ferric iron-binding periplasmic protein HitA	335	0	ATG	GGAGA	5.5	-0.2
PA4688	iron (III)-transporter permease HitB	512	12	GTG	-	10.0	0.8
PA4689	hypothetical protein	768	1	ATG	CGAGA	9.0	-0.2
PA4690a	paraquat-inducible protein A	235	3	TTG	CGAGG	6.1	0.5

protein ID	(predicted) function	length [aa]	TMH	start	RBS	pI	GRAVY
PA4693	phosphatidylserine synthase	271	6	ATG	-	6.9	0.5
PA4694	ketol-acid reductoisomerase	338	0	ATG	-	5.6	-0.1
PA4695	acetolactate synthase isozyme III small subunit	163	0	ATG	GGAGC	5.9	0.1
PA4696	acetolactate synthase 3 catalytic subunit	574	0	GTG	AGAGG	6.3	-0.1
PA4699	hypothetical protein	259	0	GTG	AGAGG	9.7	-0.2
PA4700	penicillin-binding protein 1B	774	1	ATG	-	9.2	-0.3
PA4701	hypothetical protein	520	0	GTG	AGAGG	5.7	-0.2
PA4705	PhuW	295	0	ATG	GGAGT	7.7	-0.4
PA4706	hemin importer ATP-binding subunit	255	0	ATG	-	6.2	0.0
PA4707	ABC transporter permease PhuU	327	8	GTG	GGTGC	9.3	1.0
PA4710	heme/hemoglobin uptake outer membrane receptor	764	0	ATG	GGAGT	5.7	-0.6
PA4713	hypothetical protein	149	4	ATG	CGAGG	6.6	0.7
PA4715	aminotransferase	411	0	ATG	CGAGG	7.7	-0.2
PA4717	hypothetical protein	297	1	ATG	GGAGA	5.9	-0.3
PA4718	hypothetical protein	158	0	ATG	-	9.9	0.0
PA4719	transporter	431	12	ATG	-	6.9	1.1
PA4720	tRNA (uracil-5-)-methyltransferase	363	0	ATG	-	6.5	-0.4
PA4722	probable aminotransferase	390	0	ATG	-	5.5	0.0
PA4723	suppressor protein DksA	148	0	ATG	AGAGG	5.0	-1.0
PA4725	two-component sensor CbrA	983	12	ATG	AGAGC	5.6	0.3
PA4726	two-component response regulator CbrB	478	0	ATG	CGAGA	5.5	-0.2
PA4727	poly(A) polymerase	467	0	ATG	-	9.9	-0.6
PA4728	2-amino-4-hydroxy-6-hydroxymethyl dihydropteridine pyrophosphokinase	162	0	ATG	-	4.8	0.0
PA4730	pantoate--beta-alanine ligase	283	0	ATG	-	6.1	-0.1
PA4732	glucose-6-phosphate isomerase	554	0	ATG	-	6.1	-0.2
PA4735	hypothetical protein	1088	1	ATG	AGAGA	5.3	-0.4
PA4740	polynucleotide phosphorylase	701	0	GTG	-	5.1	-0.1
PA4741	30S ribosomal protein S15	89	0	ATG	AGAGG	10.1	-0.7
PA4742	tRNA pseudouridine synthase B	304	0	GTG	CGAGG	6.4	-0.2
PA4743	ribosome-binding factor A	129	0	ATG	GGAGG	6.1	-0.4
PA4744	translation initiation factor IF-2	840	0	ATG	TGAGG	5.8	-0.4
PA4745	transcription elongation factor NusA	493	0	ATG	CGAGG	4.6	-0.3
PA4747	preprotein translocase subunit SecG	129	2	ATG	-	5.2	0.4
PA4748	triosephosphate isomerase	251	0	ATG	CGAGG	5.4	0.3
PA4749	phosphoglucosamine mutase	445	0	ATG	TGAGC	5.7	0.0
PA4750	dihydropteroate synthase	283	0	ATG	CGAGC	5.4	0.1
PA4751	cell division protein FtsH	639	2	ATG	-	5.6	-0.3
PA4754	hypothetical protein	135	4	TTG	-	8.7	1.1
PA4755	transcription elongation factor GreA	158	0	ATG	-	4.9	-0.2
PA4756	carbamoyl phosphate synthase large subunit	1073	0	ATG	CGAGA	5.1	-0.1
PA4757	leucine export protein LeuE	216	6	ATG	TGAGG	10.0	0.9
PA4758	carbamoyl phosphate synthase small subunit	378	0	TTG	GGAGG	5.3	-0.2
PA4759	4-hydroxy-tetrahydrodipicolinate reductase	268	0	ATG	GGAGT	5.7	0.1
PA4760	molecular chaperone DnaJ	377	0	ATG	TGAGA	7.0	-0.5
PA4761	molecular chaperone DnaK	637	0	ATG	GGAGA	4.8	-0.3
PA4762	heat shock protein GrpE	186	0	ATG	GGAGA	4.5	-0.6

protein ID	(predicted) function	length [aa]	TMH	start	RBS	pI	GRAVY
PA4763	DNA repair protein RecN	558	0	ATG	GGAGC	5.0	-0.3
PA4764	ferric uptake regulation protein	134	0	ATG	TGAGA	5.6	-0.3
PA4765	outer membrane lipoprotein OmlA	176	0	ATG	AGTGG	4.8	-0.5
PA4767	hypothetical protein	144	0	ATG	TGAGA	6.7	0.0
PA4769	transcriptional regulator	257	0	ATG	GGTGT	6.0	-0.4
PA4770	L-lactate permease	562	13	ATG	GGAGC	8.9	1.0
PA4771	L-lactate dehydrogenase	381	0	ATG	AGAGC	6.0	0.1
PA4772	ferredoxin	938	0	ATG	CGAGG	6.2	-0.1
PA4777	two-component regulator system signal sensor PmrB	477	2	ATG	GGAGT	6.0	0.0
PA4780	hypothetical protein	297	0	ATG	CGAGG	5.3	-0.5
PA4783	hypothetical protein	296	10	ATG	CGAGT	10.6	0.9
PA4785	acetyl-CoA acetyltransferase	425	0	ATG	GGAGT	6.7	-0.2
PA4786	3-ketoacyl-ACP reductase	451	0	ATG	GGAGC	9.4	0.1
PA4787	transcriptional regulator	333	0	ATG	-	6.5	-0.2
PA4790	hypothetical protein	249	0	ATG	-	7.8	-0.2
PA4791	hypothetical protein	206	0	ATG	GGAGC	8.6	-0.5
PA4792	hypothetical protein	311	0	ATG	GGAGA	9.4	-0.2
PA4793	hypothetical protein	187	0	ATG	GGAGA	7.8	-0.7
PA4795	hypothetical protein	125	0	TTG	-	5.0	0.0
PA4807	selenocysteine-specific elongation factor	641	0	GTG	GGAGC	7.5	-0.3
PA4808	selenocysteine synthase	468	0	ATG	TGTGG	9.1	0.0
PA4810	nitrate-inducible formate dehydrogenase subunit	208	4	ATG	CGAGG	10.2	0.3
PA4811	nitrate-inducible formate dehydrogenase subunit	309	0	ATG	TGAGG	5.6	-0.4
PA4812	formate dehydrogenase-O major subunit	1026	0	ATG	GGAGA	7.0	-0.4
PA4821	transporter	453	10	ATG	GGAGG	10.7	0.7
PA4825	Mg(2+) transport ATPase	903	8	ATG	GGAGA	5.9	0.1
PA4827	arylamine N-acetyltransferase	279	0	ATG	GGAGC	5.6	-0.1
PA4831	transcriptional regulator	186	0	ATG	-	7.0	-0.4
PA4838	hypothetical protein	384	9	ATG	-	9.9	0.7
PA4839	arginine decarboxylase (ADC)	636	0	ATG	TGAGG	5.3	-0.2
PA4842	hypothetical protein	356	1	ATG	-	5.2	-0.3
PA4843	two-component response regulator GcbA	542	0	ATG	-	6.0	-0.4
PA4845	thiol:disulfide interchange protein	591	8	ATG	CGAGA	8.4	0.4
PA4847	acetyl-CoA carboxylase biotin carboxyl carrier	156	0	ATG	GGAGT	5.0	0.1
PA4848	acetyl-CoA carboxylase biotin carboxylase	449	0	ATG	-	5.9	-0.2
PA4849	hypothetical protein	288	5	ATG	-	9.9	0.8
PA4850	50S ribosomal protein L11 methyltransferase	294	0	ATG	AGAGG	4.4	0.0
PA4851	hypothetical protein	421	1	ATG	-	4.7	-0.5
PA4854	bifunctional phosphoribosylaminoimidazolecarboxamide formyltransferase	535	0	ATG	-	6.1	-0.1
PA4855	phosphoribosylamine--glycine ligase	429	0	ATG	GGAGA	4.9	0.1
PA4856	sensor histidine kinase MifS	942	7	GTG	-	6.1	0.1
PA4857	TspR	197	6	ATG	-	9.8	1.0
PA4872	hypothetical protein	287	0	ATG	-	5.4	0.1
PA4873	heat-shock protein	421	0	ATG	-	5.3	-0.1
PA4876	OsmE family transcriptional regulator	114	0	ATG	GGAGT	8.8	-0.5

protein ID	(predicted) function	length [aa]	TMH	start	RBS	pI	GRAVY
PA4879	hypothetical protein	689	1	ATG	GGAGT	9.1	-0.2
PA4886	two-component sensor	463	2	GTG	CGAGG	6.9	0.0
PA4887	major facilitator superfamily transporter	438	12	ATG	-	6.3	0.6
PA4890	transcriptional regulator DesT	209	0	ATG	-	8.2	0.0
PA4907	short-chain dehydrogenase	253	0	ATG	CGAGG	5.3	-0.1
PA4914	transcriptional regulator	312	0	ATG	-	6.5	-0.2
PA4915	probable chemotaxis transducer	541	2	ATG	-	5.2	0.0
PA4916	Nudix-related transcriptional regulator NrtR	231	0	ATG	AGAGG	6.1	-0.1
PA4920	NAD synthetase	275	0	ATG	GGAGC	5.4	-0.2
PA4922	azurin precursor	148	0	ATG	GGAGG	6.4	-0.1
PA4924	hypothetical protein	231	0	GTG	-	10.9	-0.3
PA4925	hypothetical protein	283	3	ATG	GGTGA	6.8	0.6
PA4928	hypothetical protein	747	0	ATG	GGTGC	9.1	-0.5
PA4929	hypothetical protein	680	7	ATG	-	6.9	0.1
PA4931	replicative DNA helicase	464	0	ATG	CGAGT	5.0	-0.3
PA4932	50S ribosomal protein L9	148	0	ATG	AGAGG	5.5	0.0
PA4933	hypothetical protein	289	7	ATG	-	9.3	0.9
PA4934	30S ribosomal protein S18	76	0	ATG	TGAGG	10.5	-0.6
PA4935	30S ribosomal protein S6	139	0	ATG	GGAGC	4.9	-1.1
PA4936	23S rRNA guanosine(2251)-2'-O)-methyltransferase RlmB	248	0	ATG	-	6.7	-0.1
PA4937	exoribonuclease R	904	0	ATG	GGTGA	9.0	-0.5
PA4938	adenylosuccinate synthetase	430	0	ATG	-	5.7	-0.2
PA4941	protease subunit HflC	289	1	ATG	CGAGG	9.5	-0.5
PA4942	protease subunit HflK	400	1	ATG	GGAGA	5.2	-0.7
PA4943	GTP-binding protein	433	0	TTG	GGAGT	6.0	-0.3
PA4945	tRNA delta(2)-isopentenylpyrophosphate transferase	323	0	ATG	AGAGC	7.1	-0.2
PA4946	DNA mismatch repair protein	633	0	ATG	-	6.1	-0.3
PA4947	N-acetylmuramoyl-L-alanine amidase	475	0	ATG	GGAGC	9.8	-0.1
PA4949	hypothetical protein	502	0	ATG	-	7.2	0.4
PA4950	hypothetical protein	361	0	ATG	-	6.5	-0.3
PA4952	ribosome-associated GTPase	339	0	ATG	-	6.1	-0.2
PA4953	flagellar motor protein MotB	347	1	ATG	GGAGG	5.1	-0.5
PA4954	flagellar motor protein MotA	283	4	ATG	-	5.5	0.5
PA4955	hypothetical protein	503	0	ATG	CGAGC	9.7	-0.2
PA4957	phosphatidylserine decarboxylase	289	0	ATG	AGAGG	7.7	0.0
PA4958	protein FimW	607	0	ATG	GGAGC	7.0	-0.3
PA4959	protein FimX	691	0	ATG	TGAGC	5.1	-0.2
PA4960	phosphoserine phosphatase	429	0	ATG	GGTGG	5.1	0.0
PA4961	hypothetical protein	512	2	GTG	CGAGC	4.8	-0.1
PA4962	hypothetical protein	178	1	GTG	-	10.1	0.8
PA4963	hypothetical protein	236	0	ATG	GGTGG	9.1	-0.2
PA4964	DNA topoisomerase IV subunit A	754	0	ATG	TGAGG	5.8	-0.3
PA4965	hypothetical protein	174	1	GTG	-	9.9	-0.1
PA4967	DNA topoisomerase IV subunit B	629	0	ATG	AGAGA	5.7	-0.3
PA4972	hypothetical protein	248	0	ATG	-	6.0	-0.3
PA4974	probable outer membrane protein precursor	482	0	ATG	-	5.8	-0.5

protein ID	(predicted) function	length [aa]	TMH	start	RBS	pI	GRAVY
PA4988	3-deoxy-D-manno-octulosonic acid transferase	425	0	ATG	-	9.0	0.1
PA4991	hypothetical protein	391	0	ATG	-	7.7	-0.1
PA4992	hypothetical protein	270	0	ATG	GGAGG	6.0	-0.1
PA4996	bifunctional heptose 7-phosphate kinase/heptose 1-phosphate adenyltransferase	474	0	ATG	AGAGG	5.9	0.1
PA4997	transporter MsbA	603	5	ATG	-	6.5	0.2
PA4998	hypothetical protein	216	0	ATG	GGAGC	9.6	-0.4
PA4999	O-antigen ligase WaaL	401	11	ATG	TGAGC	10.0	0.6
PA5000	alpha-1,3-rhamnosyltransferase WapR	294	0	ATG	-	6.9	-0.3
PA5001	cell surface-sugar biosynthetic glycosyltransferase, Ssg	318	0	ATG	CGAGG	8.7	-0.2
PA5002	de-N-acetylase involved in persistence, DnpA	472	1	ATG	-	8.7	-0.3
PA5004	glycosyl transferase family protein	378	0	ATG	GGAGG	8.7	0.0
PA5005	carbamoyl transferase	585	0	GTG	AGAGG	6.5	-0.3
PA5006	putative kinase	492	0	ATG	GGAGT	9.7	-0.2
PA5008	WapP	244	0	ATG	GGAGA	10.1	-0.7
PA5010	UDP-glucose:(heptosyl) LPS alpha 1,3-glucosyltransferase WaaG	373	0	ATG	GGAGA	7.1	-0.2
PA5011	heptosyltransferase I	355	0	ATG	CGAGG	9.1	-0.2
PA5012	heptosyltransferase II	345	0	ATG	GGAGC	8.1	-0.1
PA5014	bifunctional glutamine-synthetase adenylyltransferase/deadenyltransferase	982	0	ATG	-	5.4	-0.2
PA5015	pyruvate dehydrogenase subunit E1	882	0	ATG	GGAGC	5.6	-0.4
PA5016	dihydrolipoamide acetyltransferase	547	0	GTG	GGAGA	5.2	0.0
PA5017	DipA	899	0	ATG	-	5.7	-0.3
PA5018	peptide methionine sulfoxide reductase	215	0	ATG	GGAGA	5.2	-0.2
PA5019	hypothetical protein	278	0	ATG	GGAGC	5.7	-0.4
PA5021	sodium/hydrogen antiporter	538	9	ATG	-	6.0	0.7
PA5022	potassium efflux protein KefA	1118	11	ATG	CGAGT	6.0	0.0
PA5024	hypothetical protein	323	9	ATG	-	9.6	0.7
PA5025	homocysteine synthase	425	0	ATG	-	6.0	0.1
PA5027	hypothetical protein	271	0	ATG	GGAGT	6.3	-0.1
PA5028	hypothetical protein	255	0	ATG	GGAGA	4.9	-0.2
PA5035	glutamate synthase subunit beta	477	0	ATG	TGAGG	6.1	-0.3
PA5036	glutamate synthase large chain precursor	1481	0	ATG	GGTGA	5.8	-0.1
PA5037	hypothetical protein	551	0	ATG	GGAGA	6.6	-0.1
PA5038	3-dehydroquinate synthase	368	0	ATG	-	5.5	0.1
PA5039	shikimate kinase	172	0	GTG	-	8.7	-0.3
PA5040	type 4 fimbrial biogenesis outer membrane	714	0	ATG	GGAGT	5.5	-0.3
PA5041	type 4 fimbrial biogenesis protein PilP	174	0	ATG	-	9.0	-0.3
PA5042	type 4 fimbrial biogenesis protein PilO	207	1	ATG	GGAGC	5.0	0.0
PA5043	type 4 fimbrial biogenesis protein PilN	198	1	ATG	TGAGG	9.4	-0.3
PA5044	type 4 fimbrial biogenesis protein PilM	354	0	GTG	-	4.8	0.1
PA5045	penicillin-binding protein 1A	822	1	ATG	-	5.9	-0.3
PA5046	malic enzyme	422	0	ATG	-	5.1	0.0
PA5047	hypothetical protein	479	1	ATG	-	8.5	-0.3
PA5049	50S ribosomal protein L31	71	0	ATG	CGAGG	8.9	-0.3
PA5051	arginine--tRNA ligase	587	0	ATG	GGAGA	5.4	-0.2
PA5052	hypothetical protein	231	1	ATG	GGAGT	10.2	-0.5
PA5053	heat shock protein HslV	177	0	TTG	GGAGA	6.2	0.0

protein ID	(predicted) function	length [aa]	TMH	start	RBS	pI	GRAVY
PA5054	ATP-dependent protease ATP-binding subunit HslU	447	0	ATG	GGAGT	5.5	-0.4
PA5056	poly(3-hydroxyalkanoic acid) synthase	559	0	ATG	GGAGC	8.1	-0.3
PA5057	poly(3-hydroxyalkanoic acid) depolymerase	285	0	ATG	CGAGG	9.7	0.1
PA5058	poly(3-hydroxyalkanoic acid) synthase	560	0	ATG	GGAGT	7.8	-0.3
PA5060	polyhydroxyalkanoate synthesis protein PhaF	309	0	ATG	GGAGA	10.3	-0.5
PA5061	hypothetical protein	138	0	ATG	TGAGG	9.2	-0.4
PA5063	ubiquinone/menaquinone biosynthesis methyltransferase	256	0	ATG	GGTGA	9.1	-0.3
PA5064	hypothetical protein	208	0	ATG	CGAGG	5.7	0.0
PA5065	ubiquinone biosynthetic protein UbiB	533	0	ATG	-	9.1	-0.1
PA5068	twin-arginine translocation protein TatA	82	1	ATG	CGAGG	6.7	-0.5
PA5070	transporter TatC	267	6	ATG	CGAGA	5.7	0.7
PA5072	probable chemotaxis transducer	647	2	ATG	GGAGT	5.1	-0.3
PA5074	ABC transporter ATP-binding protein	244	0	GTG	GGAGG	5.7	-0.1
PA5075	ABC transporter permease	320	5	GTG	CGAGA	7.9	0.3
PA5076	probable binding protein component of ABC transporter	266	1	ATG	-	6.9	-0.1
PA5077	glucosyltransferase MdoH	861	6	ATG	GGAGC	8.9	0.0
PA5078	glucan biosynthesis protein G	525	1	GTG	CGAGG	6.5	-0.5
PA5079	D-tyrosyl-tRNA(Tyr) deacylase	145	0	ATG	GGAGG	5.9	0.1
PA5085	transcriptional regulator DguR	318	0	ATG	-	9.1	0.0
PA5093	histidine/phenylalanine ammonia-lyase	510	0	ATG	GGTGG	5.9	0.2
PA5094	ABC transporter ATP-binding protein	276	0	ATG	CGAGA	9.1	-0.1
PA5099	transporter	480	13	ATG	GGAGT	9.4	0.8
PA5105	histidine utilization repressor HutC	250	0	GTG	GGAGT	6.9	-0.3
PA5107	outer membrane lipoprotein Blc	189	0	GTG	-	6.8	-0.4
PA5108	hypothetical protein	85	0	ATG	GGAGT	8.4	0.3
PA5110	fructose-1,6-bisphosphatase	336	0	ATG	GGAGC	5.7	-0.3
PA5112	esterase	646	0	ATG	GGAGT	4.7	-0.4
PA5113	hypothetical protein	464	1	ATG	GGAGG	6.3	-0.1
PA5114	hypothetical protein	1201	35	ATG	-	9.3	0.7
PA5115	hypothetical protein	194	0	ATG	CGAGG	5.4	0.0
PA5117	regulatory protein TypA	605	0	GTG	CGAGA	5.2	-0.3
PA5118	thiamine biosynthesis protein ThiI	484	0	ATG	-	6.2	-0.2
PA5119	glutamine synthetase	469	0	ATG	GGAGG	5.1	-0.3
PA5121	hypothetical protein	735	10	GTG	-	9.9	0.4
PA5124	two-component sensor NtrB	358	0	ATG	-	5.8	-0.2
PA5125	two-component response regulator NtrC	476	0	ATG	GGAGT	5.6	-0.4
PA5127	rRNA methylase	153	0	ATG	GGAGC	8.4	-0.3
PA5128	preprotein translocase subunit SecB	163	0	ATG	-	4.5	-0.2
PA5130	hypothetical protein	139	1	ATG	-	9.6	0.2
PA5131	phosphoglycerate mutase	515	0	ATG	AGAGC	5.1	-0.1
PA5132	hypothetical protein	272	9	ATG	-	9.8	1.0
PA5133	hypothetical protein	428	0	ATG	GGTGC	9.4	-0.7
PA5134	carboxyl-terminal protease	436	0	ATG	GGAGC	5.5	-0.2
PA5136	hypothetical protein	493	1	ATG	-	4.9	-0.3
PA5141	1-(5-phosphoribosyl)-5-[(5-phosphoribosylamino)methylideneamino] imidazole-4-carboxamide isomerase	245	0	ATG	-	5.0	0.2

protein ID	(predicted) function	length [aa]	TMH	start	RBS	pI	GRAVY
PA5142	imidazole glycerol phosphate synthase subunit	213	0	GTG	GGTGC	5.9	-0.1
PA5146	hypothetical protein	750	1	ATG	-	8.1	-0.3
PA5147	A/G-specific adenine glycosylase	355	0	ATG	-	8.6	-0.2
PA5149	hypothetical protein	360	0	ATG	GGAGG	6.3	-0.2
PA5151	hypothetical protein	229	2	ATG	-	7.8	0.7
PA5152	ABC transporter ATP-binding protein	257	0	ATG	AGAGG	6.7	-0.2
PA5154	ABC transporter permease	231	5	ATG	-	9.7	0.7
PA5155	amino acid ABC transporter permease	230	5	ATG	TGAGG	9.8	0.7
PA5159	multidrug resistance protein	394	1	ATG	CGAGG	6.0	-0.3
PA5160	drug efflux transporter	509	13	ATG	TGAGC	6.8	0.8
PA5161	dTDP-D-glucose 4,6-dehydratase	352	0	ATG	-	5.6	-0.4
PA5162	dTDP-4-dehydrorhamnose reductase	302	0	ATG	GGTGG	5.8	-0.2
PA5163	glucose-1-phosphate thymidylyltransferase	293	0	ATG	TGAGC	5.2	-0.2
PA5165	two-component sensor DctB	612	2	ATG	-	9.0	-0.2
PA5166	two-component response regulator DctD	462	0	ATG	GGAGG	5.5	-0.2
PA5167	C4-dicarboxylate-binding protein DctP	331	0	ATG	AGAGG	8.4	-0.4
PA5168	dicarboxylate transporter	210	4	ATG	AGAGG	5.5	0.7
PA5169	C4-dicarboxylate transporter DctM	427	13	ATG	CGAGG	8.7	1.3
PA5170	arginine/ornithine antiporter	482	13	ATG	GGAGA	6.5	0.9
PA5171	arginine deiminase	418	0	ATG	GGAGA	5.5	-0.2
PA5172	ornithine carbamoyltransferase	336	0	ATG	GGAGA	6.1	-0.4
PA5173	carbamate kinase	310	0	ATG	GGAGG	5.3	-0.1
PA5174	beta-acetoacetyl-acyl carrier protein synthase FabY	634	0	ATG	GGAGT	5.8	-0.1
PA5178	hypothetical protein	145	0	ATG	GGAGA	5.5	-0.1
PA5181	oxidoreductase	773	0	ATG	CGAGT	6.6	-0.3
PA5183a	hypothetical protein	71	0	ATG	-	8.2	0.0
PA5188	3-hydroxyacyl-CoA dehydrogenase	411	0	ATG	CGAGG	5.4	0.0
PA5189	transcriptional regulator	302	0	GTG	-	7.3	-0.1
PA5192	phosphoenolpyruvate carboxykinase	513	0	ATG	-	5.3	-0.2
PA5193	heat shock protein 33	297	0	ATG	-	4.7	-0.2
PA5194	hypothetical protein	267	4	ATG	-	9.6	0.6
PA5197	ribosomal protein S6 modification protein	301	0	ATG	GGTGC	9.4	0.0
PA5199	protein AmgS	439	2	ATG	-	5.9	-0.1
PA5200	osmolarity response regulator	247	0	ATG	GGAGT	6.2	-0.3
PA5201	hypothetical protein	779	0	ATG	GGTGG	6.0	-0.3
PA5203	glutamate--cysteine ligase	527	0	TTG	-	5.1	-0.3
PA5204	N-acetylglutamate synthase	432	0	ATG	-	6.1	-0.2
PA5205	multiple drug resistance protein MarC	233	5	ATG	CGAGG	6.0	0.8
PA5207	phosphate transporter	422	11	ATG	-	8.9	1.1
PA5208	hypothetical protein	225	0	ATG	GGAGG	5.4	-0.2
PA5209	hypothetical protein	454	0	ATG	CGAGC	8.9	-0.6
PA5210	secretion pathway ATPase	594	0	ATG	GGAGT	6.1	-0.2
PA5211	hypothetical protein	150	2	ATG	TGAGG	8.0	0.4
PA5215	glycine cleavage system aminomethyltransferase	360	0	ATG	GGAGA	5.4	-0.1
PA5216	iron ABC transporter substrate-binding protein	539	12	GTG	CGAGG	10.1	0.8
PA5220	hypothetical protein	273	0	ATG	GGAGG	5.8	-0.2

protein ID	(predicted) function	length [aa]	TMH	start	RBS	pI	GRAVY
PA5221	probable FAD-dependent monooxygenase	405	0	ATG	GGAGA	6.2	-0.1
PA5223	2-octaprenyl-6-methoxyphenyl hydroxylase	394	1	ATG	CGAGG	6.4	-0.1
PA5230	ABC transporter permease	374	6	ATG	GGAGG	6.2	0.5
PA5231	ABC transporter ATP-binding protein/permease	916	5	ATG	-	6.2	0.1
PA5232	hypothetical protein	357	1	ATG	CGAGG	9.1	-0.1
PA5235	sn-glycerol-3-phosphate transporter	448	12	ATG	GGAGC	9.0	0.5
PA5237	3-octaprenyl-4-hydroxybenzoate carboxy-lyase	488	0	ATG	-	6.2	-0.3
PA5239	transcription termination factor Rho	419	0	ATG	-	6.4	-0.4
PA5240	thioredoxin	108	0	ATG	GGAGA	4.7	-0.1
PA5241	exopolyphosphatase	506	0	ATG	-	6.3	-0.3
PA5242	polyphosphate kinase	736	0	ATG	-	7.3	-0.2
PA5243	delta-aminolevulinic acid dehydratase	337	0	GTG	GGAGT	5.1	-0.2
PA5244	conserved hypothetical protein	196	4	ATG	-	10.0	0.3
PA5245	glutamine amidotransferase	222	0	ATG	GGAGT	5.0	0.1
PA5247	hypothetical protein	160	0	ATG	-	7.6	-0.4
PA5248	hypothetical protein	633	7	ATG	-	5.1	0.2
PA5251	hypothetical protein	192	3	ATG	AGAGG	9.7	0.6
PA5252	ABC transporter ATP-binding protein	638	0	ATG	-	5.7	-0.4
PA5253	alginate regulatory protein AlgP	352	0	ATG	GGAGG	10.6	-0.4
PA5255	anti-RNA polymerase sigma 70 factor AlgQ	160	0	ATG	AGAGG	4.8	-0.3
PA5256	disulfide bond formation protein	163	4	ATG	TGTGG	8.3	1.0
PA5257	hypothetical protein	412	2	ATG	GGAGG	8.9	-0.2
PA5258	hypothetical protein	376	1	GTG	-	5.0	-0.3
PA5259	uroporphyrinogen-III synthase	251	0	GTG	CGAGG	5.0	-0.1
PA5260	porphobilinogen deaminase	313	0	ATG	-	5.4	-0.1
PA5261	alginate biosynthesis regulatory protein AlgR	248	0	ATG	TGAGC	6.7	-0.1
PA5262	alginate biosynthesis protein AlgZ/FimS	358	4	ATG	-	7.0	0.2
PA5268	magnesium/cobalt transporter	326	2	ATG	-	5.4	-0.2
PA5270	hypothetical protein	293	1	GTG	GGAGC	9.4	-0.3
PA5272	adenylate cyclase	950	0	ATG	-	6.3	-0.4
PA5273	hypothetical protein	237	1	ATG	-	9.2	-0.3
PA5276	lipopeptide LppL	46	1	ATG	-	9.3	-0.2
PA5277	diaminopimelate decarboxylase	415	0	ATG	TGAGA	5.4	-0.1
PA5278	diaminopimelate epimerase	276	0	ATG	TGAGG	7.2	-0.2
PA5279	hypothetical protein	233	0	ATG	CGAGA	5.4	-0.1
PA5287	ammonium transporter AmtB	442	12	ATG	GGAGA	5.5	0.9
PA5288	nitrogen regulatory protein P-II 2	112	0	ATG	GGAGA	5.4	-0.1
PA5290	hypothetical protein	497	0	ATG	GGAGC	8.2	0.0
PA5291	choline transporter BetT2	661	12	ATG	GGAGA	6.3	0.4
PA5296	ATP-dependent DNA helicase Rep	669	0	ATG	-	5.8	-0.5
PA5298	xanthine phosphoribosyltransferase	190	0	GTG	-	6.2	0.2
PA5299	hypothetical protein	619	0	ATG	-	5.6	-0.3
PA5300	cytochrome C5	136	0	ATG	GGTGA	6.7	0.0
PA5301	transcriptional regulator PauR	182	0	TTG	GGAGG	5.4	-0.3
PA5302	alanine racemase	357	0	ATG	AGAGA	6.4	0.0
PA5304	D-amino acid dehydrogenase small subunit	432	0	ATG	GGAGG	7.0	-0.2

protein ID	(predicted) function	length [aa]	TMH	start	RBS	pI	GRAVY
PA5306	hypothetical protein	63	1	ATG	GGAGA	5.0	0.6
PA5307	hypothetical protein	855	1	ATG	AGAGG	6.6	-0.2
PA5308	leucine-responsive regulatory protein	162	0	ATG	GGAGC	7.8	-0.4
PA5309	oxidoreductase	439	0	ATG	-	6.9	-0.1
PA5310	hypothetical protein	529	0	ATG	-	9.4	-0.2
PA5311	major facilitator superfamily transporter	387	12	ATG	GGAGA	9.1	1.0
PA5312	aldehyde dehydrogenase	497	0	ATG	AGAGG	5.4	0.0
PA5313	omega amino acid--pyruvate transaminase	444	0	ATG	GGTGG	6.2	0.0
PA5316	50S ribosomal protein L28	78	0	ATG	AGAGG	11.7	-0.7
PA5317	probable binding protein component of ABC dipeptide transporter	526	0	ATG	GGAGC	6.5	-0.2
PA5320	bifunctional phosphopantothenoylcysteine decarboxylase	402	0	ATG	-	5.9	0.0
PA5322	phosphomannomutase AlgC	868	2	ATG	CGAGG	5.3	-0.1
PA5323	acetylglutamate kinase	301	0	ATG	GGAGC	6.3	0.2
PA5331	orotate phosphoribosyltransferase	213	0	ATG	GGTGT	5.3	0.0
PA5332	catabolite repression control protein	259	0	ATG	-	5.3	-0.4
PA5333	hypothetical protein	123	3	ATG	GGAGA	6.5	0.9
PA5338	guanosine-3',5'-bis(diphosphate) 3'-pyrophosphohydrolase	701	0	TTG	GGTGA	9.1	-0.3
PA5339	hypothetical protein	126	0	ATG	GGAGT	5.1	0.1
PA5340	hypothetical protein	243	0	ATG	GGAGT	4.7	-0.4
PA5344	transcriptional regulator OxyR	310	0	ATG	TGAGC	6.3	0.0
PA5345	ATP-dependent DNA helicase RecG	691	0	ATG	-	6.8	-0.1
PA5346	SadB	469	0	ATG	-	5.8	0.0
PA5349	rubredoxin reductase	384	0	ATG	AGAGG	5.5	0.1
PA5354	glycolate oxidase FAD binding subunit GlcE	359	0	ATG	GGAGC	8.3	-0.1
PA5355	glycolate oxidase subunit GlcD	499	0	ATG	-	5.2	0.1
PA5356	DNA-binding transcriptional regulator GlcC	251	0	ATG	GGAGC	9.6	-0.6
PA5357	hypothetical protein	178	0	ATG	-	5.0	0.0
PA5358	4-hydroxybenzoate octaprenyltransferase	296	8	ATG	GGAGG	8.7	0.6
PA5360	two-component response regulator PhoB	229	0	ATG	CGAGG	5.3	-0.2
PA5361	two-component sensor PhoR	443	1	ATG	-	7.0	-0.3
PA5362	hypothetical protein	446	4	ATG	-	5.6	0.2
PA5364	two-component response regulator	300	0	ATG	GGAGA	9.1	-0.2
PA5365	phosphate uptake regulatory protein PhoU	242	0	ATG	-	5.2	-0.4
PA5366	phosphate ABC transporter ATP-binding protein	277	0	ATG	TGAGG	5.9	-0.2
PA5367	phosphate ABC transporter permease	558	6	GTG	GGAGG	7.9	0.2
PA5368	phosphate ABC transporter permease	677	7	ATG	-	6.0	0.2
PA5370	major facilitator superfamily transporter	438	12	ATG	AGAGA	9.2	0.8
PA5372	choline dehydrogenase	561	0	ATG	AGAGG	6.4	-0.4
PA5373	betaine aldehyde dehydrogenase	490	0	ATG	AGAGG	5.3	-0.2
PA5374	BetI family transcriptional regulator	197	0	ATG	AGAGG	8.8	-0.2
PA5376	ABC transporter ATP-binding protein CbcV	392	0	ATG	-	7.1	-0.2
PA5377	ABC transporter permease CbcW	279	6	ATG	-	6.3	1.0
PA5394	cardiolipin synthetase	490	2	ATG	GGAGA	7.2	0.1
PA5402	hypothetical protein	189	4	ATG	-	6.1	0.5
PA5412	hypothetical protein	837	2	ATG	TGAGA	5.0	-0.3
PA5413	low specificity l-threonine aldolase	346	0	ATG	AGAGG	5.2	-0.1

protein ID	(predicted) function	length [aa]	TMH	start	RBS	pI	GRAVY
PA5414	hypothetical protein	213	0	ATG	CGAGA	5.8	-0.1
PA5415	serine hydroxymethyltransferase	417	0	ATG	GGAGA	6.1	-0.1
PA5426	5-(carboxyamino)imidazole ribonucleotide mutase	163	0	ATG	AGAGG	5.8	0.2
PA5427	alcohol dehydrogenase	342	0	ATG	GGAGA	5.6	0.2
PA5428	transcriptional regulator	302	0	GTG	GGAGC	6.7	0.1
PA5429	aspartate ammonia-lyase	474	0	ATG	TGAGA	5.6	0.1
PA5430	hypothetical protein	404	10	ATG	GGAGT	10.6	0.8
PA5434	tryptophan permease	417	11	GTG	-	9.5	0.7
PA5435	probable transcarboxylase subunit	607	0	ATG	GGAGC	5.6	-0.2
PA5436	acetyl-CoA carboxylase subunit alpha	471	0	GTG	AGAGG	6.2	-0.2
PA5437	transcriptional regulator	311	0	ATG	-	7.7	0.0
PA5438	transcriptional regulator	293	0	GTG	AGAGA	6.7	0.1
PA5441	hypothetical protein	733	0	ATG	-	4.9	-0.3
PA5443	DNA-dependent helicase II	728	0	ATG	-	5.6	-0.3
PA5445	coenzyme A transferase	497	0	ATG	TGAGG	5.9	-0.1
PA5446	hypothetical protein	67	0	ATG	AGTGG	11.7	-0.8
PA5449	glycosyltransferase WbpX	460	0	ATG	GGAGA	6.4	-0.1
PA5450	ABC transporter	421	0	ATG	GGTGG	5.8	-0.2
PA5451	LPS efflux transporter membrane protein	265	6	ATG	GGTGG	9.6	0.9
PA5453	GDP-mannose 4,6-dehydratase	323	0	ATG	GGAGT	6.1	-0.3
PA5456	putative glycosyltransferase	433	0	ATG	-	5.9	-0.4
PA5457	methyltransferase	287	0	ATG	-	5.8	-0.1
PA5464	hypothetical protein	652	0	GTG	-	6.6	-0.5
PA5466	hypothetical protein	314	9	ATG	-	9.4	0.9
PA5468	citrate transporter	434	11	ATG	GGAGT	8.3	1.0
PA5470	peptide chain release factor-like protein	204	0	ATG	GGAGT	10.8	-0.3
PA5471	ArmZ	379	0	ATG	-	6.2	-0.1
PA5473	hypothetical protein	582	8	ATG	-	6.8	0.3
PA5474	metalloprotease	457	1	ATG	-	5.2	-0.3
PA5475	hypothetical protein	186	0	ATG	GGAGA	5.0	-0.3
PA5476	citrate transporter	429	12	ATG	TGAGT	9.0	0.7
PA5477	hypothetical protein	346	7	ATG	CGAGA	9.8	0.3
PA5478	hypothetical protein	409	9	ATG	-	7.7	1.0
PA5479	glutamate/aspartate:proton symporter	444	8	ATG	GGTGA	9.2	0.9
PA5483	two-component response regulator AlgB	449	0	ATG	AGAGG	5.4	-0.2
PA5484	two-component sensor KinB	595	2	ATG	-	5.5	-0.1
PA5485	protein AmpDh2	259	0	ATG	GGAGT	6.7	-0.3
PA5487	hypothetical protein	671	0	ATG	GGAGT	4.9	-0.5
PA5490	cytochrome C4	201	0	ATG	-	7.0	-0.1
PA5492	ribosome biogenesis GTP-binding protein YsxC	215	0	ATG	TGTGG	6.5	-0.2
PA5493	DNA polymerase I	913	0	ATG	-	5.0	-0.1
PA5496	class II (cobalamin-dependent) ribonucleotide-diphosphate reductase subunit, NrdJb	229	0	ATG	TGAGG	6.0	0.0
PA5497	ribonucleoside-diphosphate reductase	734	0	ATG	-	5.8	-0.5
PA5498	adhesin ZnuA	307	0	GTG	TGAGT	5.8	-0.1
PA5501	zinc ABC transporter permease ZnuB	262	8	ATG	-	7.8	1.3
PA5502	hypothetical protein	262	0	ATG	CGAGA	6.5	-0.2

protein ID	(predicted) function	length [aa]	TMH	start	RBS	pI	GRAVY
PA5503	ABC transporter ATP-binding protein	335	0	GTG	-	6.2	0.0
PA5504	D-methionine ABC transporter	225	5	ATG	GGAGG	5.8	1.0
PA5506	hypothetical protein	285	0	ATG	CGAGG	7.1	-0.3
PA5507	hypothetical protein	217	0	ATG	GGAGG	6.0	-0.3
PA5510	transporter	449	12	ATG	CGAGG	9.2	0.8
PA5511	DNA-binding response regulator MifR	447	0	ATG	CGAGC	5.7	-0.2
PA5512	sensor histidine kinase MifS	588	0	ATG	-	6.5	-0.1
PA5515	hypothetical protein	166	1	ATG	TGAGT	10.2	-0.4
PA5518	potassium efflux transporter	567	12	ATG	GGAGT	5.8	0.7
PA5521	short-chain dehydrogenase	252	0	ATG	GGAGT	5.7	0.0
PA5524	short-chain dehydrogenase	260	0	ATG	-	5.3	0.0
PA5528	hypothetical protein	284	2	ATG	AGAGA	6.1	-0.1
PA5529	sodium/proton antiporter	585	15	ATG	CGAGG	8.3	1.0
PA5530	MFS dicarboxylate transporter	435	12	ATG	AGAGG	9.0	0.5
PA5531	transporter TonB1	342	0	ATG	-	8.7	-0.7
PA5544	hypothetical protein	674	16	ATG	GGAGT	8.8	1.0
PA5546	hypothetical protein	394	0	ATG	GGAGG	5.6	-0.2
PA5549	glucosamine--fructose-6-phosphate	611	0	ATG	GGAGA	5.7	0.0
PA5552	bifunctional glucosamine-1-phosphate acetyltransferase	454	0	ATG	-	5.8	-0.1
PA5553	ATP synthase subunit epsilon	141	0	ATG	TGAGG	5.1	0.2
PA5554	ATP synthase subunit beta	458	0	ATG	AGAGG	5.0	-0.1
PA5555	ATP synthase subunit gamma	286	0	ATG	GGTGT	7.7	-0.1
PA5556	ATP synthase subunit alpha	514	0	ATG	TGAGT	5.3	-0.1
PA5557	ATP synthase subunit delta	178	0	ATG	CGAGG	5.8	-0.1
PA5558	ATP synthase subunit B	156	1	GTG	CGAGG	5.8	-0.2
PA5559	ATP synthase subunit C	85	2	ATG	GGAGG	4.9	1.3
PA5560	ATP synthase subunit A	289	6	ATG	TGAGG	6.0	0.8
PA5562	chromosome partitioning protein	290	0	ATG	-	9.4	-0.4
PA5563	chromosome partitioning protein Soj	262	0	ATG	TGAGG	5.9	0.0
PA5564	16S rRNA methyltransferase GidB	214	0	ATG	GGAGC	5.9	-0.2
PA5565	tRNA uridine 5-carboxymethylaminomethyl modification protein GidA	630	0	GTG	CGAGG	6.1	-0.3
PA5567	tRNA modification GTPase TrmE	455	0	ATG	GGAGA	5.1	-0.1
PA5568	inner membrane protein translocase subunit YidC	578	4	ATG	CGAGT	7.6	-0.1